THE PHOTOCHEMISTRY OF MONOSUBSTITUTED TRIPHENYLPHOSPHINE DERIVATIVES OF SOME METAL CARBONYL COMPLEXES

A thesis presented for the degree of Doctor of Philosophy

at

DUBLIN CITY UNIVERSITY

by

Barry Crocock B Sc

MAY 1992

Declaration

I declare that the work presented in this thesis is based entirely on my research carried out at Dublin City University under the supervison of Dr. Conor Long.

Barry Crocock

Barry Crocock

TO MY PARENTS

Acknowledgements

I would sincerely like to thank my supervisor Dr Conor Long for his constant support, guidance and generosity through out my postgraduate research

I wish to thank (Dr) Gerry Farrell my buddy, pal, mate, friend and drinking partner over the duration of my studies at D C U (N I H E)

I would also like to thank the technical staff especially the oldies, Peig, Teresa and Mick, the not so oldies Maurice, Veronica and Fintan and the youngies for their assistance in the last six years

My thanks to the people (?) in the research group past and present namely Bernie, Graham, Celia, Mick, Maureen, Mary and especially Irene my companion and friend throughout most of my postgraduate studies

I would like to thank my old classmates who have attempted to drive me bananas over the duration of my studies These include Alan (Sparkie), John (Redser), Conor (??), Peter (Pooks), Eamon (Happy), Aodhmar (?) and not forgetting Frank

How could I forget the lads and lassies in AG07, AG12, AG22(?), AG20 and the Twilight Zone who have been a constant source of humour over the years

Finally I would especially like to thank Maureen, Mary, Fiona and James who came to my rescue in my hour of need

Table of Contents

Abstract

The photochemistry of some d^6 metal carbonyl complexes is investigated In particular, the effect of the substitution of a carbon monoxide ligand by a triphenylphosphine ligand on the reactivity of the intermediates formed on photolysis of these complexes is examined The manganese complexes $(\eta^5\text{-}C_5H_4CH_3)Mn(CO)_3$ and $(\eta^5\text{-}C_5H_4CH_3)Mn(CO)_2PPh_3$ are investigated by laser flash photolysis (λ = 355nm) The laser flash photolysis (λ = 266nm, 355nm) of the Group VI $M(CO)_5PPh_3$ (M = Cr, Mo or W) complexes is also reported

The crystal structures of the $(\eta^5\text{-}C_5H_4CH_3)Mn(CO)_2L$ (L = pyridine, *cis*-cyclooctene) complexes are presented and examined to see the effects of a good σ donating ligand and a good π accepting ligand on the $(\eta^5\text{-}C_5H_4CH_3)Mn(CO)_2$ unit

A program written in GWBASIC for transient capture and analysis is described

CHAPTER 1

INTRODUCTION

1.0 INTRODUCTION

Photolysis of metal carbonyl compounds has become of increasing interest and importance in recent times The potential use of these compounds in synthesis and as homogeneous catalysts has been known for many years[1] Homogeneous catalysts frequently function efficiently under milder conditions than their heterogeneous counterparts The use of heterogeneous catalysts outweighs the use of homogeneous catalysts in industrial processes primarily because they can easily be removed from the reaction medium However, in some processes the use of homogeneous catalysts has become almost exclusive One such process is the production of ethanal which is synthesised by the Wacker process in which an aqueous HCl solution of $PdCl_2/CuCl_2$ is used to convert ethene to ethanal by air oxidation[2] Another process involves the carbonylation of methanol to produce acetic acid under low pressures of carbon monoxide (30 - 40atm) using the rhodium based catalyst $[RhI_2(CO)_2]^-$ [3] Other reactions use homogeneous catalysts to effect highly specific organic transformations Industrially, these are small scale processes producing chemicals of interest to the pharmaceutical sector Homogeneous catalysts have proved to be very effective in the areas of hydrogenation, olefin isomerisation, carbonylation, oligomerisation and polymerisation of organic molecules Certain metal carbonyl complexes are known to be homogeneous catalysts Among these are $Ni(CO)_4$ which is used in the hydrocarboxylation of olefins[1] and (arene)$Cr(CO)_3$ or photoactivated $Cr(CO)_6$ which are used in the selective hydrogenation of some conjugated dienes[4]

The central process in these reactions is the displacement of a carbonyl group by a nucleophilic ligand Thermal replacement of the carbonyl ligand is often difficult whereas photochemical decarbonylation can proceed with quantum yields approaching 1[5] Knowledge of the structure and reactivity of these intermediates has important applications in the areas of synthesis and design of homogeneous catalytic

processes[1,2] Therefore it is important to understand these processes A variety of procedures has been employed to elucidate the structure, identity and reaction kinetics of these intermediates Among the most successful have been low temperature matrix isolation and laser flash photolysis The advantages and disadvantages of these methods will be given with respect to the photochemical study of metal carbonyl complexes In addition the photochemistry of $MeCpMn(CO)_2L$ (L = CO, PPh_3) and of the GroupVIB pentacarbonyl triphenylphosphine complexes will be discussed as these are the prime concern of this thesis

1.1 Low temperature matrix isolation

This technique was developed in the 1950 by Pimentel[6] and is the oldest method employed in the detection of metal carbonyl photofragments The metal complexes are dispersed in a matrix, usually an inert noble gas at low temperature (1 5-60K) Alternative matrices such as N_2, O_2, CO and CH_4 have also been used The advantage of this technique is that reactive fragments, which would not have a long lifetime at room temperature, can be stabilised These fragments are molecules or ions which are present in vapours or discharges at high temperature, weakly bound to other molecules or transients of short lifetimes in reactions The matrices stabilise molecular ground states not excited states and the lifetimes of these species are reduced relative to gas phase[7] After irradiation of these matrices, spectroscopic techniques e g UV/visible and infra red spectroscopy, can be used to study the metal carbonyl photofragments produced This would not normally be possible because of the short lifetimes of the metal carbonyl intermediates Infra red spectroscopy is particularly useful because the carbonyl bands are sharp and to a good approximation no coupling is involved with other molecular vibrations

One of the requirements of the matrix isolation technique is that the matrix should be inert towards the photofragments produced In the majority of cases no

interaction can be observed with the noble gases or with nitrogen and methane matrices However, evidence has been found for coordination by the photoproducts to the matrix, examples of which are $Cr(CO)_5N_2$[8], $Fe(CO)_4(CH_4)$[9], $Cr(CO)_5Ar$[10] and $Mn(CO)_5Kr$[11] This demonstrates the reactivity of these photochemically produced coordinately unsaturated species

Apart from matrices of inert gases, low temperature solvent glasses are also used These consist of hydrocarbons e g isopentane, methylcyclohexane, and are maintained at higher temperatures (77K) than the inert gas matrices[12] The spectroscopic techniques used for species detection are the same as for matrix studies However, carbonyl bands in the infra red tend to be broader and may occlude other spectral features needed for accurate structural determination This problem may be overcome in some cases by isotopic enrichment of the matrix In addition, these glasses may not be inert and therefore are more likely to interact with the photofragments produced Other disadvantages which apply to both matrices and glasses are that they cannot be easily used for charged species, very little kinetic information can be obtained because of the restricted temperature range and the frozen rigid structure of the matrix can block some pathways in photochemical processes The last disadvantage is not thought to be so important in frozen glasses because of a less closely packed arrangment

As a complementary technique to matrix isolation, low temperature solutions of liquefied noble gases have been used to characterise unstable carbonyl compounds The advantage of this technique over the others is the total lack of absorption by the solvent in the infra red When combined with Fourier transform infra red spectroscopy, this allows weak absorptions arising from coordinated ligands to be detected One such example is the detection in liquid xenon of the H-H stretching vibration of coordinated

dihydrogen in $Cr(CO)_5H_2$ which is too weak to be detected using matrix isolation techniques[13]

Problems associated with low quantum yields for loss of ligand species in metal carbonyl complexes using conventional light sources have been overcome by the use of lasers for excitation[14] An example using a laser as the excitation source is the loss of hydrogen from $HMn(CO)_5$[15] Using a conventional mercury lamp $HMn(CO)_4$ is generated in a solid argon matrix but not $Mn(CO)_5$ because of low quantum yield for H loss Alternatively, $Mn(CO)_5$ is generated only in a CO matrix because recombination with CO removes $HMn(CO)_4$ When an ArF excimer laser (193nm) is used as an excitation source in an argon matrix both species are observed

1.2 Flash photolysis

Conventional flash photolysis was developed in the 1950's by Norrish and Porter[16] for which they recieved the Nobel prize They were able to identify reactive intermediates present in many photochemical systems Stationary concentrations of atoms, radicals or excited species are normally too low for intermediates to be detected by spectroscopic techniques The concentrations of these intermediates can be increased by using a very high intensity flash of light e g a discharge lamp or laser From spectroscopic observations the spectra and lifetimes of the intermediates can be obtained Nasielski pioneered flash photolysis with UV/visible detection on metal carbonyl systems with the analysis of $Cr(CO)_6$[17] Metal carbonyl intermediates are relatively easy to detect because their quantum yields for formation are high and their UV/visible absorptions are intense Solvent absorptions can be overcome by using solvents with suitable cut-off wavelengths The basic technique involves excitation of the sample solution with a high intensity flash e g a laser pulse, while simultaneously passing a monitoring beam, e g from a xenon arc lamp, through the sample Changes in absorption in the monitoring beam reflect the formation of intermediates or depletion

of parent compound (or both) Spectra are recorded using a spectrograph or are built up point by point by changing the wavelength of a monochromator Fast transient digitizers are used to record the change in voltage output from a suitable photomultiplier A diagram of a conventional flash photolysis system is shown in Figure 1 2 1

While UV/visible monitored flash photolysis is quite adequate for obtaining electronic spectra, transient decay kinetics and their variation with reaction conditions, little structural information is available from this technique Since the number of infra red bands is dependent on the symmetry of molecules, finite infra red spectral shifts are associated with minor structural changes in molecules Therefore infra red spectra have more easily accessible structural information

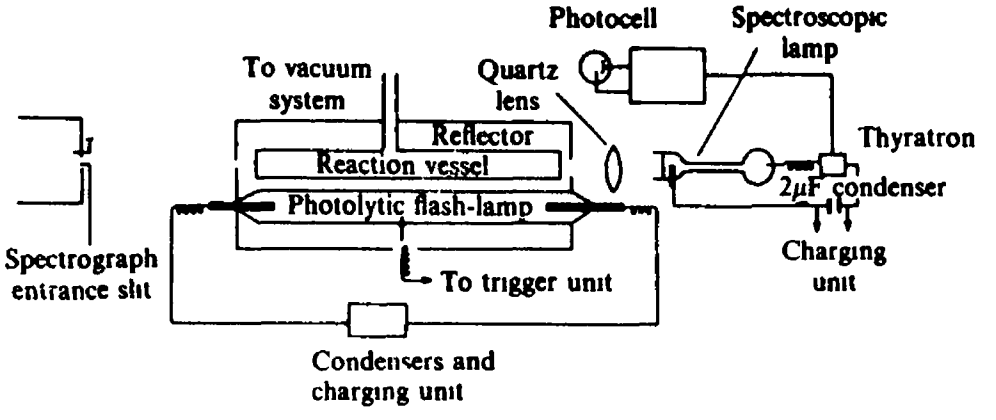

Figure 1.2.1. A schematic diagram of a typical conventional flash photolysis system

This technique is ideal for metal carbonyl compounds as CO stretching frequencies are relatively uncoupled to other vibrational modes and their positions are dependent on

the electron density on the metal[18]. The system for spectral and kinetic data collection is similar to that used in the UV/visible monitored technique. Differences arise in the absorption data and obviously the monitoring beam source. The spectrometers only measure changes in infra red absorption i.e. bands arising from the parent compound appear negative and the photoproducts as positive. Monitoring sources can be normal infra red sources such as a glowbar or the high intensity CO laser which is tunable over the carbonyl vibrational region.

1.3 Photochemistry of $MeCpMn(CO)_2L$, L=CO, $L=PPh_3$

Reports on photochemical reactions involving $MeCpMn(CO)_2L$, MeCp=(η^5-$CH_3C_5H_4$), L=CO, $L=PPh_3$, are not very common. However, reactions involving the related $CpMn(CO)_3$ complex (Cp = η^5-C_5H_5) have been comprehensively studied and are reported to behave similary to $MeCpMn(CO)_3$[19,20]. Photochemical reactions of the monosubstituted phosphine complex $MeCpMn(CO)_2PPh_3$ are rarely reported[21]. As in the case of nearly all the metal carbonyl complexes the primary photoreaction is reported to be the dissociative loss of a CO ligand[22] (Reaction 1.3.1). The primary photoprocess in the photolysis of $CpMn(CO)_3$ is also thought to be loss of a CO ligand (Reaction 1.3.2). Strohmeier *et al* reported the quantum yield for this reaction to be unity[5]. It is now known that the quantum yield is ~ 0.65 which is still quite high for dissociative loss of CO and approximates that of the isoelectronic Group VIB hexacarbonyls (Φ = 0.67)[19].

$$M(CO)_x \xrightarrow{h\nu} M(CO)_{x-1} + CO \qquad (1.3.1)$$

$$CpMn(CO)_3 \xrightarrow{h\nu} CpMn(CO)_2 + CO \qquad (1.3.2)$$

Low temperature matrix isolation studies of $CpMn(CO)_3$ in argon[23,24], methane[23,24] methylcyclohexane/Nujol[25], and nitrogen[23,24] also reveal the dicarbonyl species as the primary photoproduct. The difference in the carbonyl stretching frequencies for the

different matrices and glasses is an indication of the charge on the metal nucleus For example, the υCO for the $CpMn(CO)_2$ fragment in argon matrix are 1972 and 1903cm^{-1} and the corresponding values in Nujol are 1955 and 1886cm^{-1} This is indicitive of a 'stronger' interaction with Nujol as the CO stretching frequencies in the argon matrix approach the stretching vibration for free CO (2143cm^{-1}) In the case of the nitrogen matrix a complex was formed by replacement of the lost CO ligand with dinitrogen which agreed with the band positions found in an n-heptane solution for an authentic sample of $CpMn(CO)_2N_2$[24]

Other low temperature studies on $CpMn(CO)_3$ were performed in mixed matrices A photochemical experiment carried out on $CpMn(CO)_3$ in a CO matrix revealed no observable photochemical reactions[23] However, irradiation in a ^{13}CO doped (5%) methane matrix showed that enrichment of the $CpMn(CO)_3$ complex occurs Prolonged photolysis yielded mono-, di- and tri- ^{13}CO enriched $CpMn(CO)_3$ as well as the expected coordinately unsaturated photofragments Irradiation of $CpMn(CO)_3$ in a methylcyclohexane/isopentane 4 1 glass gave $CpMn(CO)_2$ and CpMn(CO) as photoproducts[26] The addition of ethers (L) to the glass produced $CpMn(CO)_2(L)$ and $CpMn(CO)(L)_2$ A similar type experiment was performed with alcohol glasses The production of rotamers was observed because of steric constraints involved in coordination of the alcohol to the metal centre arising from matrix interaction (Figure 1.3 1)

Photosubstitution reactions of $CpMn(CO)_3$ have been well documented and can result in the nucleophilic substitution of a CO ligand[19] (Reaction 1 3 3) or oxidative addition[27] (Reaction 1 3 4) depending on the nature of the entering ligand

$$CpMn(CO)_3 + X \xrightarrow{h\nu} CpMn(CO)_2X + CO \qquad (1\,3\,3)$$

$$CpMn(CO)_3 + Y\text{-}Z \xrightarrow{h\nu} CpMn(CO)_2(Y)(Z) + CO \qquad (1\,3\,4)$$

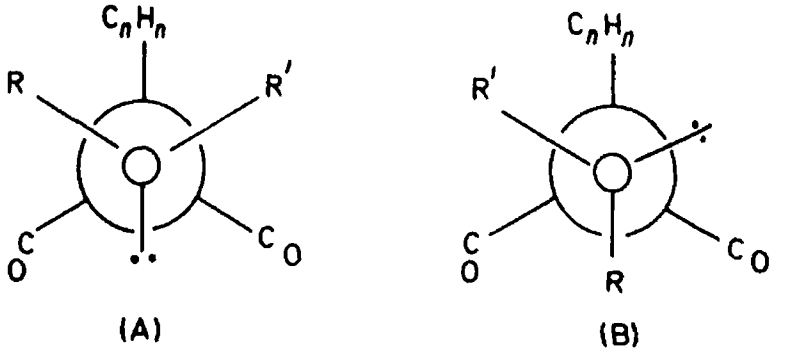

Figure 1 3.1 The rotamers produced in the photolysis of $CpMn(CO)_3$ in a methylcyclohexane/isopentane 4 1 glass at 77K ROR' = alcohol or ether, n = 5

The photochemical reactive state in $CpMn(CO)_3$ is thought to be a LF state and not a MLCT state Wrighton *et al* examined the photosubstitution behavior in $CpMn(CO)_2X$ (X = pyridine and substituted pyridine) complexes and the results showed that the only observed reaction was pyridine substitution (Reaction 1 3 3)[19] The quantum yields for these reactions were high (Φ = 0 65) An examination of the analogous rhenium complexes showed that substitution depended to a great extent on the electron accepting ability of the ligand This variation was attributed to the presence of a low lying MLCT state which could lie above or below the LF excited state depending on the nature of the ligand For the manganese complexes it was concluded that even though irradiation into the MLCT states produced photochemical substitution reactions of the pyridine ligands, the reactivity was consistent with a LF state These reactions were also independent of the nature and concentration of the entering nucleophile but dependent on the nature of the metal and the leaving ligand

The observations are characteristic of the photosubstitution reactions of d^6 metal carbonyl complexes[22]

Oxidative addition products were formed in the photolysis of (η^5-MeCp)$Mn(CO)_2L$ (L = CO, PPh_3 $P(OPh)_3$, $P(OEt)_3$, PBu_3 or PMe_3) in the presence of H_2SiPh_2 at -10°C to give the appropriate $MeCpMn(CO)(L)(H)SiPh_2H$ compounds[28] The rates of the reaction were reported to be controlled by steric rather than electronic effects The same authors also prepared similar hydrido silyl complexes containing Mn-H-Si three centred bonds[29] Reductive elimination, as in Reaction 1 3 5, can be observed when triphenyl silyl (Y) and hydrogen (Z) are replaced by addition of PPh_3 to produce $CpMn(CO)_2PPh_3$ and regenerate triphenyl silane

$$CpMn(CO)_2(Y)(Z) + L \xrightarrow{h\nu} CpMn(CO)_2L + Y\text{-}Z \qquad (1\,3\,5)$$

The cyclopentadienyl ligand is inert to substitution Photolysis of $LMn(CO)_3$ (L = η^5-C_5H_5, η^5-indenyl, η^5-fluorenyl) in the presence of PPh_3 has shown that changes in the η^5 ligand has little or no effect on the rates for carbonyl group substitution[30]

Many other photochemical reactions involving the $CpMn(CO)_2$ moiety are found in the literature Photolysis of the carbene complex $CpMn(CO)_2(CPh_2)$ in THF does not leads to any ligand substitution but to heterolytic cleavage of the Mn-carbene bond (Reaction 1 3 6)[31] The photoreactive state was a carbene centred charge transfer (CT) state In the excited CT state the complex was roughly described as containing a high spin d^5 manganese(II) and a diphenyl carbene radical anion ligand Photolysis in tetrahydrofuran (THF) provided evidence for this state as photochemical cleavage of the carbene ligand did not produce the expected $CpMn(CO)_2(THF)$ solvent adduct The carbene anion was identified by the low temperature 366nm irradiation of $CpMn(CO)_2(CPh_2)$ in a protic solvent to produce the $HCPh_2^{\bullet}$ species which was subsequently identified by electron spin resonance and emission spectroscopy

$$CpMn(CO)_2(CPh_2) \xrightarrow{h\nu} Mn(II) + CPh_2^{-\bullet} \qquad (1\,3\,6)$$

Intramolecular photochemical reactions have been observed on CO loss for ring substituted cyclopentadienyl manganese tricarbonyl complexes Examples of this type of reaction are $(C_5H_4CH_2OCH_2CHCH_2)Mn(CO)_3$[32] in which the vinyl group on the allyloxymethyl substituent coordinates to the metal centre (Figure 1 3 2 (a)) and $(Ph_2PCH_2CH_2C_5H_4)Mn(CO)_3$[33] which forms a chelate *via* the phosphine group (Figure 1 3 2 (b)) The photolysis of tetrahydrofurfurylcymantrene at 77K in Nujol produced a dicarbonyl species in which the oxygen on the tetrahydrofurfuryl was coordinated to the manganese centre to form an intramolecular chelate complex (Figure 1 3 2 (c))[34]

Several examples of dinuclear complexes formed from the photolysis of $CpMn(CO)_3$ in the presence of a bidentate ligand are known[35] There are two types of dinuclear species produced, ones containing metal-metal bonds, and ones with a bridging ligand with no metal-metal bonding The metal-metal bond complexes usually have a two electron bridging ligand e g CH_2[36] or C_8H_6[37] in which one electron is donated to each metal centre Examples of these type complexes are given in Figure 1 3 3 (a), (b) The bridging non-metal bonding complexes have ligands such as cyclopentadiene[38] or hex-2,4-diyne[39] which have two coordinating sites These dinuclear complexes are usually formed from the reaction of photochemically produced $CpMn(CO)_2S$ (S = donor solvent) with the parent complex and the bridging ligand (Figure 1 3 4 (a), (b)) Another example of a bridging ligand complex is $MeCpMn(CO)_2(\mu\text{-VP})MeCpMn(CO)_2$ where VP = 4-vinylpyridine[40] In this complex the nitrogen on the vinylpyridine ligand was σ coordinated to one of the manganese centres while the other was η^2 coordinated through the vinyl group (Figure 1 3 4 (c))

(a)

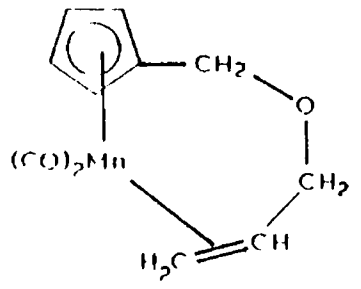

(b)

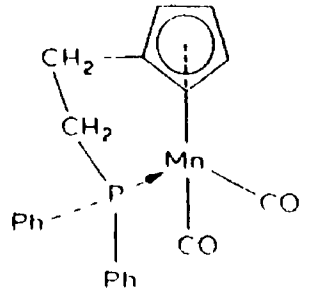

(c)

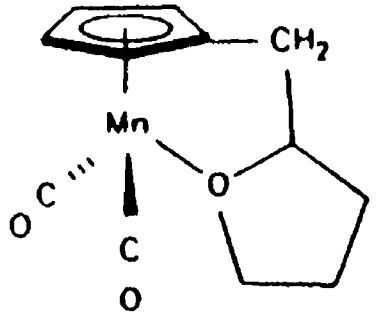

Figure 1.3.2. Examples of intramolecular coordination in $CpMn(CO)_3$ complexes

Photolysis of $MeCpMn(CO)_3$ with 4,5-dimethyl 2-phenylphosphorin yielded a dinuclear complex where a mangnese dicarbonyl moiety was σ coordinated *via* the lone pair on the phosphorus in the phosphorin ring and a second manganese was, by loss of its three carbonyl ligands, η^6 coordinated to the phosphorin ring already attached to the first manganese[41] (Figure 1 3 5)

(a)

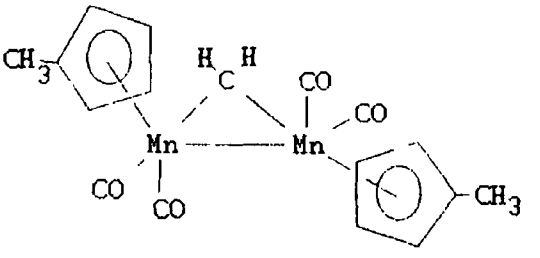

(b)

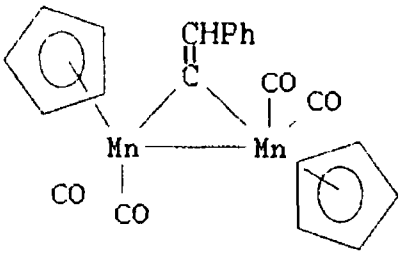

Figure 1.3.3 Dinuclear species formed from the photochemical reactions of $(\eta^5\text{-}C_5H_4R)Mn(CO)_3$ (R = H, Me) containing a Mn-Mn bond and a two electron bridging ligand

(a)

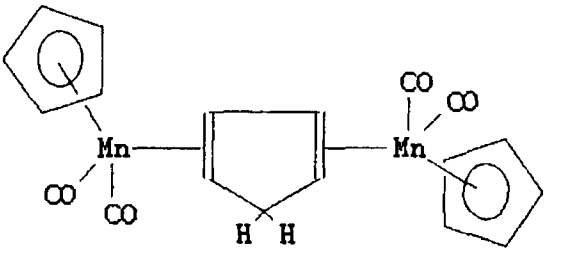

(b)

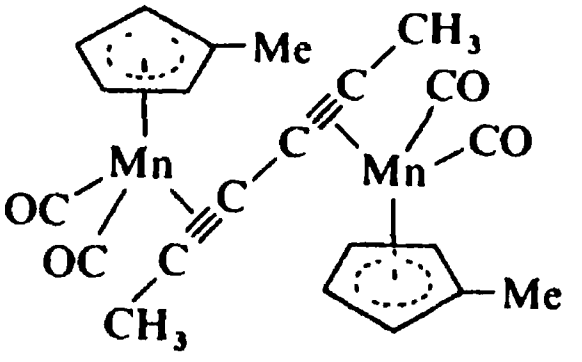

(c)

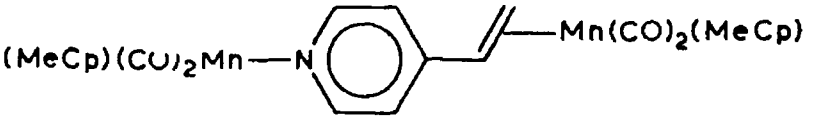

Figure 1.3.4. Dinuclear species formed from the photolysis of $(\eta^5\text{-}C_5H_4R)Mn(CO)_3$ (R = H, Me) with bidentate bridging ligands and containing no Mn-Mn bond

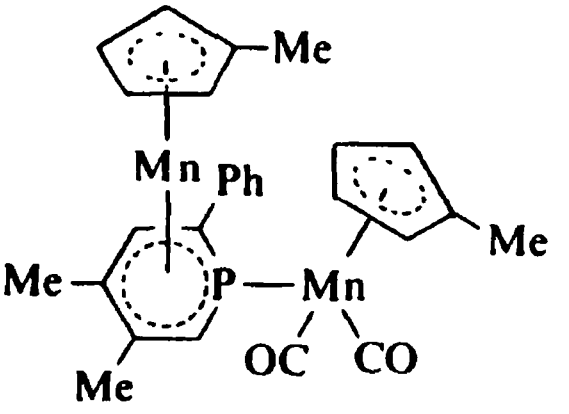

Figure 1.3.5 The unusual coordination of two manganese centres *via* a triphenyl phosphonn bridge

MeCpMn(CO)$_3$ has been observed as a photocatalyst in the cyclotrimerisation of aryl isocynates[42] Photolysis of MeCpMn(CO)$_3$ at 366nm in THF produced the solvent adduct MeCpMn(CO)$_2$(THF) Addition of isocynate to the solution produced the cyclotrimensation product phenyhsocyanurate The THF adduct was believed to be the active catalyst

1.4 Photochemistry of M(CO)$_5$L compounds (M = Cr, Mo, W).

The photochemically and thermally reactive states in M(CO)$_5$L (M = Cr, Mo, W) complexes is thought to be one and the same[43] Therefore both the thermal and photochemical reactions of these complexes will be discussed with emphasis being placed on the photochemical reactions The photochemistry of M(CO)$_5$L compounds (M = Cr, Mo, W) is complicated by the fact that three photoproducts are possible and

that the ratio of the photoproducts produced is directly dependent on the nature of the monosubstituted ligand L (Reaction 1 4 1)

$$M(CO)_5L + h\nu \begin{cases} \longrightarrow cis\text{-}M(CO)_4L + CO \\ \longrightarrow trans\text{-}M(CO)_4L + CO \\ \longrightarrow M(CO)_5 + L \end{cases} \qquad (1\,4\,1)$$

The importance of the monosubstituting ligand L is reflected in the $W(CO)_5CS$ complex where thermal substitution reactions involved CO loss and the products were in the *trans* position[44] Irradiation of this complex at 405nm produced substitution reactions of very low quantum yield ($\Phi < 0\,01$)[45] In the series where M = Cr[46], Mo[46], W[47] and L = pyridine or substituted pyridine, substitution of the pyridine ligand occurs with high quantum yields ($\Phi = 0\,6$) And in the case where M = Mo[48], W[45] and L = PPh_3, the major reaction was the loss of a CO ligand *cis* to L with the production of a significant amount of *trans* product usually in the expected statistical ratio It is obvious that the π-accepting/donating ability of the ligand L is affecting the substitution reactions. This ability is also important in determining which isomers of the pentacoordinated photofragments are the most stable. The position of the electronic excited states determines the photoreactivity of these compounds and these are ultimately controlled by the ligand

Matrix isolation studies of complexes of the type $M(CO)_5L$ coupled with infra red detection has provided valuble information in the identification of the photofragments produced on photolysis The photochemical behaviour of $Cr(CO)_5L$ (L = PMe_3[49], PCl_3[50]) was examined in an argon matrix at 12K49 CO loss was observed for L = PMe_3 and unique ligand loss for L = PCl_3 These results were explained by the existence of two photoactive states. The position of these states was dependent on the ability of the ligand L to undergo π backbonding with the metal centre. Studies of

$Cr(CO)_5$(pyridine) in argon matrix at 10K have been carried out with the dominant photoreaction being loss of the pyridine ligand at irradiation wavelengths greater than 334nm and loss of CO at wavelengths less than 313nm[50,51]

Irradiation of $W(CO)_5$(alkene) at 77K in methylcyclohexane produced evidence that twice the amount of alkene was lost on 313nm excitation than on irradiation at 254nm[52]. Longer wavelength excitation favours alkene loss by virtue of the fact that alkenes are weaker field ligands than CO and therefore the lowest excited state has more d_{z^2} character The wavelength dependency was consistent with reactivity from different one-electron excited states, the lower one having more d_{z^2} character and the upper one having more $d_{x^2-y^2}$ character even though there is little difference in the alkene and CO bonding (σ donor, π acceptor) Photolysis (436nm) of $Cr(CO)_5$(pyrazine) in an argon matrix at 10K gave one product, $Cr(CO)_5$, which was identified by infra red spectroscopy[51] Irradiation at 229nm also afforded one product However, this product was the *cis* form of $Cr(CO)_4$(pyrazine) The difference in product formation at the two wavelengths was attributed to the different energies of the σ antibonding d_{z^2} and $d_{x^2-y^2}$ orbitals Short wavelength irradiation would preferentially result in the occupation of the $d_{x^2-y^2}$ antibonding orbital causing loss of a CO ligand to form *cis*-$Cr(CO)_4$(pyrazine) On the other hand photolysis at longer wavelengths results in the population of the antibonding d_{z^2} orbital and the result is to labilize the pyrazine ligand

Thermal substitution may occur *via* one or several competing pathways[53] The first and the most common mechanism was dissociation of a CO or other ligand as the rate determining step Other mechanisms included associative processes, ligand migration to an adjacent CO and radical abstraction The general rate term for thermal reactions in metal carbonyl complexes is,

$$\frac{-d[R]}{dt} = [R](k_1 + k_2[L])$$

where [R] is the concentration of the thermally generated reactive species The rate law indicates both associative and dissociative processes The term k_2, first order in R and in entering ligand L, was often of negligible importance and therefore indicating the dominance of dissociative substitution reactions The magnitude of k_2 was determined by the basicity of ligand L, the covalent radius of the metal atom in the complexes and obviously the concentration of L Similar two term rate laws have been observed for photochemical systems[54,55]

Two further questions arise from the dissociation process with respect to $M(CO)_5L$ (M = Cr, Mo, W) complexes, (a) what are the influences of the other ligands in the complex on the dissociation rate and (b) what is the effect of the departing ligand on those which remain. The substitution of a CO ligand by PPh_3 in $Cr(CO)_6$ increased the lability of the *cis* CO groups by a factor of 300[53] Similar rate changes were seen in $Mo(CO)_5PPh_3$[56] and in *cis* -$Mo(CO)_4(PPh_3)$(piperidine)[57] This indicates that *cis* labilisation is not confined to CO loss In addition the extent of the *cis* labilisation appears to be influenced by the degree of the π bonding between the metal and the CO *trans* to a weaker π accepting ligand The presence of a strong electron releasing ligand produces the greatest labilisation of *trans* ligands Ligands which are weaker π acceptors than CO labilise preferentially in the *cis* position This is a generalisation as there is difficulty in separating the steric and electronic ground state effects and their importance in ligand substitution reactions

Crystal structure data on the $Cr(CO)_5L$ (L = phosphine) complexes indicate that the shortest Cr-P bond is found for the strongest π accepting ligand ($P(OPh)_3$[58] < $P(CH_2CH_2CN)_3$[59] < PPh_3[58]) A similar series was noted for $Mo(CO)_5L$ complexes[60] Therefore the bond distances in the complexes may reflect an energy minimum

composed of the maximum orbital overlap with minimum steric hindrance of the ligand

cis -trans/ trans -cis isomerisation of the reaction intermediates in thermal and photochemical reactions of $M(CO)_5PPh_3$ has been noted in many cases[60] The five coordinate intermediates are normally fluxional on the timescale of their expected lifetime Therefore the site of CO loss is not necessarily the position where the substituting ligand enters Darensbourg and Murphy[48] reported that in the photolysis of $Mo(CO)_5PPh_3$ with ^{13}CO the $Mo(CO)_4PPh_3$ intermediate could undergo rearrangment from the higher energy C_{4v} isomer, with the PPh_3 in the axial position, to the more stable C_s configuration In the photolysis of $Mo(CO)_5$(amine) with ^{13}CO the reaction yields exclusively the *cis*-$Mo(CO)_4(^{13}CO)$(amine) species[61] The explanation forwarded was that the rate constant for the rearrangement process to the more favourable C_s isomer in the amine complexes must be greater than the rate constant for the photochemical substitution reaction Therefore the rate constant for rearrangment in the triphenylphosphine complex must be of the same order of magnitude as the reaction rates of the photochemically produced C_{4v} isomers and so ligand scrambling can occur Other evidence points to steric crowding as an influence on the reaction intermediate *cis*-$Mo(CO)_4P(OMe)_3$(piperidine) reacts with $P(OMe)_3$ to form mainly *trans*-$Mo(CO)_4(P(OMe)_3)_2$[62] This is in contrast to its reaction with ^{13}CO where the only product is *cis*-$Mo(CO)_4(^{13}CO)P(OMe)_3$[62]

The relative size of the phosphorus ligands are known to affect the reactivities of the transition metals to which they are attached To quantify this reactivity Tolman introduced the concept of the cone angle θ[63] It is defined as the apex angle of a right cylindrical cone centred 2 28Å from the centre of a phosphorus atom that just touches the van der Waals radii of the outermost atoms Mosbo *et al* conducted a study on the relative size of the phosphorus ligands on the reaction of $W(CO)_5$(L)(pyridine) (L

= phosphines) with various phosphines[64] The distribution of the *cis* and *trans* products were measured by ^{31}P NMR and the ratios were found to decrease as the cone angle of the ligand increased Furthermore, observations in the synthesis of the $W(CO)_5(L)$(pyridine) complex from $W(CO)_4(pyridine)_2$ and the desired phosphine ligand demonstrated that large phosphine ligands (i.e ones with large cone angles) facilitated the loss of the second pyridine ligand This was in contrast to the smaller phosphines which produced predominately the monopyridine product indicating that the larger ligands accelerated loss of the *cis* ligand upon initial coordination displacing one of the pyridines

Darensbourg examined the substitution of L from *cis*-$Mo(CO)_4L_2$ by CO (L = Phosphine)[65] *cis*-$Mo(CO)_4L_2$ reacted with ^{13}CO to form specifically the *cis* ^{13}CO derivative The rate of dissociation was enhanced by the size of the phosphorus ligand and therefore with Tolman cone angle In $Mo(CO)_5L$ complexes CO loss was found to occur preferentially from equatorial sites and increased in the order $PPh_3 > P\,n\text{-}Bu_3 > P(OCH_2)CC_2H_5$ [65a] Experiments in the substitution of *trans*-$Mo(CO)_4L_2$ with ^{13}CO produced *cis* ^{13}CO labelled product indicating fluxionality with respect to the loss of a ligand *trans* to the remaining ligand[65] This indicated that the rate of *cis* - *trans* isomerisation was slower than the dissociative loss of PPh_3 from *cis*-$Mo(CO)_4(PPh_3)_2$ Smaller phosphorus ligands, e.g $P(n\text{-}Bu)_3$, PEt_3, underwent isomerisation by non-bond breaking processes which implied that the barrier to rotation with smaller ligands was less than Mo-P bond cleavage[66]

The metal centre is not necessarily the site for attack in metal carbonyl complexes as Basolo *et al.* reported on the mechanism for the CO substitution of $Mo(CO)_5PPh_3$ with L in the presence of $(CH_3)_3NO$[67] The reaction was believed to take place by the rate determining attack of $(CH_3)_3NO$ on a CO atom *cis* to the phosphorus ligand in the complex This was followed by rapid loss of CO_2 and the

uptake of PPh_3 present in the solution to form *cis*-$Mo(CO)_4(PPh_3)_2$ exclusively The sole production of the *cis* product was explained by the tighter bonding of the CO *trans* to the unique ligand in the pentacarbonyl species because the ligand was not a good π acceptor relative to CO This greater electron density on the *trans* CO, with respect to the *cis* CO ligands, made it less suceptible to nucleophilic attack by $(CH_3)_3NO$ The oxygen atom transfer takes place because the carbon atoms of CO have a partial positive charge while the oxygen atom of $(CH_3)_3NO$ has a partial negative charge The different reactivities of the Group VIB metal centres to the $(CH_3)_3NO$ has been attributed to the σ donor capacities of CO in the complexes to the metal centre (W > Mo > Cr) and to the metal size (Cr < Mo ~ W) This indicates that there was a correlation between π backbonding in the metal complexes and the reactivity of the carbon atom on CO to nucleophiles

Irradiation into the LF band is believed to produce the photochemistry observed with these complexes i e ligand loss[22] The MLCT band is reported as being unreactive with any photochemistry associated with MLCT irradiation arising from intersystem crossing to the reactive LF state Therefore the depopulation of the $d\pi$ orbitals involved in the backbonding to a ligand orbital does not appear to cause sufficient destabilization to cause M-CO dissociation LF excitation would result in the population of a σ^* level (either d_{z^2} or $d_{x^2-y^2}$ in origin) which would be expected to labilise a σ donating ligand In addition, the promoted electron would also have been involved in the backdonation of electron density from the metal into the ligand orbitals and so affect the metal-ligand π bonding Therefore any ligand involved in the σ and π bonding would be expected to be labilised upon excitation into the LF band This in effect means that CO loss and unique ligand loss would be expected in the irradiation of $M(CO)_5PPh_3$ (M = Cr, Mo, W) complexes A point to note is that irradiation into the MLCT band of $W(CO)_4$(1,10 phenanthroline) in the presence of PEt_3 produces photochemistry *via* an associative mechanism[68] This means in effect that the

depopulation of the weakly backbonding orbitals producing a partially oxidised metal centre provides a route for an associative mechanism This may explain in part why the rate laws in the photosubstitution of metal carbonyl complexes have two competing terms, one dissociative and one associative (*vide supra*)

The ligand photosubstitution reactions in THF solutions of $Mo(CO)_5PPh_3$ at 366nm in the presence of PPh_3 and ^{13}CO have shown that both *cis* and *trans* products were observed[48] The yield of the *cis* product was much higher than the corresponding *trans* analogue in the reactions with both ligands In the reaction with ^{13}CO a small quantity of ^{13}CO enriched $Mo(CO)_6$ was produced indicating loss of the unique ligand *trans*-$Mo(CO)_4(PPh_3)_2$ photoisomerised to the *cis* form by loss of PPh_3, rearrangment to the C_s form and recapture of PPh_3 Thermal rearrangment back to the *trans* isomer was possible at elevated temperatures where the more energetic form of the intermediate (C_{4v}) predominates Therefore the loss of a *trans* ligand was thermodynamically less favourable at ambient temperature with rearrangment of the intermediate to the less energic C_s form

The excitation wavelength is also important in ligand labilisation In many cases wavelength dependent substitution of $M(CO)_5L$, (M = Mo, L = PPh_3[61], M = W, L = pyridine[69], L = alkene[52]) complexes has been observed In $Mo(CO)_5PPh_3$ the reaction displays a significant decline in quantum efficiency on irradiation at shorter wavelengths The reason proposed was that longer wavelength irradiation promotes an electron preferentially into a d_{z^2} antibonding orbital and therefore labilising ligands along the z axis as opposed to shorter wavelength irradiation which could populate both the antibonding σ^* orbitals and labilise on all axes In the $W(CO)_5$(pyridine) case, irradiation across the region of LF singlet absorption produces an increase in quantum yield as the excitation wavelength decreases. Irradiation into the LF triplet region produces quantum yields smaller relative to the LF singlet region. This was

explained in terms of more efficient substitution on irradiation into the lower electronic state ^1E rather than the upper state ^1A (^1E and ^1A are components of C_{4v} symmetry) ^1E irradiation gives a excited state relaxation pathway which releases a pyridine ligand, ^1A excitation leads to a relaxation pathway which exposes a CO ligand not a pyridine ligand

Wavelength dependence was also observed for the photochemical substitution of $W(CO)_5L$ L = pyridine, piperidine) with 1-hexene[70] This dependency was attributed to solvent effects as the quantum yields varied from solvent to solvent In the piperidine and pyridine complexes, irradiation at 436nm populates the ^1E excited state directly. This was thought to be the reactive state as excitation at this wavelength produces higher yields However the yields were less than unity and it was assumed that competition between intersystem crossing to the ^3E (488nm) state and radiationless decay were responsible The quantum yields varied from 0 68 in CCl_4 to 0 41 in CH_2Cl_2 This was accounted for by collisions with the solvent molecules The CCl_4 molecule is considerably larger than the corresponding CH_2Cl_2 molecule. It was suggested that collisions with CCl_4 leads to inefficient energy transfer which prolongs the excited state and allows for greater internal conversion between the ^1A and the ^1E states and greater intersystem crossing between ^1E and ^3E states This would explain the observation that the quantum yield decreases with decreasing excitation wavelength therefore allowing an increase in intersystem crossing to the ^3E state which was less reactive

In time resolved spectroscopy the solvent interactions have been the subject of much interest Flash photolysis studies on the Group VIB metal hexacarbonyls has provided evidence that the $M(CO)_5$ photoproducts are solvated in alkane solutions within picoseconds of irradiation to form $M(CO)_5S$ (S = alkane)[71] Flash photolysis studies of $Cr(CO)_6$ in alcohol[72] and alkyl bromide[73] solvents demonstrated that the

coordinately unsaturated photofragment, generated in the flash reacts with the solvent molecule either at the alkane end or the functional end (i e -OH or Br) The alkane intermediate then rearranges to a more stable complex coordinating either to the oxygen of the hydroxyl group or to the bromide atom depending on the solvent used Similar observations were for noted for picosecond studies carried out in tetrahydrofuran solvent[74] In alkane nitrile solvents the photofragment coordinates preferentially at the cyano end of the solvent molecule[73] The reaction dynamics were faster in nitrile solvent than in the corresponding alcohol series This was accounted for by the preferential coordination of the pentacarbonyl photofragment to the dipolar end of the nitrile solvent molecule Photolysis in benzene solution produces a $Cr(CO)_5(\eta^2$-benzene) complex where the benzene was coordinated to Cr *via* an 'isolated' carbon double bond[75] The strength of the solvent interaction with the photo-generated metal pentacarbonyl fragment appears in the order perfluoroalkane < alkane < arene < alcohol < nitrile. Two mechanisms were proposed for the displacement of the solvent molecule by ligands from the metal/solvent complex[54]. The first process involved an interchange between the solvent and the incoming ligand (path A) The second involved dissociation of the solvent molecule from the photogenerated metal complex followed by a reaction with the ligand (path B)

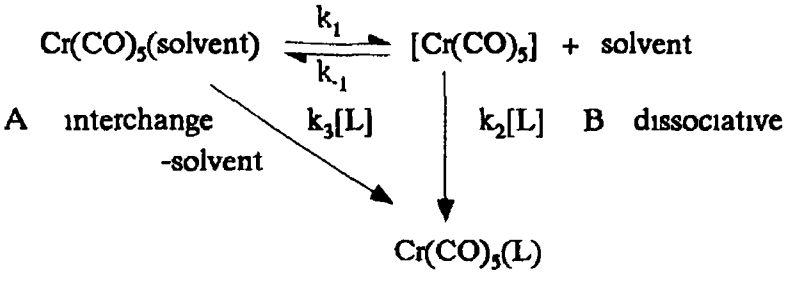

The contribution of each mechanism to the overall reaction was influenced by the type of solvent and the size of the metal atom An interchange mechanism was proposed for the solvent displacement of n-heptane and a dissociative mechanism for arenes based

on the observed volumes of activation The contribution of the solvent interchange process was found to increase in the order Cr < Mo ~ W

Flash photolysis of the $M(CO)_5L$ (L = ligand) complexes has been investigated but only in modified experiments where one of the CO ligands was replaced by a nitrogen based ligand which would be labilized preferentially to a CO and so reduce the number of primary photoproducts Dobson *et al* carried out pulsed laser time resolved studies on $Mo(CO)_4(NP)$ (NP = 1-(diethylamino)-2-(diphenylphosphino)ethane)[55] The reaction proceeds by cleavage of the Mo-N bond to form a solvated complex where the vacant coordination sites were *cis* and *trans* to the coordinated phosphorus The formation of a *trans* species from the parent complex was indicative of a ligand scrambling process This process is thought occur prior to solvation, which when measured for other carbonyl complexes e.g $Cr(CO)_5$, using picosecond spectroscopy occurred in under 1ps[71] In other words, the excited state species, following loss of a carbonyl ligand, decayed by a ligand randomization process to form two square pyramidial species, one with the phosphorus ligand in the axial site and one with the ligand in an equatorial site, at a rate faster than the solvation process. The reactivities of the *cis* and *trans* solvated complexes were different by a factor of 100 The effect of the phosphorus atom on the *trans* site would be more stabilising on the solvent-metal interaction because of the electron releasing nature of the phosphorus atom Similar type experiments were also carried out by Dobson *et al.* on *cis*-$W(CO)_4(L)(L')$, where L = PPh_3 and L' = piperidine, using both time resolved UV/visible[76] and infra red detection[77] He observed loss of the piperidine ligand to form [*cis* -$W(CO)_4L$] which reacted with chlorobenzene to form the solvated intermediate *cis*-$W(CO)_4L$(chlorobenzene). This subsequently reacted with L" (L" = phosphines) to form the *cis* -$W(CO)_4LL"$ complex which may undergo thermal isomerisation to the *trans* product

The investigation of the lower metal to ligand charge transfer state of $W(CO)_5$(4-cyanopyridine) was carried out using time resolved infra red spectroscopy[78] Visible irradiation of the complex resulted in a shift to higher frequency for the CO stretching vibrations indicating that an electron was lost from the metal centre This excited state decays to the ground state *via* an LF state and fragments into $W(CO)_5$ and 4-cyanopyridine

1.5 Summary

Both the manganese and the Group VIB complexes are very photoreactive and the dominant photoreaction appears to be the loss of a CO ligand The π accepting/donating effect of the unique ligand in the pentacarbonyl compounds affects the extent of the CO loss The cyclopentadienyl ring is substitutionally inert in the manganese carbonyl complexes Ligand loss in both types of compounds is thought to occur *via* the LF state by promotion of an electron from the t_{2g} orbitals to the antibonding e_g orbitals In the Group VIB complexes these e_g orbitals are split and this splitting is believed to account for the wavelength dependency observed in their photochemical reactions The lowest energy MLCT states appear to be unreactive but evidence exists that implicates these states as accounting, in part, for the associative term in the two term rate law noted in the photochemical reactions of the Group VIB systems, particulary the larger metal complexes

REFERENCES

1 Parshall, G , W , *Homogeneous Catalysis*, Wiley-Interscience, New York, 1980

2 Nakamura, A , Tsutsiu, M ; *Homogeneous Catalysis*, Wiley-Interscience, New York, 1980

3 Forster, D , *J Am Chem. Soc*, 1976, 98, 846

4 (a) Platbrood, G , Wilputte-Steinert, L , *J Mol. Catal*, 1976, 1, 263 (b) Farona, M F , *Organomet React Syth*, 1977, 6, 246

5 Strohmeier, W , *Agnew Chem Internat Ed*, 1964, 3(11), 730

6 Pimentel, G , C , Whittle, E , Dows, D A , *J Phys. Chem*, 1954, 22, 1943

7 Fournier, J , Mohammed, H H , Deson, J ; Malliard, D , *Chem Phys*, 1982, 70 ,39

8 Burdett, J K , Downs, A J , Gaskill, G P , Graham, M A., Turner, J. J , Turner, R F , *Inorg Chem*, 1978, 17, 532

9 Poliakoff, M , Turner, J J , *J Chem Soc , Dalton Trans*, 1974, 2276.

10 Perutz, R N , Turner, J J , *J Am Chem Soc*, 1975, 97, 4791

11 Fairhurst, S A , Morton, J R , Perutz, R N , Preston, K F , *Organometallics*, 1984, 3, 1389

12 Burdett, J K , *Coord Chem Rev*, 1978, 27, 1

13 Poliakoff, M , Weitz, E , *Adv Organomet Chem*, 1986, 25, 277

14 Perutz, R N , *Annu Rep Prog Chem , Sect. C*, 1985, 157

15 Abbate, A D , Moore, C B , *J Phys Chem*, 1985, 82, 1255

16 Norrish, R G W , Porter, G , *Nature*, 1950, 164, 685

17 Nasielski, J ,Kirsch, P , Wilputte-Steinert, L , *J Organomet Chem*, 1971, 29, 269

18 Purcell, K F , Kotz, J C , *Inorganic Chemistry*, Saunders and Co , Philidelphia, 1977

19 Giordano, P ; Wrighton, M. S., *Inorg Chem*, 1977, 16(1), 160

20 Wrighton, M S, *Chem Rev*, 1974, 74(4), 401

21 Teixeira, G, Avilés, T, Dias, A R, Pina, F, *J Organomet Chem*, 1988, **353**, 83

22 Geoffroy,G L, Wrighton, M S, *Organometallic Photochemistry* Academic Press, New York, 1979

23 Herberhold, M,Kremnitz, W, Trampsich, H, Hitam, R B, Rest, A J; Taylor, D J, *J. Chem Soc., Dalton Trans*, 1982, 1261

24 Rest, A J, Sodeau, J R; Taylor, D J, *J Chem Soc, Dalton Trans*, 1978, 651

25 Black, J D, Braterman, P S, *J Organomet Chem*, 1972, **39**, C3

26 Black, J D, Boylan, M J, Braterman, P S, *J Chem Soc, Dalton Trans*, 1981, 673

27 Graham, W A G, Hart-Davis, A J, *J Am Chem Soc*, 1971, **94**, 4388

28 Schubert, U., Kraft, G, Kalbas, C, *Transition Met. Chem*, 1984, **9**, 161

29 Kraft, G, Kalbas, C, Schubert, U, *J Organomet Chem*, 1985, **289**, 247

30 Zhdanovich, V I, Ezernitskaya, M G, *Ivz Akad. Nauk. SSSR, Ser Khim*, 1981, 685

31 Wright, R E; Vogler, A, *J. Organomet Chem*, 1978, **160**, 197

32 Rybinskaya, M. I, Korneva, L M, *J Organomet Chem*, 1982, **231**, 25

33 Charner, C, Mathey, F, *J Organomet Chem*, 1979, **170**, C41

34 Bitterwolf, T. E, Lott, K A, Rest, A J, *J Organomet Chem*, 1991, **408**, 137

35 Caulton, K G, *Coord Chem Rev* 1981, **38**, 1

36 Creswick, M, Bernal, I, Herrmann, W, *J Organomet Chem*, 1979, **172**, C39

37 Nesmeyanov,A N, Aleksandrov, G G, Antonova, A B, Anismov, K N; Kolobova, N E, Struuchkov, Y T, *J Organomet Chem*, 1976, **110**, C36

38 Bathelt, W, Herberhold, M, Fischer, E O, *J Organomet Chem*, 1970, **21**, 395

39 Cash, G G , Pettersen, R C , *J Chem. Soc , Dalton Trans*, 1979, 1630

40 Kelly, J M , Long, C , *J Organomet Chem*, 1982, 231, C9

41 Neıf, F , Charner, C , Mathey, F , Sımalty, M ; *J. Organomet Chem*, 1980, 187, 277

42 Martellı, E , Pelızzı, C , Predıerı, G , *J Mol Catal*, 1983, 22, 89

43 Dobson, G R., Asalı, K J , Basson, S S , Dobson, C. B , *Polyhedron*, 1987, 6, 337

44 Dombek, B D , Angelıcı, R J ; *J Am Chem Soc*, 1976, 98, 4110

45 Dahlgren, R M , Zınk, J I , *Inorg Chem*, 1977, 16, 3154

46 Kolodzıej, R M , Lees, A J , *Organometallics*, 1986, 5, 450.

47 Wrighton, M S , Abrahamson, H B , Morse, D L , *J. Am Chem Soc*, 1976, 98, 4105

48 Darensbourg, D J , Murphy, M A , *J. Am Chem. Soc*, 1978, 100, 463

49 Boxhoorn, G , Shoemaker,G C.; Stufkens, D J , Oskam, A , *Inorg Chım Acta*, 1981, 42, 241

50 Oskam, A ,Boxhoorn, G , *Inorg Chım Acta*, 1978, 29, L207

51 Boxhoorn, G , Stufkens, D J , Oskam, A , *Inorg Chım. Acta*, 1979, 33, 215.

52 Pope, K R , Wrighton, M S , *Inorg, Chem*, 1985, 24, 2792

53 Atwood J D , Brown, T L , *J. Am. Chem Soc*, 1976, 98, 3160

54 Zhang, S , Zang, V , Bajaj, H C ; Dobson, G R , van Eldık, R ; *J Organomet. Chem*, 1990, 397, 279

55 Dobson, G R , Bernal, I , Reısner, G M , Dobson, C B , Mansour, S E ; *J Am. Chem Soc*, 1985, 107, 525

56 Covey, W ; Brown, T L , *Inorg, Chem*, 1973, 12, 2820

57 Darensbourg, D J , Hyde, C , *Inorg, Chem*, 1973, 12, 1286

58 Plastas, H J , Stewart, M J ; Grım, S O , *Inorg Chem*, 1973, 12, 265

59 Cotton, F A ; Darensbourg, D. J ; Ilsley, W. H., *Inorg. Chem*, 1981, 20, 578

60 Howell, J A S , Burkınshaw, P M , *Chem Rev*, 1983, **83**, 557

61 Darensbourg, D J , Murphy, M A , *Inorg Chem*, 1978, 17,884

62 (a) Darensbourg, D J , *Inorg Chem*, 1979, 18,2821 (b) Darensbourg, D J ; Dobson, G R , Moradı-Araghı, A , *J Organomet Chem*, 1976, **116**, C17

63 Tolman, A C , *J Am Chem Soc*, 1970, **92**, 2956

64 Boyles, M L ; Brown, D V , Drake, D A , Hostetler, C K , Maves, C K , Mosbo, J A , *Inorg. Chem*, 1985, **24**, 3126

65 (a) Darensbourg, D J , Graves, A H , *Inorg Chem*, 1979, 18, 1257 (b) Darensbourg, D J , Kudaroskı, R , Schenk, W , *Inorg Chem*, 1982, **21**, 2488

66 Darensbourg, D J ; Kump, R L , *Inorg Chem*, 1978, 17, 2680

67 Gao,Y C , Shı, Q Z , Kershner, D L , Basolo, F , *Inorg Chem*, 1988, **27**, 188

68 Wıeland, S ; van Eldık, R , *J Chem Soc Chem Commun*, 1989, 367

69 Moralejo, C ; Langford, C H , Sharma, D K , *Inorg Chem*, 1989, 28,2205

70 Moralejo, C , Langford, C H , *Inorg Chem*, 1991, **30**, 567

71 Sımon, J. D , Xıe, X , *J Phys Chem*, 1986, **90**, 6751

72 (a) Sımon, J D , Xıe, X , *J Am. Chem Soc*, 1990, **112**, 1130 (b) Sımon, J D ; Xıe, X ; *J Phys Chem*, 1989, **93**, 291 (c) Sımon, J. D , Xıe, X , *J. Phys Chem*, 1987, **91**, 5538

73 O'Dnscoll, E , Sımon, J D , *J Am. Chem Soc*, 1990, **112**, 6580

74 Wang, L , Zhu, X , Spears, K G , *J Phys Chem*, 1989, **93**, 2.

75 Zhang, S , Dobson, G R , Zang, V , Bajaj, H C , van Eldık, R , *Inorg Chem*, 1990, **29**, 3477

76 Asalı, K J , Basson, S S , Tucker, J S , Hester, B C , Cortés, J E ; Awad, H H , Dobson, G R , *J Am Chem Soc*, 1987, **109**, 5386

77 Dobson, G R , Hodges, P M , Healy, M A , Polıakoff, M , Turner, J J , Fırth. S , Asalı, K J , *J Am Chem Soc*, 1987, **109**, 4218

78 Glyn, P, Johnson, F P A; George, M W, Lees, A J, Turner, J J, *Inorg. Chem*, 1991, **30**, 3543

CHAPTER 2

355nm LASER FLASH PHOTOLYSIS OF $MeCpMn(CO)_3$ AND $MeCpMn(CO)_2PPh_3$ WITH UV/VISIBLE MONITORING

2.0 Laser flash photolysis of $MeCpMn(CO)_3$

The laser flash photolysis with UV/visible monitoring of $MeCpMn(CO)_3$ (MeCp = η^5-$C_5H_4CH_3$) in cyclohexane at 355nm produced evidence for the formation of two transient species The first transient species was identified as the the solvated $MeCpMn(CO)_2$(cyclohexane) complex from its UV/visible difference spectrum and its reaction kinetics A second transient species was observed and similarly identified as the dinuclear $MeCp_2Mn_2(CO)_5$ complex

2.1 Electronic spectrum of $MeCpMn(CO)_3$

A UV/visible spectrum of $MeCpMn(CO)_3$ in cyclohexane solution is shown in Figure 2 1 1 The low energy absorption spectrum of $MeCpMn(CO)_3$ is dominated by a band centred at 330nm This band has been assigned as a charge transfer (CT) transition, having mainly Mn --> (η^5-$C_5H_4CH_3$) CT character[1]

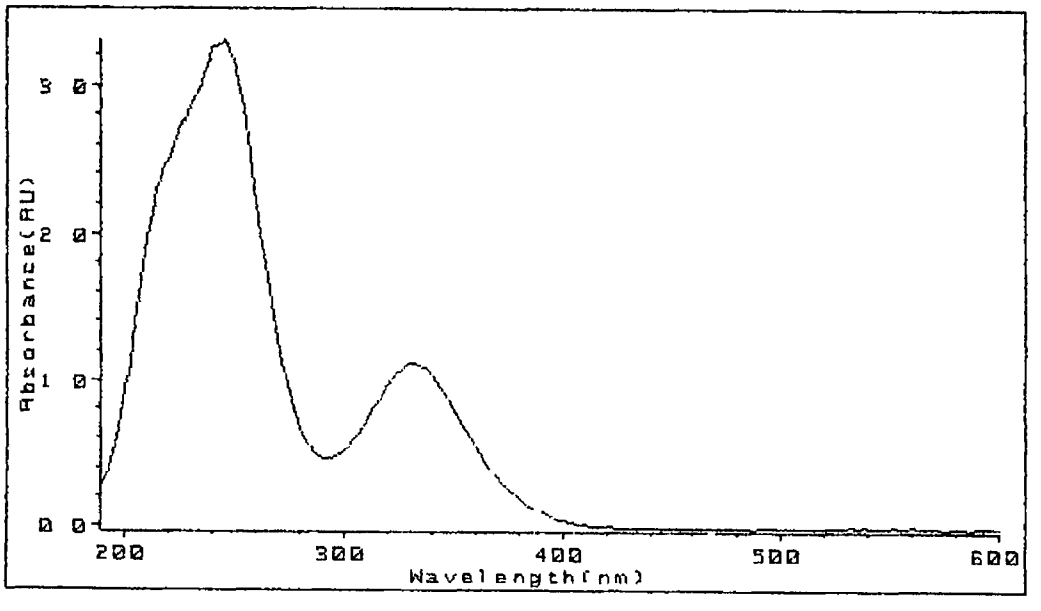

Figure 2.1 1 A UV/visible spectrum of $MeCpMn(CO)_3$ (1 08 x 10^{-3} mol dm^{-3}) in cyclohexane

This region of the spectrum is also thought to contain the LF transitions which are obscured by the more intense Mn --> (η^5-$C_5H_4CH_3$) CT transition The large absorption at ~250nm is probably a Mn --> π^*CO CT transition

2.2 Primary photoproduct: MeCpMn(CO)$_2$(cyclohexane)

Photolysis of MeCpMn(CO)$_3$ in hydrocarbon glasses at 80K is reported to undergo loss of CO as the primary photoprocess[2] The resulting photoproduct has been identified by infra red spectroscopy as the coordinately unsaturated 16e$^-$ complex MeCpMn(CO)$_2$ These highly reactive 16e$^-$ species of metal carbonyl complexes are known to coordinate weakly to the matrices and even those consisting of inert nobel gases[3] The coordinately unsaturated isoelectronic M(CO)$_5$ (M = Cr, Mo, W) complexes are now recognised as coordinating to solvent molecules in solution photolysis[4] This rate of this coordination has been measured, using picosecond spectroscopy, in alkane solvent to occur within 1ps of the flash[5] Consistent with CO loss from the M(CO)$_6$ complexes the isoelectronic manganese complex CpMn(CO)$_3$ is also known to lose a CO ligand and coordinate a solvent molecule when photolysed in solution[6] MeCpMn(CO)$_3$ has been shown to behave similarly to CpMn(CO)$_3$ in photochemical reactions[7] i e the primary photoproduct is reported to be loss of a CO ligand Therefore on the 355nm photolysis of MeCpMn(CO)$_3$ (ε = 650 dm^3 mol^{-1} cm^{-1}) the first transient species observed was MeCpMn(CO)$_2$(cyclohexane) and this species was probably formed within the duration of the flash (10ns) as in the case of the Group VIB pentacarbonyl solvated species[5] The reaction is sumarised in Equation 2 1.1

$$\text{MeCpMn(CO)}_3 \xrightarrow{h\nu} \text{MeCpMn(CO)}_2 + \text{CO} \xrightarrow{S} \text{MeCpMn(CO)}_2\text{S} \qquad (2\,2\,1)$$

S=cyclohexane

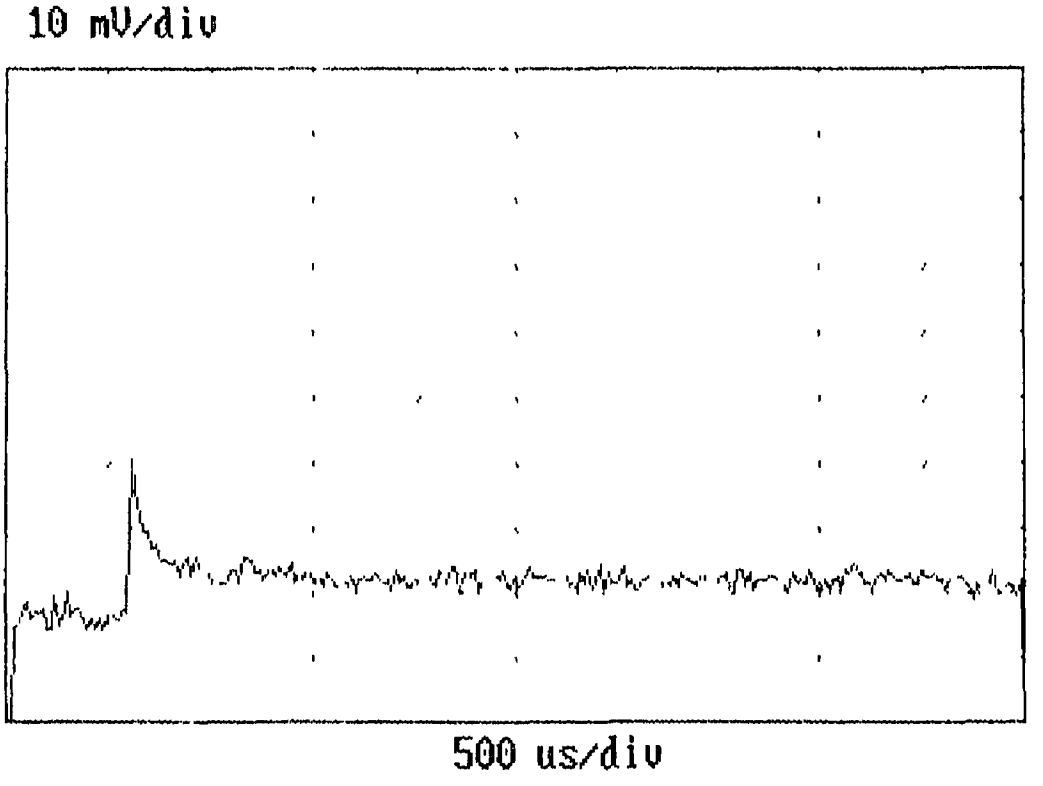

Figure 2.2.1 Transient for the decay of the $MeCpMn(CO)_2$(cyclohexane) complex at 640nm

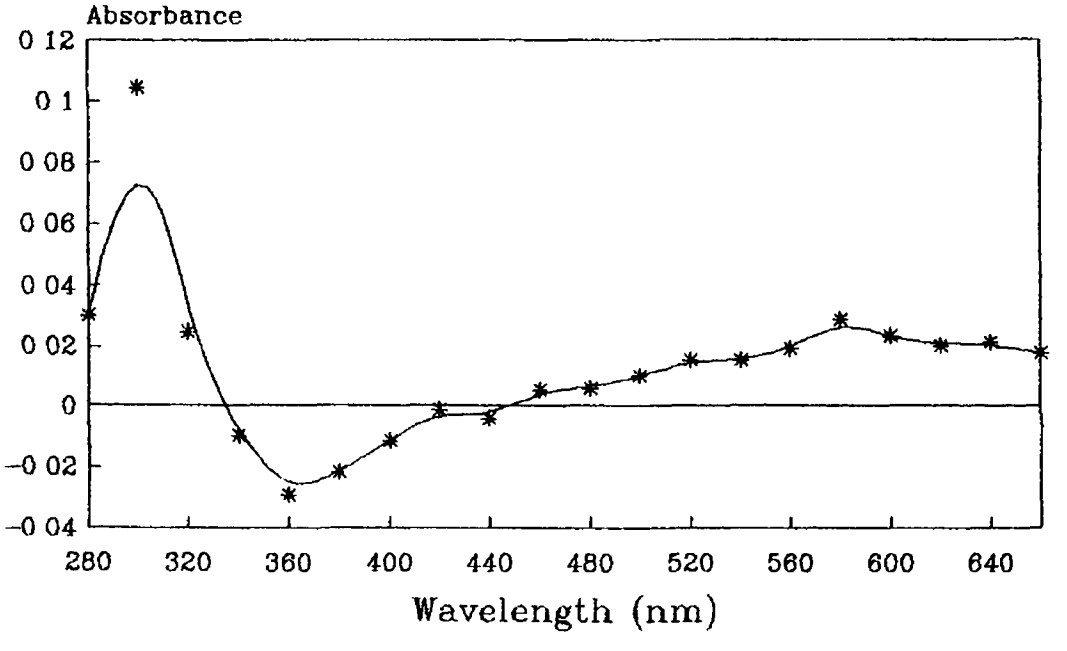

Figure 2.2.2 A UV/visible difference spectrum of $MeCpMn(CO)_2$(cyclohexane) obtained in cyclohexane solution 1 μs after the laser pulse

A typical transient obtained in the 355nm photolysis of $MeCpMn(CO)_3$ monitored at 640nm is shown in Figure 2 2 1 where the decay curve corresponds to the decay of the solvated complex $MeCpMn(CO)_2$(cyclohexane) This assignment can be supported by evidence from the 308nm TRIR (TRIR = Time Resolved Infra Red) spectroscopy studies of $CpMn(CO)_3$ in hydrocarbon solvents where the first observable species was the solvated $CpMn(CO)_2S$ (S = n-heptane[6]) complex A parallel study of $CpMn(CO)_3$ carried out in cyclohexane solution using UV/visible detection obtained a UV/visible difference spectrum of the solvated complex $CpMn(CO)_2$(cyclohexane) 5μs after the flash This spectrum consisted of a broad band with a maximum near 580nm The UV/visible difference spectrum of $MeCpMn(CO)_2$(cyclohexane) (Figure 2 2 2) has two maxima at 290nm and 580nm The broad absorption at 580nm and is similar to that obtained for $CpMn(CO)_2$(cyclohexane) The region less than 300nm was not measured in the $CpMn(CO)_3$ experiment so the strong absorption at 290nm was not observed in the spectrum obtained for $CpMn(CO)_2$(cyclohexane)[6] The valley in the UV/visible spectrum of $MeCpMn(CO)_3$ (Figure 2 1 1) corresponded to the maximum at 290nm for $MeCpMn(CO)_2$(cyclohexane) in the UV/visible difference spectrum

As with $CpMn(CO)_2S$ (S = cyclohexane[6], n-heptane[6]) the addition of CO to the solution reduced the lifetime of the solvated complex but had little effect on its overall yield However the second order rate constant for the reaction of $MeCpMn(CO)_2$(cyclohexane) with CO (Figure 2 2 3) was twice that of the corresponding rate for the unsubstituted ring complex $CpMn(CO)_2$(cyclohexane) (Table 2 2 1) In the manganese complexes, the electron donating effect of the methyl substituent on the cyclopentadienyl ring should decrease the reaction rate by forming a more stable manganese dicarbonyl complex This should increase the stability of the dicarbonyl photofragment and so decrease its reaction rate However, the opposite was observed and this suggests that steric effects are involved in the coordination of cyclohexane to the metal centre

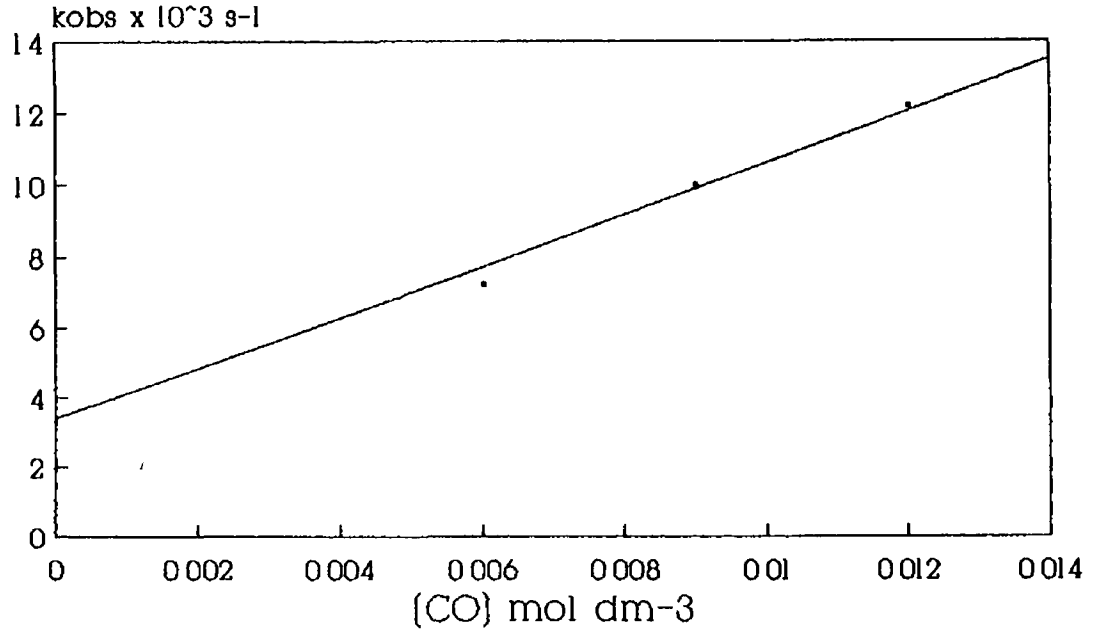

[CO] mol dm^{-3}	$k_{obs} \times 10^{-3}$ (s^{-1})
0 003	5 89
0 006	7 22
0 009	9 99
0 012	12 19

$k_{[CO]} = 7\ 21 \times 10^{5} \pm 6\ 6 \times 10^{4}\ dm^{3}\ mol^{-1}\ s^{-1}$

Intercept = $3\ 41 \times 10^{3} \pm 445\ s^{-1}$

Corr coeff = 0 991

Figure 2.2.3 A plot of concentration of CO (mol dm^{-3}) against the observed rate constant for the reaction of CO with the $MeCpMn(CO)_2$(cyclohexane) complex at 298K

$(C_5H_4R)Mn(CO)_2S$	CO	$(C_5H_4R)Mn(CO)_3$
R=H	3.4×10^{5} [a]	1.1×10^{6} [a]
R=Me	7.2×10^{5}	1.08×10^{6}

Table 2.2.1 Second order rate constants (dm^3 mol^{-1} s^{-1}) for the reaction of $(C_5H_4R)Mn(CO)_3S$ (S = cyclohexane) with CO and parent compound in cyclohexane solution [a] ref 6

This trend was also observed in the TRIR studies of pentasubstituted cyclopentadienyl manganese tricarbonyl complexes in n-heptane solution[8] The two fold increase in the second order rate observed in these experiments for the monomethylsubstituted complex in cyclohexane corresponded to a two fold increase for the pentamethylsubstituted complex in n-heptane This suggests that the orientation of the single methyl group on the cyclopentadienyl ring has a steric influence on the solvent coordination site and that this effect is independent of the number of methyl substituents Therefore this indicates that the substitution on the cyclopentadienyl ring affects the rates of reaction of these solvated intermediates and that it is more likely to be a steric effect rather than an electronic one

An interesting point to note is the difference in rate constants between experiments carried out in n-heptane and cyclohexane solutions The rates observed in n-heptane are approximately twice as fast as those observed in cyclohexane. This shows that different interaction energies are involved in the coordination of cyclohexane to the metal as chemically both solvents are the same, differing only in shape This difference has also been noted indirectly in photoacoustic calorimetry experiments of the metal-ligand bond dissociation energies of $CpMn(CO)_3$ in n-heptane[9] Using previously obtained activation parameters for the substitution

reaction of $CpMn(CO)_2$(*cis* -cyclooctene) by PPh_3 in methylcyclohexane and comparing it to data which they calculated in n-heptane they found that the activation energy for the Mn-ligand bond strength was 42 kJ mol^{-1} greater in methylcyclohexane solution than in the corresponding n-heptane solution This suggests that the higher activation energy associated with methylcyclohexane may be attributed to stronger coordination of the methylcyclohexane molecule to the metal centre and perhaps to steric effects or a different mechanism of desolvation.

The possibility exists of photochemical ring slippage as a primary photoprocess[10] However, photochemically induced ring slippage has not been observed in η^5-cyclopentadienyl coordinated manganese complexes[11] The η^3 coordinated ring slipped dianion $[\eta^3\text{-}MeCpMn(CO)_3]^{2-}$ has been synthesised and indicates that ring slippage in $MeCpMn(CO)_3$ appears to be a function of charge on the metal centre If ring slippage did occur in the photolysis of $MeCpMn(CO)_3$ this species would be expected to be stabilised under 1 0 atmosphere of CO, forming a tetracarbonyl complex No new transients were observed in photolysis experiments under CO

2.3 Secondary photoprocess: $MeCp_2Mn_2(CO)_5$

The second transient species observed in the 355nm laser flash photolysis of $MeCpMn(CO)_3$ has been attributed to the dinuclear $MeCp_2Mn_2(CO)_5$ species The UV/visible difference spectrum obtained at 1700μs for the longer lived transient decay (Figure 2 3 1) was identical to that which was observed for the $CpMn(CO)_3$ system with two maxima at 360nm and 530nm[6] The 360nm region of the spectrum is often assigned to metal σ-σ^* transitions in dinuclear species[1] and the presence of the methyl group on the cyclopentadienyl ring should not affect this transition The corresponding TRIR spectrum for the $CpMn(CO)_3$ system revealed four CO bands which were assigned to the single carbonyl bridging $Cp_2Mn_2(CO)_4(\mu\text{-}CO)$ complex

$MeCpMn(CO)_3$ has often been reported to have photochemical behaviour very similar to $CpMn(CO)_3$[7] Therefore it was unlikely that $MeCpMn(CO)_3$ formed a different dinuclear complex given the close agreement in the UV/visible difference spectra

The $MeCp_2Mn_2(CO)_5$ complex must be formed by reaction of the solvated primary photoproduct $MeCpMn(CO)_2$(cyclohexane) with unreacted parent (Reaction 2 3 2).

$$MeCpMn(CO)_2S + MeCpMn(CO)_3 \xrightarrow{-S} MeCp_2Mn_2(CO)_5 \qquad (2\,3\,2)$$

S = cyclohexane

The transient in Figure 2 3 2 shows the 'grow-in' of the dinuclear species As in experiments carried out on the $CpMn(CO)_3$ complex the rate of reaction of $MeCpMn(CO)_2$(cyclohexane) was found to increase linearly with increasing $MeCpMn(CO)_3$ concentration (Figure 2 3 3) The second order rate constant for this reaction was $1\,08 \times 10^6$ dm^3 mol^{-1} s^{-1} This was consistent with $1\,1 \times 10^6$ dm^{-3} mol^{-1} s^{-1} for $CpMn(CO)_3$ Kinetic observations in the photoreactions of various pentasubstituted cyclopentadienyl manganese compounds in n-heptane indicated that PPh_3 reacts with the solvated intermediates of these complexes at the same rate regardless of the cyclopentadienyl substitution[8] This was attributed to the steric factors in the approach of the PPh_3 ligand Similarly large steric interactions would be expected in the reaction of $MeCpMn(CO)_2S$ (S = cyclohexane) with the parent complex This would explain the close second order rate constant agreement between the reaction of the ring substituted and unsubstituted cyclopentadienyl manganese dicarbonyl solvent complexes with their respective parent complexes

The decay of the dinuclear species was dependent on the concentration of CO (Figure 2.3 4) The CO dependence indicated that the dinuclear species reacted with CO in solution to regenerate parent complex (Reaction 2 3.3)

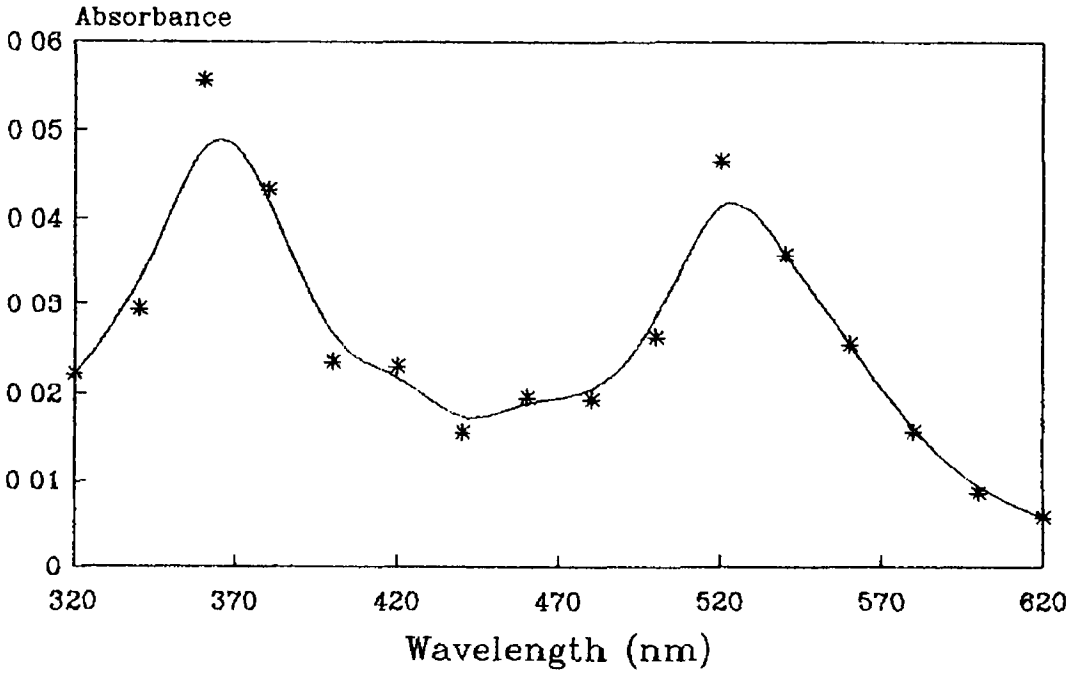

Figure 2.3.1 A UV/visible difference spectrum of $MeCp_2Mn_2(CO)_5$ in cyclohexane obtained after 1700μs

$$MeCp_2Mn_2(CO)_5 + CO \text{ --------> } 2MeCpMn(CO)_3 \quad (2\,3.3)$$

A typical transient for the decay of the dinuclear species is shown in Figure 2 3 5 The second order rate constant for this reaction was calculated as 5 733 x 10^3 dm^{-3} mol^{-1} s^{-1}. The lifetime of this species (~80ms) was longer than that observed for the $Cp_2Mn_2(CO)_5$ complex (~50ms) This extra stability is most likely from the presence of the electron donating methyl group on the cyclopentadienyl ring

Activation parameters have been calculated for the reaction of $MeCpMn(CO)_2$(cyclohexane) with parent compound (Figure 2 3 6) The value for $E_{act}^{\#}$ of 34.5 kJ mol^{-1} was very similar to the value calculated for the reaction of the $CpMn(CO)_2$(cyclohexane) species with parent complex of 32 kJ mol^{-1} In a study of the activation parameters for $CpMn(CO)_2$(cyclohexane) with various ligand types, the value for the activation energies showed no significant difference from 30 kJ mol^{-1} [13]

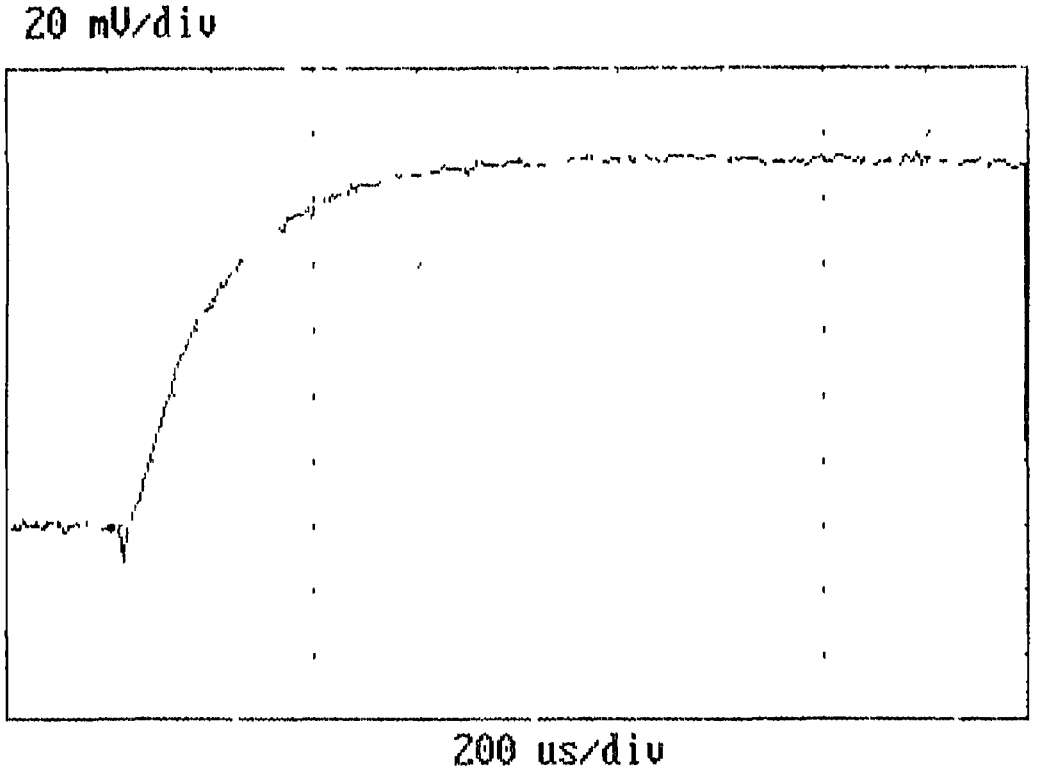

Figure 2.3.2 Grow-in of the dinuclear $MeCp_2Mn_2(CO)_5$ species at 370nm corresponding to the reaction of $MeCpMn(CO)_2$(cyclohexane) with parent complex

This value was very similar to the value reported for the low temperature oxidition of a range of R_3SiH compounds to $CpMn(CO)_3$[14] The $\Delta S^{\ddagger}$value for the reaction with parent complex was slightly negative. This indicates that the reaction was associative in nature However $\Delta S^{\ddagger}$is subject to large errors and the data were inconclusive

2.4 Infra red monitored photolysis of $MeCpMn(CO)_3$

Infra red experiments involving solution cell laser photolysis (355nm) of $MeCpMn(CO)_3$ in argon degassed cyclohexane indicate the formation of 5 new bands (Figure 2 4 1) These bands to some extent are in agreement with the υCO's obtained in TRIR experiments in n-heptane solution[6] and in low temperature matrix isolation experiments at 77K in nujol[13] (Table 2 4 1) Differences in the frequencies could be accounted for by the difference in solvent and in timescale in the recording of the spectra The dinuclear species observed in the time resolved experiments had a lifetime

of ~80ms The unknown species was observed to have a longer lifetime as its infra red spectrum was recorded ~30 seconds after 355nm photolysis with the laser The lifetime of this species indicated that it was not the $MeCp_2Mn_2(CO)_4(\mu\text{-}CO)$ complex proposed in the photolysis of $MeCpMn(CO)_3$ It was therefore another dinuclear species perhaps formed from the thermal decay of the $MeCp_2Mn_2(CO)_4(\mu\text{-}CO)$ dinuclear complex. The lower frequencies could be accounted for by the extra electron density on the metal centre because of the donating effect of the methyl group on the cyclopentadienyl ring The presence of a weak vibration at $1777cm^{-1}$ shows that this photoproduct contained a bridging carbonyl ligand with the same frequency as the $Cp_2Mn_2(CO)_5$ complex The close agreement of the bands in Table 2.4 1 indicated that this species may be a *cis* or *trans* analogue of $MeCp_2Mn_2(CO)_4(\mu\text{-}CO)$ The species observed in the time resolved experiments may have the cyclopentadienyl rings in a *cis* configuration while the species observed in the infra red experiments may be the more stable *trans* analogue

Compound	υCO terminal (cm^{-1})	υCO bridge (cm^{-1})
$Cp_2Mn_2(CO)_5$ [a]	1993, 1955, 1934, 1907	1777
$MeCp_2Mn_2(CO)_5$ [b]	1973, 1948, 1920, 1885	1762
Unknown [c]	1991, 1963, 1907, 1880	1777

Table 2.4.1 Infra red data for the υCO of the dinuclear species from the photochemical reactions of $CpMn(CO)_3$ [a] Ref 6 in n-heptane solution after 1500μs [b] Ref 13 at 77K in nujol [c] this work in cyclohexane solution

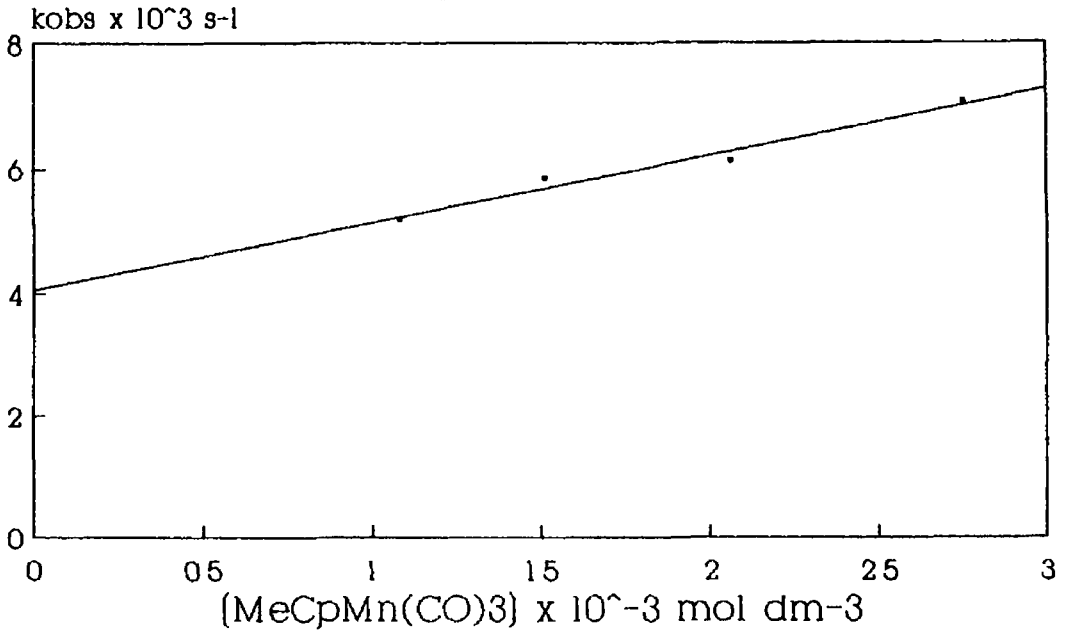

$[MeCpMn(CO)_3] \times 10^3$ mol dm^{-3}	$k_{obs} \times 10^{-3}$ (s^{-1})
1 08	5 17
1.51	5 84
2 06	6 11
2 75	7 07

$k[MeCpMn(CO)_3] = 1\ 08 \times 10^6 \pm 1\ 36 \times 10^5\ dm^3\ mol^{-1}\ s^{-1}$

Intercept = $4\ 06 \times 10^3 \pm 170\ s^{-1}$

Corr coeff. = 0 984

Figure 2.3.3 Plot of k_{obs} for the reaction of $MeCpMn(CO)_2$(cyclohexane) against the initial concentration of $MeCpMn(CO)_3$ in cyclohexane at 298K.

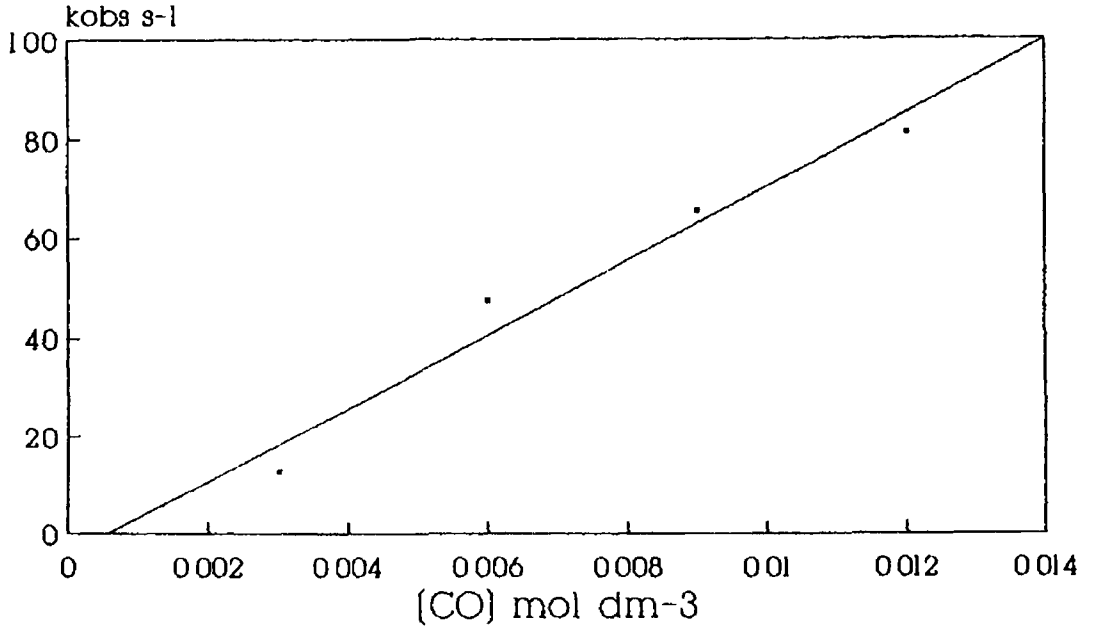

[CO] mol dm^{-3}	k_{obs} (s^{-1})
0 003	12 7
0 006	47 3
0 009	65 2
0 012	81 1

$k_{[CO]} = 5\ 733 \times 10^3 \pm 73\ 2\ dm^3\ mol^{-1}\ s^{-1}$

Intercept = 12 89 ± 0 6 s^{-1}

Corr coeff = 0 999

Figure 2 3.4 Plot of CO concentration (mol dm^{-3}) against the observed rate constant for the decay of the dinuclear $MeCp_2Mn_2(CO)_5$ complex at 298K

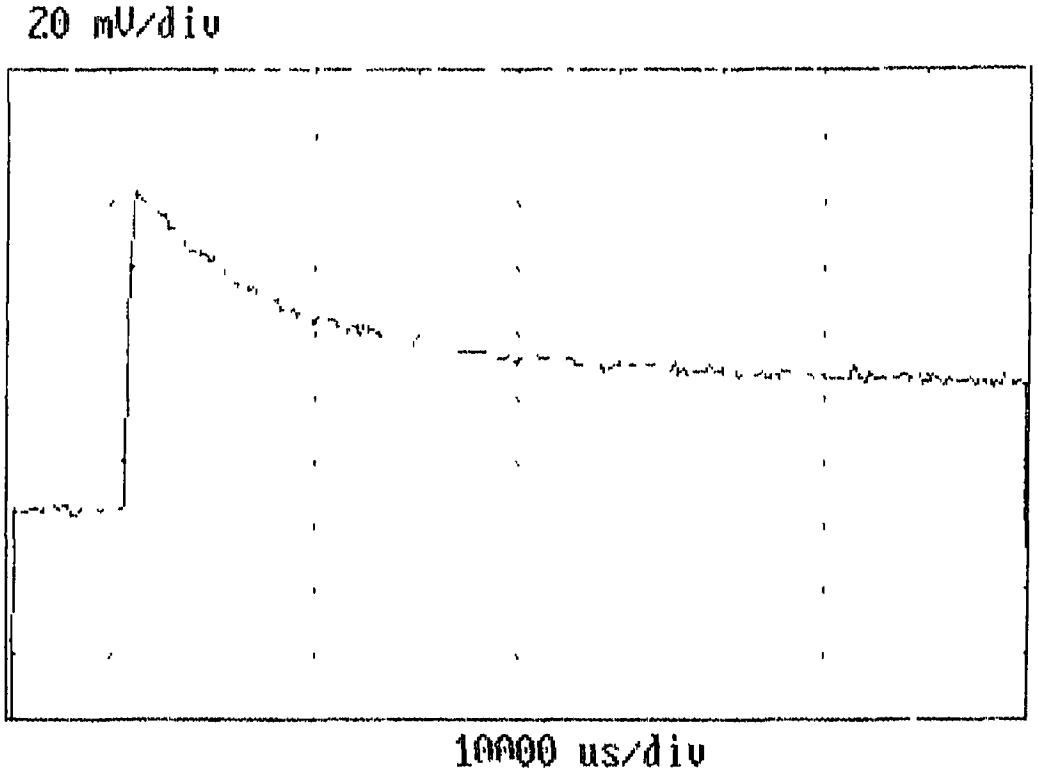

Figure 2.3.5 Transient for the decay of $MeCp_2Mn_2(CO)_5$ monitored at 370nm under 1 0 atmosphere of argon

$\frac{1}{T} \times 10^{-3}$ K^{-1}	$\ln \frac{k_{obs}}{[M]^a}$	$\ln \frac{k_{obs}}{[M]^a T}$
3 5211	8 521	9 310
3 4783	8 705	9 482
3 4423	8 888	9 654
3 3670	9 173	9 918
3 3445	9 347	10 084
3 3058	9 360	10 086
3 2573	9 637	10 348

a = [M] concentration of $MeCpMn(CO)_3$ = 1 6 x 10^{-3} mol dm^{-3}

Arrhenius plot	Eyring plot
slope = -4148 ± 207	slope = -3853 ± 207
intercept = 23 14 ± 0.7	intercept = 22 9 ± 0.704
Corr. Coeff = 0.994	Corr Coeff = 0 993

$E_{act}^{\ddagger}$ =34.5 ± 1 7 kJ mol^{-1} $\Delta H^{\ddagger}$ = 32 0 ± 1 7 kJmol^{-1} $\Delta S^{\ddagger}$ = -7 5 ± 20 J mol^{-1} K^{-1}

Table 2.3.2 Experimental data for the calculation of the energy, entalphy and entropy of activation for the formation of $MeCp_2Mn_2(CO)_5$ as determined from UV/visible flash photolysis experiments

(a)

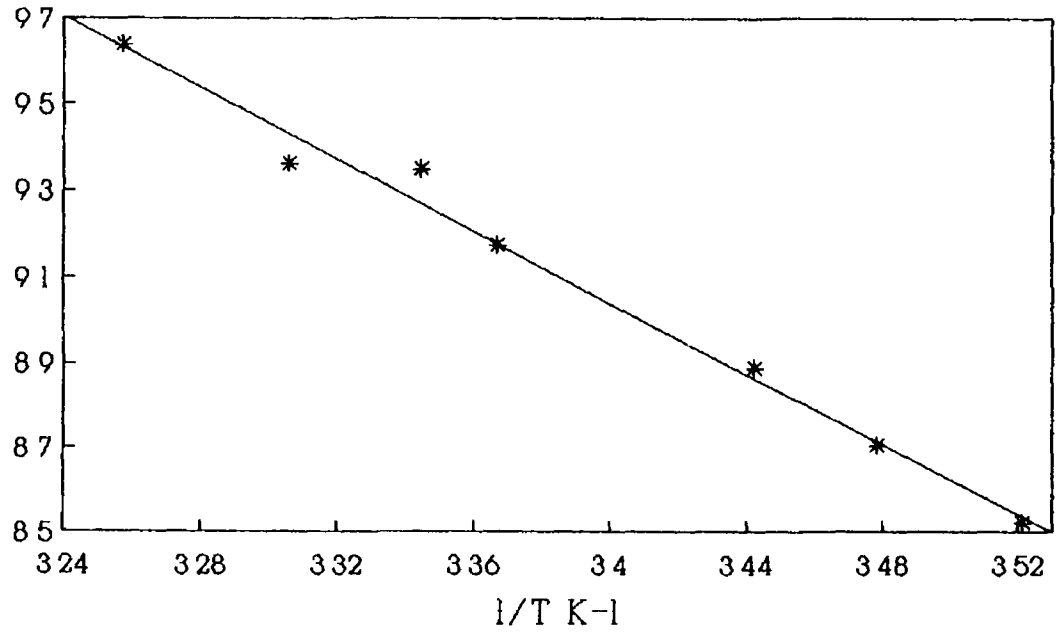

(b)

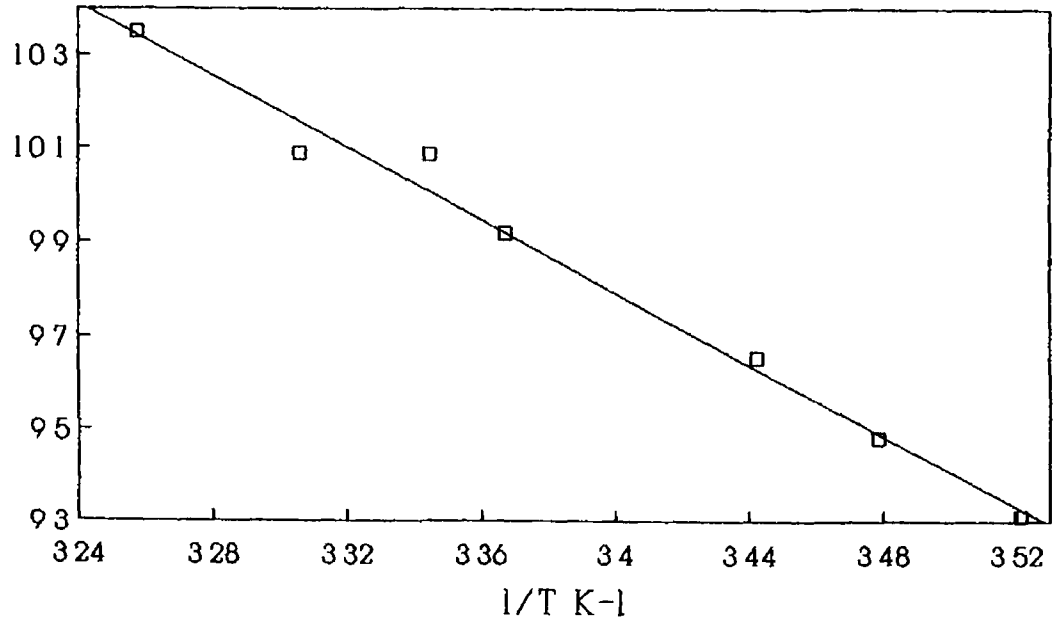

Figure 2.3.6 (a) Arrhenius and (b) Eyring plots for the formation of $MeCp_2Mn_2(CO)_5$ obtained from 355nm laser flash photolysis experiments of $MeCpMn(CO)_3$

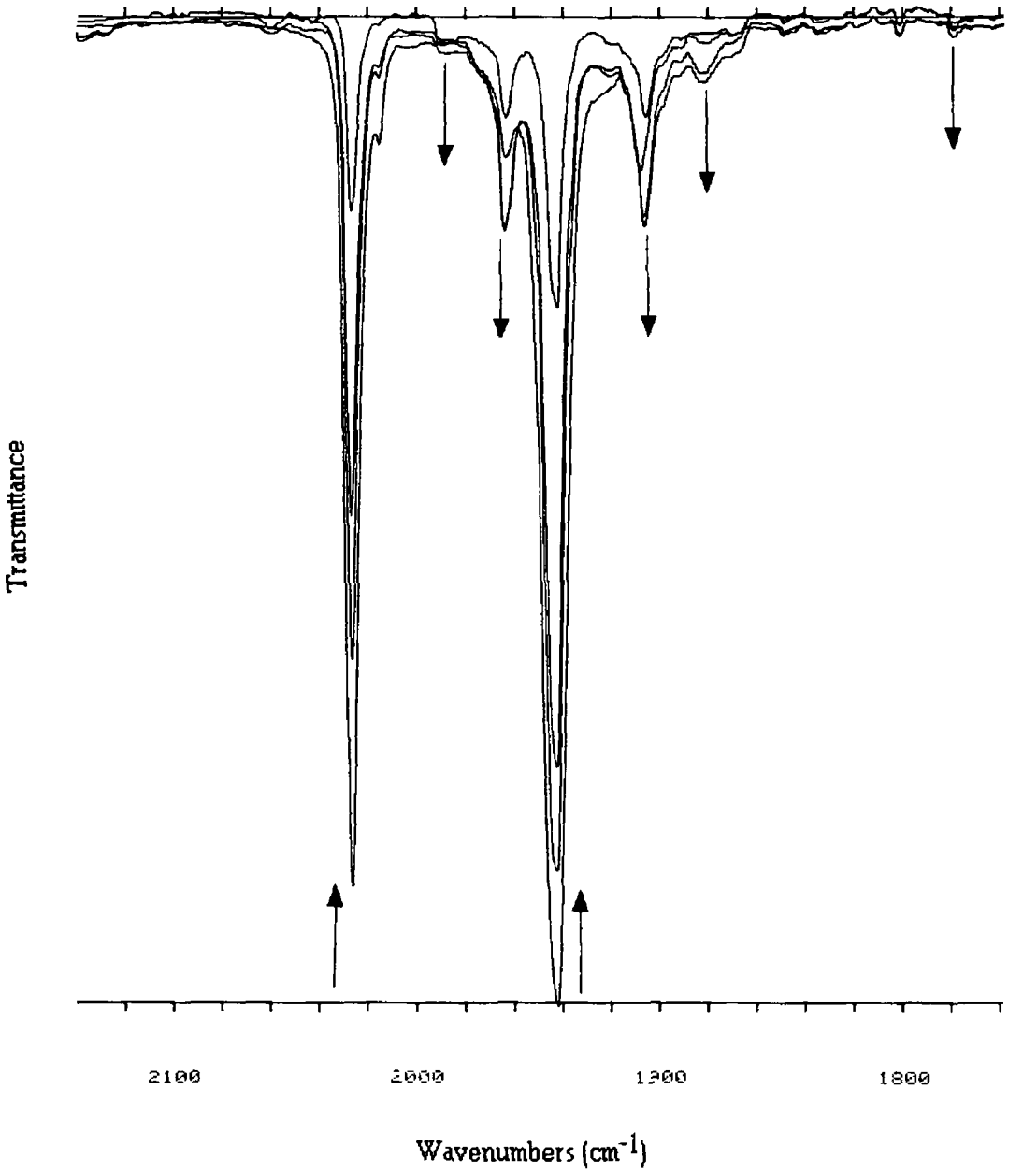

Figure 2.4.1 An infra red spectrum of the carbonyl region obtained after 355nm photolysis of $MeCpMn(CO)_3$ in an argon degassed cyclohexane solution

2.5 Conclusion

Flash photolysis experiment of $MeCpMn(CO)_3$ demonstrated that the reactions of this complex are analogous to those reported for $CpMn(CO)_3$ Differences arise from kinetic data which demonstrated that the methyl group on the cyclopentadienyl ring has an influence on the solvation/desolvation of the cyclohexane molecule from the metal coordination sphere Reactions of the solvated dicarbonyl species are twice as fast with CO as the corresponding $CpMn(CO)_2$(cyclohexane) species This was probably because of a more weakly coordinated cyclohexane arising from the steric influence of the methyl group It appears that the methyl group has a direct influence on the coordination site as previous work carried out in n-hexane produced a two fold increase for the pentamethylsubstituted $Me_5CpMn(CO)_3$ complex[8] The solvated complex $MeCpMn(CO)_2$(cyclohexane) also reacts with parent tricarbonyl complex to form a dinuclear species The existence of the dinuclear species was confirmed by its UV/visible difference spectrum This spectrum was similar to one identified in the photolysis of $CpMn(CO)_3$[6] TRIR studies of $CpMn(CO)_3$ identified the dinuclear complex as a pentacarbonyl compound with four terminal CO's and a bridging CO A similar structure was postulated for $MeCpMn(CO)_3$ The dinuclear complex reacted with CO presumably to reform the parent complex Solution infra red studies indicated the possibility of a second and more stable dinuclear complex

2 6 Laser flash photolysis of $MeCpMn(CO)_2PPh_3$

UV/visible photolysis of $MeCpMn(CO)_2PPh_3$ ($MeCp = \eta^5\text{-}C_5H_4CH_3$) in n-heptane solution (λ = 366nm) was reported to lose a CO molecule as its primary photoprocess[16] No loss of the triphenylphosphine ligand was observed as shown by experiments performed in the presence of CO and the absence of PPh_3 Laser flash photolysis experiments on $MeCpMn(CO)_2PPh_3$ at 355nm produced evidence for the production of one dominant transient species This species was identified and proposed as the non-solvated $MeCpMn(CO)PPh_3$ complex principally from its reaction kinetics and from its UV/visible difference spectrum Evidence exists for other transient species which were presumably formed as a result of loss of a triphenylphosphine ligand from $MeCpMn(CO)_2PPh_3$

2.7 Electronic spectrum of $MeCpMn(CO)_2PPh_3$

Figure 2 7 1 contains the electronic absorption spectrum of $MeCpMn(CO)_2PPh_3$ in cyclohexane solvent The first low energy absorption band appears at ~350nm with the next lowest absorption at ~290nm in $MeCpMn(CO)_2PPh_3$ In the corresponding tricarbonyl complex the lowest absorption band was found at 330nm in alkane solvent This band was assigned to a Mn to (η^5- $CH_3C_5H_4$) charge transfer (Mn --> CpCT) band[1] In addition, the LF transitions were also assigned unresolved to the same energy region It is likely that the band at 350nm is the LF transition because of a lowering of the LF energy on the coordination of the triphenylphosphine ligand The substitution of a carbonyl group in $MeCpMn(CO)_3$ by a ligand with less accepting power than a CO ligand has the effect of inducing a higher negative charge on the metal This charge can be distributed over the metal centre and on the remaining carbonyl groups The cyclopentadienyl ring has been shown in infra red studies of $CpMn(CO)_3$ not to accept any electron density as a result of carbonyl

substitution with most of the charge distribution occuring over the carbonyl groups[17] Therefore the Mn-->CpCT band for $MeCpMn(CO)_2PPh_3$ is present unresolved at 330nm The assignment of the transition at 290nm may possibly be a Mn-->dπ* CT band arising from the phosphine ligand as this band was absent in the UV/visible spectrum of $MeCpMn(CO)_3$ (Figure 2 1 1) The band at 250nm is probably a Mn-->COπ*CT transition

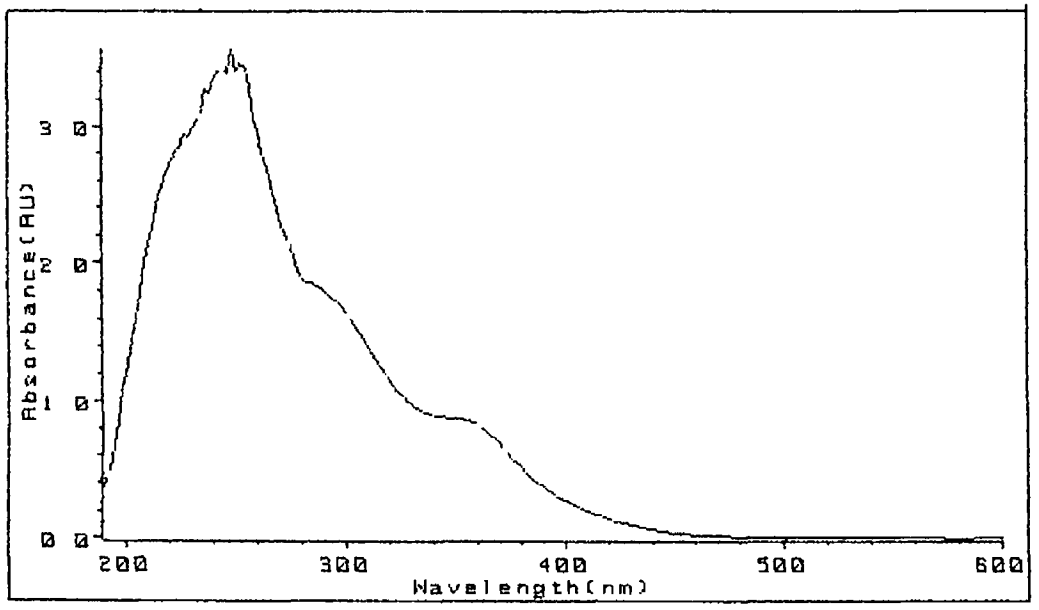

Figure 2.7.1 A UV/visible spectrum of $MeCpMn(CO)_2PPh_3$ (6 3 x 10^{-4} mol dm^{-3}) in cyclohexane solution

2.8 355nm Laser flash photolysis of $MeCpMn(CO)_2PPh_3$

$MeCpMn(CO)_2PPh_3$ is produced from the photoelimination of a CO ligand from the η^5-methylcyclopentadienylmanganese(I)tricarbonyl complex $MeCpMn(CO)_3$ Flash photolysis of $MeCpMn(CO)_2PPh_3$ in cyclohexane at 355nm (ε = 1367 dm^3 mol^{-1} cm^{-1}) produced one transient species. This species had an absorbance maximum

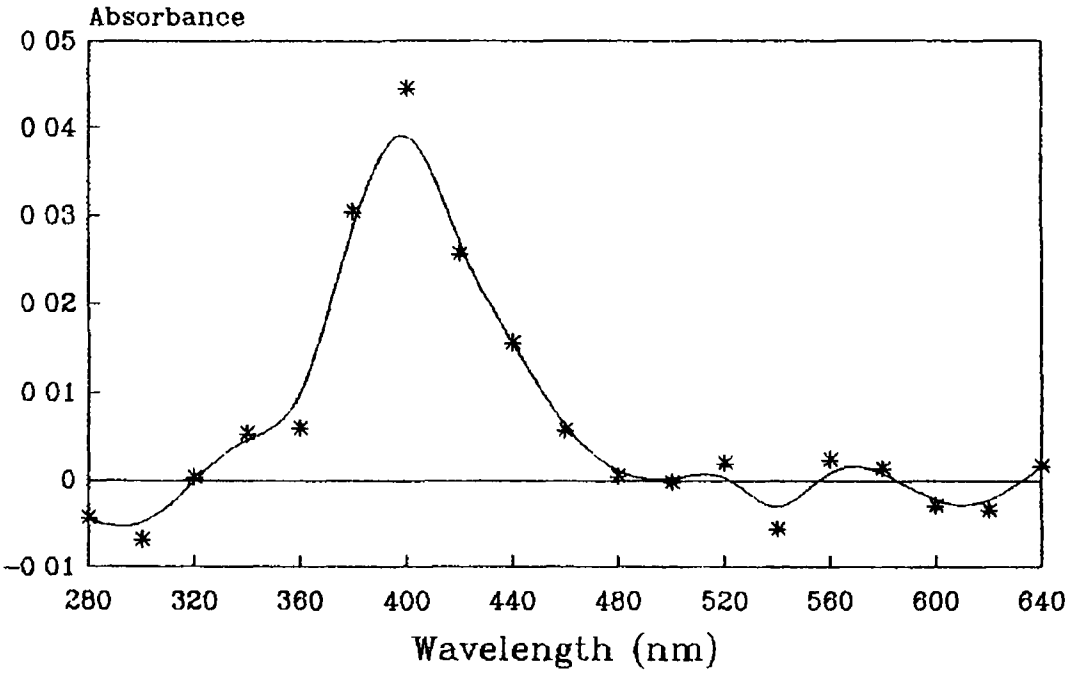

Figure 2 8.1 A UV/visible difference spectrum of the MeCpMn(CO)PPh_3 complex in cyclohexane recorded after 1 0μs under 1 0 atmosphere of argon

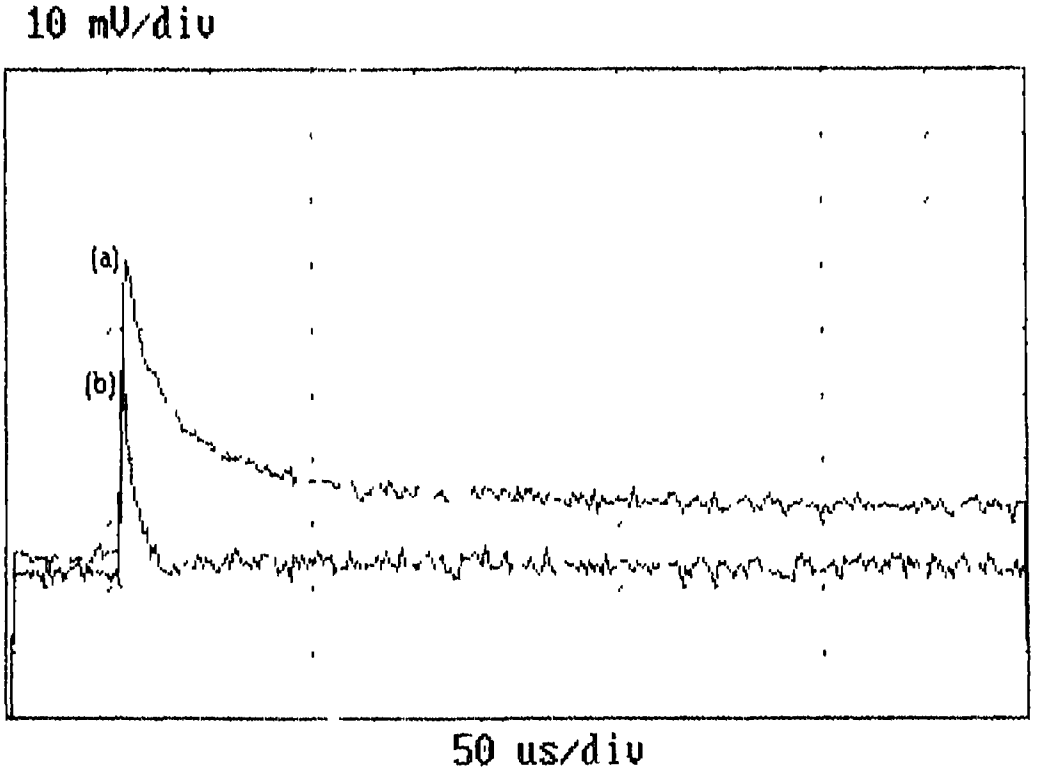

Figure 2.8.2 Decay of the transient species, (a) under one atmosphere of argon and (b) under 0.25 atmospheres of carbonmonoxide, monitored at 400nm

at 400nm as can be seen in the UV/visible difference spectrum in Figure 2 8 1. This species was not $MeCpMn(CO)_2$(cyclohexane) as its UV/visible difference spectrum consisted of a broad band with a maximum at 580nm (Figure 2 2 2)

This transient species was originally thought to be the solvated $MeCpMn(CO)PPh_3$(cyclohexane) complex produced from photochemical loss of a CO ligand Under 1 atmosphere of argon the decay of this photoproduct was detected and follows a first order decay process However, under 1 atmosphere of CO the formation of this species was suppressed, the transient returned to baseline The decay of the transient species again followed a psuedo-first order process This indicated that this transient species was not a primary photoproduct as the addition of CO greatly affected its yield Figure 2 8.2 demonstrates the loss in yield upon addition of CO to the sample solution This suggests that perhaps two transient species of varying reactivity were formed, an extremely reactive one, with a lifetime too short to be measured on the present instrumentation (<200ns), and the one that was detected, a secondary photoproduct Similar type behaviour was noted in the flash photolysis of $CH_3Mn(CO)_5$ in cyclohexane[18] Time resolved infra red and UV/visible detection were used to determine that the primary photoproduct was $CH_3Mn(CO)_4$ produced form the loss of a CO *cis* to the methyl group Under an argon atmosphere this species was identified as the solvated *cis*-$CH_3Mn(CO)_4$(cyclohexane) complex Under a CO atmosphere however, the yield of this solvatocomplex was reduced to one fifth its intensity under argon The solution proposed was that the coordinately unsaturated species competed with CO and cyclohexane to form either the *cis* - $CH_3Mn(CO)_4$(cyclohexane) complex or parent $CH_3Mn(CO)_5$ This implied that the 16e- intermediate was not solvated as quickly as for example the $Cr(CO)_5$ species[5] The authors indicated some geometric rearrangment in $CH_3Mn(CO)_4$ to form a more stable trigonal-bipyrimadal C_{3v} complex to account for this behaviour This species would have, because of geometric or electronic constraints, a sufficient lifetime to

discriminate in the coordination of a sixth ligand The second order rate constant for the reaction of $CH_3Mn(CO)_4$ with CO is 2 2 x 10^6 dm^3 mol^{-1} s^{-1} The corresponding second order rate constant for the reaction of $MeCpMn(CO)PPh_3$ with CO is 1 05 x 10^8 dm^3 mol^{-1} s^{-1} (Figure 2 8 3) The increase in rate constant by two orders of magnitude indicates that perhaps a molecule of solvent does not occupy the vacant coordination site in the $MeCpMn(CO)PPh_3$ photoproduct The reacting species could not be the $MeCpMn(CO)_2$(cyclohexane) complex as the second order rate constant for the reaction of this species with CO is 7 2 x 10^5 dm^3 mol^{-1} s^{-1} (*vide infra*) The explanation for this observation may he in an intramolecular reaction and not in a geometric rearrangment as with $CH_3Mn(CO)_5$ Manganese carbonyl compounds are well known in ortho-metallation reactions involving phosphine ligands[19] Triphenylphosphine is a very bulky ligand and could prevent the usual coordination of a solvent to the vacant ligand site This action would facilitate an ortho-metallated type product The CO molecule is small and would be able to coordinate to the metal centre This is important as it means that the intermediate can discriminate between different sizes of molecules This would account for the extremely fast second order rate constant The intermediate formed could compete with the ortho hydrogens on the phenyl rings of the triphenylphosphine ligand and with CO in a similar fashion as the $CH_3Mn(CO)_4$ intermediate competes with cyclohexane and CO The reaction is summarised in Scheme 2 8 1 Laser flash photolysis experiments of $MeCpMn(CO)_3$ in cyclohexane indicated that the methyl group on the cyclopentadienyl ring had a direct effect on the 'vacant' coordination site (*vide infra*) It is possible that the methyl group also contributed in these experiments to the non-solvation of the $MeCpMn(CO)PPh_3$ species

In solution, metal centres of electron rich complexes have been observed to react with C-H bonds on their own ligands more rapidly than with saturated hydrocarbons[20] Many examples exist showing this type of interaction

$(C_5Me_5)(PPh_3)IrH_2$ irradiated in benzene solution undergoes loss of H_2 to form a hydrido phenyl complex where the coordinately unsaturated intermediate formed on photolysis reacted with benzene solvent In addition, an orthometallated complex was formed by intramolecular oxidative addition to the triphenylphosphine ligand Irradiation in cyclohexane produced predominately the orthometallated product indicating that perhaps the intermediate in the reaction was not solvated on photolysis because of steric effects in coordinating a cyclohexane molecule The methyl groups on the cyclopentadienyl ring remained uninvolved in the reaction However this is not always the case Hydrogen atoms on the methyl group on the cyclopentadienyl ring can also participate in intramolecular C-H activation $(C_5Me_5)_2ZrH_2$ can activate a methyl group on the cyclopentadienyl ring *via* loss of the dihydrogen ligand[20] With respect to manganese, indium and zirconium have much larger atomic radii The probability of a metallation reaction is increased for the larger metals Manganese analogues would be expected to have shorter lifetimes arising from more unstable complexes because of increased ring strain

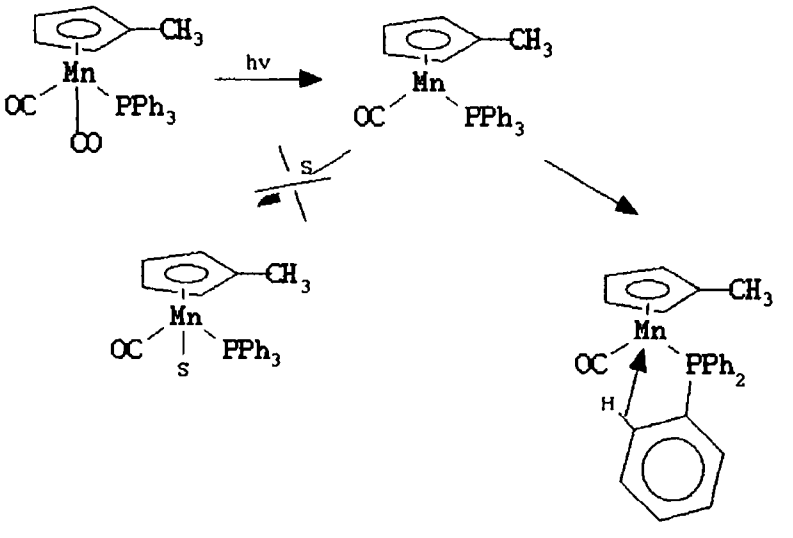

Scheme 2.8.1 Scheme for the photolysis of $MeCpMn(CO)_2PPh_3$ in cyclohexane for loss of a CO ligand

The intermediate may not necessarily involve an orthometallated type reaction Many cases are known for the metal centre to coordinate to a benzene ring *via* a 'double bond'[21] or to an alkyl silane in a three centred Si-Mn-H bond[22] The possibility exists that a phenyl ring may coordinate *via* an 'isolated double' bond as postulated in the coordination of $Cr(CO)_5$ to benzene[21] Alternately the phenyl ring may be weakly coordinated *via* a three centred 'agostic' bond where the metal coordinates to the carbon hydrogen bond[23] A fourth possibility is 'end on' agostic bonding where the C-H σ bond interacts with the metal to form a linear weak σ bond[24] This type of interaction would provide the least strain in the proposed ring system

Another explaination may be a rearrangment in the $MeCpMn(CO)PPh_3$ unit Extended Huckel metal orbital calculations and perturbation theory have shown that the $MeCpMn(CO)_2$ species exists in a pyramidal geometry with the remaining ligands retaining a constant angle between them[25] This pyrimidal geometry was very sensitive to the nature of the ligands and to the cyclopentadienyl ring The effect of the electron donating methyl group and the replacement of a CO ligand with a PPh_3 may cause a planar ground state geometry to predominate and give a structure analogous to $CpCo(CO)_2$ Therefore the steric influence of the ligands would be greater, preventing coordination of the cyclohexane molecule and again facilitating coordination of smaller ligands to the metal However, given the nature of the triphenylphosphine ligand i e σ donor, π acceptor, the bonding for a triphenylphosphine ligand is not very different to a CO ligand and so it is likely that the pyramidal geometry would predominate

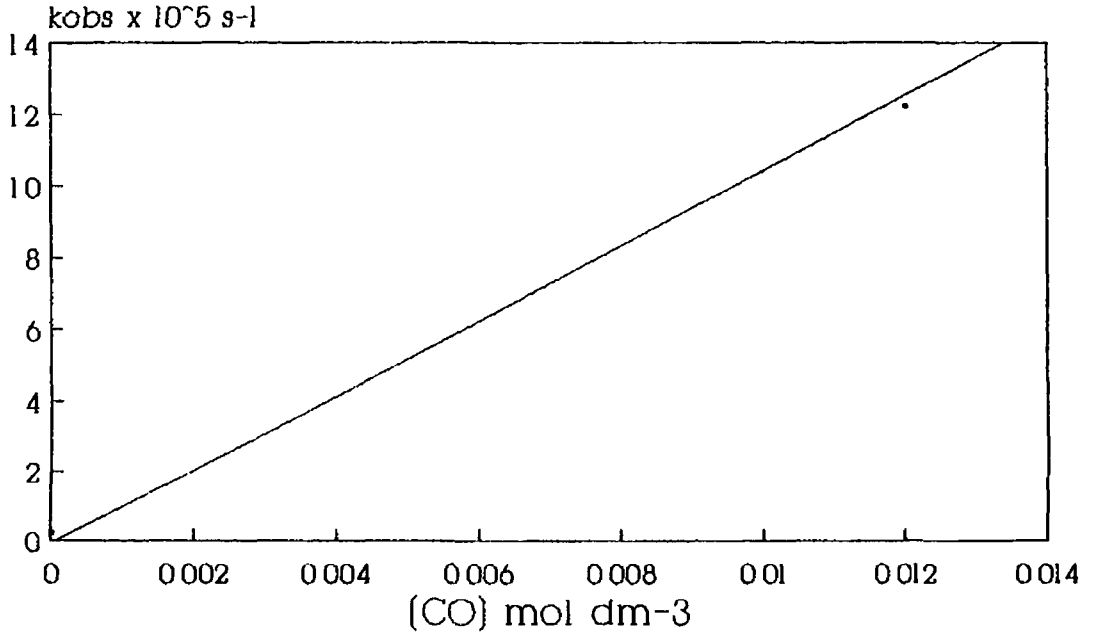

[CO] mol dm^{-3}	$k_{obs} \times 10^{-5}$ (s^{-1})
0 000	0 204
0 003	2 236
0 006	6 786
0 009	9 680
0 012	12 226

$k_{[CO]} = 1\ 05 \times 10^{8} \pm 6\ 88 \times 10^{6}\ dm^{3}\ mol^{-1}\ s^{-1}$

Intercept = $-7075 \pm 6\ 5 \times 10^{4}\ s^{-1}$

Corr coeff = 0 993

Figure 2.8.3 A plot of the observed rate constant for the decay of $MeCpMn(CO)PPh_3$ against concentration of CO in cyclohexane solution at 298K

Ring dechelation is another possibility in the explaination of loss of yield on addition of CO[10] However, the cyclopentadienyl ring has been shown in all photochemical reactions involving a manganese metal centre to be inert and therefore could be described as a rigid ligand[11] Even when the cyclopentadienyl ring has been replaced by other η^5 ligands such as indenyl and fluorenyl no reaction involving these ligands was observed in contrast to the photochemical systems of the isoelectronic arene chromium tricarbonyl complexes[26] Hapticity changes in the cyclopentadienyl ring from η^5 to η^3 has been observed in the thermal reactions of $MeCpMn(CO)_3$[12] The production of this hapticity change involved the reduction of the manganese centre to produce the dianion $[\eta^3\text{-}MeCpMn(CO)_3]^{2-}$ which was detected and identified by infra red spectroscopy If a photochemically induced ring slipped complex was formed in this experiment, it would be expected to be stabilised in the presence of CO forming a tricarbonyl complex No new transients were observed on addition of CO to the sample solution

The non-solvation of the $MeCpMn(CO)PPh_3$ complex because of steric hindrance from the intramolecular stabilisation reaction would also prevent the formation of a dinuclear species These dinuclear species are thought to be common in photochemical reactions of organometallic complexes and are unwanted side reactions as they would reduce the efficiency of these complexes as homogeneous catalysts The isoelectronic cyclopentadienyl manganese tricarbonyl, arene chromium tricarbonyl and cyclobutadienyl iron tricarbonyl complexes are known to form these dinuclear complexes[13] The parent $MeCpMn(CO)_2PPh_3$ complex is much larger than a cyclohexane solvent molecule Since the triphenylphosphine ligand prevents coordination of a cyclohexane molecule it is also unlikely that the non-solvated intermediate would coordinate to $MeCpMn(CO)_2PPh_3$ This lack of a dinuclear complex greatly simplifies the task of transient identification and this was reflected in this experiment as only one transient was detected

The production of the dicarbonyl species cannot be ruled as infra red experiments which involved irradiating a solution of $MeCpMn(CO)_2PPh_3$ in argon degassed cyclohexane produced evidence for the production of the tricarbonyl complex (Figure 2 8 4). The irradiation was carried out using the 355nm line of the laser so as to reproduce the conditions in the transient experiments The $MeCpMn(CO)_3$ complex could be produced from the loss of a triphenylphosphine ligand. The source of CO was most probably from the observed photoproduct, $MeCpMn(CO)PPh_3$ The weak band at 1836cm^{-1} may be the monocarbonyl complex $MeCpMn(CO)(PPh_3)_2$ Four weak bands were observed at 1975, 1961, 1919 and 1903 cm^{-1} These bands correspond to similar ones observed in identical experiments with $MeCpMn(CO)_3$ and were assigned to an unknown dinuclear complex (Table 2.3 1) Under one atmosphere of argon the transient decay of $MeCpMn(CO)PPh_3$ did not return to the baseline This may indicate a reaction of the undetected $MeCpMn(CO)_2$(cyclohexane) species with parent $MeCpMn(CO)_2PPh_3$ to form a dinuclear species A UV/visible difference spectrum of this species is shown in Figure 2 8 5 $MeCpMn(CO)_2$(cyclohexane) has been shown to react with parent in the laser flash photolysis of $MeCpMn(CO)_3$ In addition, the extinction coefficient of the $MeCpMn(CO)_2$(cyclohexane) complex produced from the photolysis of $MeCpMn(CO)_3$ appeared to be very low and this may account for its non-detection in the laser flash photolysis of $MeCpMn(CO)_2PPh_3$ On the other hand metal carbonyl dinuclear species have high extinction coefficients for metal centred σ-σ^* transitions[1] and so this would facilitate the detection of a photochemically produced transient dinuclear species The strong absorption at 290nm detected in the time resolved spectrum of $MeCpMn(CO)_2$(cyclohexane) would be absent in this experiment because there is no valley at 290nm in the absorbance spectrum of $MeCpMn(CO)_2PPh_3$

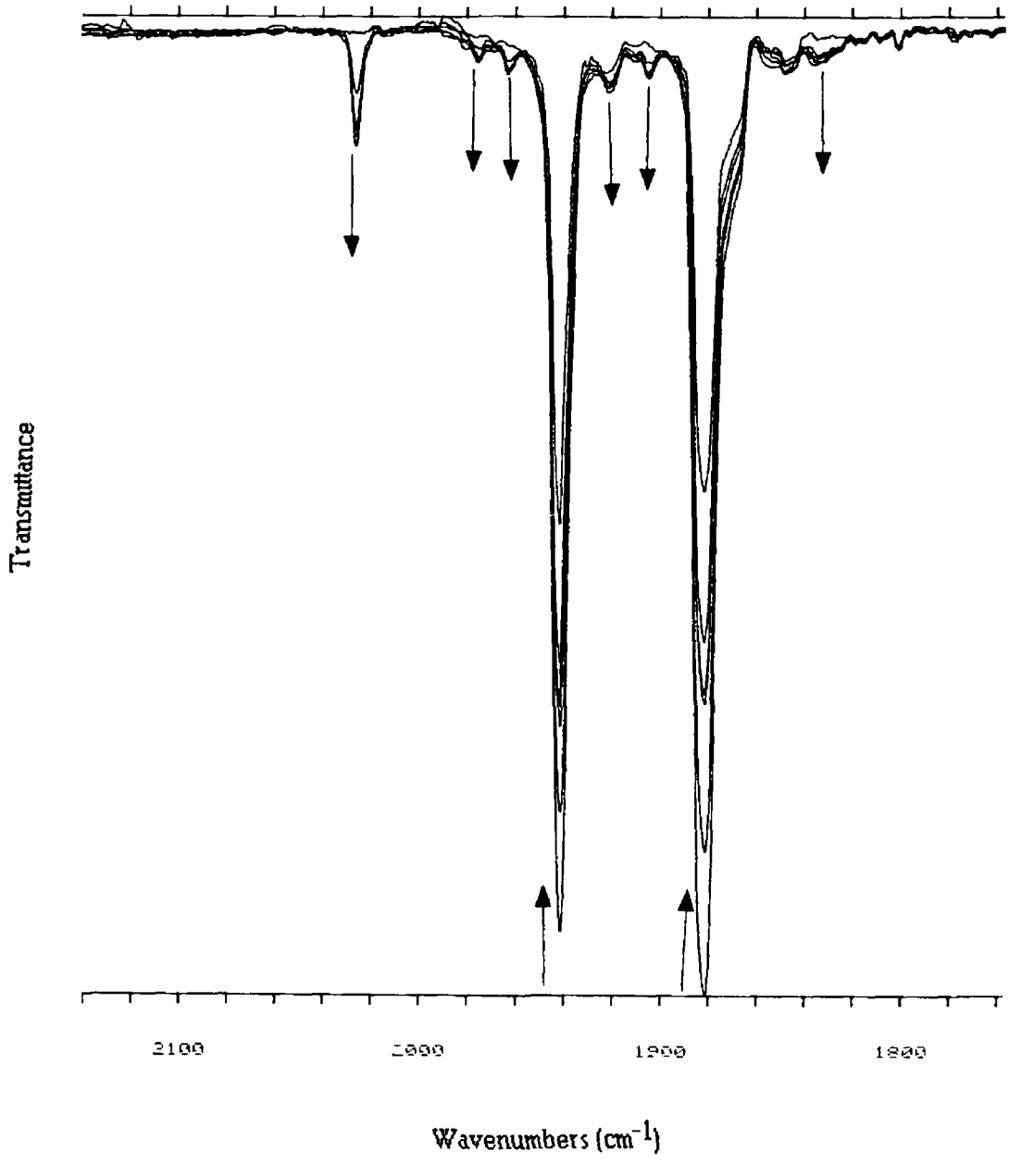

Figure 2.8.4 Infra red carbonyl region after the photolysis of $MeCpMn(CO)_2PPh_3$ in cyclohexane using the 355nm laser line The bands at 1941 and 1881 cm^{-1} correspond to the parent complex and at 2026cm^{-1} for $MeCpMn(CO)_3$

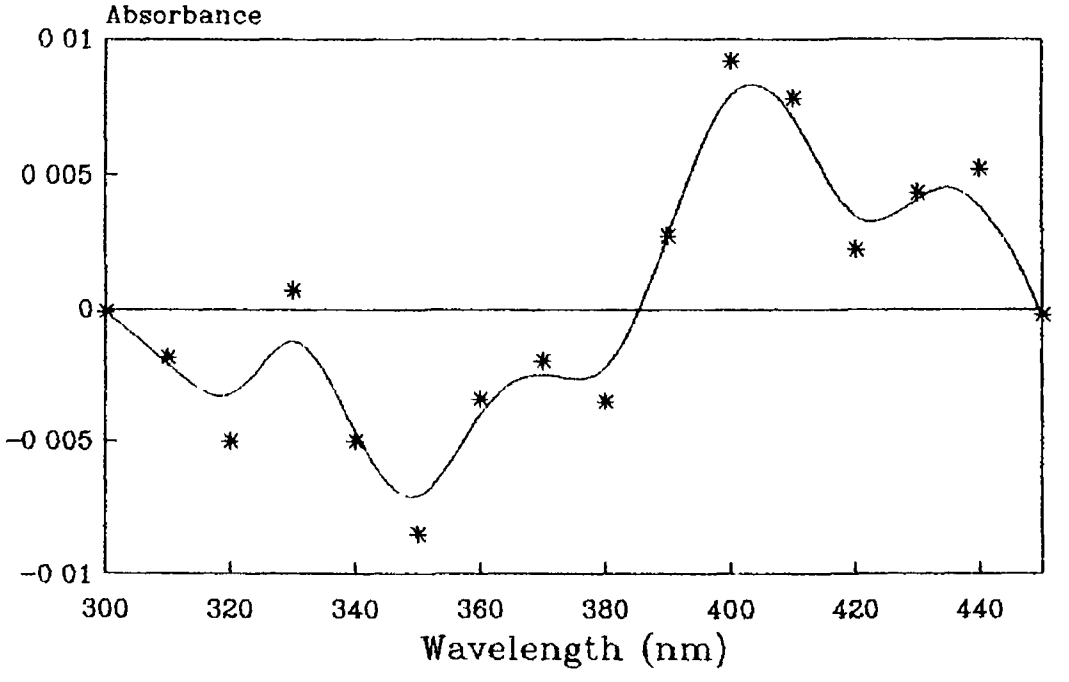

Figure 2.8.5 A UV/visible difference spectrum of the unknown dinuclear species taken after 300μs under 1 0 atmosphere of argon

2.9 Conclusion

Photolysis of $MeCpMn(CO)_2PPh_3$ in cyclohexane solution produced evidence for the formation of two transient species The first transient was identified from reaction kinetics as the non-solvated $MeCpMn(CO)PPh_3$ complex The bulky triphenylphosphine ligand stencally prevented the cyclohexane molecule from coordinating to the metal centre The coordinately unsaturated complex was stabilised by an intramolecular reaction The nature of this interaction was unknown but is believed to involve possibly an orthometallation type reaction The fast second order

rate constant for the reaction of this species with CO indicated that the CO molecule was able to coordinate to the manganese atom while the larger cyclohexane solvent molecule was not The orientation of the methyl group may also have contributed to the non-solvation of the intermediate as it appears to directly influence the 'vacant' coordination site in experiments involving $MeCpMn(CO)_3$ Loss of triphenylphosphine ligand was observed in infra red monitored solution photolysis of $MeCpMn(CO)_2PPh_3$ In time resolved experiments the presence of $MeCpMn(CO)_2$(cyclohexane) was not detected although it was thought to contribute to the transient decay not returning to the baseline in experiments carried out under argon No dinuclear complex was formed from the $MeCpMn(CO)PPh_3$ species because of combined steric effects involving the triphenylphosphine ligand and the cyclopentadienyl methyl group

REFERENCES

1 Geoffroy,G L , Wrighton, M S , *Organometallic Photochemistry*, Academic Press, New York, 1979

2 Braterman, P S , Black, J D , *J Organomet Chem*, 1972, **39**, C3

3 Perutz, R N , Turner, J J , *J Am Chem Soc*, 1975, **97**, 4791

4 Kelly, J M , Long, C , Bonneau, R , *J Phys Chem*, 1983, **87**, 3344

5 Simon, J D , Xie, X , *J Phys Chem*, 1986, **90**, 6751

6 Creaven, B S , Dixon, A J , Kelly, J M , Long, C , Poliakoff, M , *Organometallics*, 1987, **6**, 2600

7 (a) Giordano, P , Wrighton, M S , *Inorg. Chem*, 1977, **16(1)**, 160 ,(b) Wrighton, M S , *Chem Rev*, 1974, **74(4)**, 401

8 Johnson, F P A , George, M W , Bagratashvili, V N ; Vereshchagina, L N , Poliakoff, M , *J Chem Soc , Mendeleev Commun*, 1991, 26

9 Klassen, J K , Selke, M , Sorenson, A A , Yang, G K., *J. Am Chem. Soc*, 1990, **112**, 1267

10 O'Connor, J M , Casey, C P , *Chem Rev*, 1987, **87**, 307

11 Zhdanovich, V I , Ezernitskaya, M G , *Ivz Akad Nauk SSSR, Ser Khim*, 1981, 685

12 Lee, S , Cooper, N J , *J Am Chem Soc*, 1991, **113**, 716.

13 Bitterwolf, T E ; Lott, K A , Rest, A J ; Mascetti, J , *J. Organomet. Chem*, 1991, **419**, 113

14 Creaven, B S , Ph D thesis, Dublin City University, 1989

15 Hill, R S , Wrighton, M S , *Organometallics*, 1987, **6**, 632 ,

16 Teixeira, G , Avilés, T , Dias, A R , Pina, F , *J. Organomet Chem*, 1988, **353**, 83

17 Barbeau, C ; *J Can Chem*, 1967, **15**, 161

18 Belt, S T , Ryba, D W ; Ford, P C , *Inorg. Chem*, 1990, **29**, 3633

19 Wilkinson, G; Stone, F G A, Abel, E. W, *Comprehensive Organometalhc Chemistry, Vol IV,* Pergamon Press, Oxford, 1982

20 Janowicz, A H; Bergman, R G, *J. Am Chem Soc*, **1983, 105**, 3929

21 Zhang, S, Dobson, G R, Zang, V, Bajaj, H C, van Eldik, R, *Inorg Chem*, **1990, 29**, 3477

22 Carré, F; Colomer, E, Corriu, R P J, Vioux, A, *Organometallics*, **1983, 3**, 1272

23 Brookhart, M, Green, M L H, *J Organomet Chem*, **1983, 250**, 395

24 Saillard, J Y, Hoffmann, R, *J Am Chem Soc*, **1984, 106**, 2006

25 Hofmann, P, *Angew. Chem Int Ed. Engl*, **1977, 16**, 536

26 Gilbert, A, Kelly, J M, Budzwait, M, Koerner von Gustorf, E, *Z. Naturforsch*, **1976, 31b**, 1091

CHAPTER 3

355nm AND 266nm LASER FLASH PHOTOLYSIS OF $M(CO)_5PPh_3$ COMPLEXES

(M = Cr, Mo or W)

3 0 Laser flash photolysis of $M(CO)_5PPh_3$ complexes (M = Cr, Mo or W)

3.1 Introduction

The irradiation into the LF bands of the GroupVIB hexacarbonyls produces loss of a CO ligand by depopulation of an electron from the t_{2g} orbitals, which are involved in the π backbonding from the metal to the CO ligands, and population of the e_g^* orbitals, which are antibonding with respect to the metal-CO σ bond The substitution of a CO ligand in the $M(CO)_6$ complexes by a ligand with less π accepting capacity has the effect of splitting the doubly degenerate antibonding orbitals of e symmetry in the hexacarbonyl complex into two discrete orbitals having $d_{x^2-y^2}$ and d_{z^2} character in the pentacarbonyl complex[1] The extent of the splitting of the e orbitals is determined by the strength of the π accepting capability of the unique ligand By convention the unique ligand is placed on the z axis Therefore, it should be possible by irradiating into the LF band, using different excitation wavelengths, to selectively labilise a ligand on the z axis or a CO group on the x and y axes The loss of the unique ligand or a CO ligand on the z axis is dependent again on the extent of the π accepting ability of the unique ligand However this is a generalisation as the non radiative deactivation pathways of the excited states are not taken into account in this argument The effect of these pathways was clearly seen in quantum yield measurements for the $Cr(CO)_6$ complex where a quantum yield of 1 0 was predicted for CO loss[2] The actual measurement was 0 67 with the difference being accounted for by recombination of the photoejected CO ligand with the $Cr(CO)_5$ photofragment[3]

A study of the fast photochemical reactions of the Group VIB monosubstituted triphenylphosphine pentacarbonyls in cyclohexane was undertaken to see the different effects produced on 355nm and 266nm laser irradiation The major problem associated with such a study is the relatively similar UV/visible spectra of the three expected

photoproducts ($M(CO)_5$, *cis*-$M(CO)_4PPh_3$ and *trans*-$M(CO)_4PPh_3$ photocomplexes) Such problems can be overcome to a certain extent by examining the relative reaction rates of the various photoproducts with CO which, in previous experiments using related compounds, have been shown to differ significantly

3.1.1 Electronic spectra of $M(CO)_5PPh_3$ (M = Cr, Mo or W).

The low energy absorption features of $M(CO)_5PPh_3$ (M = Cr, Mo or W) are shown in Figure 3 1 1 1 The first absorption band is noted at ~350nm for each of the complexes This band has been assigned as the LF ($e^4b_2^2$ --> $e^3b_2^2a_1^1$) (LF = ligand field) transition[4] The more intense absorption at ~300nm corresponds to the M-->π^*CO CT (CT = charge transfer) band

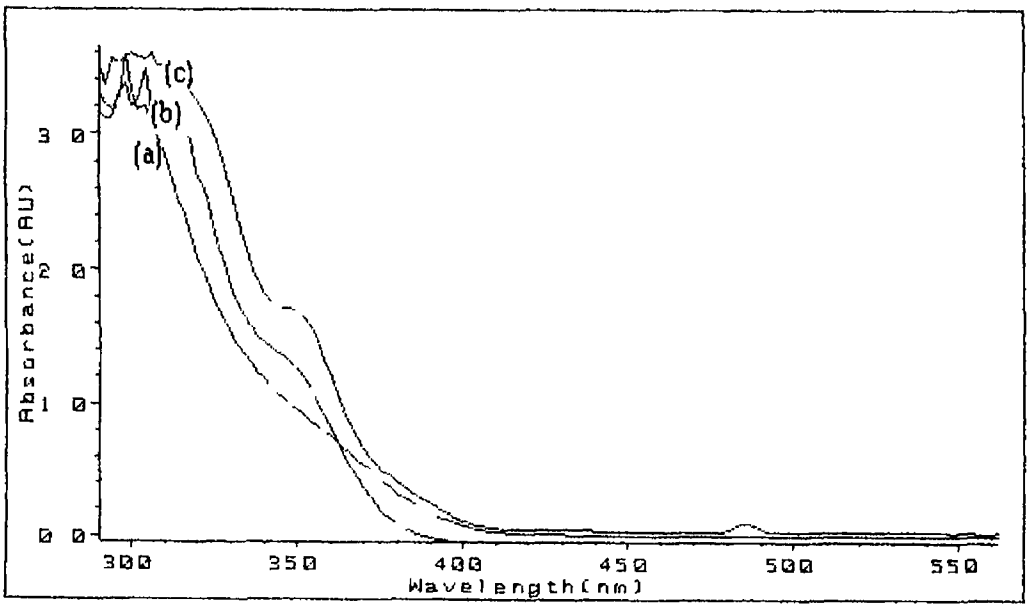

Figure 3.1.1.1 The electronic spectra of (a) $Cr(CO)_5PPh_3$ (7 0 x 10^{-4} mol dm^{-3}) (b) $Mo(CO)_5PPh_3$ (6 4 x 10^{-4} mol dm^{-3}) and (c) $W(CO)_5PPh_3$ (7 9 x 10^{-4} mol dm^{-3}) in cyclohexane solution at room temperature

3.2 Photolysis of $Cr(CO)_5PPh_3$

3.2.1 Infra red monitored photolysis of $Cr(CO)_5PPh_3$

Room temperature 355nm laser photolysis of argon degassed cyclohexane solutions of $Cr(CO)_5PPh_3$ in NaCl solution cells (path length = 0 1mm) reveal the production of $Cr(CO)_6$ and a *trans* product (Figure 3 2 1 1) The bands at 2064, 1982 and 1944cm^{-1} correspond to the A_1, A_2 and E modes of $Cr(CO)_5PPh_3$ These bands were depleted as a result of photolysis at 355nm New bands were observed at 2010, 1987, 1919, and 1895cm^{-1} The band at 1987cm^{-1} was characteristic of the T_{1u} band observed for the Group VIB metal hexacarbonyl complexes and was assigned to $Cr(CO)_6$. The formation of the hexacarbonyl complex indicated that the triphenylphosphine ligand was lost from the parent compound As the experiment was carried out in a sealed cell any CO released during the photolysis could react with the pentacarbonyl $Cr(CO)_5$ produced from photoliberation of triphenylphosphine Triphenylphosphine loss has been observed in other related systems i e $Mo(CO)_5PPh_3$[5] and occured at low quantum yield for 366nm excitation The carbonyl stretching frequencies at 2010 and 1896cm^{-1} were indicative of the A_{1g} and E_u modes of a *trans* complex This complex was probably formed from the reaction of a $Cr(CO)_4PPh_3$ intermediate, produced from photochemical loss of a CO ligand, with triphenylphosphine liberated from the parent complex The small band at 1919cm^{-1} indicated the formation of some *cis* configuration $Cr(CO)_4(PPh_3)_2$ In order to investigate the reaction intermediates of the $Cr(CO)_5PPh_3$ further a photolysis study was carried out with excess triphenylphosphine in an argon degassed cyclohexane/$Cr(CO)_5PPh_3$ solution The result of this experiment is presented in Figure 3.2 1 2 The parent complex bands correspond to 2064, 1982 and 1944cm^{-1} for the A_1, A_2 and E modes respectively New bands were observed at 2012, 1920 and 1895cm-1 and correlate well with those observed in the photolysis of $Cr(CO)_5PPh_3$ in the

absence of ligand The band at 1895cm^{-1} was the most intense and again suggests the formation of a *trans*-$M(CO)_4L_2$ complex The band intensity indicates the E_u mode of a *trans* complex The weaker band at 2010cm^{-1} corresponds to the A_{1g} band observed in *trans* complexes of the type $M(CO)_4L_2$ (M = Cr, Mo or W)[6] Another band, the B_{1g} mode at 1945cm^{-1}, is usually observed for these compounds but was masked in these experiments by the very intense E mode of the parent complex The band at 1920cm^{-1} again suggests the formation of some *cis*-$Cr(CO)_4(PPh_3)_2$ The other bands usually observed for *cis* complexes are at approximately 2010, 1901 and 1876cm^{-1} The band at 2010cm^{-1} is obscured by the 2010cm^{-1} band of the *trans* complex The other bands could be masked by the very intense E_u mode of *trans*-$Cr(CO)_4(PPh_3)_2$ A shoulder on the E_u band at ~1870cm^{-1} may correspond to the B_2 mode observed in *cis*-$M(CO)_4L_2$ complexes. From these results it may be concluded that the room temperature photolysis of $Cr(CO)_5PPh_3$ results in the formation of the *trans* -$Cr(CO)_4(PPh_3)_2$ complex as the major photoproduct with the formation of *cis*-$Cr(CO)_4(PPh_3)_2$ as a minor product The loss of a triphenylphosphine ligand also occurs however this appears to be a minor photoproduct No evidence for *cis* - *trans* photoisomerisation was observed

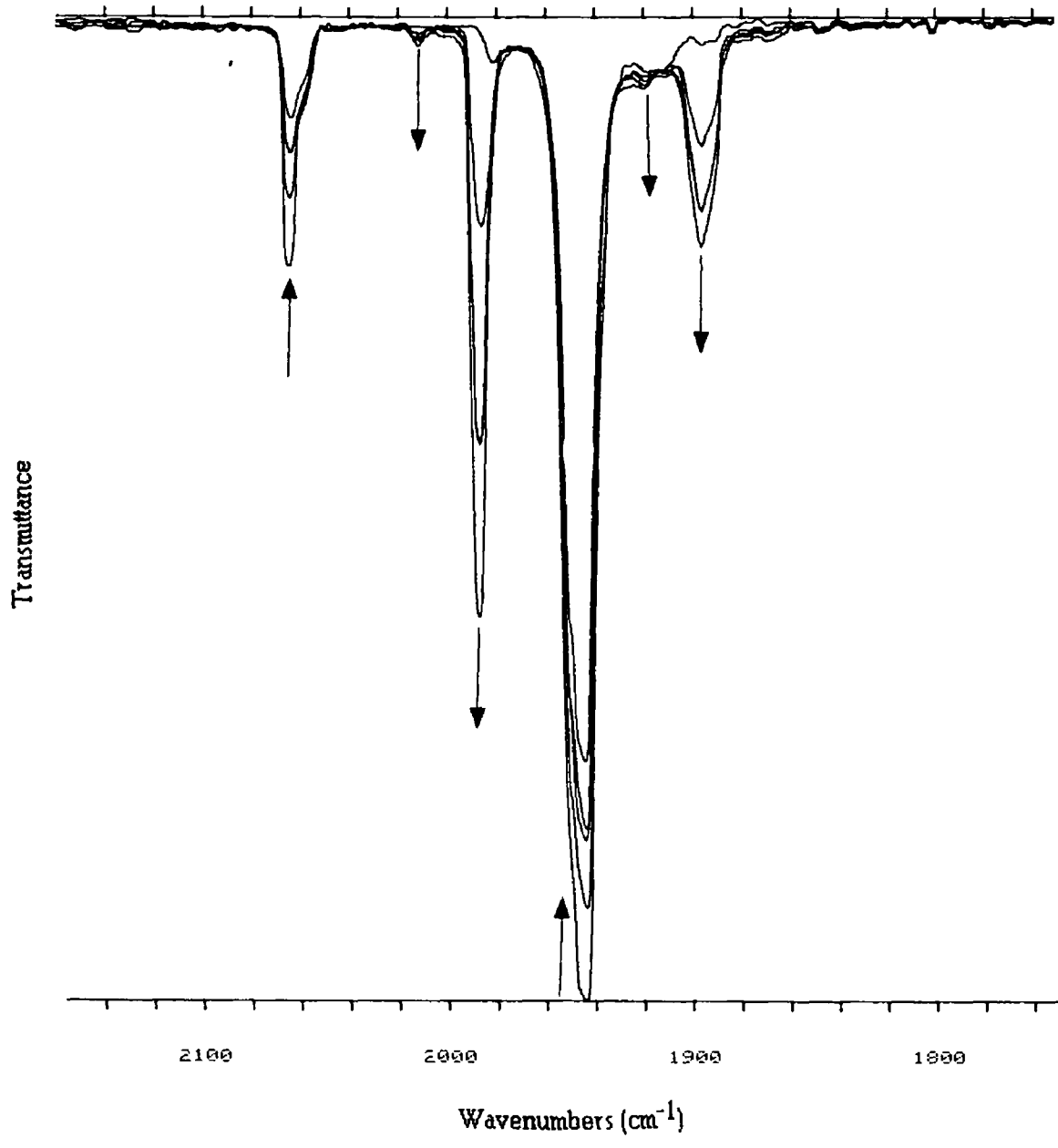

Figure 3.2.1.1 An infra red spectrum of the carbonyl bands produced following the 355nm photolysis of $Cr(CO)_5PPh_3$ in an argon degassed cyclohexane solution

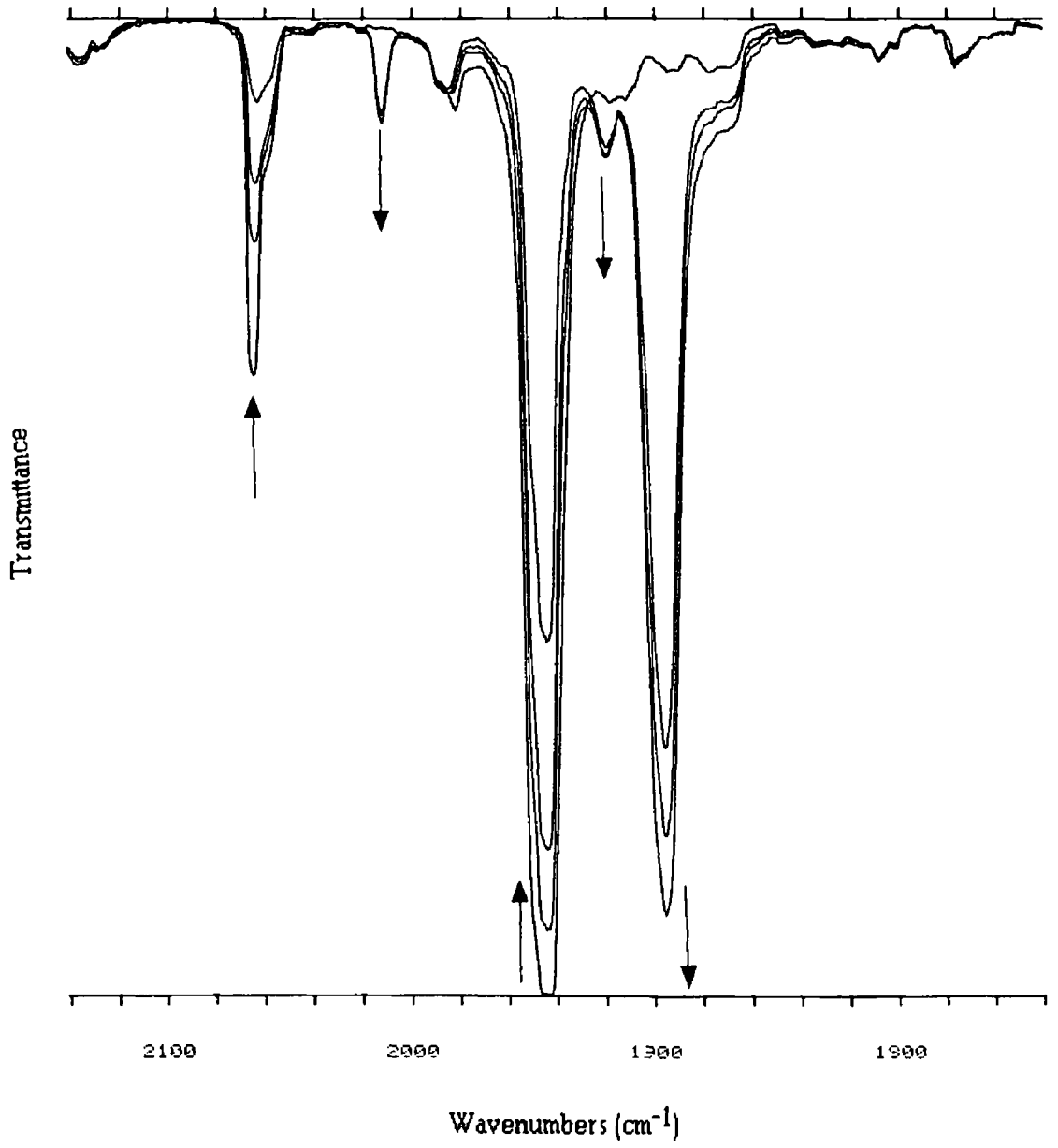

Figure 3.2.1.2 An infra red spectrum in the υCO region produced following the 355nm photolysis of $Cr(CO)_5PPh_3$ in an argon degassed cyclohexane solution with excess triphenylphosphine

3.2.2 355nm laser flash photolysis of $Cr(CO)_5PPh_3$ with UV/visible monitoring

Laser flash photolysis of $Cr(CO)_5PPh_3$ using the 355nm line of the laser produced evidence for the formation of four transient species These species were identified primarily from their reaction kinetics and to a lesser extent their UV/visible difference spectra The species were identified as *cis* -$Cr(CO)_4PPh_3$, *trans* -$Cr(CO)_4PPh_3$(cyclohexane) and two dinuclear species whose identities remain uncertain

3.2.2.1 First transient species

The first observable transient species was *cis*-$Cr(CO)_4PPh_3$ This species was identified from its UV/visible difference spectrum and from kinetic studies of its reaction with CO The UV/visible difference spectrum can be seen in Figure 3 2 2 1 1 The spectrum consists of a broad band with two maxima at 400nm and 500nm This spectrum was different to that observed for $Cr(CO)_5S$ (S = cyclohexane) which consisted of a single broad band with a maximum centred around 500nm A spectrum of $Cr(CO)_5$(cyclohexane) obtained by photolysis of $Cr(CO)_6$ in cyclohexane solution under one atmosphere of CO can be seen in Figure 3 2 2 1 2 The absence of the small band at 400nm in the spectrum obtained for *cis*-$Cr(CO)_4PPh_3$ indicated that the UV/visible difference spectrum for this species was different to that obtained for $Cr(CO)_5$(cyclohexane)

The reaction of this species with CO demonstrates unequivocally that this species was not $Cr(CO)_5$(cyclohexane) The second order rate constant for the reaction of this first transient species was obtained by varying the concentration of CO in the cyclohexane solution A typical transient for this reaction is given in Figure 3 2 2 1 3

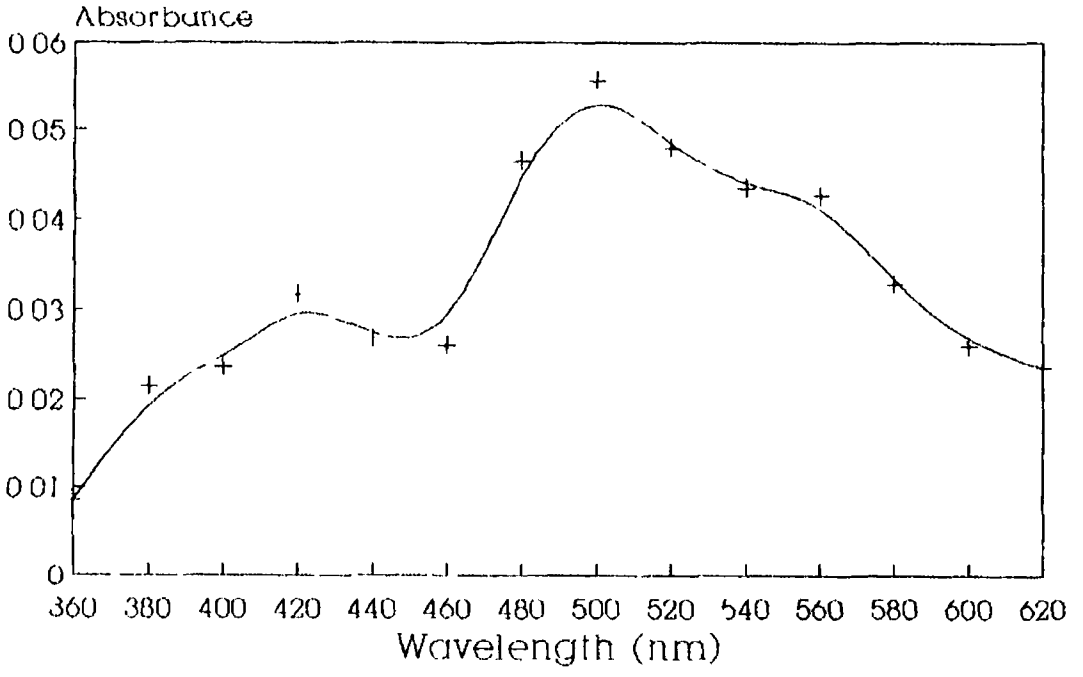

Figure 3.2.2.1.1 A UV/visible difference spectrum of *cis*-$Cr(CO)_4PPh_3$ obtained at 0 5μs after the laser pulse

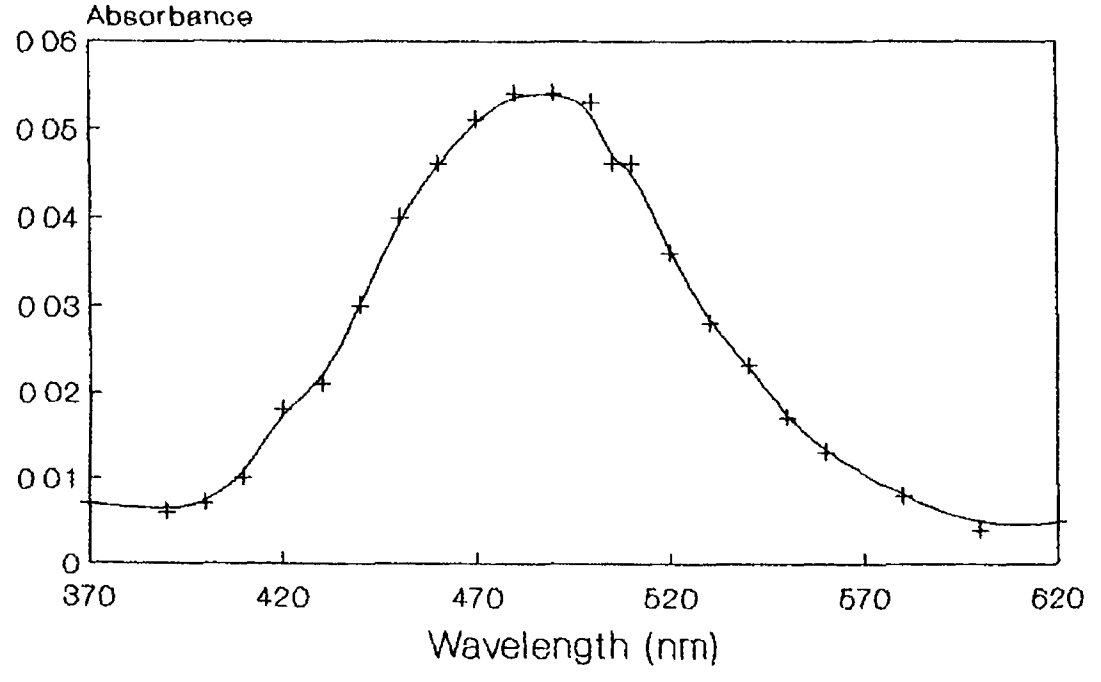

Figure 3.2.2.1.2 A UV/visible difference spectrum of $Cr(CO)_5$(cyclohexane) obtained from 266nm laser flash photolysis of $Cr(CO)_6$ under 1.0 atmosphere of CO after 20μs after the laser pulse.

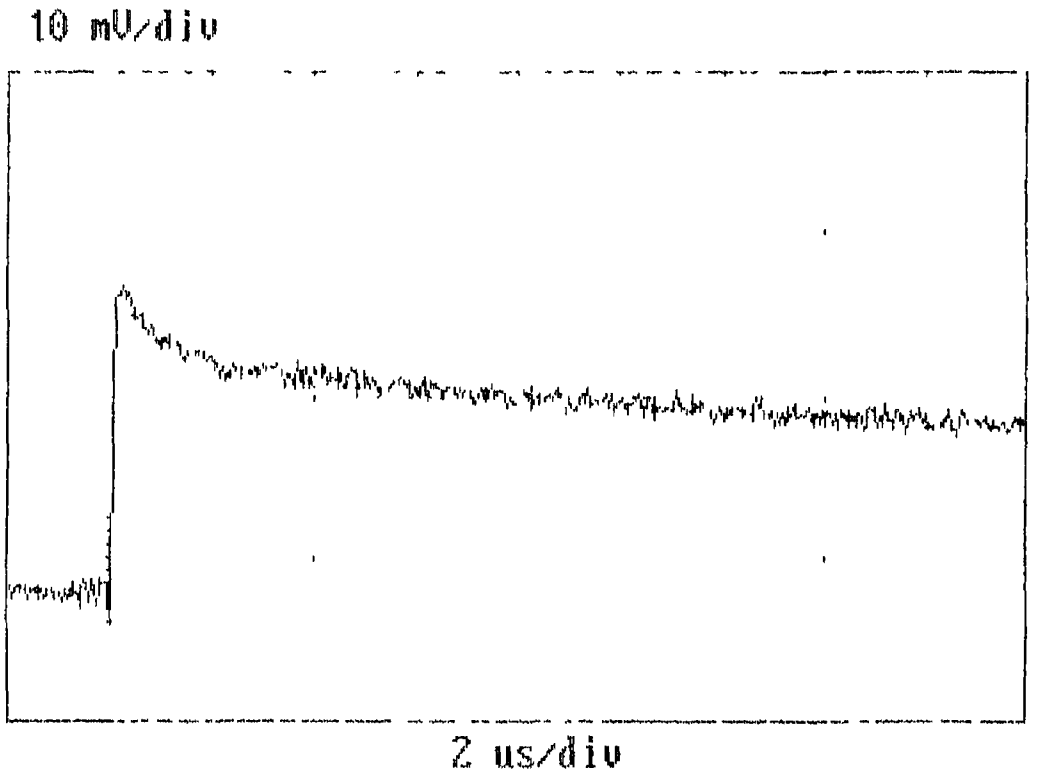

Figure 3.2 2 1 3 A typical transient obtained for the decay of *cis* -$Cr(CO)_4PPh_3$ obtained at 500nm under 0 25 atmospheres of CO

The data for the reaction of this transient species with CO and a graph of the concentration of CO (mol dm^{-3}) against the observed rate constant (s^{-1}) is shown in Figure 3 2 2 1 4 The slope of the line and hence the second order rate constant was 2 0 x 10^8 dm^3 mol^{-1} s^{-1} The second order rate constant for the reaction of CO with $Cr(CO)_5$(cyclohexane) was quoted by Kelly *et al* [7] as 3 0 x 10^6 dm^3 mol^{-1} s^{-1} The value obtained from the photolysis of $Cr(CO)_6$ under 1 atmosphere of CO in these experiments was 2 8 x 10^6 dm^3 mol^{-1} s^{-1} The second order rate constant obtained for the species obtained from the photolysis of $Cr(CO)_5PPh_3$ was almost two orders of magnitude greater than that obtained for $Cr(CO)_5$(cyclohexane) This confirms that the photoproduct observed was not $Cr(CO)_5$(cyclohexane) A possible explanation for the marked increase in the second order rate constant for this species could be that the *cis* species cannot coordinate a solvent molecule because of the bulky triphenylphosphine ligand However in the presence of CO, the *cis* species may be able to coordinate

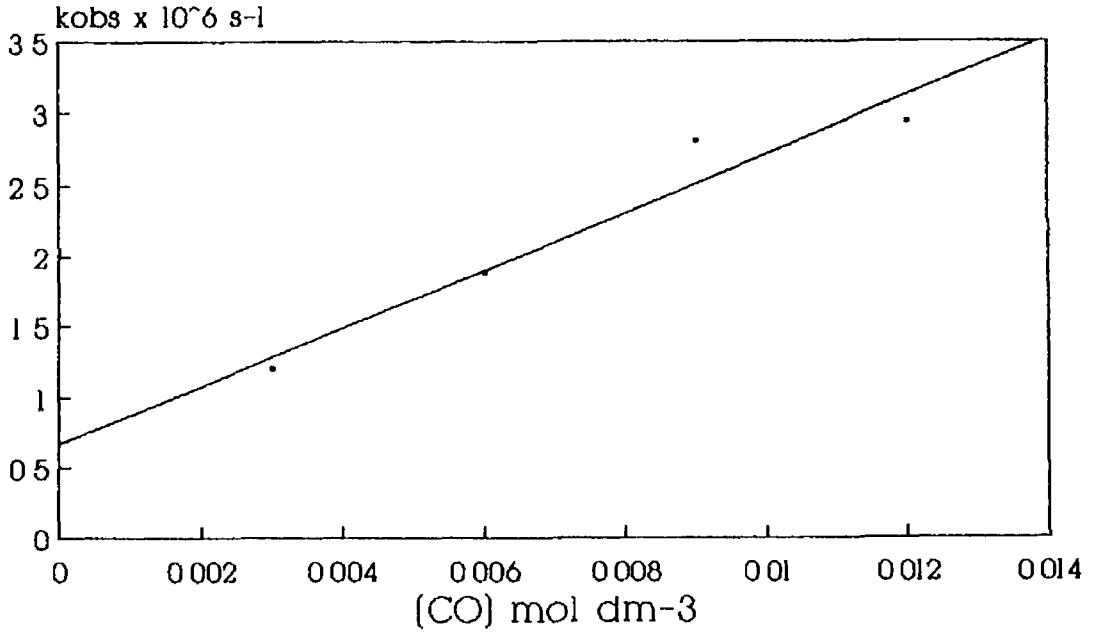

[CO] mol dm^{-3}	k_{obs} x 10^{-6} (s^{-1})
0 003	1 200
0 006	1 880
0 009	2 803
0 012	2.930

$k_{[CO]} = 2.04 \times 10^{8} \pm 3\,81 \times 10^{7}$ dm^3 mol^{-1} s^{-1}

Intercept = $6.75 \times 10^{5} \pm 2\,55 \times 10^{5}$ s^{-1}

Corr Coeff 0 967

Figure 3.2.2.1.4 A second order plot of the observed rate constant k_{obs} (s^{-1}) for the reaction of *cis*-$Cr(CO)_4PPh_3$ against the concentration of CO (mol dm^{-3}) at 298K

to a CO because a CO molecule is much smaller than a corresponding cyclohexane molecule This would account for the increased rate for reaction of *cis*-$Cr(CO)_4PPh_3$ with CO The rate constant was faster than that obtained for the non-solvated $MeCpMn(CO)PPh_3$ intermediate and may, like $MeCpMn(CO)PPh_3$, be stabilised by an intramolecular interaction with the bulky triphenylphosphine ligand Chromium carbonyl complexes stabilised by intramolecular reactions have been observed $Cr(CO)_3(PCy_3)_2$ has been synthesised and characterised by X-ray crystallography where the sixth coordination site was occupied by an 'agostic' hydrogen from one of the cyclohexyl rings[8]

In thermal reactions of complexes of the type $Cr(CO)_5L$ a site preference was shown for loss of a CO ligand, or other ligand, *cis* to the unique ligand L[9] Substitution of a CO ligand in $Cr(CO)_6$ by phosphine ligands increased the lability of the *cis* CO ligands by a factor of approximately 300 Time resolved infra red analysis of $W(CO)_5PPh_3$ in n-heptane solution has demonstrated that the *cis* CO loss intermediate reacted faster than the *trans* intermediate and faster than the pentacarbonyl intermediate produced from photolysis of $W(CO)_6$[10] Therefore the first transient species is proposed as *cis*-$Cr(CO)_4PPh_3$ If this is the case then this transient species would be a primary photoproduct produced from the loss of a CO group *cis* to the triphenylphosphine ligand Deconvoluting the transient decay curves using non linear regression (see expenmental section) can give the initial absorbances of the species involved in the decay process This can be used as an indicator at fast timescales to determine if the first species in the transient was a primary photoproduct as a steady absorbance value under various CO atmospheres would serve as evidence of a primary photoproduct A plot of the absorbance values calculated from the transient decay curves obtained at various concentrations of CO against the concentration of carbon monoxide monitored at 500nm (Figure 3 2 2 1 5) revealed that the initial absorbance value calculated for the fast species remained constant regardless

of CO concentration This indicates that the yield of this photoproduct was unaffected by the presence of CO and therefore a primary photoproduct In photolysis experiments where a liquid pumping phase was omitted from the sample preparation this first transient species was not observed This indicates that the transient species is sensitive to impurities in the solvent, most probably water Grevels *et al* have shown that water can easily be removed from cyclohexane solutions by the addition of a liquid pumping phase to the sample preparation[11] The absence of this species when there is no liquid pumping phase suggests that it may be obscured by another band formed form the reaction of one of the other photoproducts with water Another explanation possible is that the reactivity of the first transient species with water may be beyond the detection range of the instrumentation

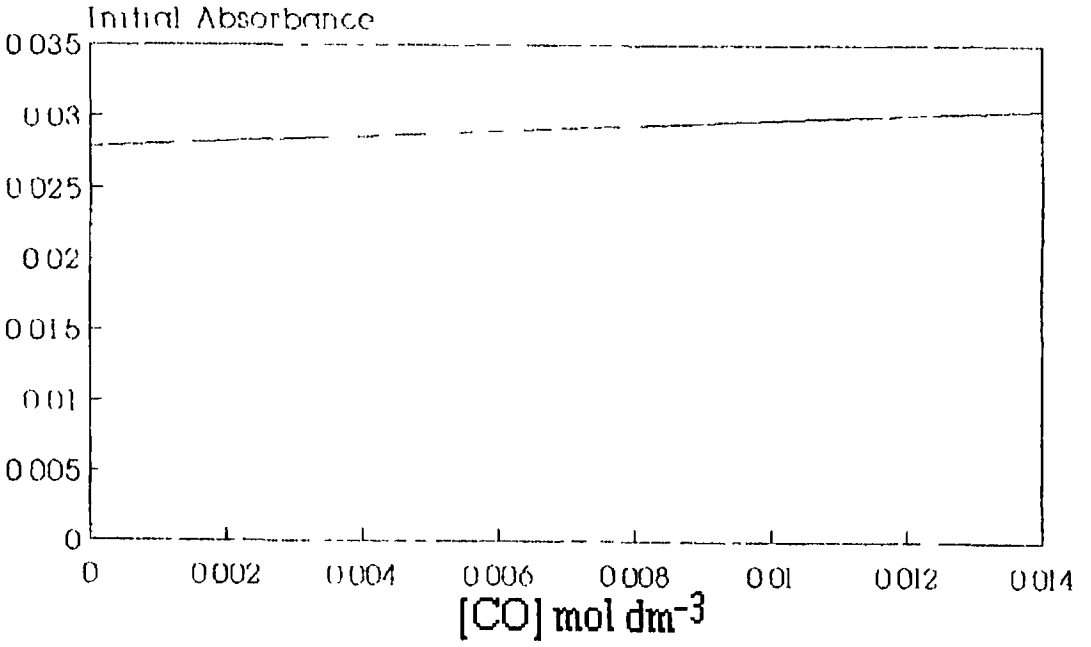

Figure 3.2.2.1.5 A plot of the initial absorbances of *cis*-$Cr(CO)_4PPh_3$ against the concentration of CO

3.2.2.2 Second transient species

The second transient species was assigned to *trans* - $Cr(CO)_4PPh_3$(cyclohexane) In the infra red monitored solution cell experiments *trans* products were identified as being the dominant photoproducts A UV/visible difference absorption spectrum of *trans*-$Cr(CO)_4PPh_3$(cyclohexane) obtained from 355nm laser flash photolysis experiments in cyclohexane solution is shown in Figure 3 2 2 2 1 It consists of a broad band with a maximum at 480nm Again the $Cr(CO)_5$(cyclohexane) species can be ruled out as it has a maximum of ~500nm A transient of this species is shown in Figure 3 2 2 2 2 This species reacts with CO and a graph of various concentrations of CO against the observed rate constant is depicted in Figure 3 2 2 2 3 The second order rate constant for the reaction of this species with CO was 2 0 x 10^6 dm^3 mol^{-1} s^{-1} This value was close to that obtained for the $Cr(CO)_5$(cyclohexane) complex at 3 0 x 10^6 dm^3 mol^{-1} s^{-1} [7] However given the difference in the UV/visible difference spectra it was concluded that this species was the *trans*-$Cr(CO)_4PPh_3$(cyclohexane) complex To further support this conclusion the low temperature matrix isolation study of the related $Cr(CO)_5PMe_3$ complex in argon matrix at 10K revealed that two photoproducts were observed on photolysis between 229 and 366nm and identified as the *cis* and *trans* configurations of $Cr(CO)_4PMe_3$[12] A small amount of $Cr(CO)_5$ was also observed and consistent with the low quantum yield for unique ligand loss in other related systems e g $Mo(CO)_5PPh_3$[5], $W(CO)_5PPh_3$[13] As before deconvolution of the transients under various pressures of CO revealed that this species was a primary photoproduct i e the yield of this species was unaffected by changing the CO concentration in solution A graph of CO concentration against initial absorbance is shown in Figure 3 2 2 2 4 This species was probably solvated in solution The loss of a CO ligand *trans* to the triphenylphosphine ligand would facilitate solvation of the *trans*-$Cr(CO)_4PPh_3$ intermediate

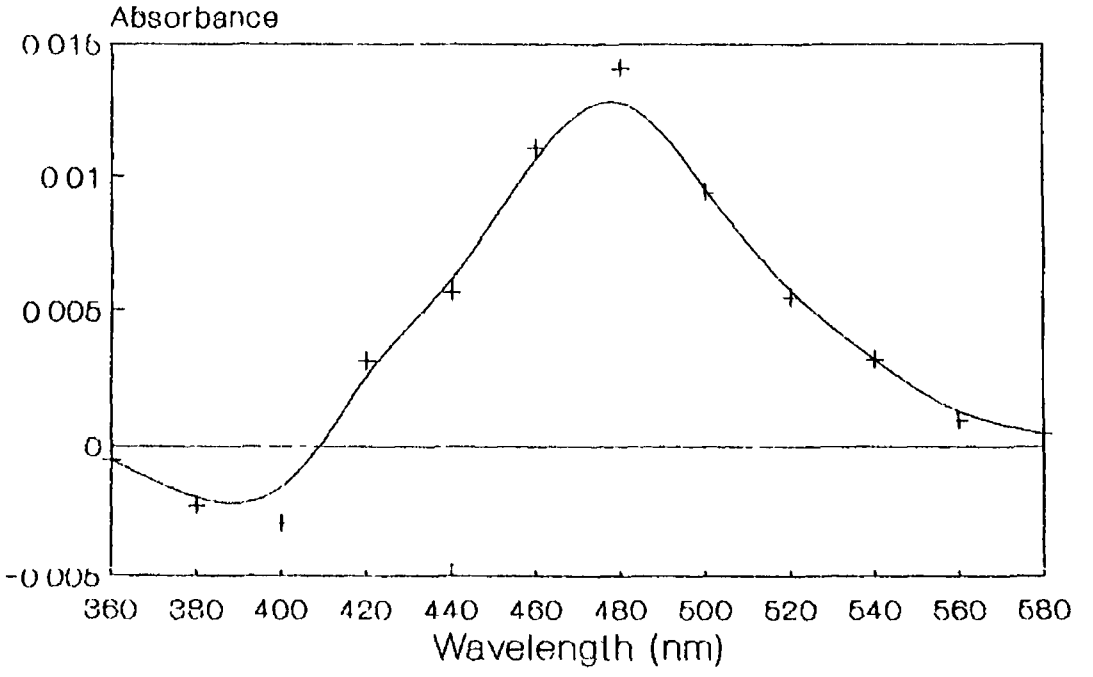

Figure 3.2.2.2.1 UV/visible difference spectrum of *trans*-$Cr(CO)_4PPh_3$(cyclohexane) obtained at 10μs after the laser pulse

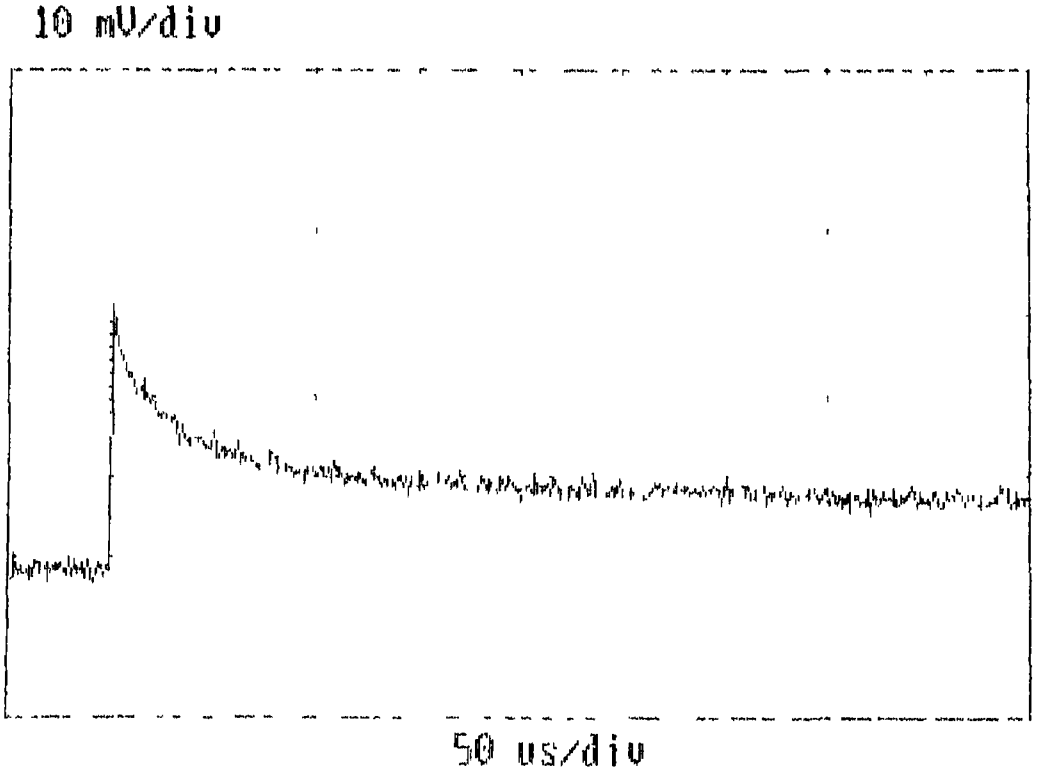

Figure 3.2.2.2.2 A typical transient for *trans*-$Cr(CO)_4PPh_3$(cyclohexane) monitored at 500nm under 0 25 atmospheres of CO

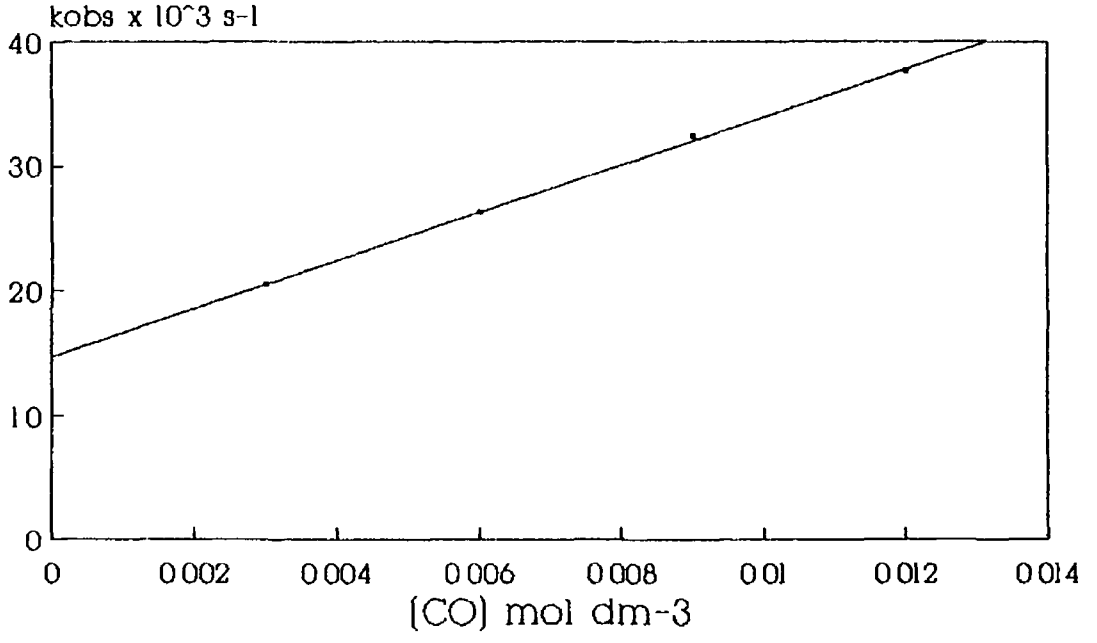

[CO] mol dm^{-3}	$k_{obs} \times 10^{-4}$ (s^{-1})
0 003	2 040
0 006	2 619
0 009	3 236
0 012	3 754

$k_{[CO]} = 1\ 92 \times 10^{6} \pm 4\ 56 \times 10^{4}\ dm^{3}\ mol^{-1}\ s^{-1}$

Intercept = $1.47 \times 10^{4} \pm 3\ 05 \times 10^{2}\ s^{-1}$

Corr Coeff 0 999

Figure 3.2 2.2.3 A second order plot of the observed rate constant k_{obs} (s^{-1}) for the reaction of *trans*-$Cr(CO)_4PPh_3$(cyclohexane) against the concentration of CO (mol dm^{-3}) at 298K

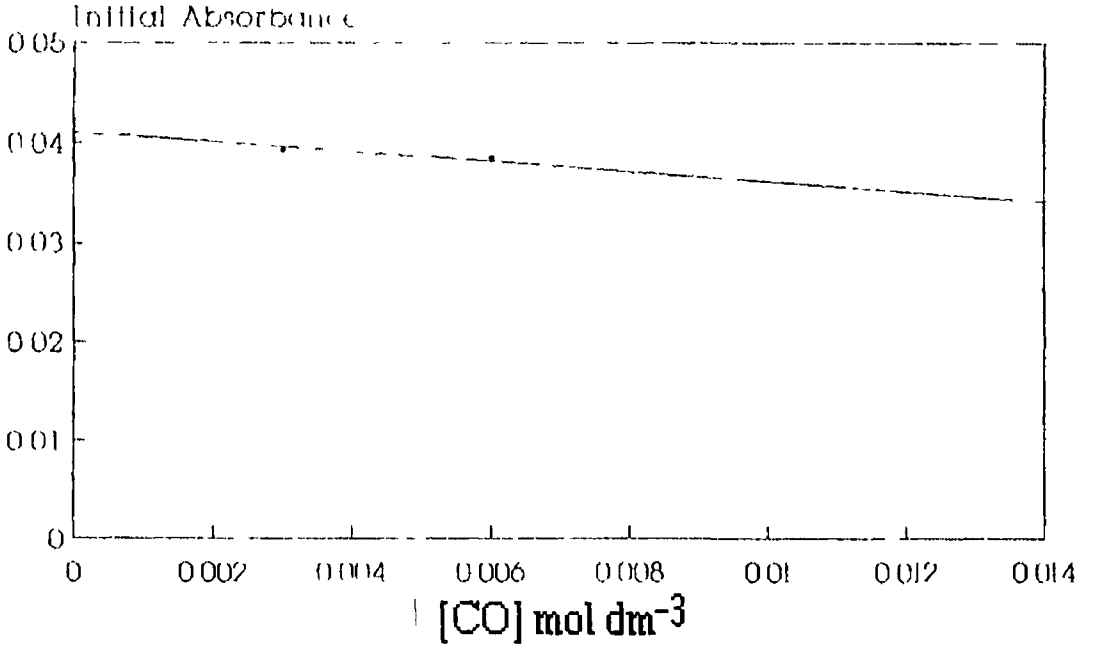

Figure 3.2.2.2.4 A plot of initial absorbance of *trans* -$Cr(CO)_4PPh_3$(cyclohexane) against concentration of CO in solution

The bulky triphenylphosphine ligand *trans* to the vacant site would provide the least steric effects to solvation

3.2.2.3 Third transient species

The third transient species observed for the 355nm photolysis of $Cr(CO)_5PPh_3$ had a λmax at 460nm A UV/visible spectrum of this species is shown in Figure 3 2 2 3 1 The λmax observed for this species was different to that observed for both *cis* -$Cr(CO)_4PPh_3$ and *trans* -$Cr(CO)_4PPh_3$(cyclohexane) A transient of this species obtained at 500nm is shown in Figure 3 2 2 3 2 The decay of the fast portion of the curve followed psuedo first order kinetics A plot of the observed rate constant against concentration of CO (Figure 3 2 2 3 3) revealed that this species appeared not to react with CO A plot of initial absorbance against concentration of CO in cyclohexane solution (Figure 3 2 2 3 4) indicated that yield of this species was affected by the

presence of CO and is therefore a secondary photoproduct This secondary photoproduct may have been a dinuclear species formed from the reaction of a primary photoproduct with parent or from an intramolecular reaction with one of the ligands Such dinuclear species have been observed in the photochemical reactions of a number of metal carbonyl systems[14, 15, 16]

Another possibility is the formation of a water complex Time resolved infra red studies carried out on $Cr(CO)_6$ in cyclohexane revealed the presence of $Cr(CO)_5(H_2O)$ as a result of reaction of $Cr(CO)_5$(cyclohexane) with trace amounts of water in the solvent[11] The infra red frequencies of this complex at 1946 and 1916cm^{-1} indicated that H_2O was a good donor ligand comparable with diethyl ether and tetrahydrofuran as ligands Therefore it is possible that this intermediate was a water complex formed from the reaction of either *cis*-$Cr(CO)_4PPh_3$ or *trans*-$Cr(CO)_4PPh_3$(cyclohexane) with H_2O However, in the time resolved infra red experiments on $Cr(CO)_6$, it was reported that the the water could easily be removed by a liquid pumping phase in the sample preparation[11] Therefore the inclusion of a liquid pumping phase in the sample preparation in the photolysis of $Cr(CO)_5PPh_3$ should remove transient species produced as a result of reaction with water This third transient species was present with and without a liquid pumping phase and was therefore not formed from the reaction of one of the photochemically produced intermediates with water

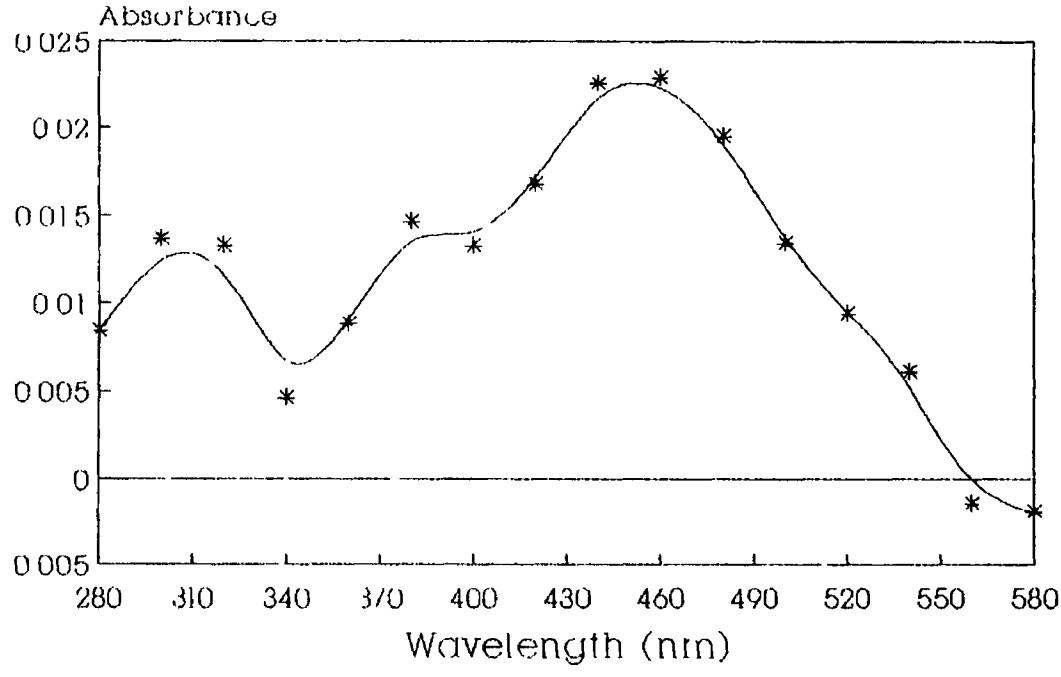

Figure 3.2.2.3.1 A UV/visible difference spectrum of the third transient species obtained 1000μs after the flash under 1 0 atmospheres of argon

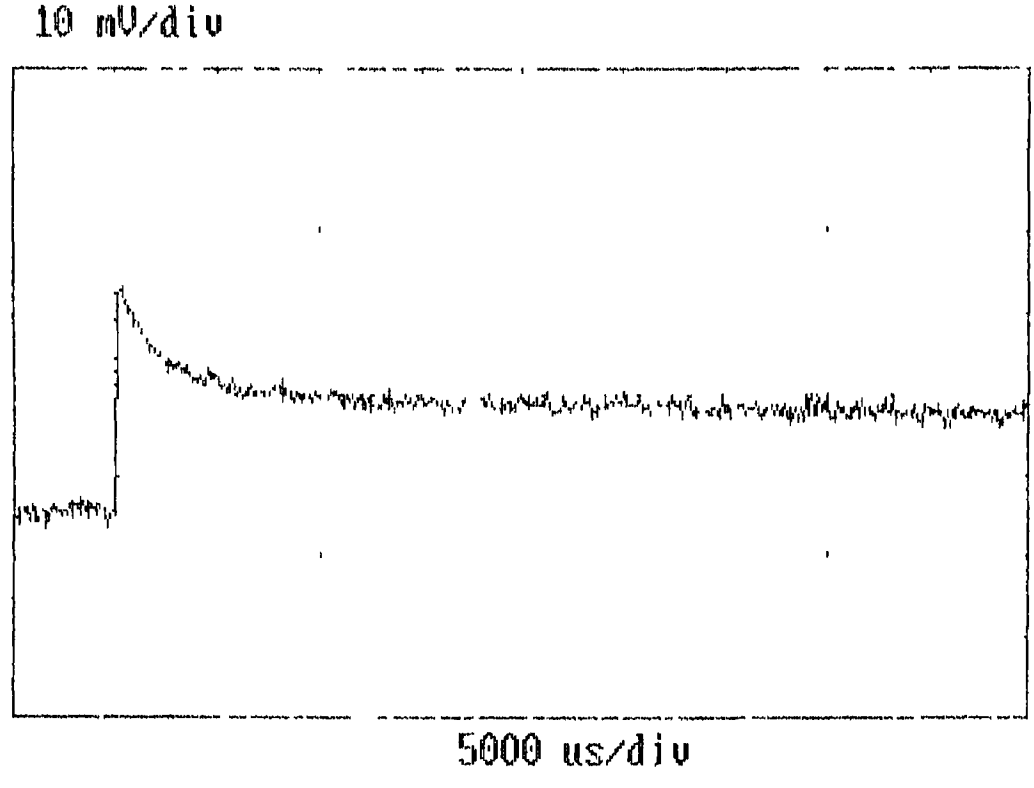

Figure 3.2 2 3 2 A transient signal obtained for the third transient species monitored at 500nm under 0 25 atmospheres of CO

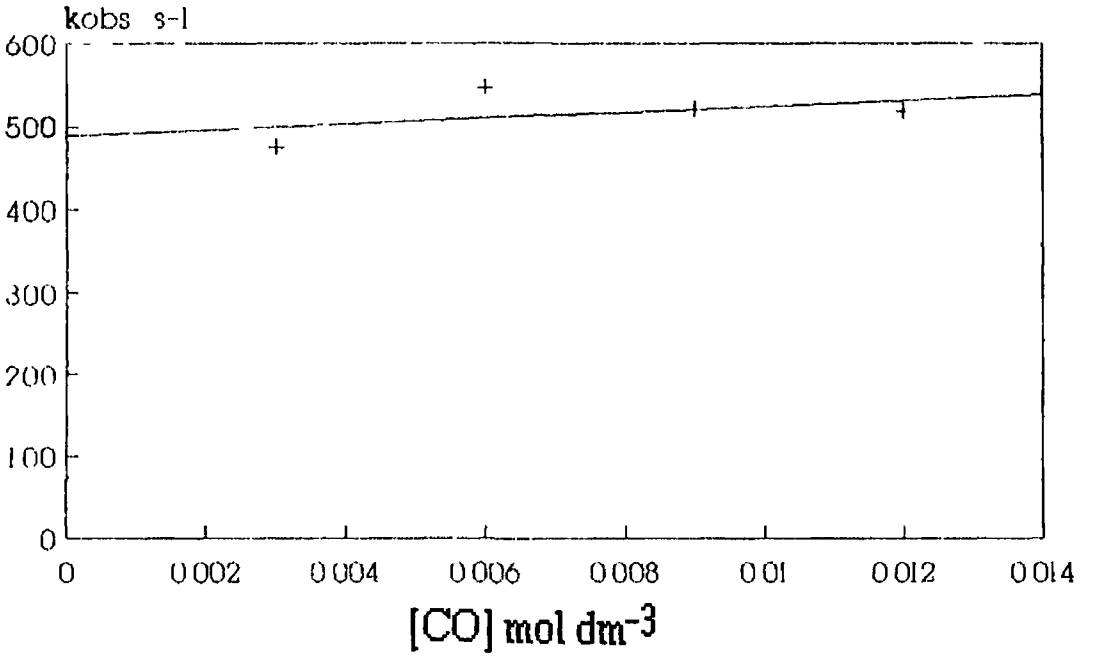

[CO] mol dm^{-3}	k_{obs} (s^{-1})
0 003	475
0 006	546
0.009	520
0 012	518

Figure 3.2.2.3.3 A graphical representation and the experimental data of the concentration of CO (mol dm^{-3}) and the corresponding first order rate constants (s^{-1}) demonstrating the non-reaction of the third transient species with CO at 298K.

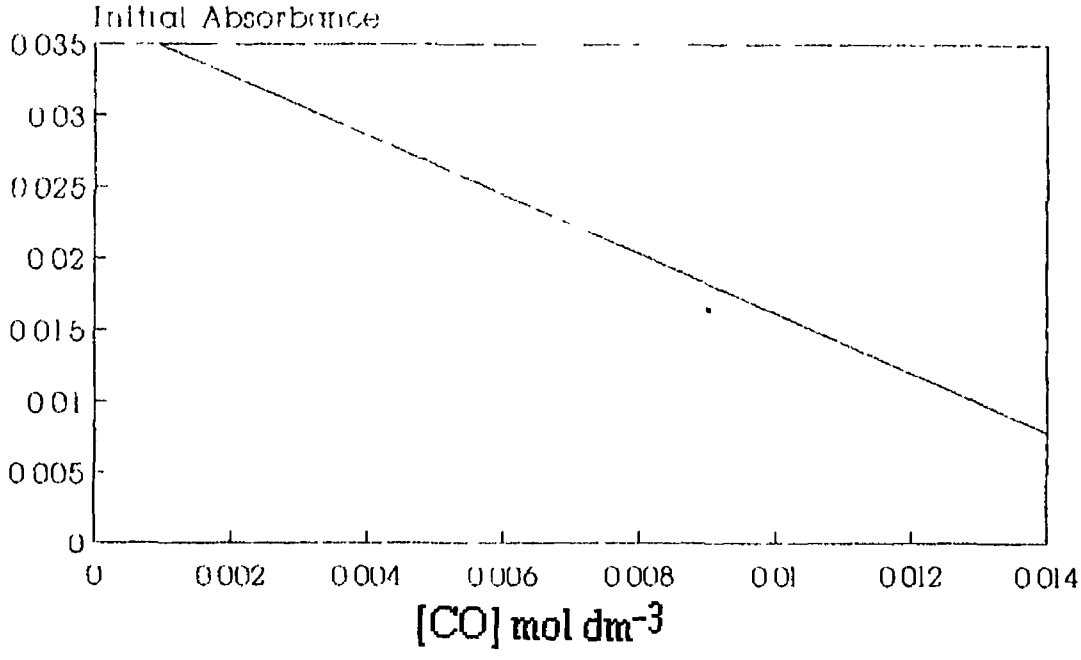

Figure 3 2.2 3 4 A plot of initial absorbance for the third transient species against concentration of CO

3.2.2 4 Fourth transient species

A fourth transient species was observed with a relatively long lifetime of ~1 0 seconds A UV/visible difference spectrum of this complex is shown in Figure 3 2 2 4 1 It can be seen from this spectrum that the maximum absorption for this complex was also at 460nm A transient obtained for this species is shown in Figure 3 2 2 4 2 This species reacted with CO to give a second order rate constant of 489 dm^3 mol^{-1} s^{-1} (Figure 3 2 2 4 3) The kinetic data obtained from long lived transient species are not as accurate as those obtained at shorter timescales because of the added effect of diffusion of photoproduct from the path of the monitoring beam However the diffusion effect is a systematic one and should not affect second order rate constant calculation This species was not a primary photoproduct as again employing transient absorption deconvolution of the transient signal demonstrated that the yield of this species was sensitive to the presence of CO in solution (Figure 3 2 2 4 4)

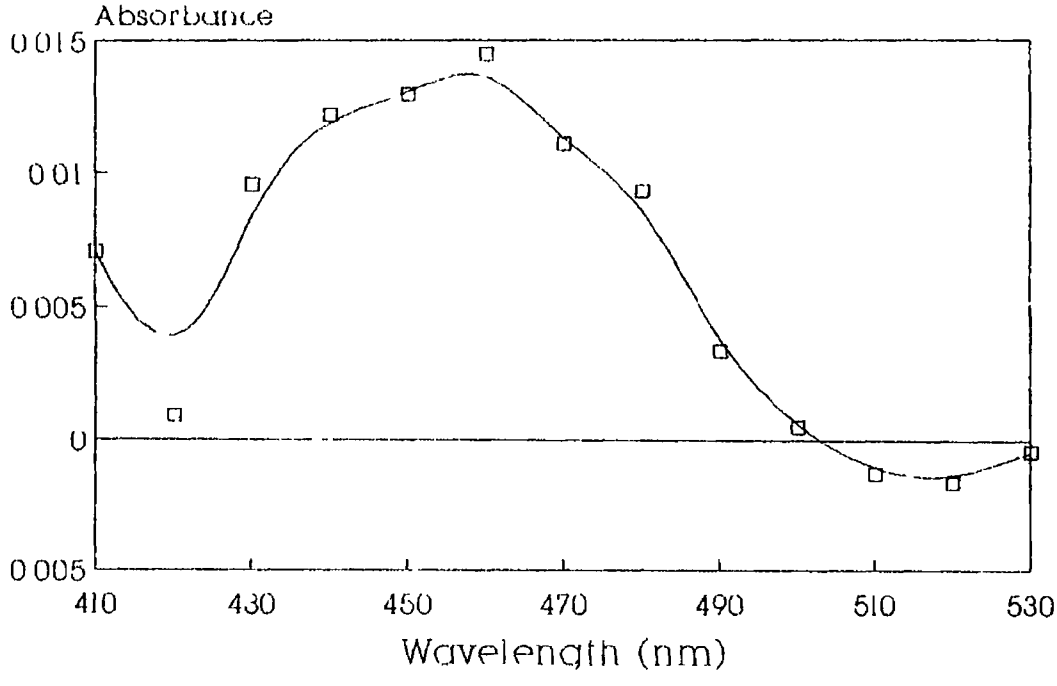

Figure 3.2.2.4.1 A UV/visible difference spectrum of the fourth transient species taken after 40000μs

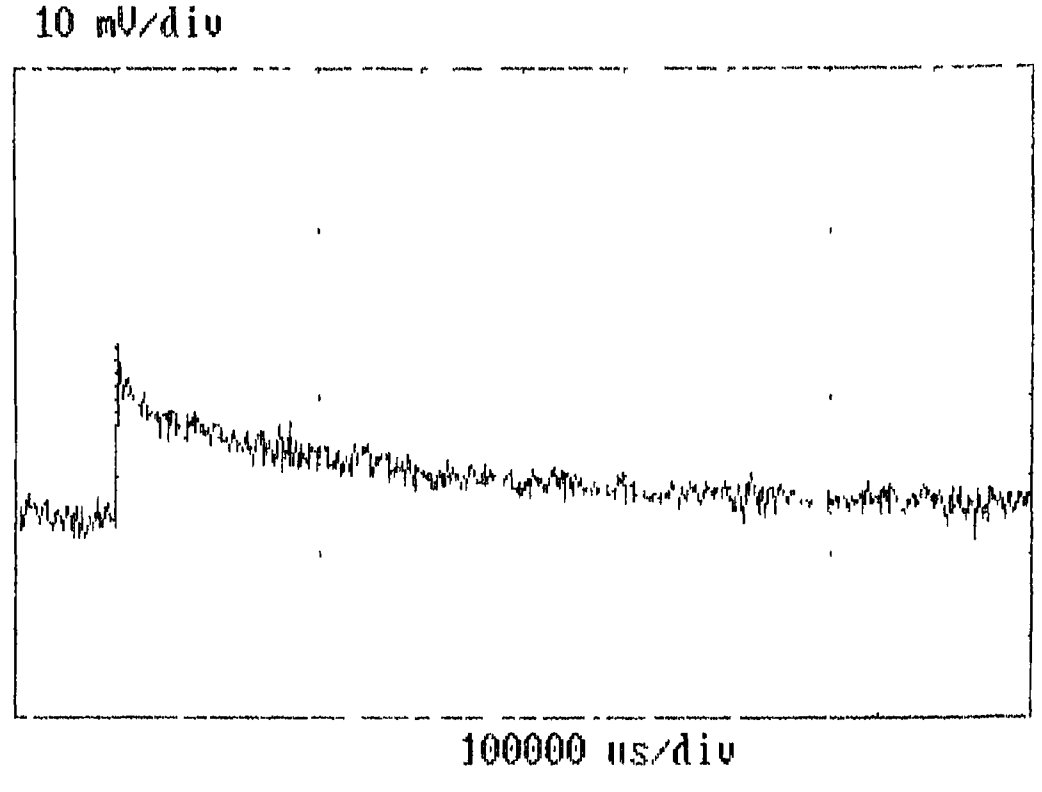

Figure 3.2.2.4.2 A typical transient decay obtained for the decay of the fourth transient species monitored at 500nm under 0 25 atmospheres of CO

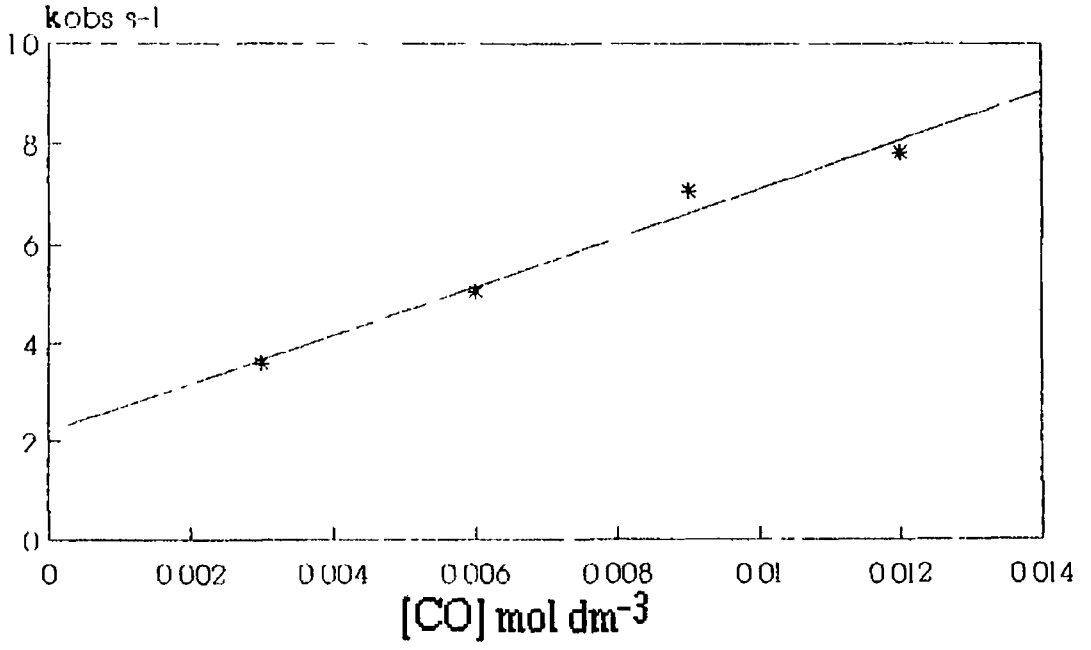

[CO] mol dm^{-3}	k_{obs} (s^{-1})
0.003	3 59
0 006	5 04
0 009	7 04
0.012	7 82

$k_{[CO]} = 489 \pm 55\ dm^3\ mol^{-1}\ s^{-1}$

Intercept = $2\ 2 \pm 0\ 4\ s^{-1}$

Corr coeff = 0 988

Figure 3.2.2.4.3 A table of the concentration of CO (mol dm^{-3}) and the corresponding first order rate constants (s^{-1}) for the reaction of the fourth transient species with CO at 298K

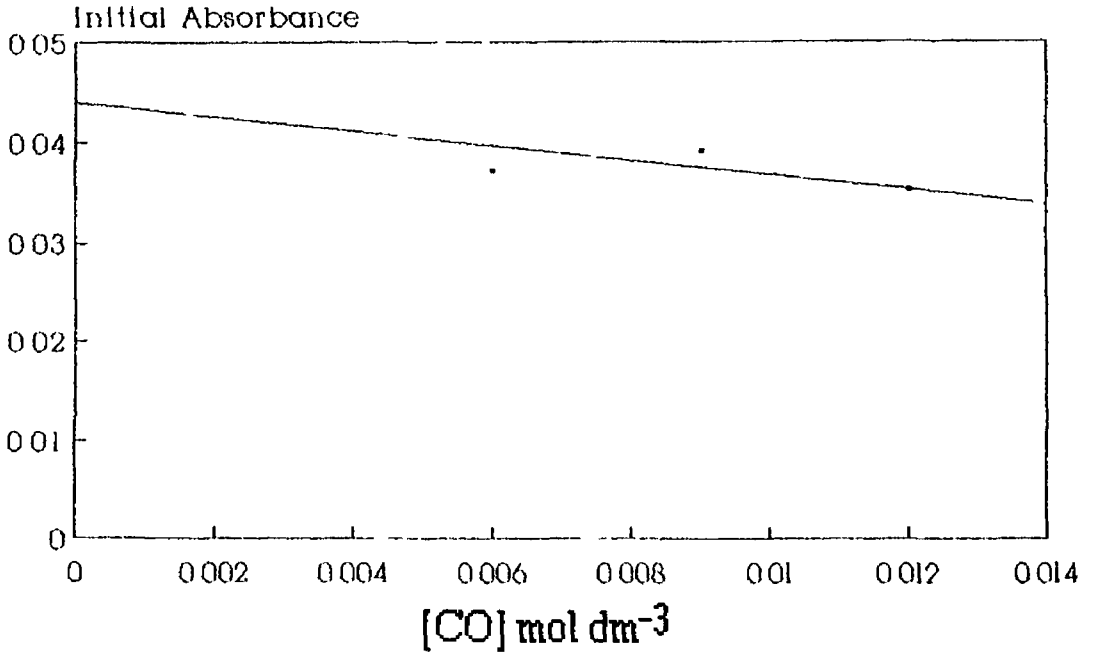

Figure 3.2.2.4.4 A plot of initial absorbance against concentration of CO for the fourth transient species

This fourth transient species was also presumed to be a dinuclear complex. It was present with or without a liquid pumping phase in the sample preparation and therefore was not the result of reaction with water in the solvent

3.2.3 266nm laser flash photolysis of $Cr(CO)_5PPh_3$ with UV/visible monitoring

The 266nm laser flash photolysis of $Cr(CO)_5PPh_3$ in cyclohexane produced evidence for the formation of two transient species These species were identified as a primary photoproduct and a secondary photoproduct Other transient species were observed but were very weak and difficult to analyse Room temperature infra red analysis of this species was not possible because of significant absorption of the infra red cells at 266nm

3.2.3.1 First transient species

The first transient species observed for the 266nm photolysis of $Cr(CO)_5PPh_3$ was surprisingly not *cis* -$Cr(CO)_4PPh_3$ but the *trans* -$Cr(CO)_4PPh_3$(cyclohexane) complex A UV/visible difference spectrum of the first transient species is shown in Figure 3 2 3 1 1 and has a λmax at 480nm the same maximum as the *trans* -$Cr(CO)_4PPh_3$(cyclohexane) species proposed on 355nm excitation The reaction kinetics of this species with CO was the same as for the second transient species compared to the 355nm laser photolysis of $Cr(CO)_5PPh_3$ yielding a second order rate constant of $1\,9 \times 10^6 \pm 2\,0 \times 10^5$ $dm^3\ mol^{-1}\ s^{-1}$ at 298K ($k_{[CO]}$ 355nm = $1\,9 \times 10^6$ $dm^3\ mol^{-1}\ s^{-1}$ at 298K) Therefore this species was identified as *trans* -$Cr(CO)_4PPh_3$(cyclohexane)

3 2 3.2 Second transient species

The characteristics of the second transient species were the same as those observed for the third transient species on 355nm excitation A UV/visible difference spectrum of this complex is shown in Figure 3 2 3 2 1 and has a λmax at 460nm, the same as that observed for the 355nm third species The reaction kinetics of this species were also consistent with the 355nm observations demonstrating that this photocomplex decayed independent of CO concentration

Weak transients were observed on the timebase of the fourth species on 355nm excitation indicating that this species was formed but that its yield had been affected An obvious conclusion from this was that this species was a dinuclear complex formed from the reaction of a primary photoproduct with parent The difference in yield of the dinuclear complexes between 355 and 266nm excitation could be accounted for by the relative extinction coefficients between 355 and 266nm i e 355nm (ε = 1223 $dm^3\ mol^{-1}\ cm^{-1}$), 266nm (ε = 14220 $dm^3\ mol^{-1}\ cm^{-1}$) The difference in magnitude of the extinction coefficients of ~10 corresponds to a difference of ~10 in the concentration of $Cr(CO)_5PPh_3$ at 355nm and 266nm excitation Therefore, the concentration of parent

at 266nm was 10 times less than at 355nm and so preventing the formation of a dinuclear species The overall scheme for the photolysis reactions of $Cr(CO)_5PPh_3$ on 355nm and 266nm excitation is given in Scheme 3 5 1

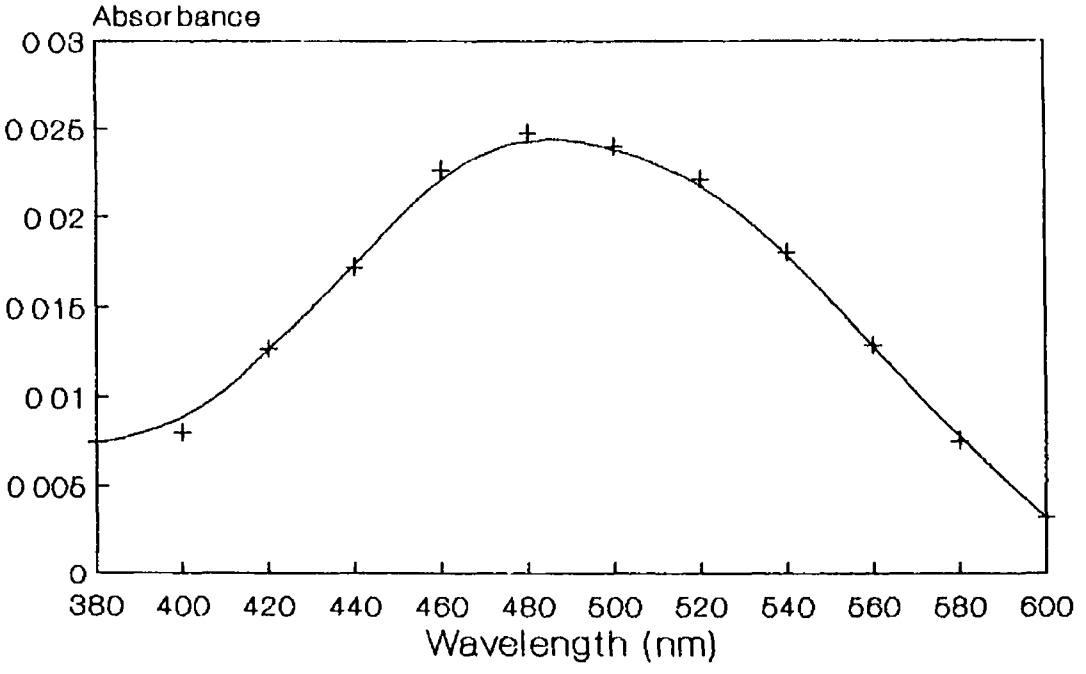

Figure 3.2.3.1.1 A UV/visible difference spectrum of *trans*-$Cr(CO)_4PPh_3$ taken 10μs after the laser pulse

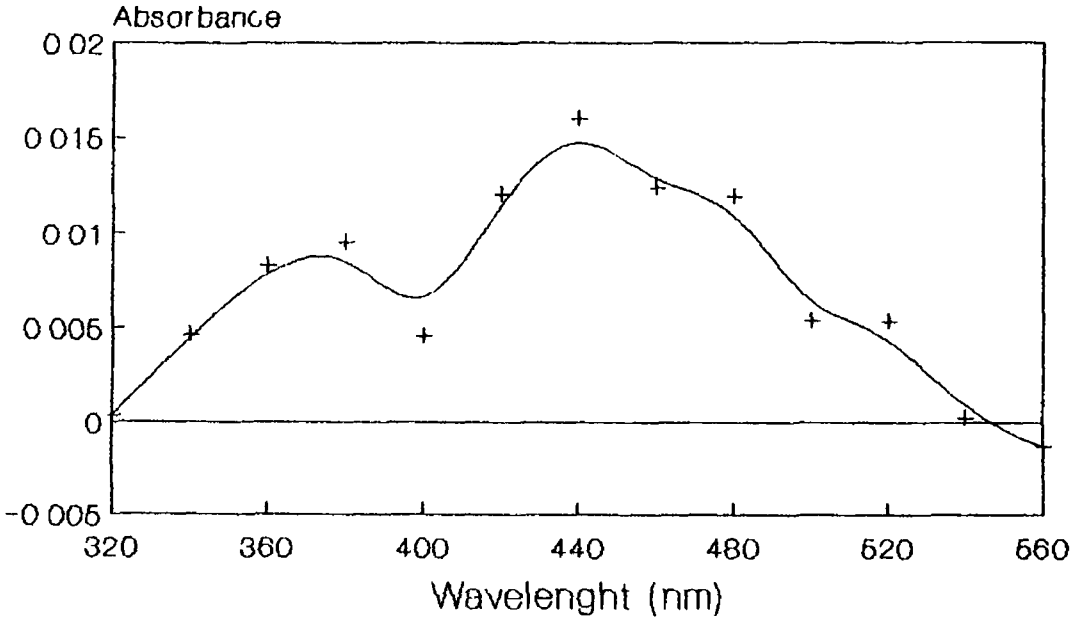

Figure 3.2.3 2.1 A UV/visible difference spectrum of the second transient species taken 2500μs after the laser pulse

3.3 Photolysis of $Mo(CO)_5PPh_3$

3.3.1 Infra red monitored photolysis of $Mo(CO)_5PPh_3$

355nm photolysis, using an Nd YAG laser of room temperature argon degassed cyclohexane solutions of $Mo(CO)_5PPh_3$, was carried out to determine which ligands were lost on photolysis at this wavelength An infra red spectrum of the photolysis result is given in Figure 3 3 1 1 The bands at 2074 and 1952cm^{-1} correspond to the A_1 and E modes respectively of the parent complex The A_2 mode at 1988cm^{-1} usually observed was masked by the photolysis products The parent bands were depleted to produce five new bands at 2024, 1988, 1931, 1907 and 1868cm^{-1} The band at 1988cm^{-1} was indicative of the T_{1u} band of the $Mo(CO)_6$ complex Therefore a triphenylphosphine ligand was lost on photolysis As the experiment was carried out in a sealed system the source of CO must have come from the photoejection of a CO from the parent complex This result was not unexpected as 366nm photolysis of $Mo(CO)_5PPh_3$ in tetrahydrofuran solution also revealed the loss of a triphenylphosphine ligand with a quantum yield of 0 11[5] The CO stretching frequencies at 2024 and 1907cm^{-1} suggested the formation of a *trans* complex. The most likely explanation for this observation was that a $Mo(CO)_4PPh_3$ intermediate produced on photolysis of $Mo(CO)_5PPh_3$ reacted with the free triphenylphosphine generated from unique ligand loss from the parent. The intensity of the 1907cm^{-1} band indicated that this may be the major photoproduct The bands at 1931 and 1868cm^{-1} point to the formation of a *cis* complex, probably $Mo(CO)_4(PPh_3)_2$ Four bands are usually observed for *cis*-$M(CO)_4L_2$ complexes however overlapping of νCO bands prevented the 1945 and 2020cm^{-1} bands being observed. To investigate the reactions further and prevent the formation of $Mo(CO)_6$ excess triphenylphosphine was added to a solution of argon degassed cyclohexane and $Mo(CO)_5PPh_3$ and subsequently photolysed at 355nm as before The photolysis result is shown in Figure 3 3 1 2.

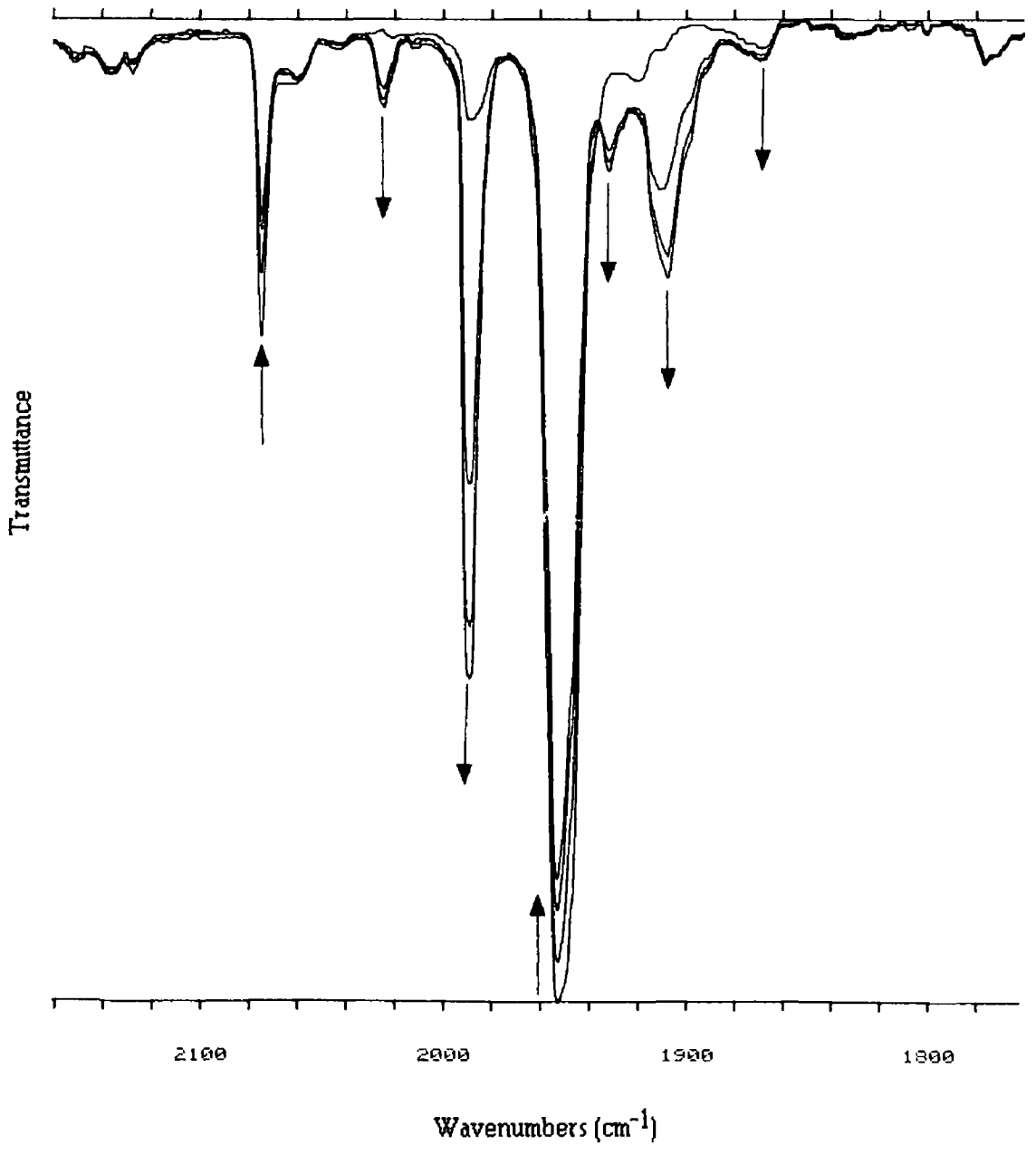

Figure 3.3.1.1 The infra red carbonyl region following 355nm photolysis of $Mo(CO)_5PPh_3$ in argon degassed cyclohexane solution

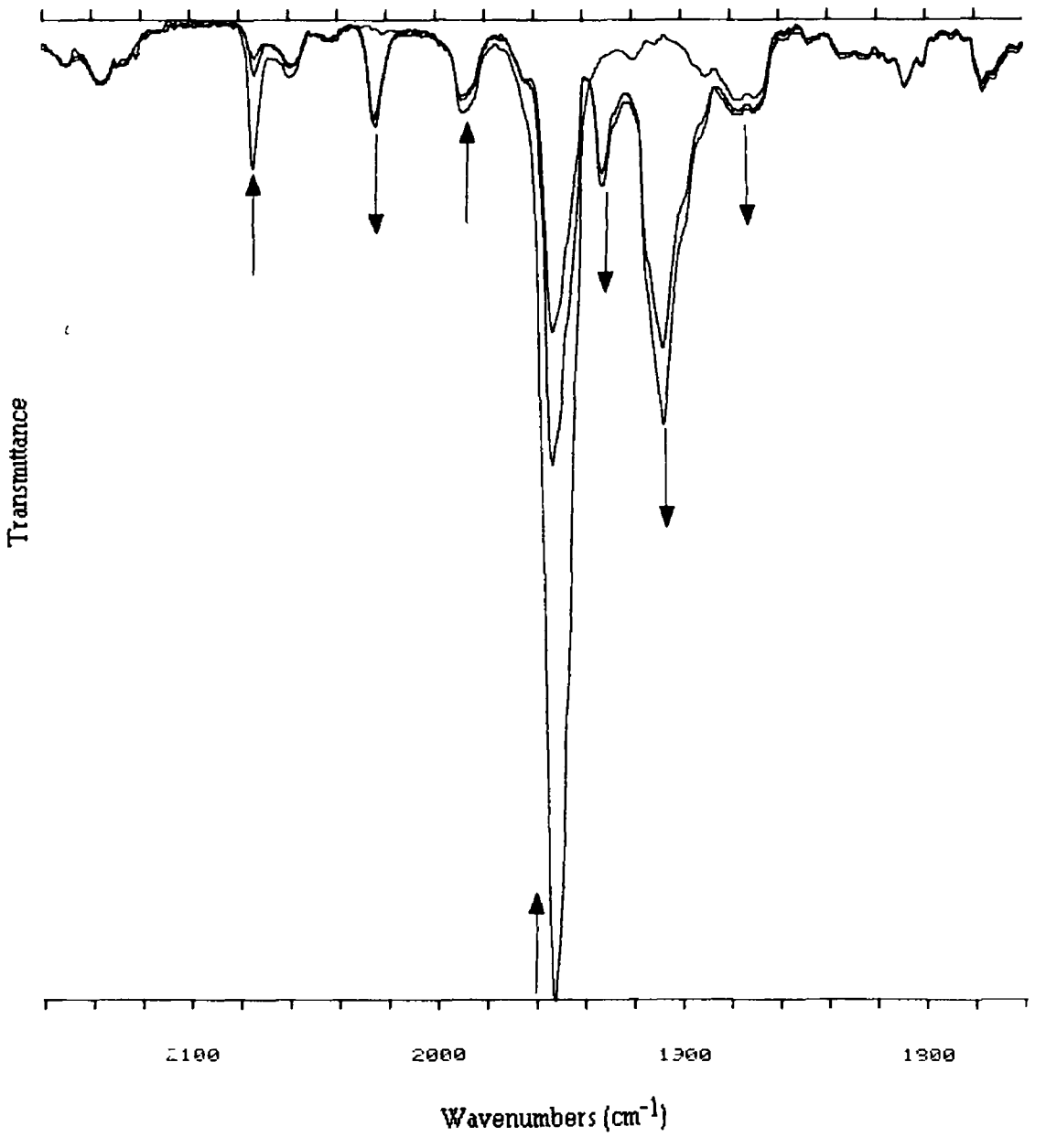

Figure 3.3 1.2 The infra red carbonyl region following the 355nm photolysis of $Mo(CO)_5PPh_3$ with excess triphenylphosphine in argon degassed cyclohexane solution

The infra red spectrum was identical to that obtained for the photolysis of $Mo(CO)_5PPh_3$ in the absence of added ligand except the band indicating the formation of $Mo(CO)_6$ at 1988cm^{-1} was no longer observable presumably because of reaction of any pentacarbonyl produced on photolysis with free triphenylphosphine Again the dominant photoproduct appeared to be the *trans*-$Mo(CO)_4(PPh_3)_2$ complex with a strong absorption at 1907cm^{-1} *cis* configuration $Mo(CO)_4(PPh_3)_2$ was also observed at 1932 and 1876cm^{-1} These observations were in contrast to those observed in tetrahydrofuran solutions by Darensbourg *et al* [5] The dominant photoproduct in this system was the *cis*-$Mo(CO)_4(PPh_3)_2$ complex The difference in the photolysis products may be because of the solvents used in the reactions Tetrahydrofuran is a good σ-donor solvent while cyclohexane has little σ-donating capacity Therefore, the intermediates produced on photolysis would have very different lifetimes The $Mo(CO)_4PPh_3(THF)$ (THF = tetrahydrofuran) intermediate produced on photolysis would be much longer lived than the corresponding cyclohexane intermediate because of a greater capacity of THF to stabilise the intermediate and a significantly higher activation barrier to the displacement of the solvent molecule As a consequence of this longer lifetime the possibility of a rearrangment to the thermodynamically more stable *cis* configuration increases Photolysis experiments carried out by Darensbourg and Murphy on *trans* -$Mo(CO)_4(PPh_3)_2$ in the presence of triphenylphosphine afforded the *cis*-$Mo(CO)_4(PPh_3)_2$ product[5] They observed that *cis*-$Mo(CO)_4(PPh_3)_2$ undergoes thermal rearrangement to *trans*-$Mo(CO)_4(PPh_3)_2$ at elevated temperatures Therefore the *cis* product was the thermodynamically more stable configuration In cyclohexane solution the cyclohexane solvated intermediates produced would have less time to rearrange to the *cis* form and trap an incoming ligand more quickly than the corresponding tetrahydrofuran intermediates Therefore it is possible that initial loss position of a CO ligand may be *trans* to a triphenylphosphine ligand.

3.3.2 355nm laser flash photolysis of $Mo(CO)_5PPh_3$ with UV/visible monitoring

The 355nm laser flash photolysis of $Mo(CO)_5PPh_3$ produced evidence for the formation of five transient species One of these species was identified as the primary photoproduct *cis*-$Mo(CO)_4PPh_3$ The identities of the other species are unknown Tentative assignment of two of these species to possibly *trans* - $Mo(CO)_4PPh_3$(cyclohexane) and $Mo(CO)_5$(cyclohexane) is proposed It was likely that the long lived transients were dinuclear species formed from the reaction of the primary photoproducts with parent complex

3.3 2 1 First transient species

This species was identified as *cis*-$Mo(CO)_4PPh_3$ on the basis of its reactivity with CO and to a lesser extent on its UV/visible difference spectrum A typical transient obtained for this species is shown in Figure 3 3 2 1 1 The fast portion of the transient corresponded to the decay of *cis*-$Mo(CO)_4PPh_3$ complex The slower part of the decay corresponded to the second transient species The difference in reactivity of *cis* and *trans* phosphine substituted molydenum tetracarbonyl intermediates has been reported by Dobson and coworkers on work carried out on $Mo(CO)_4$(NP) where NP = 1-(diethylamino)-2-(diphenylphosphino)ethane[17] The chelating ligand NP contained both nitrogen and phosphorus coordinated moities Laser flash photolysis (λ = 355nm) of this complex in chlorobenzene produced both *cis* and *trans* intermediates from the photocleavage of the nitrogen coordinated ligand site and rearrangment of the intermediate to form a mixture of *cis* and *trans*-$Mo(CO)_4(\eta^1$-NP)(chlorobenzene) isomers The *cis* isomer reacted with added ligand L (L = phosphines and phosphites) two orders of magnitude faster than the corresponding *trans* intermediate to form the *cis* and *trans*-$Mo(CO)_4(\eta^1$-NP)L products In other systems such as *cis*-$W(CO)_4(PPh_3)$(pip)[18] and $W(CO)_5PPh_3$[10] studied by laser flash photolysis the *cis* solvated intermediates formed have been the most reactive

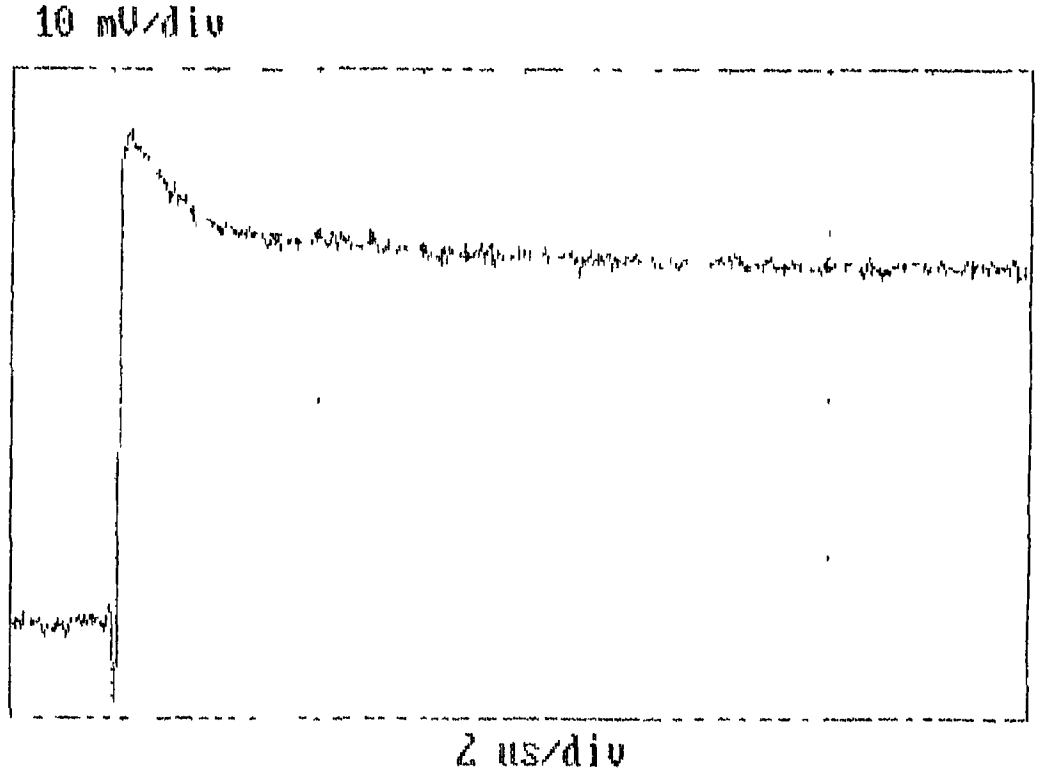

Figure 3.3.2.1.1 A typical transient obtained for the fast species in the 355nm laser flash photolysis of $Mo(CO)_5PPh_3$ under 0 5 atmospheres of CO monitored at 420nm The fast portion of the curve corresponds to the *cis*-$Mo(CO)_4PPh_3$ species

A UV/visible difference spectrum of *cis*-$Mo(CO)_4PPh_3$ can be seen in Figure 3.3 2 1 2 A UV/visible difference spectrum of $Mo(CO)_5$(cyclohexane) obtained from the 355nm photolysis of $Mo(CO)_6$ is displayed in Figure 3 3 2 1 3 These spectra were different with maxima at 420nm and 480nm for *cis*-$Mo(CO)_4PPh_3$ and a single maximum for $Mo(CO)_5$(cyclohexane) at 420nm In order to demonstrate conclusively that this species was not $Mo(CO)_5$(cyclohexane) a study was carried out by varying the concentration of CO in the cyclohexane solution to calculate the second order rate constant for the reaction of *cis*-$Mo(CO)_4PPh_3$ with CO A graph of the concentration of CO against the observed rate constant is shown in Figure 3 3 2 1 4 The slope of this graph corresponded to the second order rate constant and was calculated as 1.51×10^8 $dm^3\ mol^{-1}\ s^{-1}$ This experiment demonstrated that this species was not

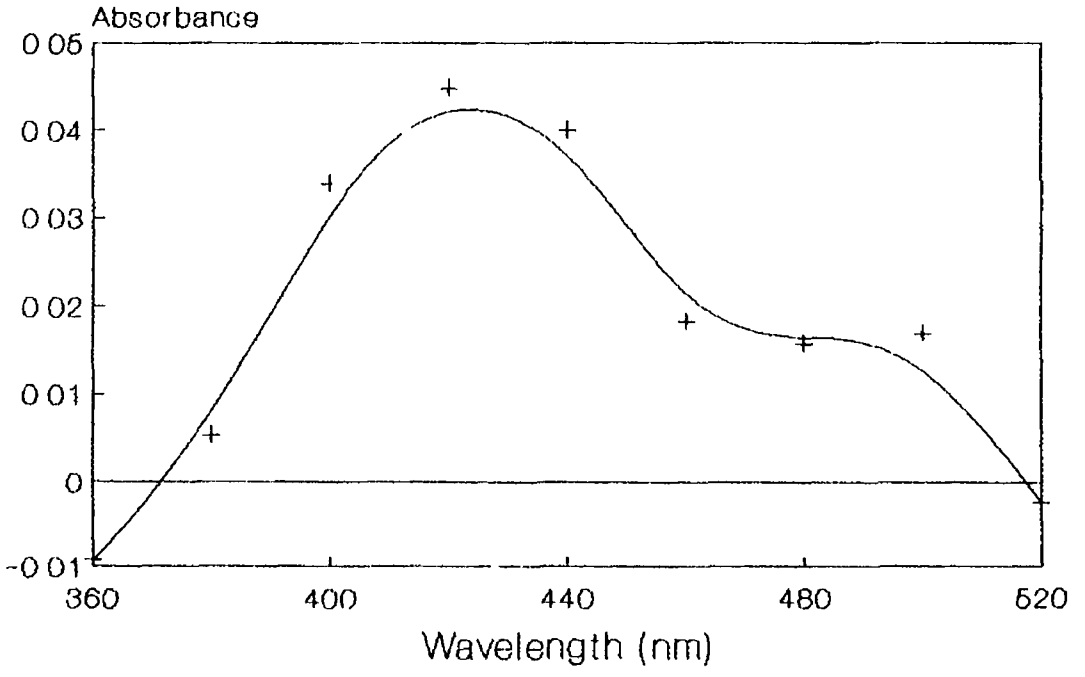

Figure 3.3.2.1.2 A UV/visible difference spectrum of *cis* -$Mo(CO)_4PPh_3$ obtained from the 355nm laser flash photolysis of $Mo(CO)_5PPh_3$ 2μs after the laser pulse

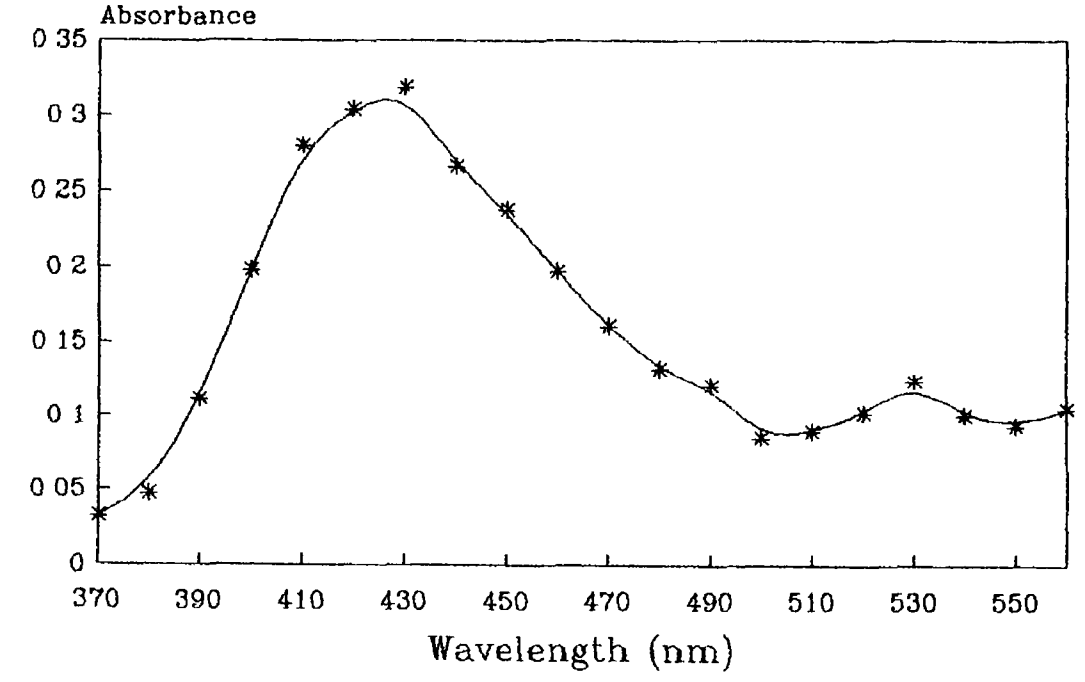

Figure 3.3.2.1.3 A spectrum of $Mo(CO)_5$(cyclohexane) obtained from the 355nm photolysis of $Mo(CO)_6$ in cyclohexane 0.2μs after the laser pulse

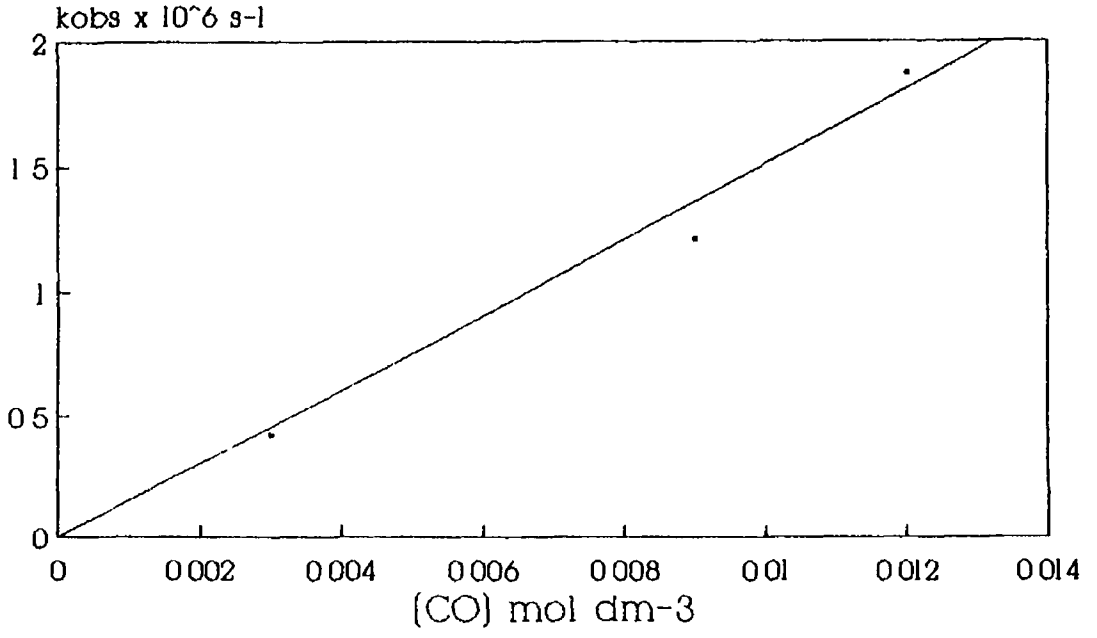

[CO] mol dm^{-3}	$k_{obs} \times 10^{-6}$ (s^{-1})
0 003	0 42
0 006	1 03
0 009	1 21
0 012	1 87

$$k_{[CO]} = 1\ 51 \times 10^{8} \pm 2\ 16 \times 10^{7}\ dm^{3}\ mol^{-1}\ s^{-1}$$

$$\text{Intercept} = 4\ 88 \times 10^{-4} \pm 1\ 45 \times 10^{5}\ s^{-1}$$

$$\text{Corr Coeff} = 0\ 98$$

Figure 3.3.2.1 4 A plot of k_{obs} (s^{-1}) against concentration of CO (mol dm^{-3}) for the reaction of *cis*-$Mo(CO)_4PPh_3$ with CO at 298K

$Mo(CO)_5$(cyclohexane) as the second order rate constant for the reaction of $Mo(CO)_5$(cyclohexane) with CO was calculated as 2 4 x 10^6 dm^3 mol^{-1} s^{-1} from the 355nm photolysis of $Mo(CO)_6$ in a CO saturated cyclohexane solution The second order rate constant for *cis*-$Mo(CO)_4PPh_3$ was very fast for a reaction in cyclohexane solution and indicates that perhaps the intermediate was not solvated on the timescale of the experiment Therefore as in the case of the chromium analogue the bulky triphenylphosphine ligand may be preventing coordination of a solvent molecule to the metal centre The formation of this species indicates that it may be a primary photoproduct In order to prove that *cis* -$Mo(CO)_4PPh_3$ was indeed a primary photoproduct the transients obtained at various concentrations of CO were fitted with a double exponential curve The parameter corresponding to the intercept of the decay of the *cis*-$Mo(CO)_4PPh_3$ component and hence the initial absorbance of this species was plotted against CO concentration (Figure 3 3 2 1 5) The initial absorbance of *cis*-$Mo(CO)_4PPh_3$ and therefore its concentration did not change with varying CO concentration after 0 5 atmospheres of added CO This demonstrated that the yield of *cis*-$Mo(CO)_4PPh_3$ was unaffected by changing CO concentration indicating that it was a primary photoproduct The loss in yield indicated in the graph for a CO concentration of 0 003 mol dm^{-3} may be because of an isomerisation process from *cis* to *trans*-$Mo(CO)_4PPh_3$ which could have taken place on the timescale of the reaction of the *cis*-$Mo(CO)_4PPh_3$ intermediate with CO The addition of CO would prevent the isomerisation process and therefore increase the yield of $Mo(CO)_5PPh_3$ produced from a *cis* derivative

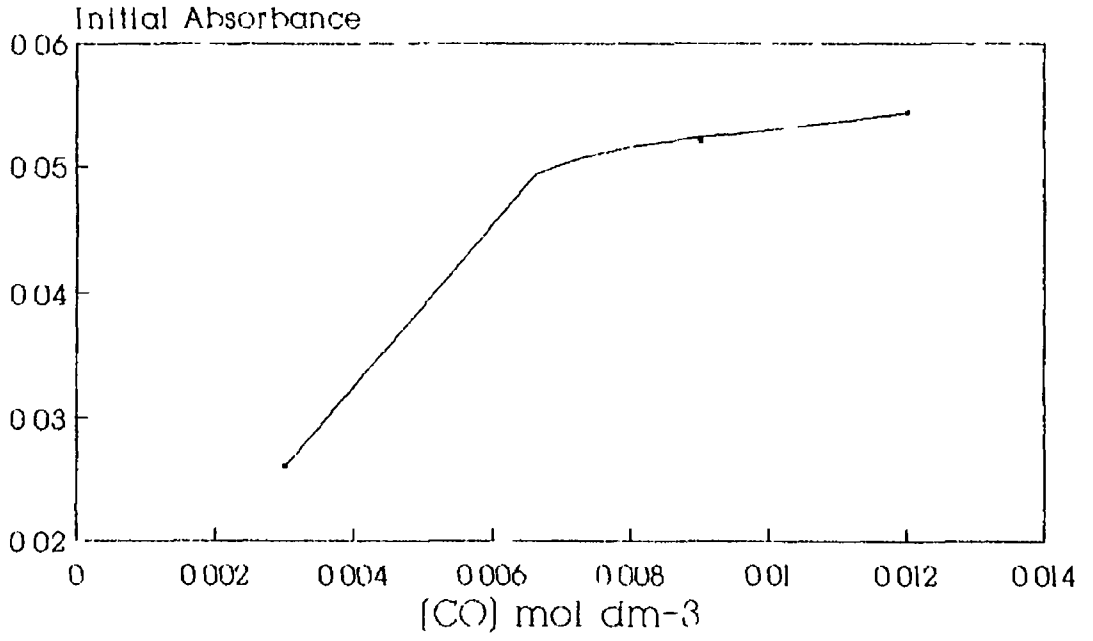

Figure 3.3.2 1.5 A plot of the initial absorbance of *cis* -$Mo(CO)_4PPh_3$ against concentration of CO in cyclohexane solution

3.3.2 2 Second transient species

The second transient species could not be unambiguously assigned but could be $Mo(CO)_5$(cyclohexane) A UV/visible difference spectrum of this intermediate obtained after 50 μs is presented in Figure 3 3 2 2 1 The spectral feature of this species was similar to those observed for $Mo(CO)_5$(cyclohexane) i e. λmax ~420nm A typical transient of this species is depicted in Figure 3 3 2 2 2 Its decay follows psuedo first order reaction kinetics A plot of the observed rate constant against different concentrations of CO gave a straight line with a slope of 3 8 x 10^6 dm^3 mol^{-1} s^{-1} This second order rate constant was not very different to that obtained for $Mo(CO)_5$(cyclohexane) at 2 4 x 10^6 dm^3 mol^{-1} s^{-1} and therefore it was possible that this species was $Mo(CO)_5$(cyclohexane) A graph of initial absorbance against concentration of CO in solution, shown in Figure 3.3 2 2 4, indicated that the yield of this species increased with increasing CO concentration. This observation was

consistent with loss of unique ligand from the parent complex because in the presence of CO, any $Mo(CO)_5$(cyclohexane) formed would react with CO to form $Mo(CO)_6$ Since a flow through sample cell was not used in the experiments the concentration of $Mo(CO)_6$ in the sample cell would increase with increasing laser photolysis This would increase the concentration of $Mo(CO)_5$(cyclohexane) in the sample solution as both $Mo(CO)_6$ and $Mo(CO)_5PPh_3$ would be photolysed in subsequent laser pulses The inclusion of a liquid pumping phase did not affect the formation of transient species so it was not produced from the reaction of a transient intermediate with water in the solvent

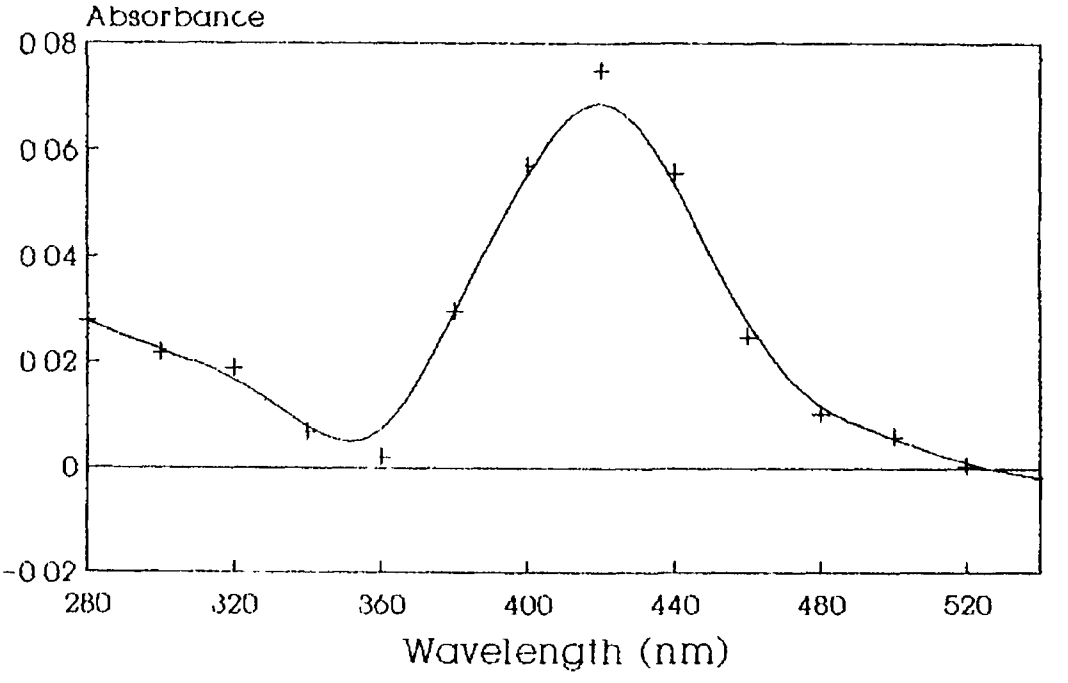

Figure 3.3.2.2.1 A UV/visible difference spectrum obtained 50μs after the laser pulse for the second transient species

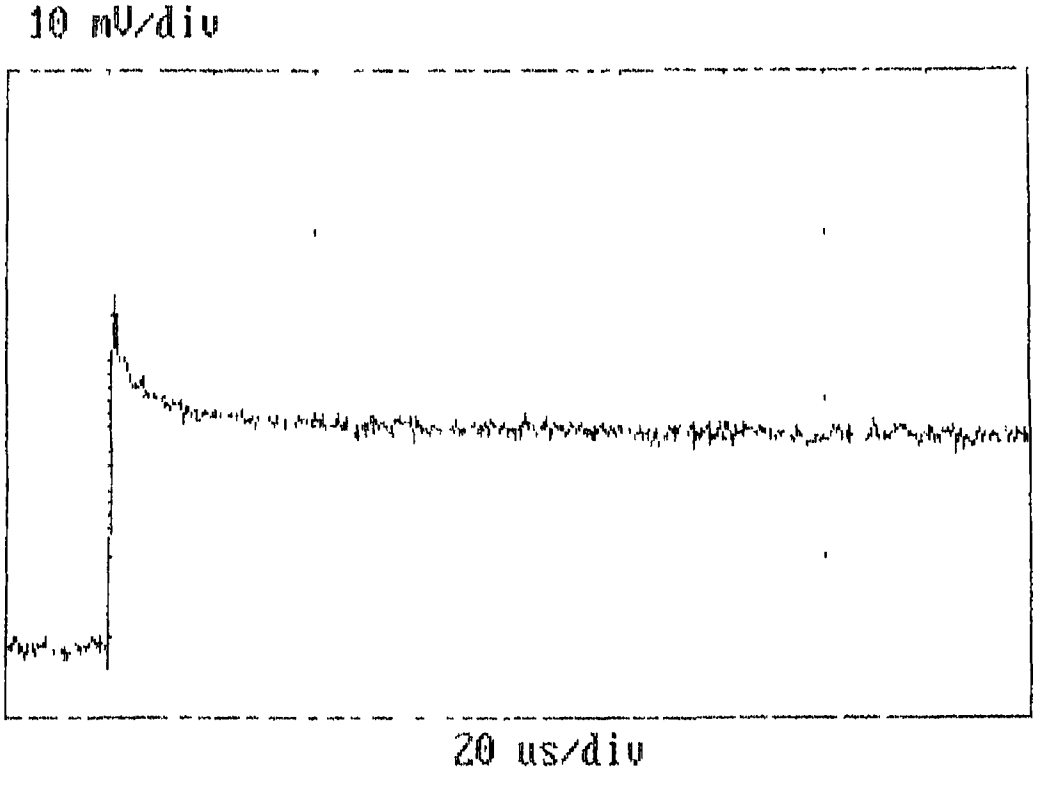

Figure 3.3 2.2.2 A typical transient obtained for the second transient species obtained under 1 0 atmosphere of CO monitored at 420nm

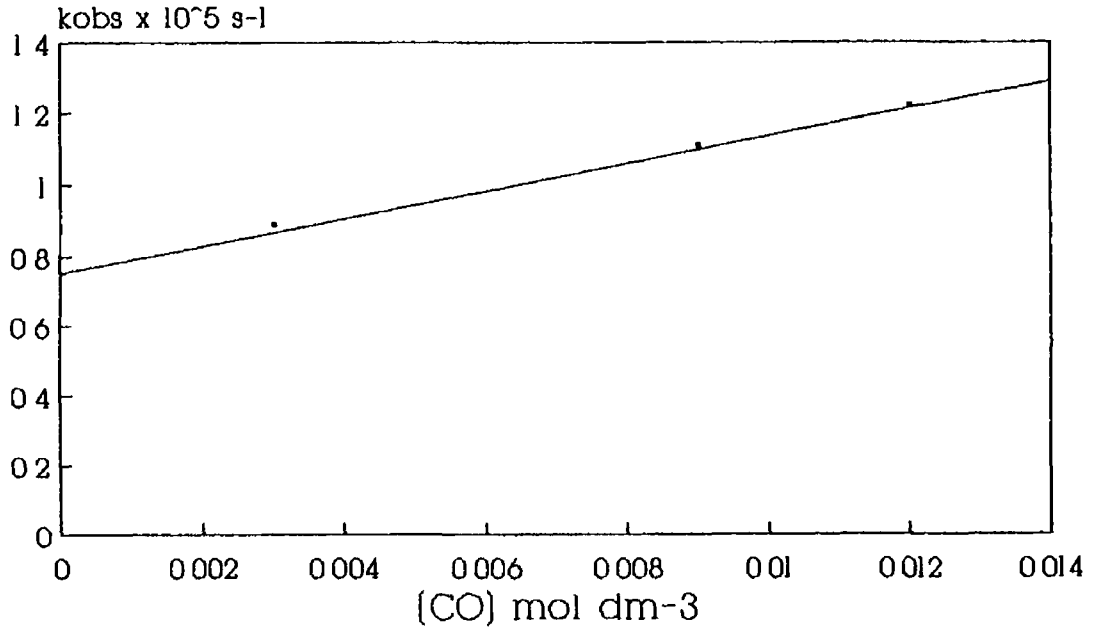

[CO] mol dm^{-3}	k_{obs} x 10^{-5} (s^{-1})
0 003	0 89
0 006	0 95
0 009	1 11
0 012	1 22

$k_{[CO]} = 3\ 83 \times 10^{6} \pm 4\ 41 \times 10^{5}\ dm^{3}\ mol^{-1}\ s^{-1}$

Intercept = $7\ 55 \times 10^{4} \pm 2\ 96 \times 10^{3}\ s^{-1}$

Corr Coeff = 0 985

Figure 3.3.2 2.3 A plot of the observed rate constant (s^{-1}) for the second transient species against the concentration of CO (mol dm^{-3}) in solution at 298K

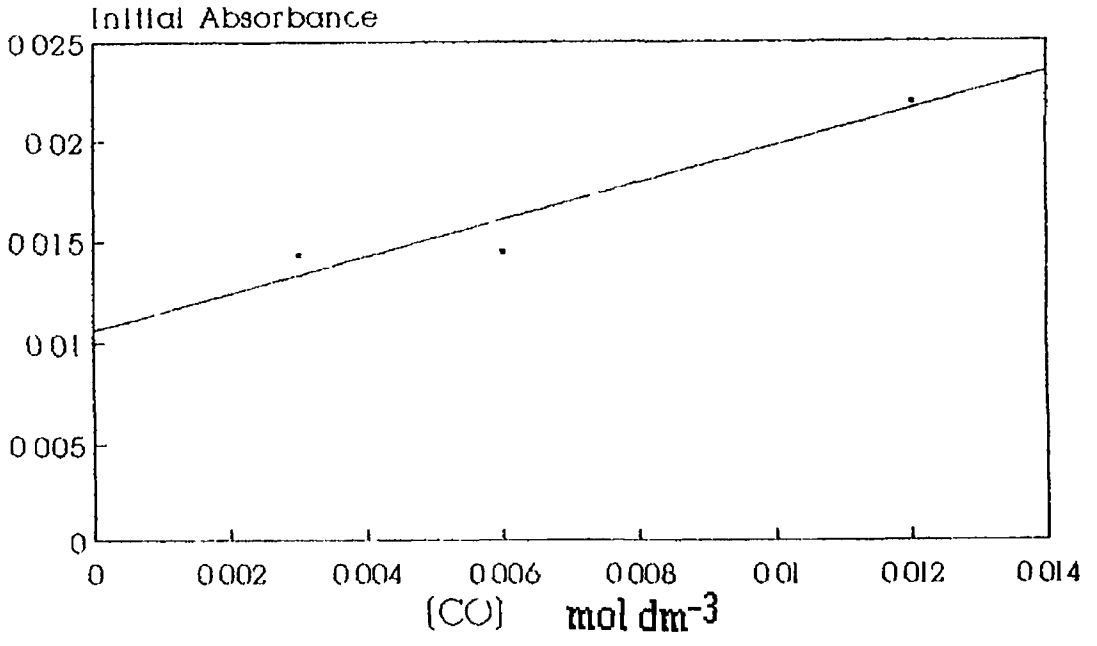

Figure 3.3.2.2.4 A plot of initial absorbance of the second transient species against concentration of CO in cyclohexane solution

3.3 2.3 Third transient species

The identity of this species was unknown but it reacts with parent complex and therefore it appears that it is a primary photoproduct possibly *trans*-$Mo(CO)_4PPh_3$ A UV/visible difference spectrum of this intermediate is shown in Figure 3 3.2 3 1 and consists of a single broad band with a λmax at 410nm not unlike the spectra of the other species A typical transient of this species is depicted in Figure 3 3 2 3.2 with the fast part of the decay corresponding to the third transient species. This species showed dependence on CO concentration and a plot of the observed rate constant against CO concentration is shown in Figure 3 3 2 3 3 The slope of this graph yielded a second order rate constant of $4\ 0 \times 10^5$ $dm^3\ mol^{-1}\ s^{-1}$ The decay of this species at 420nm was accompanied by the grow in of a band at 360nm The rate of this grow in was dependent on the concentration of $Mo(CO)_5PPh_3$ in the solution

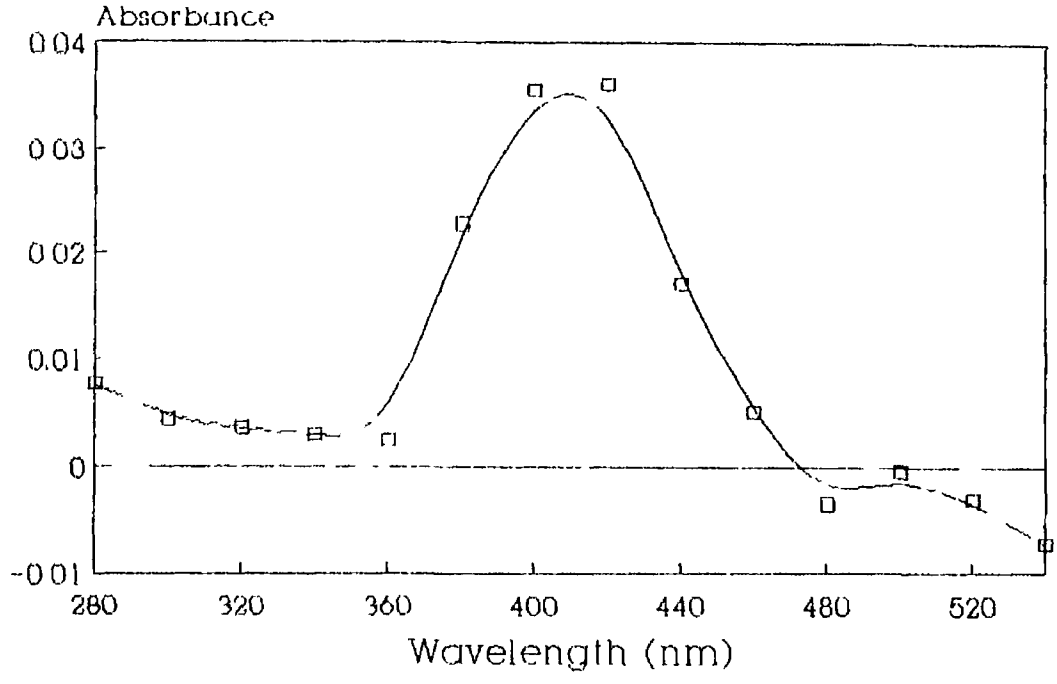

Figure 3.3.2.3.1 A UV/visible difference spectrum obtained for the third transient species 600μs after the laser pulse

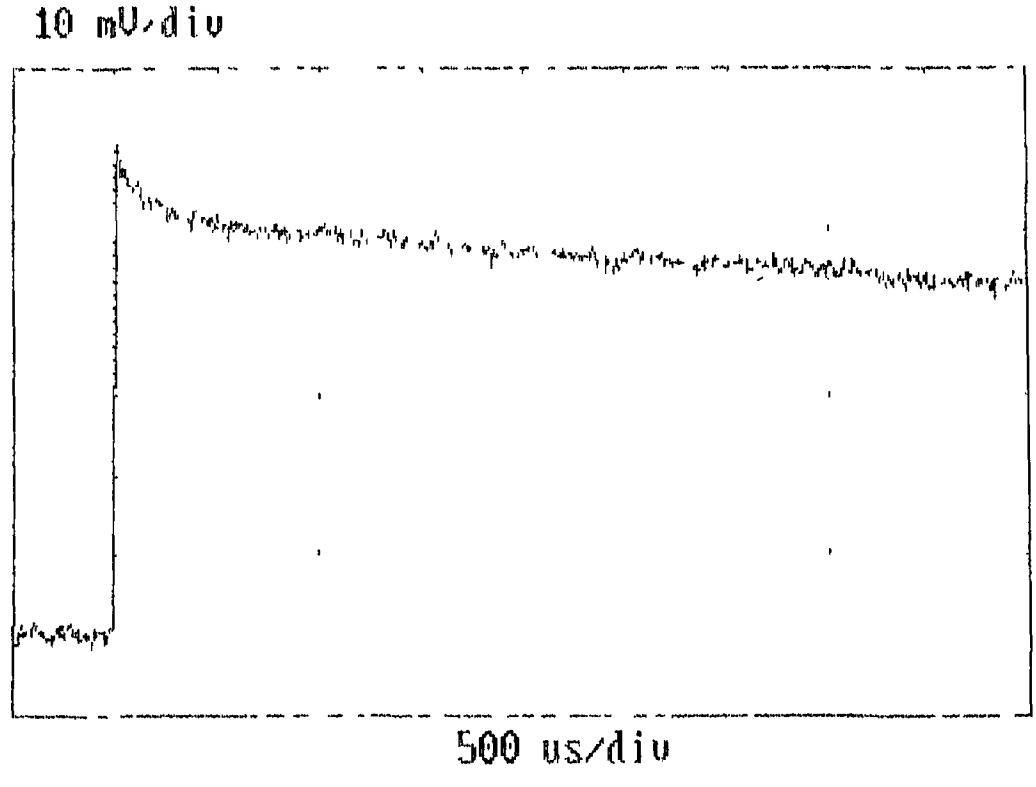

Figure 3.3.2.3.2 A typical transient for the third species obtained from the 355nm photolysis of $Mo(CO)_5PPh_3$ in cyclohexane containing 0.25 atmospheres of CO monitored at 420nm

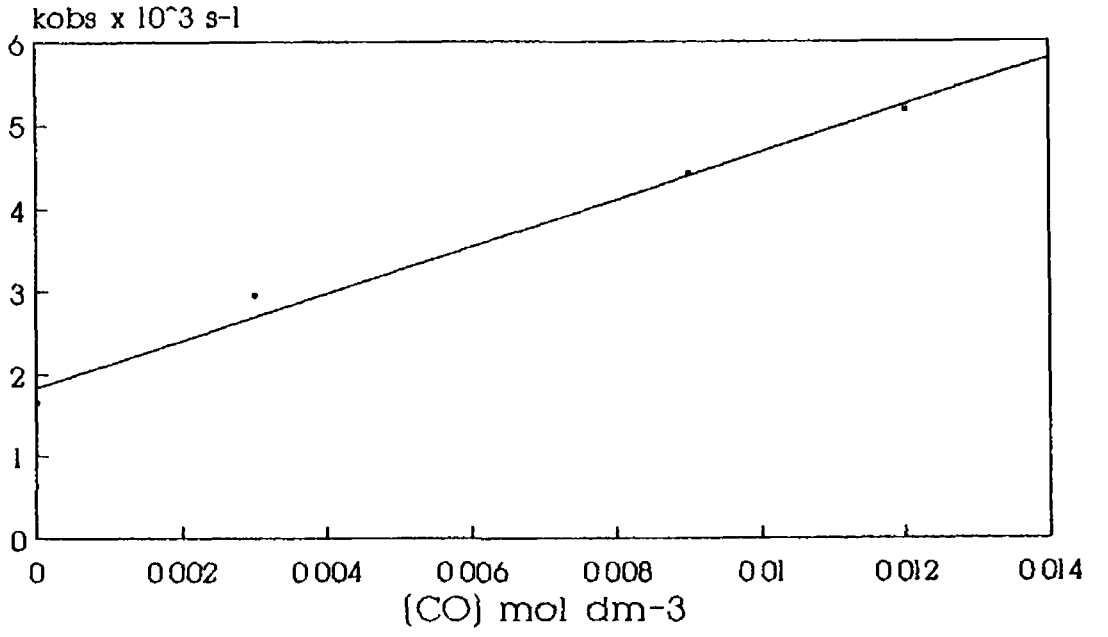

[CO] mol dm^{-3}	k_{obs} x 10^{-3} (s^{-1})
0 000	1 64
0 003	2 94
0 009	4 40
0 012	5 16

$k_{[CO]} = 4\ 00 \times 10^{5} \pm 3\ 49 \times 10^{4}\ dm^{3}\ mol^{-1}\ s^{-1}$

Intercept = $5\ 30 \times 10^{2} \pm 2\ 48 \times 10^{2}\ s^{-1}$

Corr Coeff = 0 993

Figure 3.3.2.3.3 A plot of the observed rate constant (s^{-1}) for the third transient species against the concentration of CO (mol dm^{-3}) in cyclohexane solution at 298K

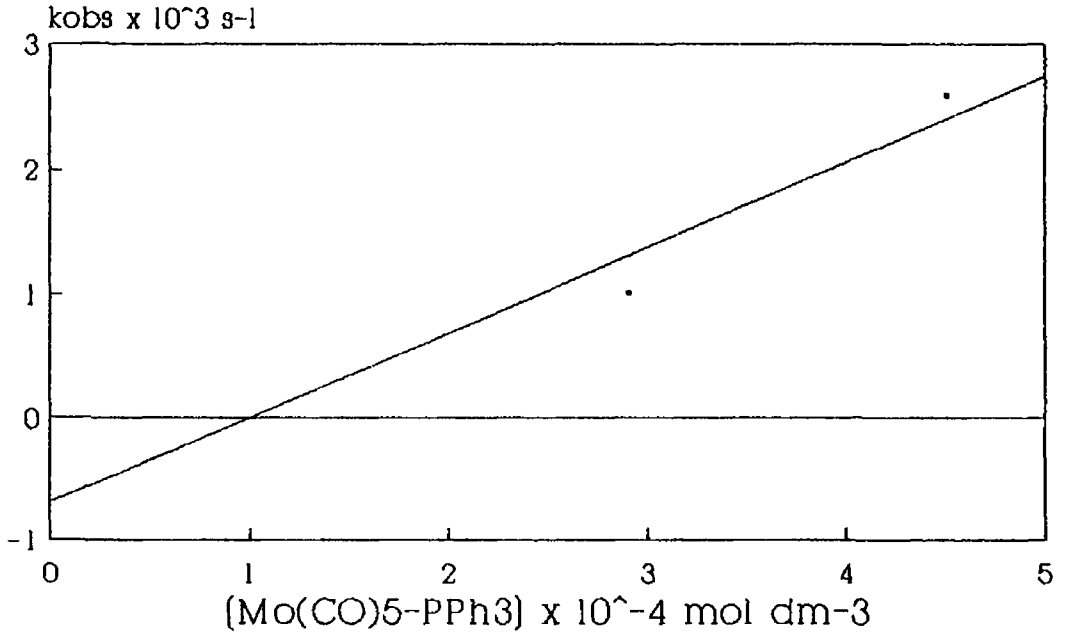

$[Mo(CO)_5PPh_3]$ x 10^{-4} mol dm^{-3}	k_{obs} (s^{-1})
1 2	356
2 2	721
2 9	1004
4 5	2590

$k[Mo(CO)_4PPh_3] = 6.95 \times 10^6 \pm 1\ 21 \times 10^6\ dm^3\ mol^{-1}\ s^{-1}$

Intercept = $-694 \pm 289\ s^{-1}$

Corr Coeff = 0 971

Figure 3.3.2.3.4 A plot of concentration of parent complex (mol dm^{-3}) against the observed rate constants (s^{-1}) for the reaction of the third transient species at 298K

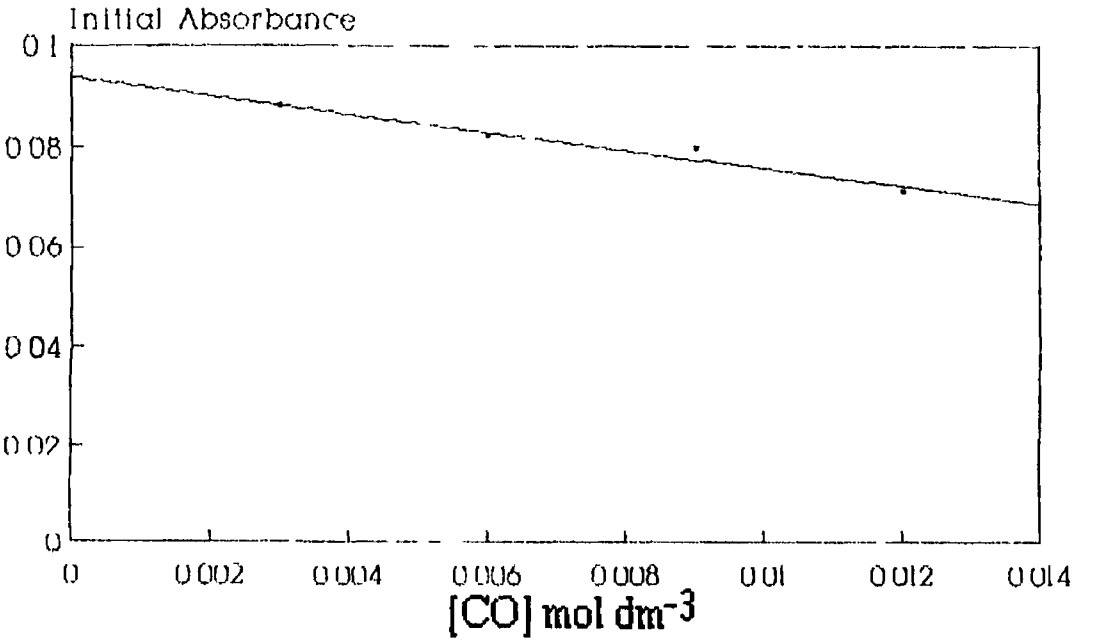

Figure 3.3.2.3.5 A plot of initial absorbance of the third transient species against concentration of CO in cyclohexane solution

A plot of concentration of parent against the observed rate constant (Figure 3 3 2 3 4) gave a second order rate constant of 6 95 x 10^6 dm^3 mol^{-1} s^{-1} This indicates that perhaps this species is a primary photoproduct which was reacting with parent to form a dinuclear species in solution A plot of the initial absorbance of this species against the concentration of CO in cyclohexane shows that the initial absorbance of this species decreased by a small amount as the CO concentration increased This observation may be because of the isomerisation process which was proposed for the drop in yield of the *cis* -$Mo(CO)_4PPh_3$ intermediate The prevention of the *cis* intermediate from isomerising to the *trans* configuration would decrease the yield of *trans* in the solution Another possibility which may not be overlooked is the loss of parent complex by the formation of $Mo(CO)_6$ which would also decrease the amount of *trans*-$Mo(CO)_4PPh_3$ Given the lifetime and the configuration of the intermediate it was most likely that it was solvated in solution The bulky triphenylphosphine ligand, in a *trans* configuration, would be in an axial position at the furthest point from the

vacant coordination site Therefore, like $Mo(CO)_5$(cyclohexane) this intermediate was probably solvated The transient species was not the result of the reaction with water in the solvent as it was present with or without a liquid pumping stage in the sample preparation

3 3.2.4 Fourth transient species

The fourth transient species was most probably a dinuclear species produced from the reaction of one of the primary photoproducts with an unphotolysed parent complex A UV/visible difference spectrum of this complex is presented in Figure 3 3 2 4 1 and has a λmax of 400nm unlike the other species A typical transient for this species is depicted in Figure 3 3 2 4 2 This species reacted with CO and a graph of the observed rate constant against the concentration of CO in cyclohexane solution is shown in Figure 3 3 2 4 3 and yielded a second order rate constant of 6 0 x 10^3 dm^3 mol^{-1} s^{-1} The yield of this product was sensitive to the presence of CO in the solution and a graph of initial absorbance against concentration of CO (Figure 3 3 2 4 4) shows the loss in yield as the concentration of CO increased Therefore this species was a secondary photoproduct

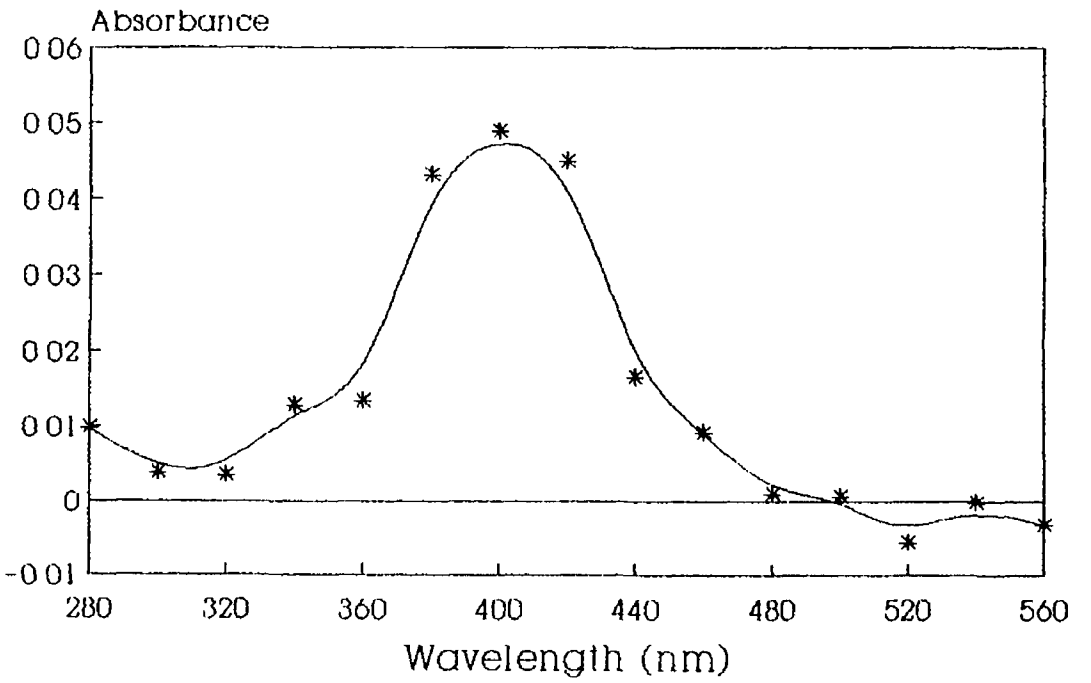

Figure 3.3.2.4.1 A UV/visible difference spectrum obtained for the fourth transient species under 1 0 atmospheres of argon at 20000μs after the laser pulse

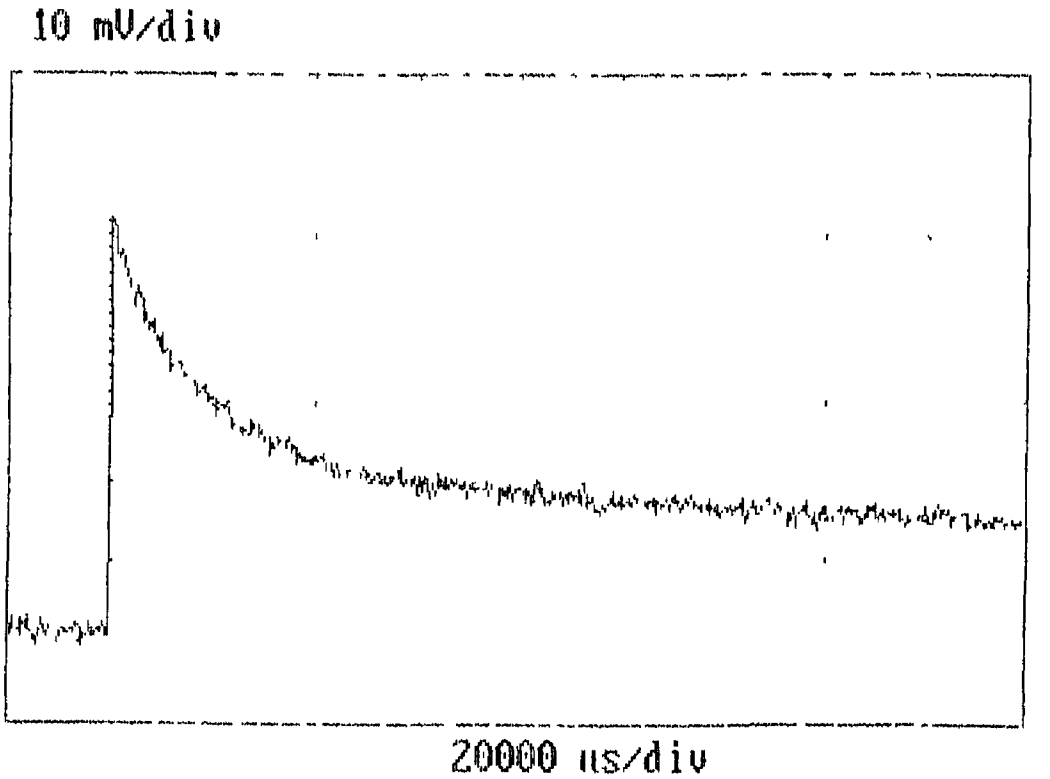

Figure 3.3.2 4.2 A typical transient of the fourth species obtained at 420nm under 0 25 atmospheres CO

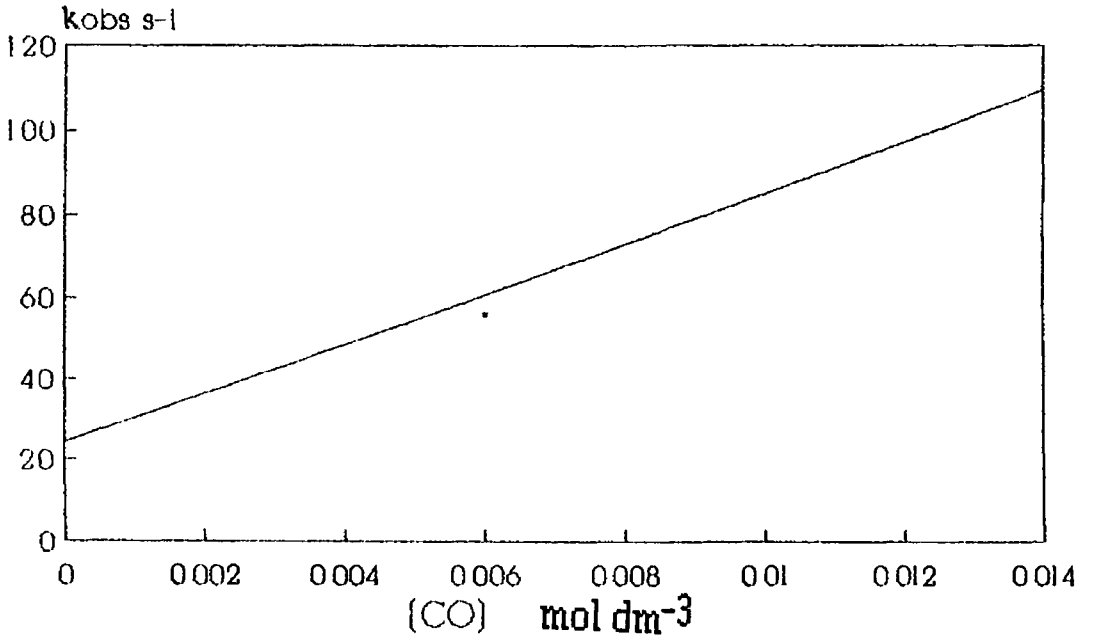

[CO] mol dm^{-3}	k_{obs} (s^{-1})
0 003	49 9
0 006	55.9
0 009	75 4
0 012	101 3

$$k_{[CO]} = 5\ 79 \times 10^{3} \pm 1\ 06 \times 10^{3}\ dm^{3}\ mol^{-1}\ s^{-1}$$

Intercept = 27 2 ± 7 12 s^{-1}

Corr Coeff = 0 967

Figure 3.3.2.4.3 A plot and the experimental data of the observed rate constant (s^{-1}) for the fourth transient species against the concentration of CO (mol dm^{-3}) in solution at 298K

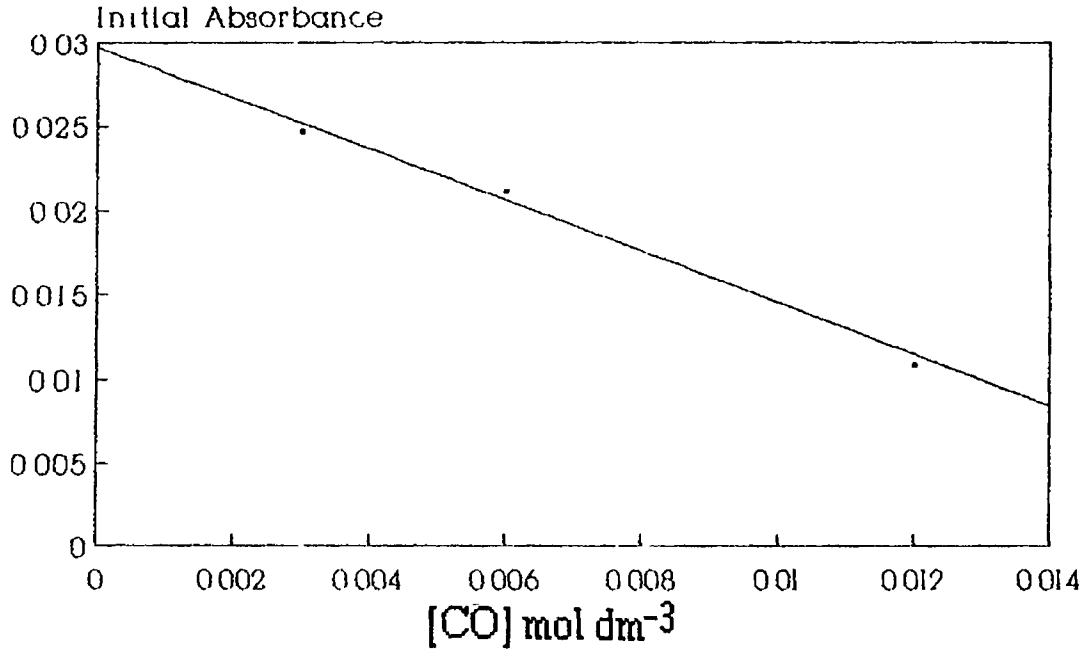

Figure 3.3.2.4 4 A plot of initial absorbance for the fourth transient species against the concentration of CO in cyclohexane solution

3.3.2.5 Fifth transient species

The presence of a fifth transient species suggested that the *trans* - $Mo(CO)_4PPh_3$(cyclohexane) and the $Mo(CO)_5$(cyclohexane) intermediates were formed on photolysis and reacted with the parent to produce two dinuclear species the fourth and the fifth transients This is because both these intermediates were presumed to adopt a square planar configuration in solution[18] This type of orientation would be the most sterically favourable for dinuclear species formation A UV/visible difference spectrum of the fifth transient species is shown in Figure 3 3 2 5 1 and has a maximum at 400nm In the typical transient presented in Figure 3 3 2 5 2 the fast portion of the decay represents the fourth transient species while one can clearly see that the fifth transient species was decaying at a slower rate In line with the other species in this system this transient reacted with CO added to the cyclohexane solution.

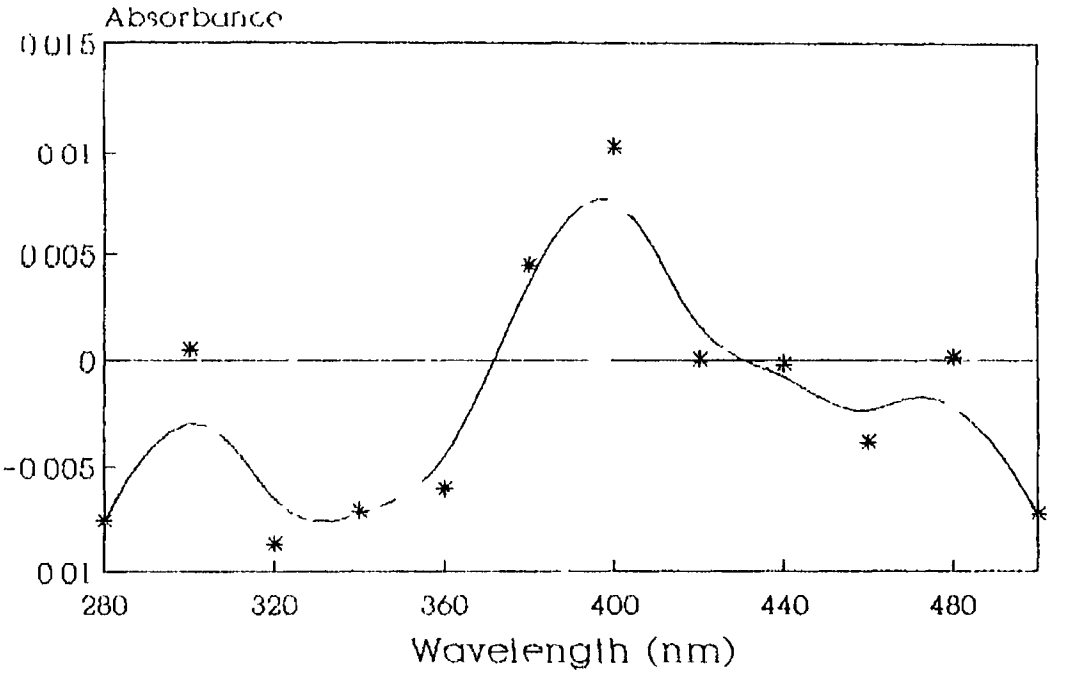

Figure 3.3.2.5.1 A UV/visible spectrum of the fifth transient species obtained 50000μs after the laser pulse under 1 0 atmosphere of CO

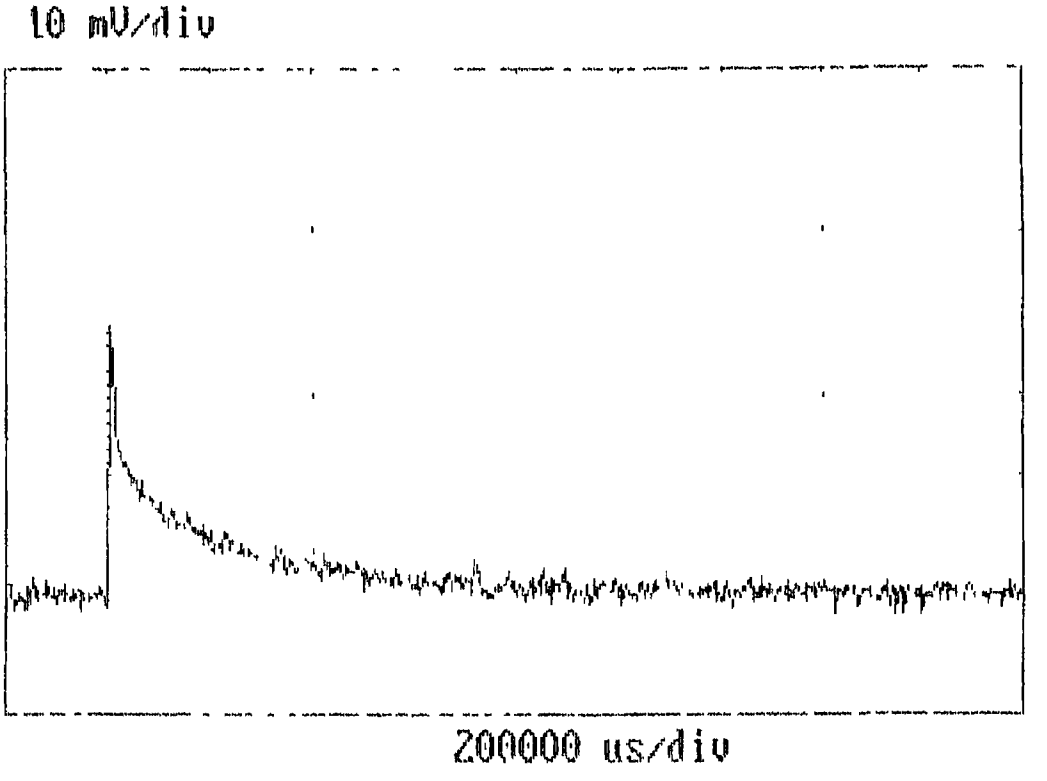

Figure 3.3 2.5 2 A typical transient obtained for the fifth transient species monitored at 420nm under 0 5 atmospheres of CO

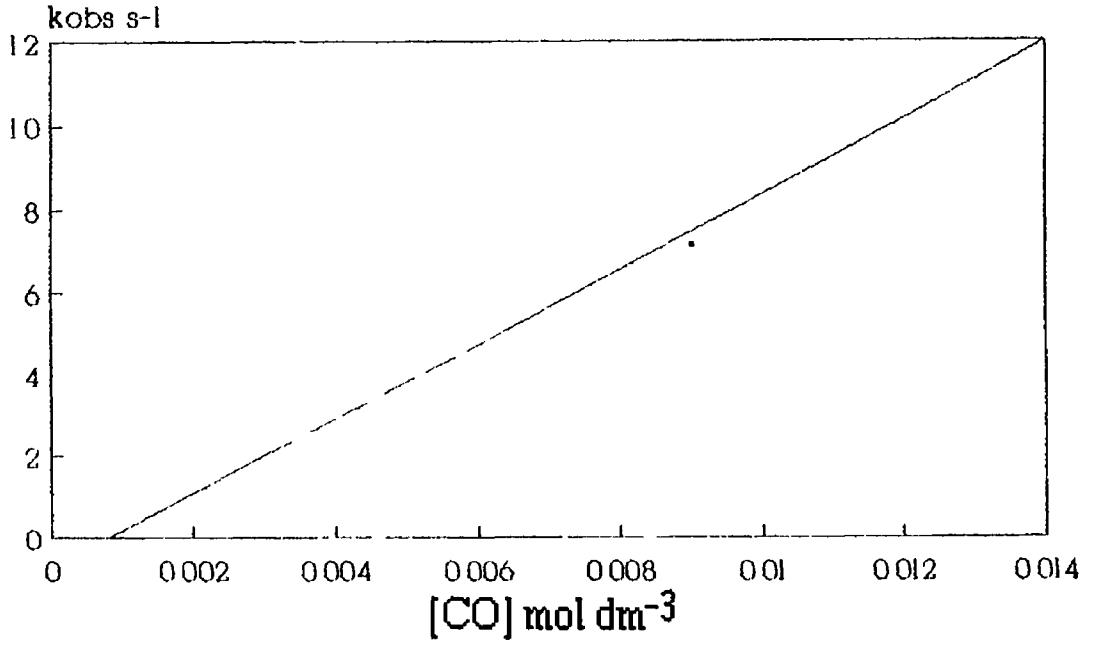

[CO] mol dm^{-3}	k_{obs} (s^{-1})
0 003	2 32
0 006	4 40
0 009	7 11
0 012	10 5

$k_{[CO]} = 908 \pm 69\ dm^3\ mol^{-1}\ s^{-1}$

Intercept = $-0\ 7 \pm 0\ 5\ s^{-1}$

Corr Coeff = 0 994

Figure 3.3.2.5.3 A plot of the observed rate constant (s^{-1}) for the fifth transient species against the concentration of CO (mol dm^{-3}) in cyclohexane solution at 298K

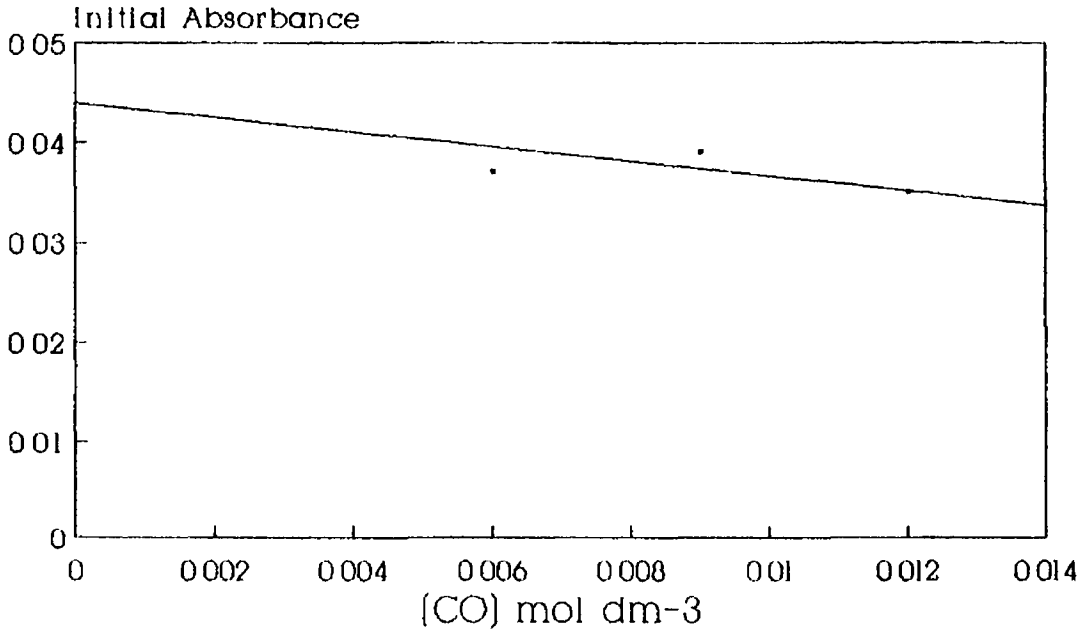

Figure 3.3.2 5 4 A plot of initial absorbance against concentration of CO in cyclohexane solution showing the dependance of yield on CO concentration

A graph of the observed rate constant of this species against CO concentration, as shown in Figure 3 3 2 5 3, yielded a second order rate constant of 908 dm^3 mol^{-1} s^{-1} Again the presence or absence of a liquid pumping phase did not affect formation of this transient species The graphical representation in Figure 3 3 4.5 4 of the yield of the photoproduct as a function of concentration of CO shows that the yield of this product is dependent on the concentration of CO and therefore is a secondary photoproduct

3 3 3 266nm laser flash photolysis of $Mo(CO)_5PPh_3$ with UV/visible monitoring

The 266nm laser flash photolysis of $Mo(CO)_5PPh_3$ produced evidence for the production of two transient species These species were the same as those produced on 355nm photolysis of $Mo(CO)_5PPh_3$ and were the primary photoproducts Significantly the third, fourth and fifth transients observed on 355nm photolysis were only present as weak transients For the fourth and fifth transient species this is presumably because

of the difference in concentration of $Mo(CO)_5PPh_3$ between the 355nm and 266nm photolysis experiments as these were assigned to dinuclear species on 355nm photolysis. Room temperature infra red studies were not possible because of the strong absorption of sodium chloride plates in the UV region

3.3.3.1 First transient species

The first transient species was identified as *cis*-$Mo(CO)_4PPh_3$ as in the 355nm analysis A UV/visible difference spectrum of this species is shown in Figure 3.3 3 1 1 and has the same absorption characteristics as the spectrum obtained for the 355nm excitation of $Mo(CO)_5PPh_3$ i e λmax = 420nm and 480nm The reaction kinetics of this species with CO indicate that this species was the same as that obtained at 355nm excitation The second order rate constant for the reaction of the first transient species with CO ($1\ 2 \times 10^7 \pm 2\ 8 \times 10^7$ $dm^3\ mol^{-1}\ s^{-1}$) on 266nm excitation was similar to that

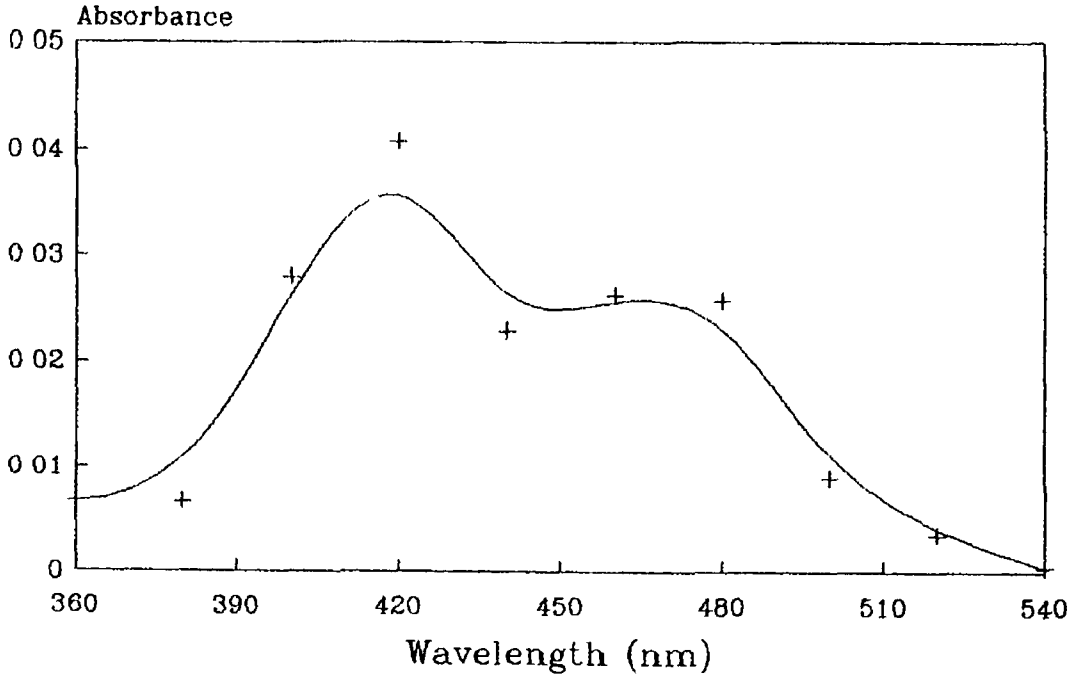

Figure 3.3.3.1.1 A UV/visible difference spectrum of *cis*-$Mo(CO)_4PPh_3$ obtained 1μs after the pulse

obtained for the first transient species on 355nm excitation

3.3.3.2 Second transient species

The results obtained for the second transient species were similar to those for the second transient species observed for 355nm excitation Therefore it was presumably the same species proposed on 355nm excitation, i e $Mo(CO)_5$(cyclohexane) The UV visible spectrum shown in Figure 3 3 3 2 1 was identical to that obtained for the second species in the 355nm excitation The reaction kinetics of this species with CO suggests that these species were the same The second order rate constant obtained for the reaction of this species with CO was $4\ 2 \times 10^6 \pm 9\ 7 \times 10^5$ $dm^3\ mol^{-1}\ s^{-1}$ and compared favourably with the rate constant obtained at 355nm of $3\ 8 \times 10^6$ $dm^3\ mol^{-1}\ s^{-1}$

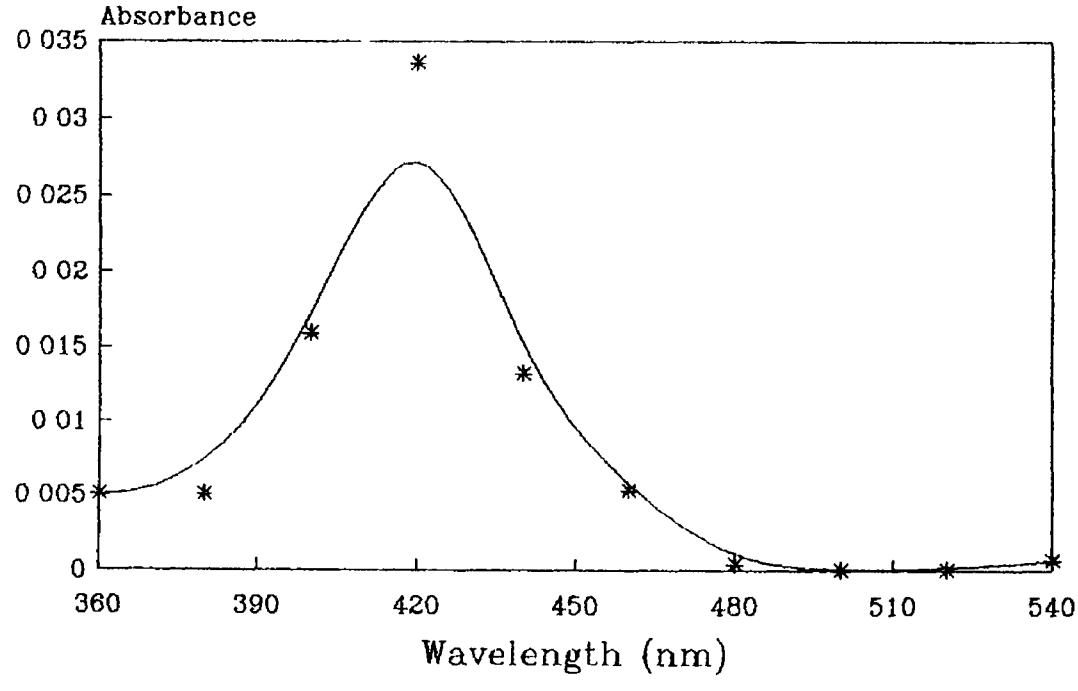

Figure 3 3.3.2 1 A UV/visible difference spectrum of the second transient species obtained 20μs after the laser pulse

The absence of the other transients indicated that they may have been dependent on the parent concentration Constraints on the absorbance values of the sample solution at the excitation wavelengths i e between 0 5 and 2 0 absorbance units, means that because of the differences in exctinction coefficients for $Mo(CO)_5PPh_3$ at 355nm and 266nm the concentration of $Mo(CO)_5PPh_3$ at 266nm is ~10 less than at 355nm Therefore the probability of formation of a dinuclear species at 266nm is less than at 355nm The presence of a weak transient at the timescale of the third transient was interesting because this species, on 355nm excitation, reacted with $Mo(CO)_5PPh_3$ This may point to wavelength dependency for the production of the third transient species It was suggested that this species may have been *trans*-$Mo(CO)_5PPh_3$(cyclohexane) and so this points to a change in the labilisation along the z axes for 355nm and 266nm excitation where the 266nm excitation favoured loss of a triphenylphosphine ligand A full reaction scheme of the photolysis products formed on 355nm and 266nm excitation is given in Figure 3 5 2

3.4 Photolysis of $W(CO)_5PPh_3$

3.4.1 Infra red monitored photolysis of $W(CO)_5PPh_3$

An argon degassed cyclohexane solution of $W(CO)_5PPh_3$ was photolysed using the 355nm laser line of an Nd YAG laser in 0 1mm pathlength sodium chloride cells The resultant infra red spectrum of the carbonyl region is displayed in Figure 3 4 1 1 The parent complex carbonyl bands were at 2073, 1981 and 1942cm^{-1} and corresponded to the A_1, A_2, E modes respectively of $W(CO)_5PPh_3$ The bands at 2073 and 1942cm^{-1} were depleted on photolysis while the band at 1981cm^{-1} increased in intensity and moved to 1983cm^{-1} This increase was because of the formation of $W(CO)_6$ arising from the loss of a triphenylphosphine ligand from the parent and its subsequent reaction with a CO molecule photochemically lost from another parent complex The band at 1983cm^{-1} corresponds to the T_{1u} mode of $W(CO)_6$ Other new bands were formed at 2021, 1926, 1903 and 1870cm^{-1} The most intense of these new bands was the νCO at 1903cm^{-1} This band suggests the formation of a *trans* complex as complexes of the type *trans*-$M(CO)_4L_2$ have a very strong absorption at ~1890cm^{-1} [6] This complex could have been formed from the reaction of photochemically produced $W(CO)_4PPh_3$ with free triphenylphosphine ligands lost from the parent complex The νCO at 2010cm^{-1} could arise from the A_{1g} band observed in *trans* complexes or the 2010cm^{-1} band observed in *cis* complexes. The band at 1926cm^{-1} also indicates the formation of some *cis* complex This complex may have been formed from the reaction of *cis*-$W(CO)_4PPh_3$ with triphenylphosphine or the isomerisation of the *trans* complex to the *cis* complex To investigate if the products were triphenylphosphine disubstituted tetracarbonyl complexes the photolysis was carried out in excess triphenylphosphine The infra red spectrum of the carbonyl region from the photolysis is shown in Figure 3 4 1 2 The band arising from the $W(CO)_6$ complex was absent presumably because of efficient reformation of the parent complex by the

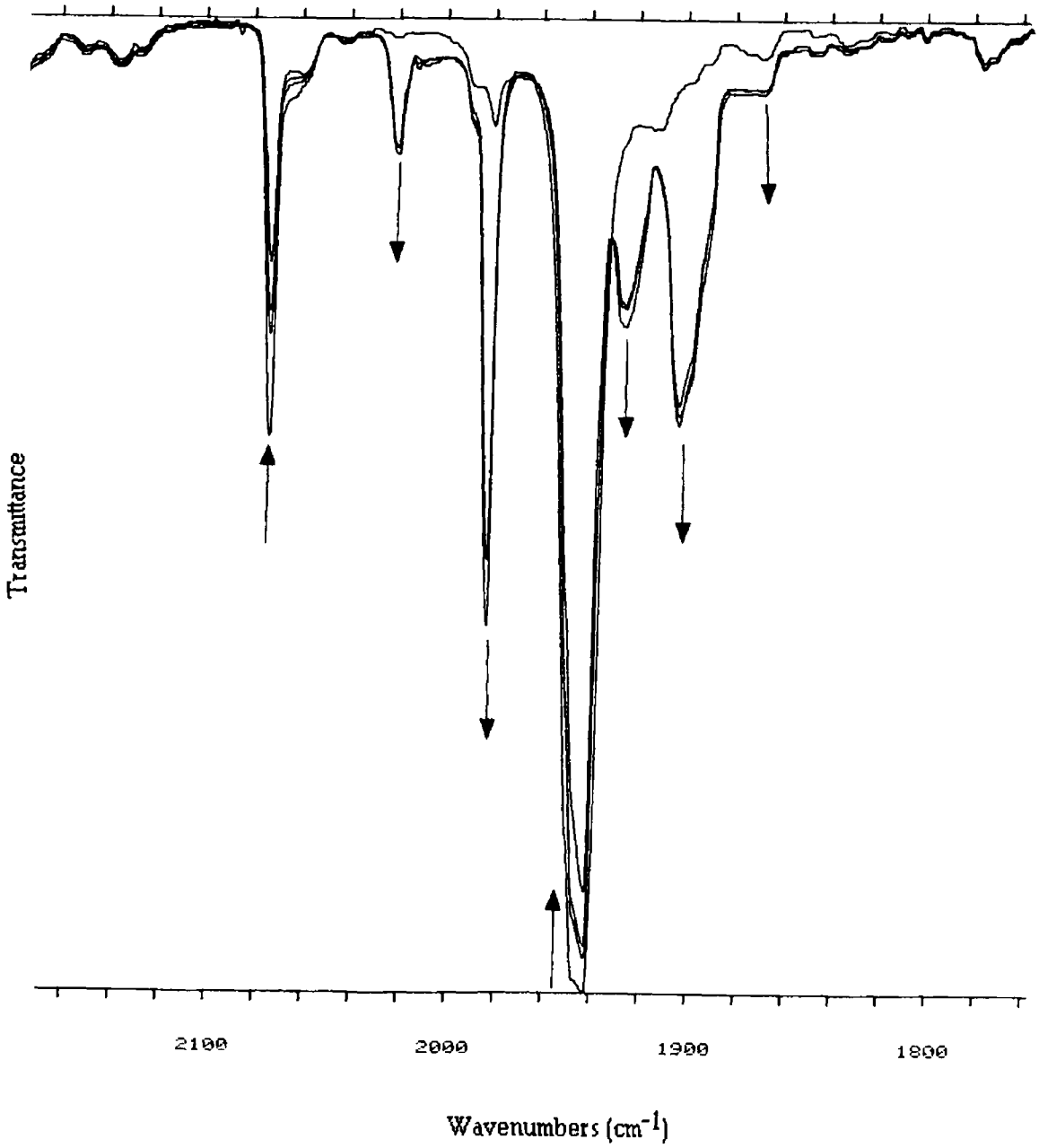

Figure 3.4.1.1 The infra red carbonyl region after the 355nm photolysis of $W(CO)_5PPh_3$

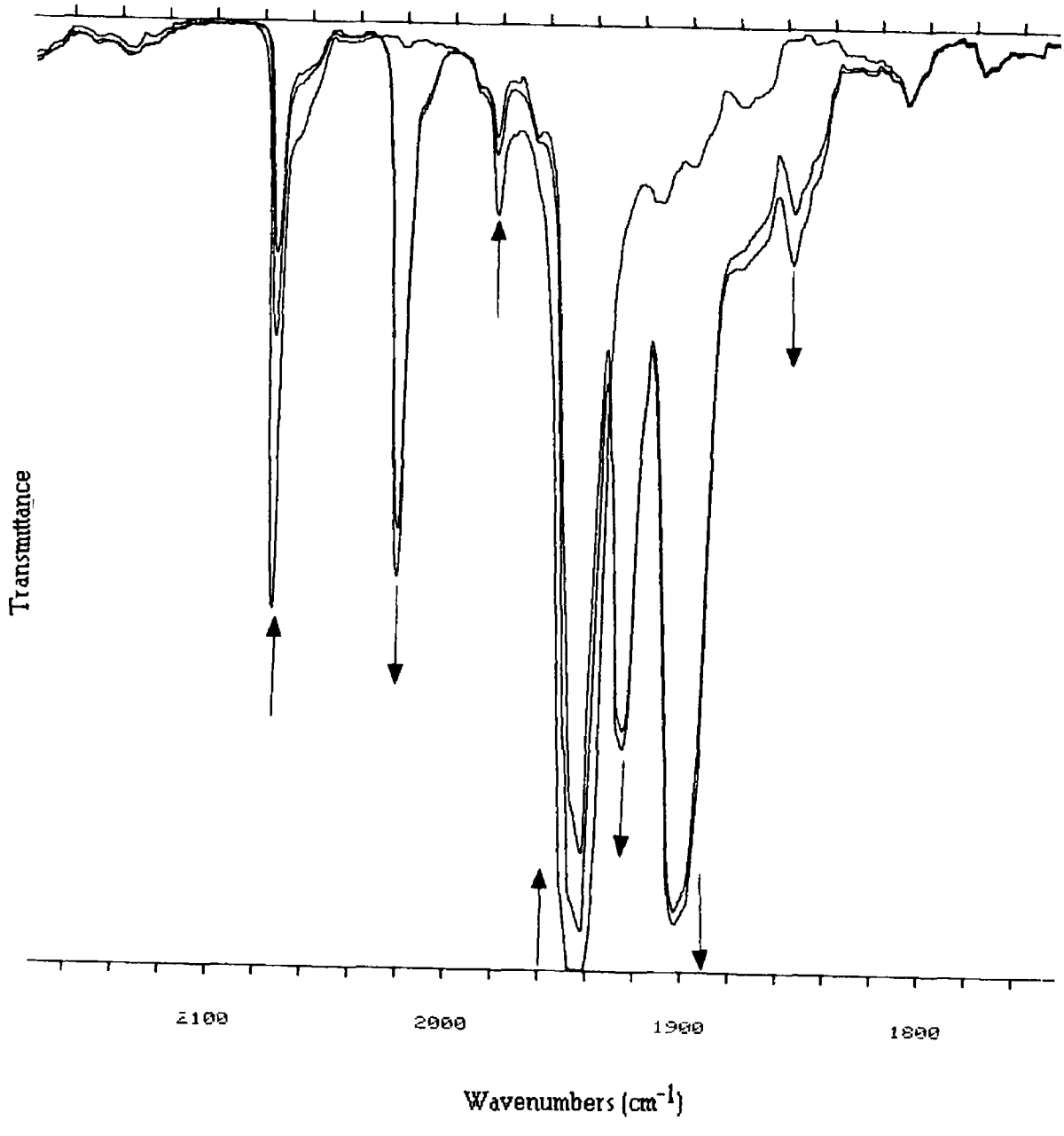

Figure 3.4.1.2 The infra red carbonyl region following the 355nm photolysis of $W(CO)_5PPh_3$ with an excess of PPh_3

reaction of the pentacarbonyl intermediate with the excess ligand All other bands were present as in the previous experiment leading to the conclusion that *cis* and *trans* complexes were formed from one or more $W(CO)_4PPh_3$ intermediates The *trans* νCO band at 1903cm^{-1} was again the most intense indicating that this was perhaps the major product of the photoreaction

3.4.2 355nm laser flash photolysis of $W(CO)_5PPh_3$ with UV/Visible monitoring

The 355nm laser flash photolysis of $W(CO)_5PPh_3$ produced evidence for the existence of five transient species of which three were identified as primary photoproducts One was identified as *cis*-$W(CO)_4PPh_3$ and the others were tentatively assigned as $W(CO)_5$(cyclohexane) and *trans* -$W(CO)_4PPh_3$(cyclohexane) The identities of the other two species were unknown but were presumed to be dinuclear species as a result of the reactions of the primary photoproducts with parent complex.

3.4.2.1 First transient species

The first transient species was identified as *cis*-$W(CO)_4PPh_3$ primarily on the basis of its reaction kinetics as spectral data were ambiguous The UV/visible difference spectrum of the first transient species is shown in Figure 3 4 2 1 1 The spectrum consisted of a broad band with a maximum at ~425nm. The UV/visible difference spectrum of $W(CO)_5$(cyclohexane) obtained from the 355nm laser flash photolysis of $W(CO)_6$ is presented in Figure 3 4 2 1 2 and has a λmax at 430nm Therefore given the close agreement of the spectra of the two transient intermediates it is difficult to exclude the possibility that this species is $W(CO)_5$(cyclohexane) The laser flash photolysis of $W(CO)_5PPh_3$ in a cyclohexane solution containing different concentrations of carbon monoxide was used to determine if the reacting species was $W(CO)_5$(cyclohexane) or *cis*-$W(CO)_4PPh_3$ A typical transient obtained under a 0 5 atmosphere of CO is depicted in Figure 3 4 2 1 3 The reaction of *cis*-$W(CO)_4PPh_3$

with CO followed psuedo first order conditions The kinetic data obtained from this experiment is displayed in Figure 3 4 2 1 4 and shows a linear dependence of the rate on the concentration of CO The slope of this graph yielded a second order rate constant of 6 05 x 10^7 dm^3 mol^{-1} s^{-1} Dobson and coworkers[10] carried out time resolved infra red laser flash photolysis (λ = 308nm) on $W(CO)_5PPh_3$ in n-heptane solution and obtained a second order rate constant of 1 17 x 10^7 dm^3 mol^{-1} s^{-1} for the reaction of *cis*-$W(CO)_4PPh_3$(n-heptane) with CO In photolysis experiments with n-heptane and cyclohexane the rate constants obtained in n-heptane are normally twice as fast as those obtained in cyclohexane because of different interaction energies between the solvents and the metal centre[19] The second order rate constant obtained in this experiment indicated that the *cis*-$W(CO)_4PPh_3$ species may not be solvated in solution This observation points to steric hinderance in the *cis* position by the presence of the bulky triphenylphosphine group allowing the relatively small CO ligand to coordinate in the *cis* position but not the larger solvent molecule One possible solution was that the *cis*-$W(CO)_4PPh_3$ intermediate could fill the vacant coordination site by an 'agostic' interaction with one of the hydrogens on the triphenylphosphine ligand, most likely in an ortho position A tungsten carbonyl complex $W(CO)_3(PCy_3)_2$ has been isolated and its structure determined where the complex, although apparently coordinately unsaturated, has an ortho hydrogen atom from one of the cyclohexyl rings filling the sixth coordination site and stabilising the complex[8]

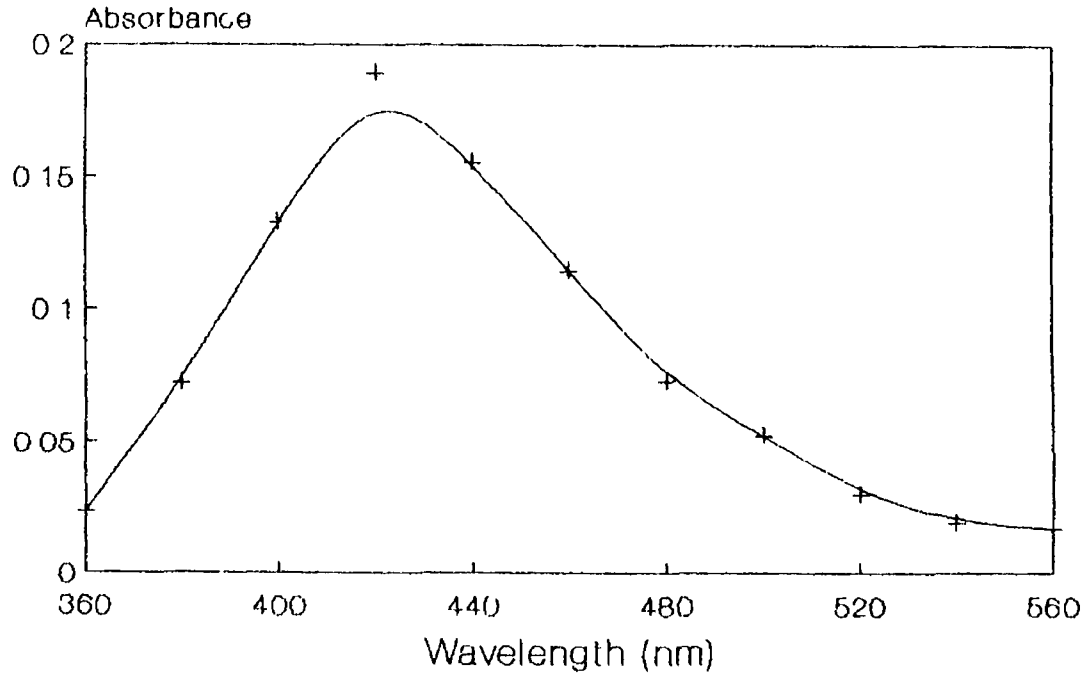

Figure 3.4.2.1.1 A UV/visible difference spectrum of *cis*-$W(CO)_4PPh_3$ obtained 2μs after the laser pulse from the photolysis of $W(CO)_5PPh_3$ in cyclohexane under 0 5atmospheres of CO

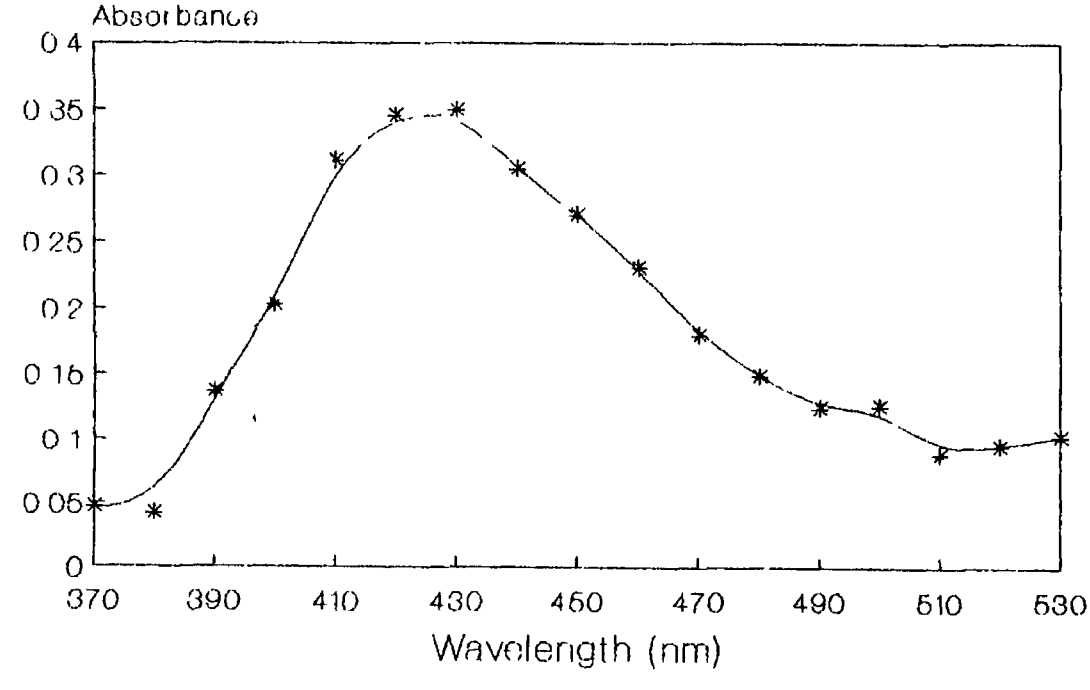

Figure 3.4.2.1.2 A UV/visible difference spectrum of $W(CO)_5$(cyclohexane) obtained 0 2μs after the laser pulse in the 355nm photolysis of $W(CO)_6$ under 1 0 atmospheres of CO

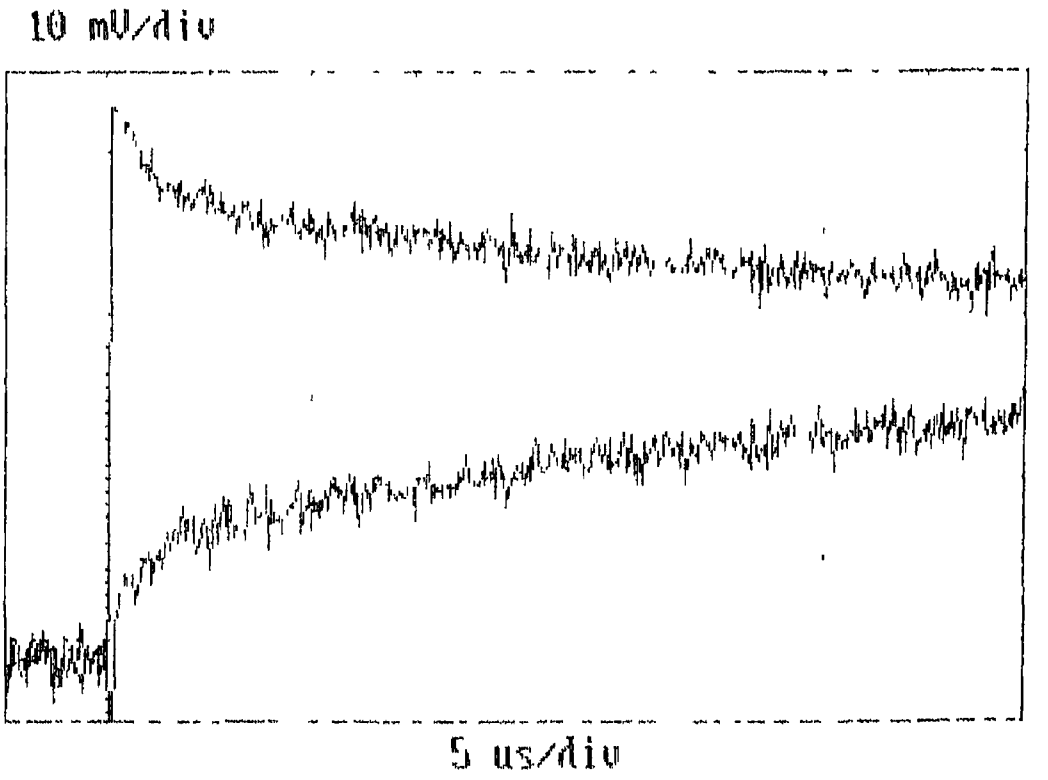

Figure 3.4.2.1.3 A typical transient for the decay of *cis*-$W(CO)_5PPh_3$ in cyclohexane under 0.5 atmospheres of CO monitored at 440nm with a simultaneous grow in monitored at 360nm

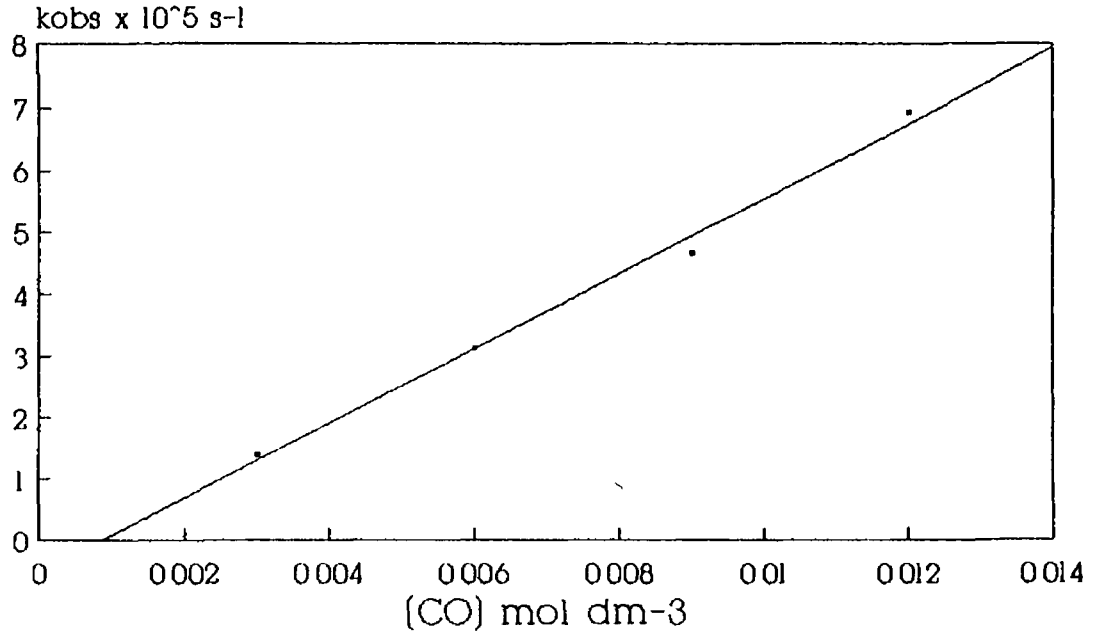

[CO] mol dm^{-3}	k_{obs} x 10^{-5} (s^{-1})
0.003	1 38
0 006	3 11
0 009	4 64
0 012	6 92

$k_{[CO]} = 6\ 05 \times 10^{7} \pm 3\ 66 \times 10^{6}\ dm^{3}\ mol^{-1}\ s^{-1}$

Intercept = $-5\ 25 \times 10^{4} \pm 2\ 45 \times 10^{4}$

Corr Coeff = 0 996

Figure 3.4.2.1.4 The graph and kinetic data obtained from the 355nm photolysis of $W(CO)_5PPh_3$ with various concentrations of CO (mol dm^{-3}) for the first transient species

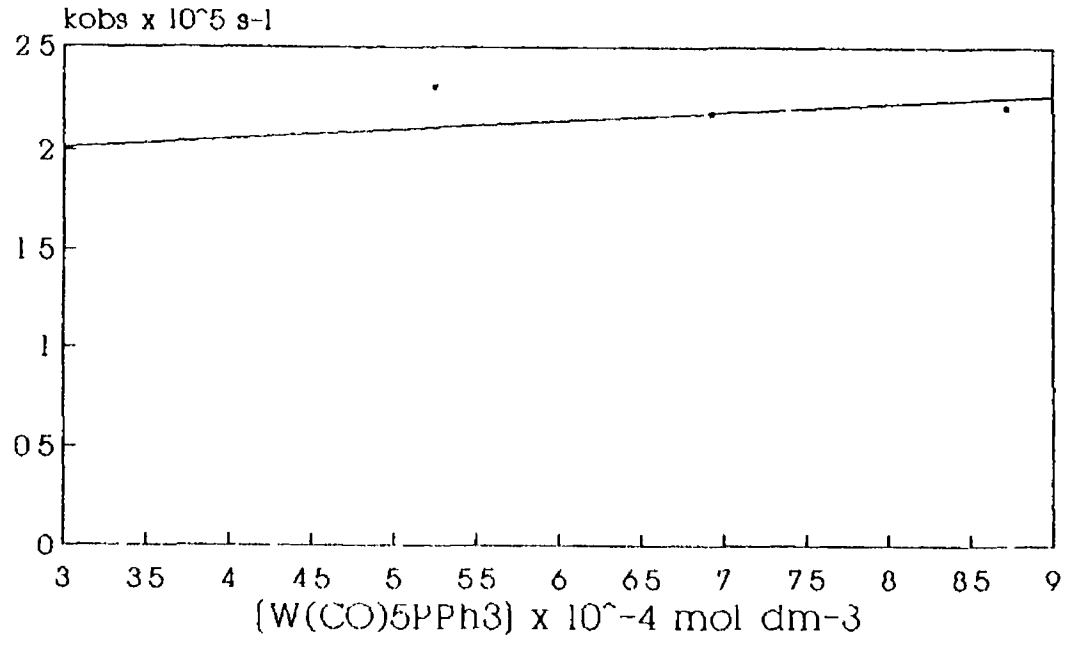

Figure 3 4.2.1.5 A plot of concentration of $W(CO)_5PPh_3$ (mol dm^{-3}) against k_{obs} (s^{-1}) for *cis*-$W(CO)_5PPh_3$ demonstrating the non-dependence of the transient species on parent concentration

In addition, the rate of decay of the *cis*-$W(CO)_4PPh_3$ intermediate was mirrored by a concomitant grow in at ~360nm, indicating that this species was reacting to form a secondary transient photoproduct with a λmax ~415nm The rate of this grow in was constant regardless of the concentration of $W(CO)_5PPh_3$ as can be seen in Figure 3 4 2 1 5 ruling out the possibility of dinuclear complex formation The identity of this secondary photoproduct is uncertain but could be the intramoleculaly stabilised *cis*-$W(CO)_4PPh_3$ complex It may also be the result of isomerisation of the *cis* form of $W(CO)_4PPh_3$ to the *trans* configuration Another possible solution was that the $W(CO)_5PPh_3$ intermediate could have reacted with impurities in the cyclohexane solvent even though the sample was subjected to a liquid pumping stage to remove impurities such as H_2O or CO_2 prior to photolysis However H_2O can be easily removed by three liquid pumping cycles prior to analysis[11] In the absence of a liquid pumping stage in sample preparation, like the Cr and Mo analogues of this transient

species, the first transient was absent This may be because of fast reaction of the *cis* intermediate with water beyond the detection limit of the instrumentation or the production of a water complex from one of the other photoproducts which obscures the band arising from the *cis* complex

A plot of initial absorbance against CO concentration showed that the yield of this species increased with increasing CO concentration (Figure 3 4 2 1 6) A possible explanation for this observation was that the *cis* intermediate was undergoing isomerisation to the *trans* form on a timescale similar to the reaction of *cis* - $W(CO)_4PPh_3$ with CO Increasing the CO concentration would increase the rate of formation of $W(CO)_5PPh_3$ from a *cis* intermediate and so reduce the amount isomerising to *trans*-$W(CO)_4PPh_3$

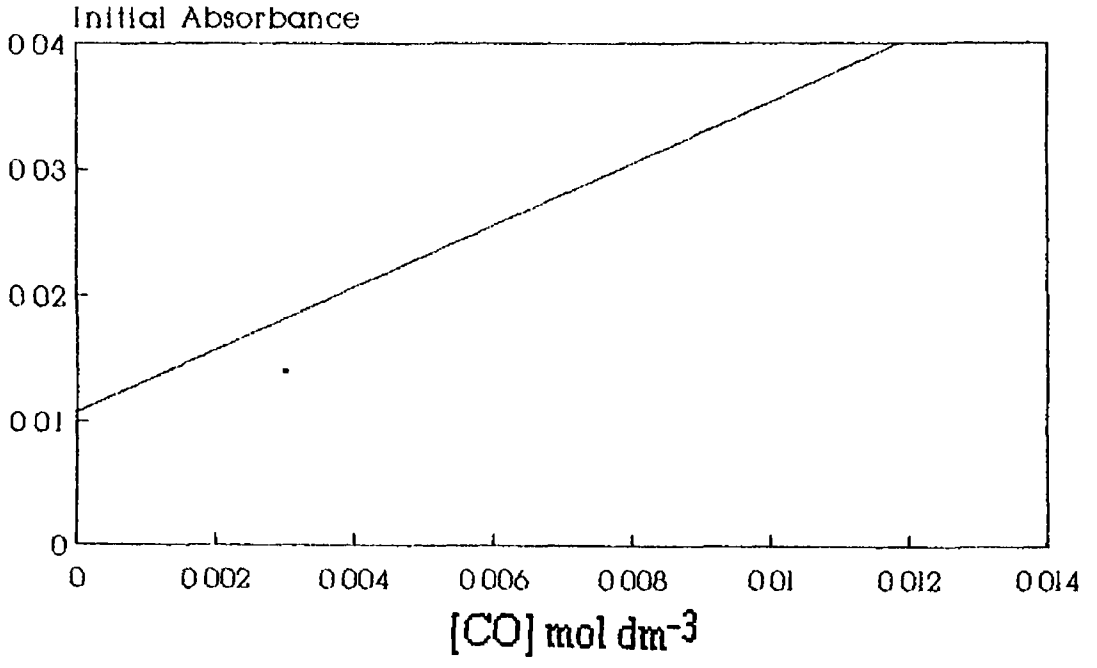

Figure 3.4 2.1.6 A plot of initial absorbance against concentration of CO indicating an increase in yield of *cis*-$W(CO)_5PPh_3$ on increasing CO concentration

3.4.2 2 Second transient species

The identification of the second transient species was tentative A UV/visible difference spectrum is shown in Figure 3 4 2 2 1 and has a maximum at ~420nm Again it was practically indistinguishable from other spectra obtained for this system This species also reacted with CO and a plot of absorbance against time exhibited a logarithmic decay an example of which is shown in Figure 3 4 2 2 2 Psuedo first order rate constants (k_{obs}) were extracted from the decay curve of this species A plot of the observed rate constant against CO ligand concentration showed a linear dependence of the decay of this species with varying CO concentration A graph of the observed rate constant against CO concentration is displayed in Figure 3 4 2.2.3 The second order rate constant calculated for the reaction of this species with CO was 6 6 x 10^5 dm^3 mol^{-1} s^{-1} This value was close to that observed in an experiment carried out on $W(CO)_6$ in CO saturated cyclohexane for the reaction of $W(CO)_5$(cyclohexane) with CO at 6 x 10^5 dm^3 mol^{-1} s^{-1} This species did not react with the parent complex as can be seen from Figure 3 4 2 2 4 The observed rate constant remained unchanged regardless of the parent concentration The decay of the species was mirrored by a simultaneous grow in at the same rate It may well be that the decaying species was reacting with free triphenylphosphine in solution generated from the loss of a triphenylphosphine ligand from the parent to form a *cis* or *trans* isomer of $W(CO)_4(PPh_3)_2$ Alternatively it may be the result of a *cis - trans* isomerisation reaction However, Dobson and coworkers, on their experiments with $W(CO)_4L(pip)$ (L = phosphines, phosphites, pip = pipendine), reported that the interconversion of the intermediates was not as fast as their bimolecular reactions[18] In contrast to this these workers report that in the photolysis of $Mo(CO)_4(NP)$[17] (NP = 1-(diethylamino)-2-(diphenylphosphino)ethane) a single primary photoproduct was formed from the cleavage of the nitrogen coordinated atom in the chelate followed by rearrangment of

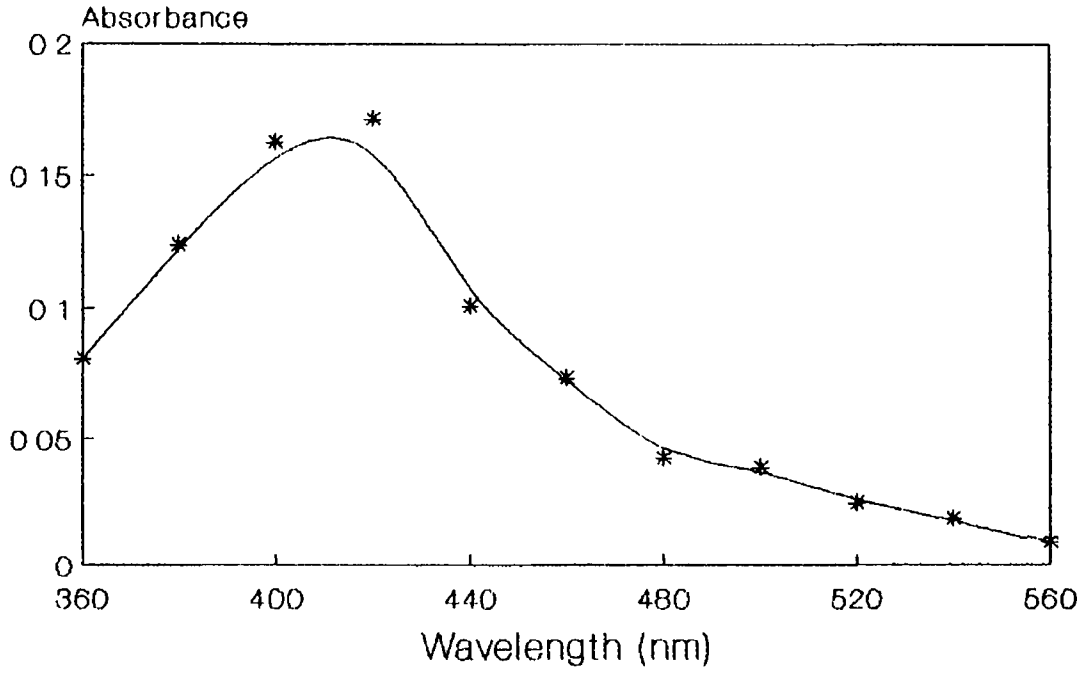

Figure 3 4 2.2.1 A UV/visible difference spectrum of the second transient species obtained 50μs after the laser pulse under 0 5 atmospheres of CO

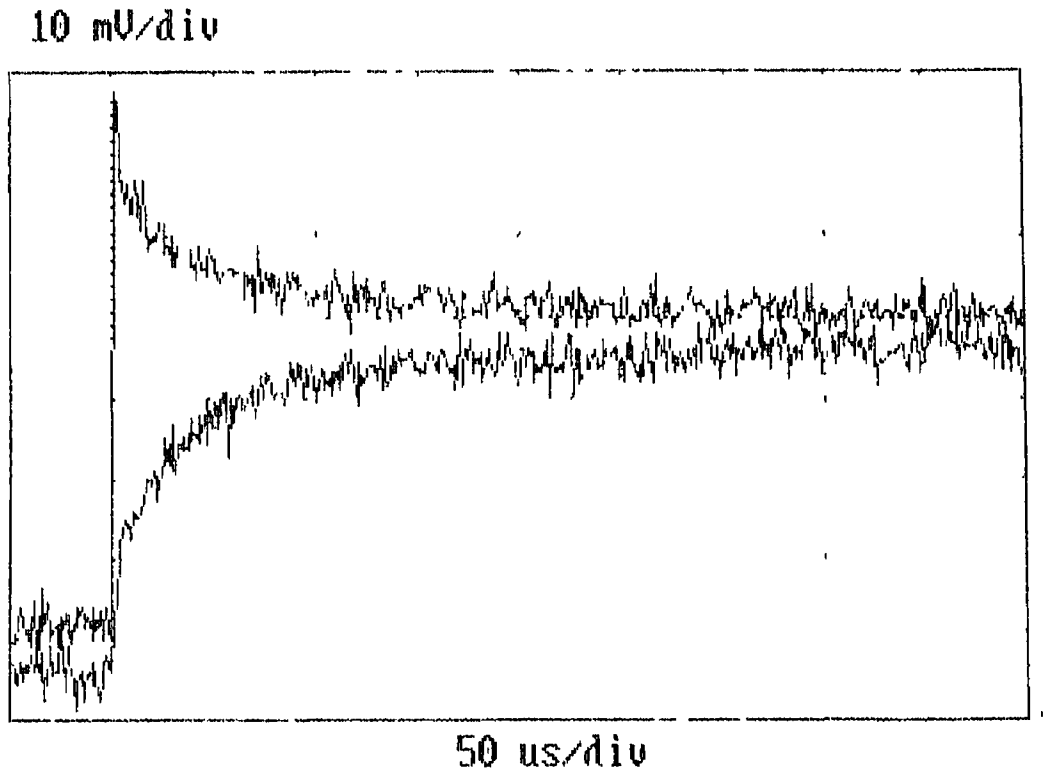

Figure 3.4.2.2.2 A typical transient signal obtained for the second transient species showing a decay at 440nm and a concomitant grow in at 360nm

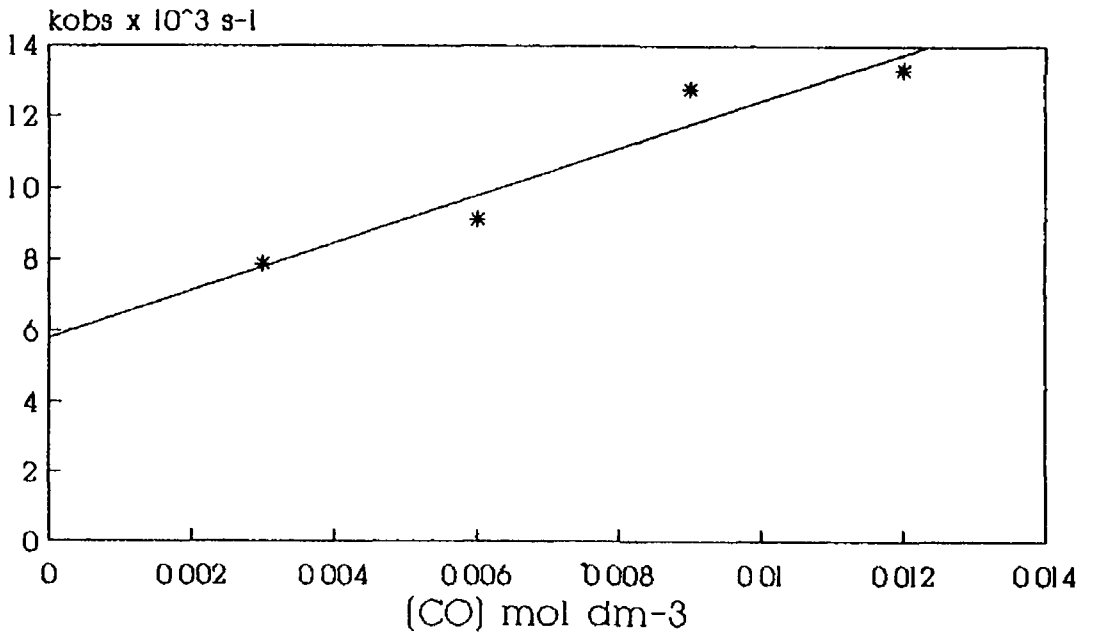

[CO] mol dm^{-3}	$k_{obs} \times 10^{-4}$ (s^{-1})
0 003	0 79
0 006	0 91
0 009	1 28
0 012	1 33

$k_{[CO]} = 6\ 63 \times 10^5 \pm 1\ 39 \times 10^5\ dm^3\ mol^{-1}\ s^{-1}$

Intercept = $5\ 80 \times 10^3 \pm 9\ 34 \times 10^2\ s^{-1}$

Corr Coeff = 0 959

Figure 3.4.2.2.3 The graph and data of the observed rate constants (s^{-1}) and the corresponding concentrations of CO (mol dm^{-3}) for the reaction of the second transient species with CO

the intermediate, prior to solvation, to form a mixture of *cis* and *trans* solvatocomplexes Another possible solution was a recombination reaction of a photochemically generated $W(CO)_5$(cyclohexane) moiety with triphenylphosphine The triphenylphosphine ligand is large and bulky and may not have diffused sufficiently far from the other photofragment produced from photolysis of $W(CO)_5PPh_3$, i e $W(CO)_5$(cyclohexane) Photolysis at 355nm at room temperature of $W(CO)_5PPh_3$ in infra red cells demonstrated that loss of a triphenylphosphine occured *vide infra*

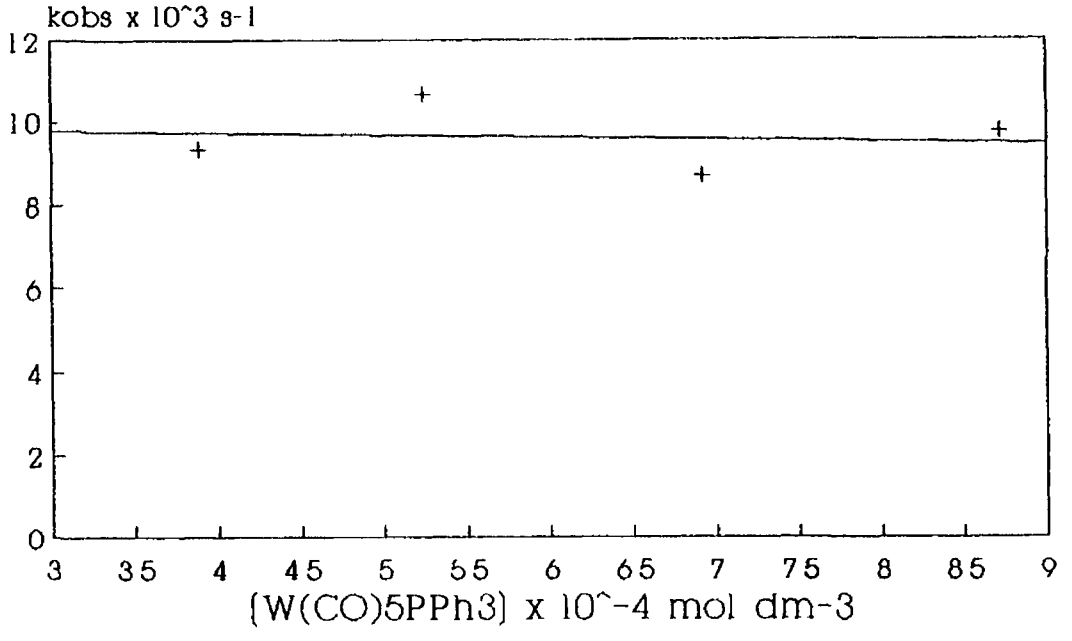

Figure 3.4.2.2.4 A plot of k_{obs} (s^{-1}) against $W(CO)_5PPh_3$ concentration (mol dm^{-3}) monitored at 360nm

Additionally, Dalgren and Zink calculated the quantum yield for unique ligand loss as 0 29 for the 366nm excitation of $W(CO)_5PPh_3$ in cyclohexane solution[13] As the experiments to calculate the second order rate constant of this species were carried out on the same sample the loss of a triphenylphosphine ligand from $W(CO)_5PPh_3$ would be expected to produce $W(CO)_6$ in solution The presence of $W(CO)_6$ would increase the concentration of $W(CO)_5$(cyclohexane) formed in solution as the laser pulse would photolyse both $W(CO)_6$ and $W(CO)_5PPh_3$ Deconvolution of the kinetic decays at various concentrations of CO showed that the yield of this transient species increased with increasing CO concentration (Figure 3 4 2 2 5) Time resolved infra red experiments carried out by Dobson *et al* on $W(CO)_5PPh_3$ in n-heptane solution yielded a second order rate constant of 3×10^6 dm^3 mol^{-1} s^{-1} for the reaction of *trans*-$W(CO)_4PPh_3$(n-heptane) with CO[10] Given the different interaction energies of cyclohexane and n-heptane with the coordinately unsaturated intermediates produced in photolysis experiments, reactions of n-heptane solvated complexes tends to be faster by a factor of two compared to the corresponding cyclohexane solvated species Therefore the second order reaction rate of *trans*-$W(CO)_4PPh_3$(cyclohexane) with CO would be expected to be ~1 5 x 10^6 dm^3 mol^{-1} s^{-1}, twice the rate constant obtained in this experiment Given the above data this species can be tentatively assigned as $W(CO)_5$(cyclohexane)

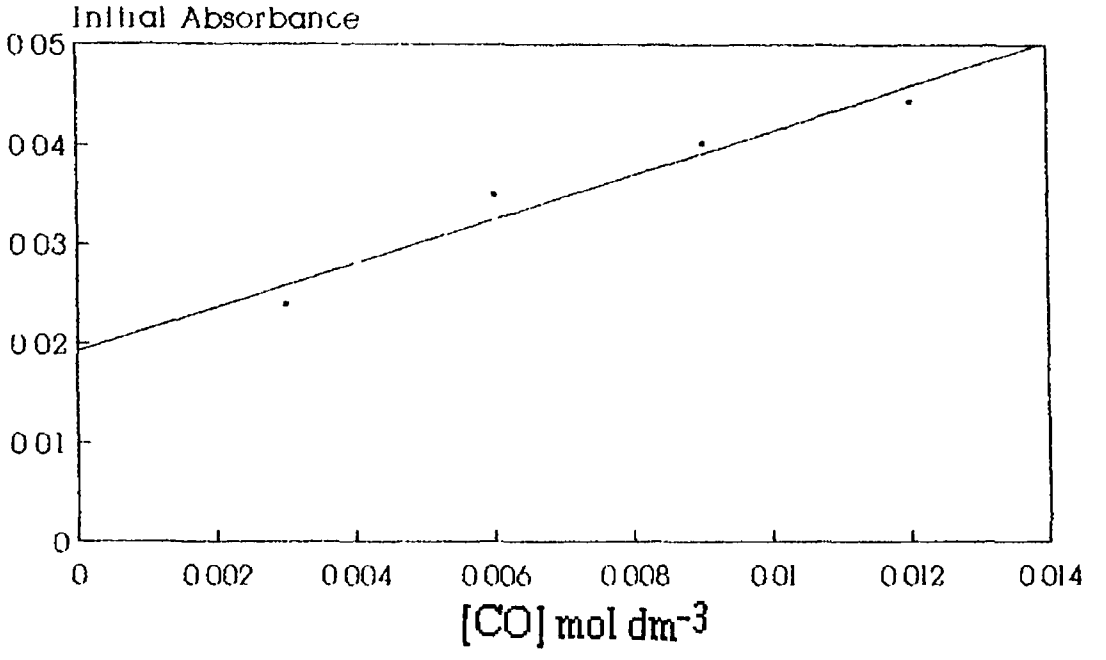

Figure 3.4.2 2.5 A plot of initial absorbance against concentration of CO for the second transient species

3.4.2 3 Third transient species

The identity of this third transient species was unknown A UV/visible difference spectrum of this species is shown in Figure 3 4 2.3 1 and contains a broad band with a maximum at ~430nm A typical transient representing the decay profile of this species is depicted in Figure 3 4 2 3 2 The decay of this species was dependent on the concentration of CO in solution A graph of the concentration of CO against the observed rate constant is displayed in Figure 3 4 2 3 3 The second order rate constant for the reaction of this species with CO was calculated from the slope of the line as $1\ 27 \times 10^4$ dm^3 mol^{-1} s^{-1} This second order rate constant was slow in comparison to the rates observed for primary photoproducts in cyclohexane solution which are usually of the order of $10^6 s^{-1}$ Figure 3 4 2 3 4 shows the dependence of the yield of this photoproduct on CO concentration and indicates that this intermediate is not a primary photoproduct

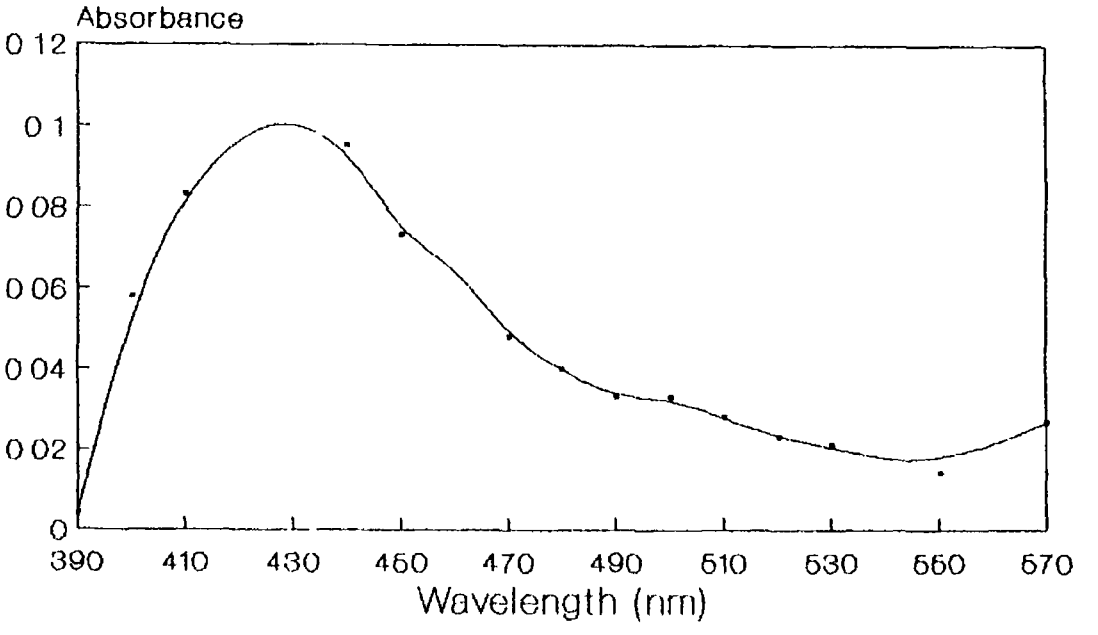

Figure 3 4 2.3.1. A UV/visible difference spectrum obtained for the third transient species 800μs after the laser pulse

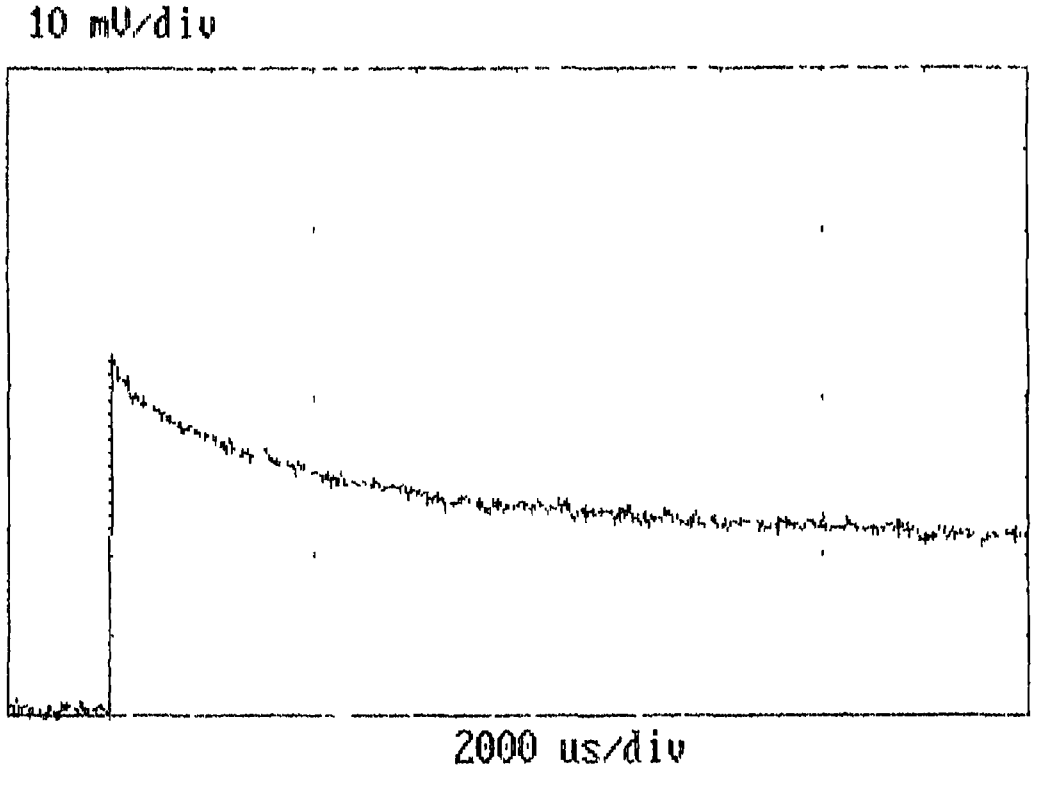

Figure 3 4.2.3 2 A typical transient obtained for the third transient species under 0 25 atmospheres of CO at 420nm

The loss in yield may be explained by the isomerisation process implied for the *cis*-$W(CO)_4PPh_3$ intermediate However, the rate of disappearance of this transient species at 430nm was echoed by a simultaneous grow in monitored at 360nm when measured under an argon atmosphere The formation of this photoproduct was dependent on the concentration of the parent Therefore this species must be reacting with $W(CO)_5PPh_3$ in solution to yield a dinuclear species A graph of the observed rate constant against the parent concentration is displayed in Figure 3 4 2 3 5 The second order rate constant for the formation of this species was 3 0 x 10^6 dm^3 mol^{-1} s^{-1} The reactive intermediate may be *trans*-$W(CO)_4PPh_3$(cyclohexane) The presence of the electronegative phosphorus group *trans* to the vacant coordination site would be better able to stablise a solvated intermediate than an intermediate with the vacant site *trans* to a CO ligand[17]. In addition, the square planar intermediate with a PPh_3 in the axial position would facilitate attack on a parent complex because of less steric hindrance compared to a square planar intermediate with the relatively large PPh_3 ligand in an equatorial position As stated before intermediates generated in n-heptane solution tend to react twice as fast as those in cyclohexane solution In Dobson and coworkers time resolved infra red (TRIR) 308nm excitation of $W(CO)_5PPh_3$ the second order rate constant for the reaction of *trans*-$W(CO)_4PPh_3$(n-heptane) with CO was 3 x 10^6 dm^3 mol^{-1} s^{-1} [10] On this basis the reactivity of *trans*-$W(CO)_4PPh_3$(cyclohexane) would be 1 5 x 10^6 dm^3 mol^{-1} s^{-1} Therefore, given that TRIR is a better method for the elucidation of structure than time resolved UV, this species may not be *trans*-$W(CO)_4PPh_3$(cyclohexane)

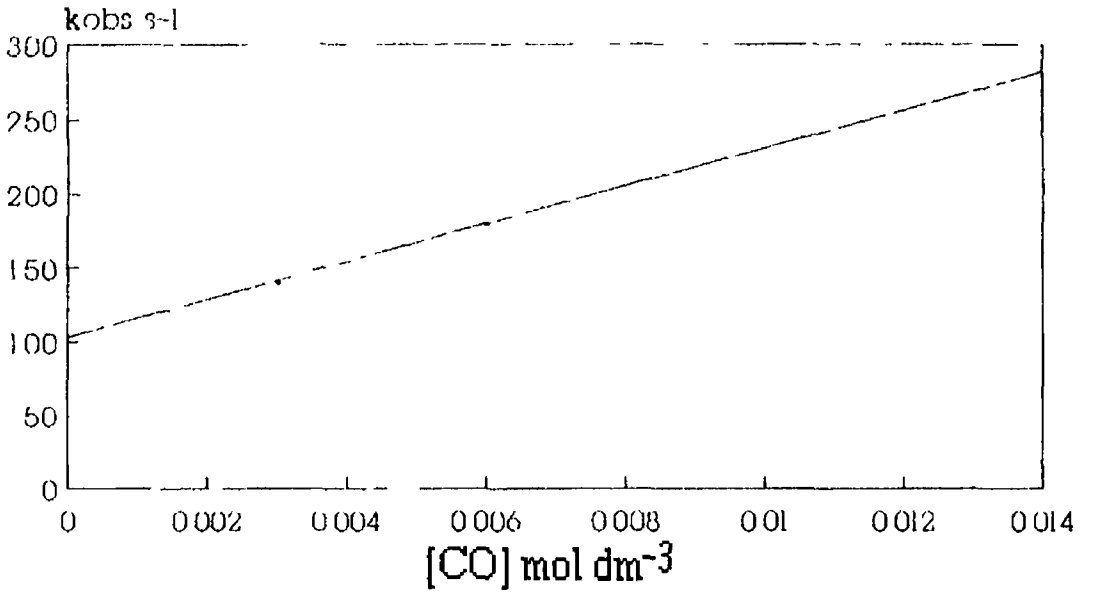

[CO] mol dm^{-3}	k_{obs} (s^{-1})
0 003	140
0 006	179
0 009	224
0 012	252

$k_{[CO]} = 1\ 27 \times 10^4 \pm 7\ 93 \times 10^2\ dm^3\ mol^{-1}\ s^{-1}$

Intercept = $103 \pm 5\ 3\ s^{-1}$

Corr Coeff = 0 996

Figure 3.4.2.3.3 A plot of the observed rate constants (s^{-1}) for the decay of the third transient species with different concentrations of CO (mol dm^{-3}) at 298K

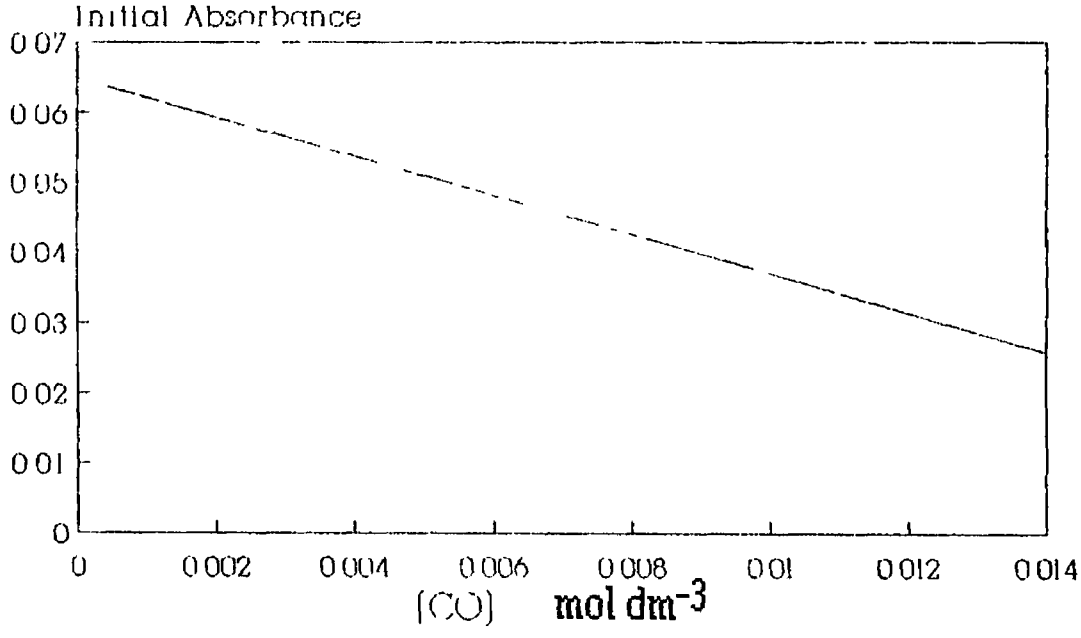

Figure 3.4.2.3.4 A plot of initial absorbance of the third transient species against concentration of CO

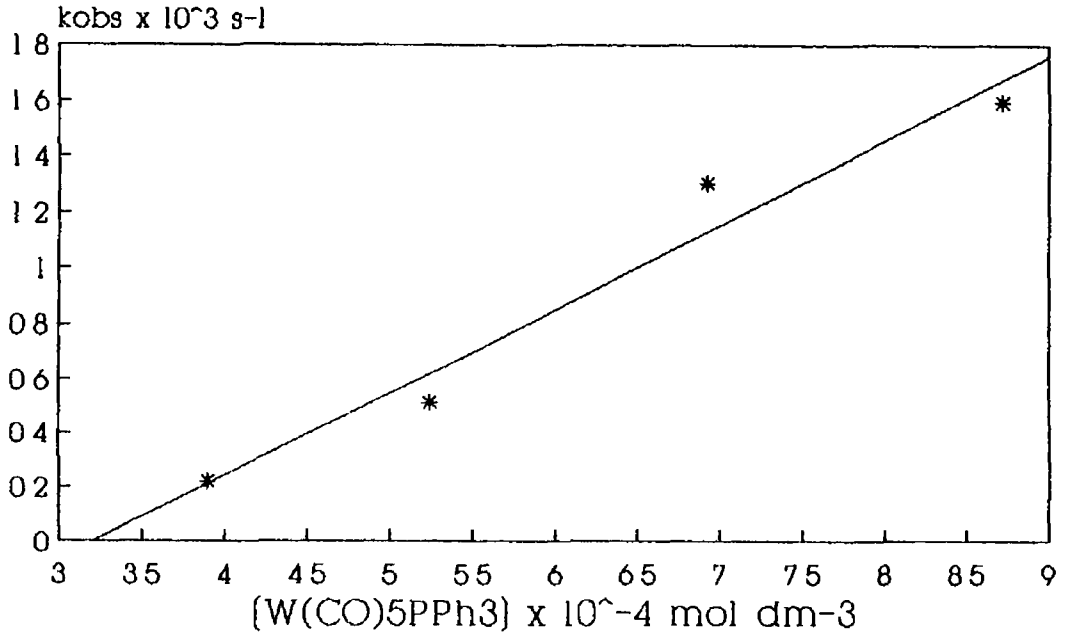

$[W(CO)_5PPh_3]$ x 10^{-4} mol dm^{-3}	k_{obs} (s^{-1})
3 89	221
5 24	511
6 92	1303
8 72	1593

$k[W(CO)_5PPh_3] = 3\ 04 \times 10^6 \pm 4\ 3 \times 10^5\ dm^3\ mol^{-1}\ s^{-1}$

Intercept = -969 ± 156 s^{-1}

Corr Coeff = 0 980

Figure 3.4 2.3.5 A plot of concentration of $W(CO)_5PPh_3$ (mol dm^{-3}) against the observed rate constants (s^{-1}) obtained for the third transient species at 298K.

3.4.2.4 Fourth transient species

A UV/visible difference of the fourth transient species observed in the 355nm laser flash photolysis of $W(CO)_5PPh_3$ is shown in Figure 3 4 2 4 1 and had a broad band with a λmax at ~430nm The nature of this species was unknown but it may be the decay of the dinuclear species formed from the third transient species and the parent complex or the decay of the intramolecularly stabilised complex described for the first transient The first option was the most likely solution given the reactivity of the *cis*-$W(CO)_4PPh_3$ to CO A typical transient for the decay of this species can be seen in Figure 3 4 2 4 2 This photoproduct like the others appeared to react with CO and yielded a second order rate constant of 1 14 x 10^3 dm^3 mol^{-1} s^{-1} A graph of the dependence on CO concentration is shown in Figure 3 4 2 4 3 As expected the yield of this product depended on the concentration of CO. The plot in Figure 3.4.2 4 4 of the initial absorbance of the species against CO concentration shows the decrease in yield with increasing CO concentration This therefore indicates that the fourth transient species is a secondary photoproduct

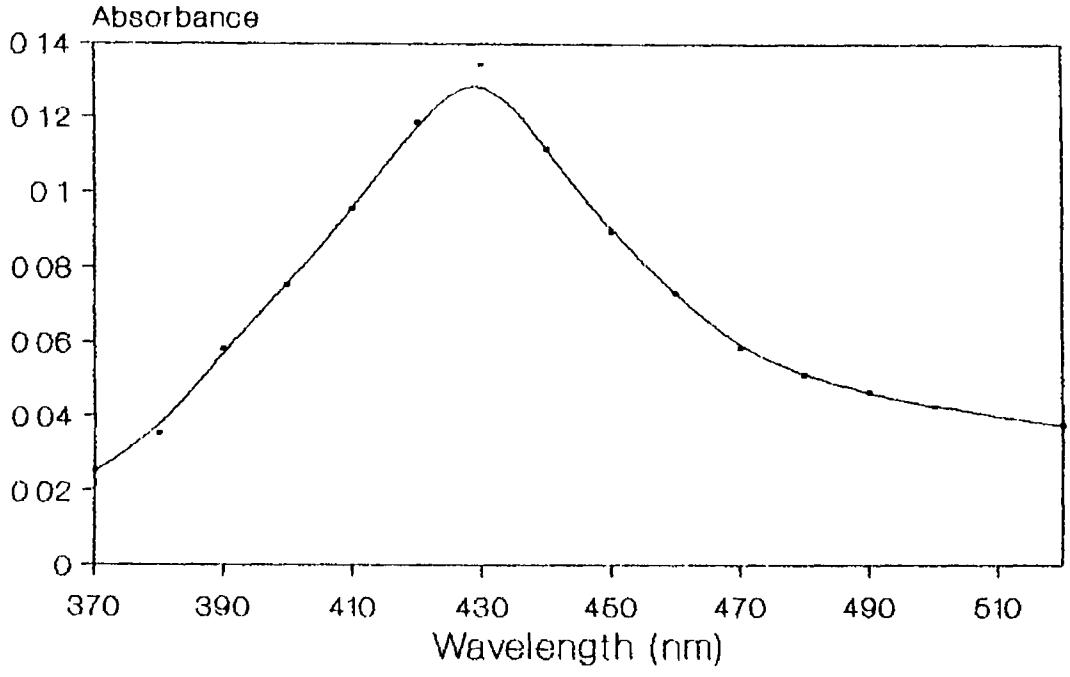

Figure 3.4.2.4.1 A UV/visible difference spectrum of the fourth transient species obtained 20000μs after the laser pulse

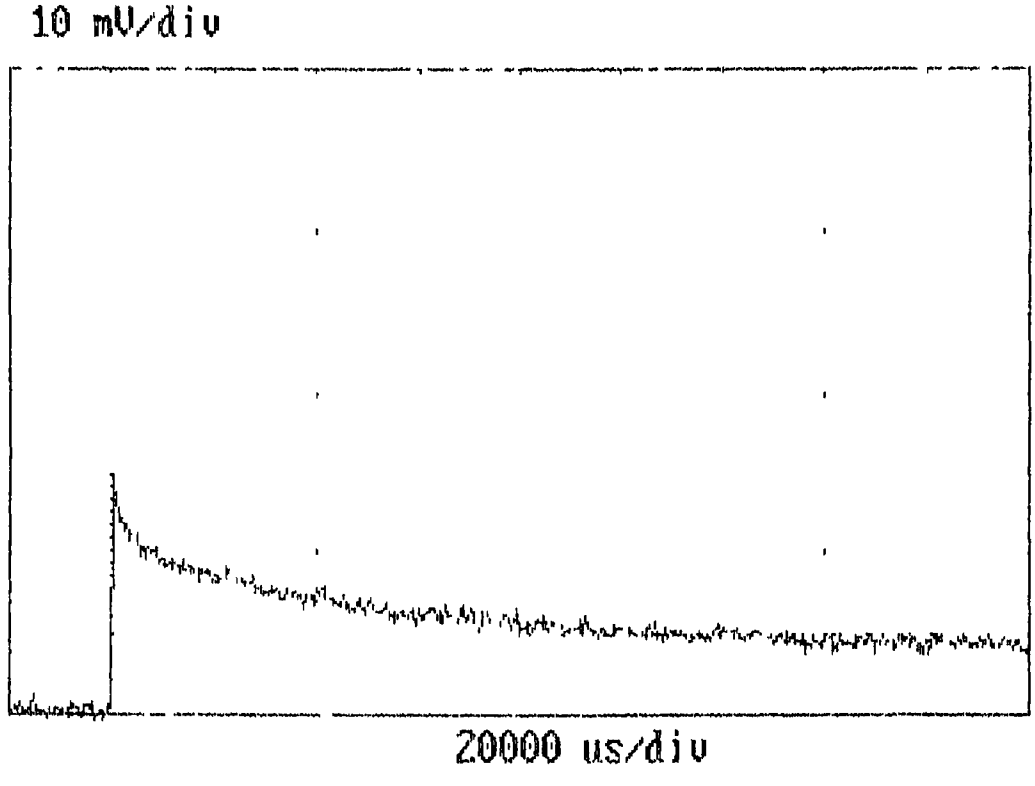

Figure 3.4 2 4 2 A typical transient signal obtained for the fourth transient species under 1 0 atmospheres of CO monitored at 420nm

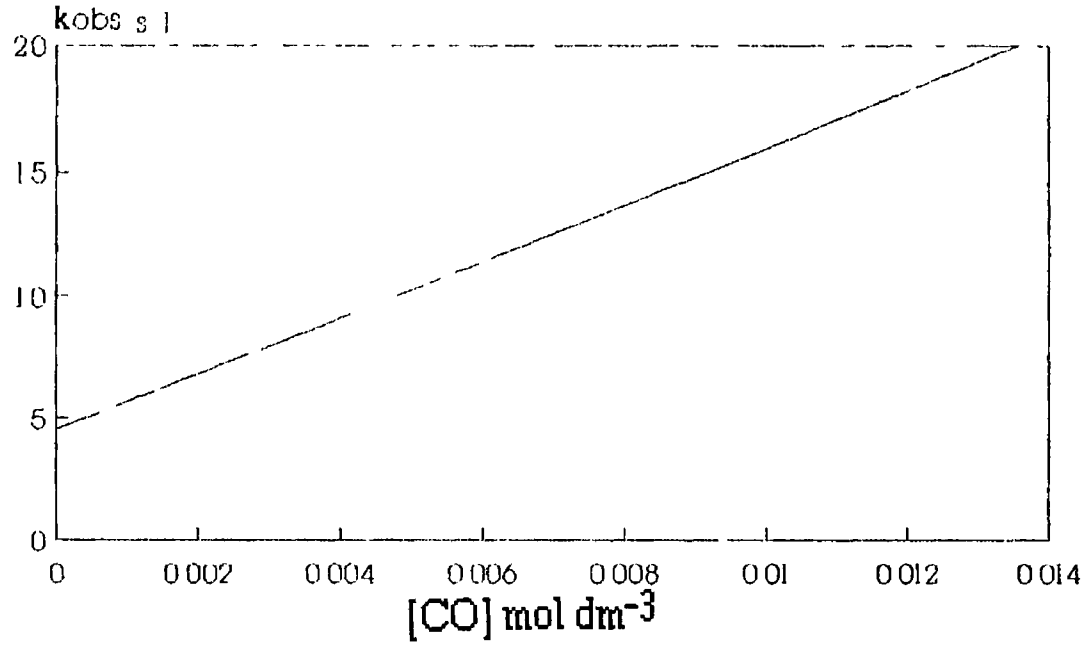

[CO] mol dm^{-3}	k_{obs} (s^{-1})
0 003	6 99
0 006	12 6
0 009	15 26
0 012	17 51

$k_{[CO]} = 1\ 14 \times 10^{3} \pm 1\ 86 \times 10^{2}\ dm^{3}\ mol^{-1}\ s^{-1}$

Intercept = 4 53 ± 1 52 s^{-1}

Corr Coeff = 0 974

Figure 3.4.2.4.3 The experimental data obtained for the graph of the observed rate constants (s^{-1}) for the fourth transient species with concentration of CO (mol dm^{-3}) at 298K.

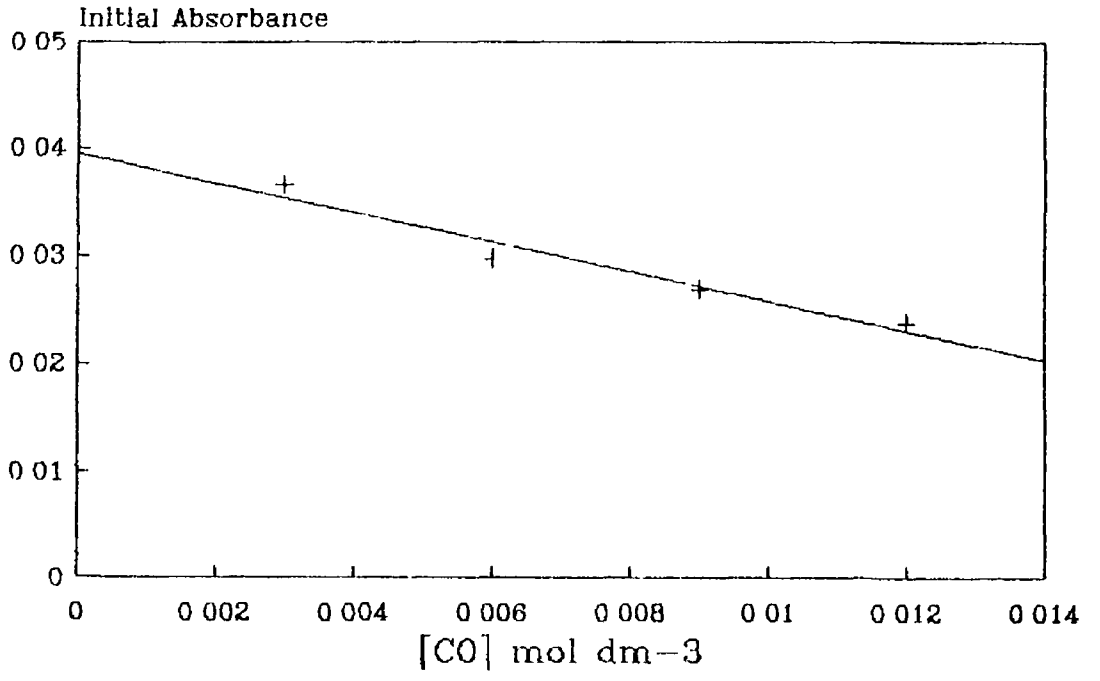

Figure 3.4.2 4 4 A plot of the initial absorbance of the fourth transient species against CO concentration showing the dependence of the yield on concentration of CO

3 4 2.5 Fifth transient species

A UV/visible difference spectrum of the fifth transient species is shown in Figure 3 4 2 5 1 and it can be seen that, like the other transient species, it has a λmax at ~400nm A typical transient signal obtained for this species is shown in Figure 3 4 2 5 2 This species appears to be stable even under a CO atmosphere However kinetic measurements at long timescales is difficult because of the effect of diffusion of product from the monitoring beam This species was affected by the presence of CO in the sample solution A plot of initial absorbance against CO is given in Figure 3 4 2 5 3 and shows a drop in yield of this photoproduct with increasing CO concentration This species was not the result of reaction with water in the cyclohexane solution as it was present with and without a liquid pumping phase in the sample preparation and so therefore it probably is a dinuclear complex

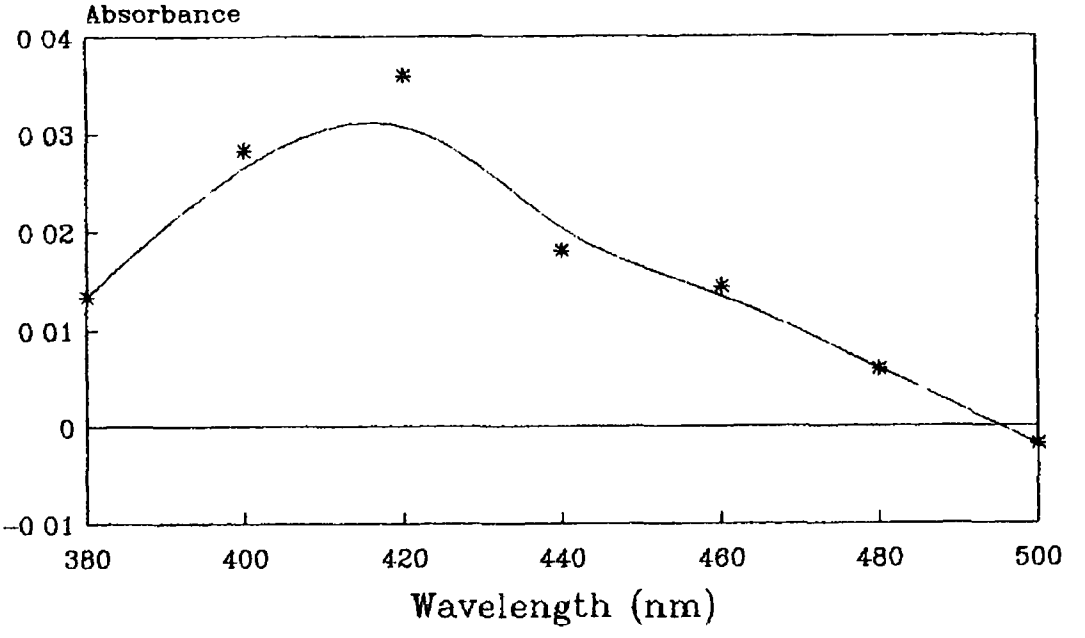

Figure 3.4 2.5.1 A UV/visible difference spectrum of the fifth transient species obtained 0 3 s after the laser pulse

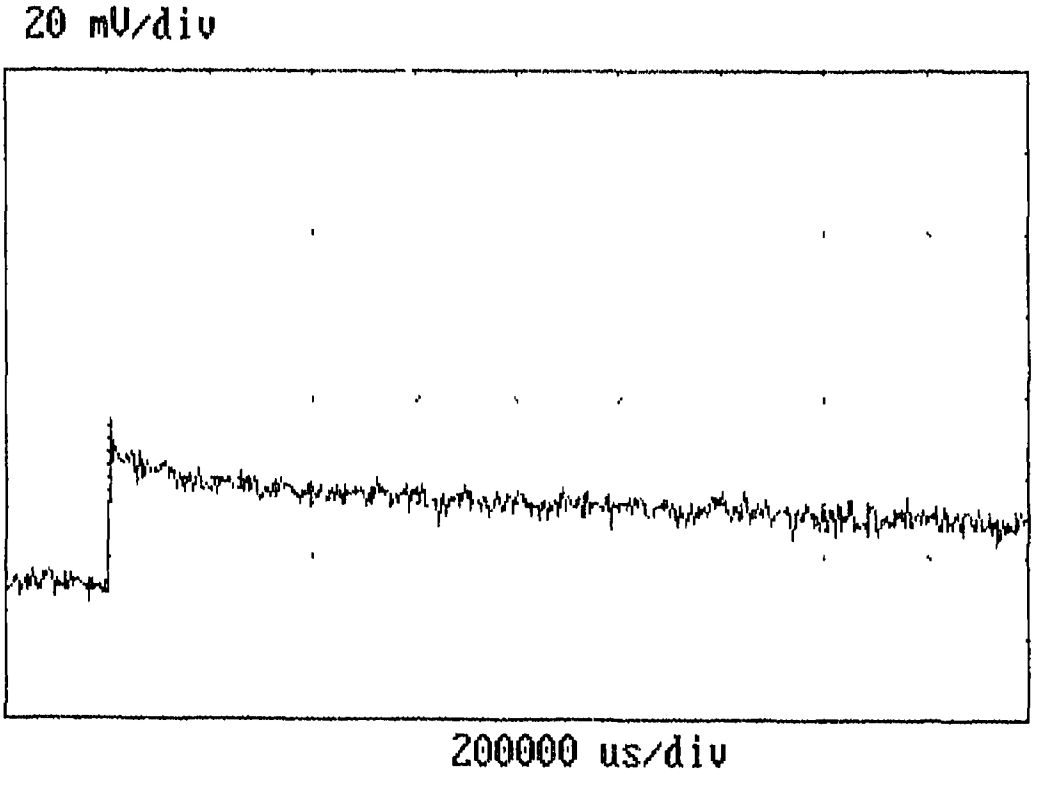

Figure 3.4.2.5.2 A typical transient obtained for the fifth transient species under 0 25 atmospheres of CO

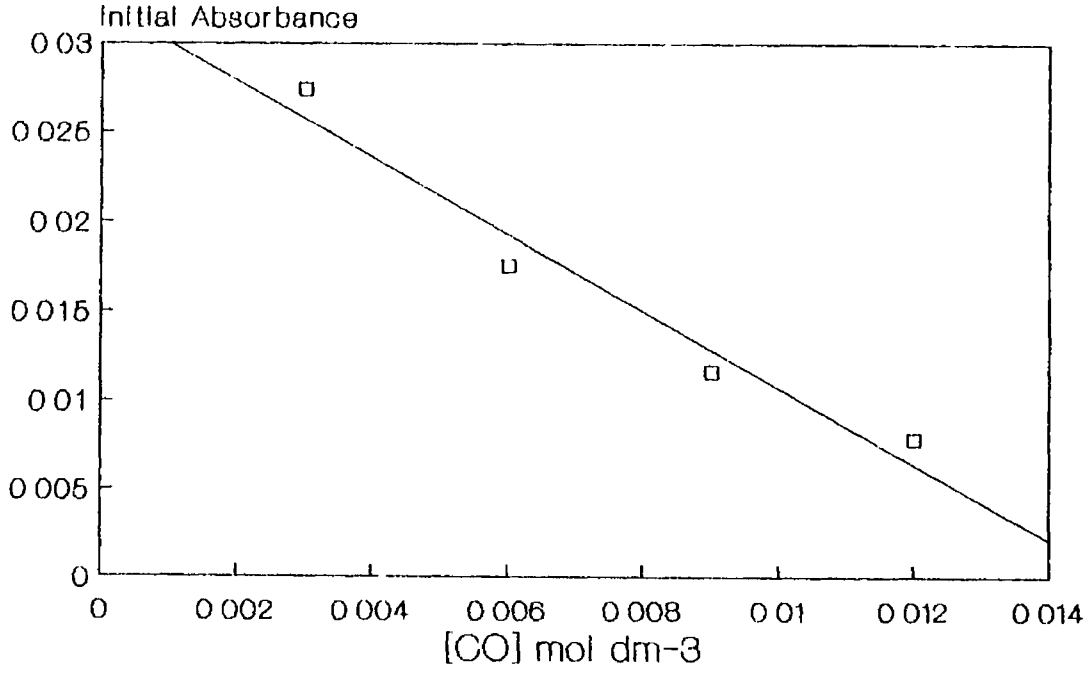

Figure 3 4.2.5.3 A plot of initial absorbance against CO concentration for the fifth transient species

3 4.3 266nm laser flash photolysis of $W(CO)_5PPh_3$ with UV/visible monitoring

Laser flash photolysis of $W(CO)_5PPh_3$ at 266nm produced evidence for the formation of three photoproducts Room temperature infra red experiments were not possible because of significant absorption by the sodium chloride plates and the large extinction coefficient of $W(CO)_5PPh_3$ at 266nm (ε = 20040 cm mol dm^{-3}) Identities for these photoproducts were suggested primarily on the basis of their reaction kinetics UV/visible difference spectra were also used to aid in the identification of the photoproducts The species produced on 266nm photolysis of $W(CO)_5PPh_3$ were *cis*-$W(CO)_4PPh_3$, $W(CO)_5$(cyclohexane) and *trans*-$W(CO)_4PPh_3$(cyclohexane)

3 4.3.1 First transient species

A UV/visible difference spectrum of the first transient species is shown in Figure 3.4 3 1 1 and contains a broad band with a λmax at ~430nm commonplace in

these tungsten carbonyl photoproducts No significant conclusions could be drawn from this spectrum The reaction of this intermediate with CO was extremely important in determining the identity of this species A plot of the observed psuedo first order rate constant against differing CO concentrations in cyclohexane solution revealed that the change in k_{obs} with CO concentration was linear The bimolecular rate constant was obtained from the slope and calculated as $3\,2 \times 10^7$ dm^3 mol^{-1} s^{-1} $\pm$ $1\,9 \times 10^6$ This rate was half that observed for the *cis* -$W(CO)_4PPh_3$ intermediate on 355nm excitation The reason for this change was unknown but it may be because of discrete changes in the transient profile as 266nm irradiation was prone to shock waves The reaction rate of the first species in the 266nm photolysis was significantly faster than the corresponding rate for $W(CO)_5$(cyclohexane) at $6\,6 \times 10^5$ dm^3 mol^{-1} s^{-1} and therefore was not $W(CO)_5$(cyclohexane) Alternatively the species could be *trans*-$W(CO)_4PPh_3$ However *trans*-$W(CO)_4PPh_3$(n-heptane) reacted significantly slower than the corresponding *cis*-$W(CO)_4PPh_3$(n-heptane) in Dobson and coworkers TRIR 308nm excitation of $W(CO)_5PPh_3$ (*cis* $1\,4 \times 10^5$ s^{-1} , *trans* $3\,5 \times 10^4$ s^{-1})[10] Knowing that photolysis of metal carbonyl species in cyclohexane slows down the rate of decay of the species produced relative to n-heptane because of different interaction energies of the solvent with the metal centre, this species could not be assigned to *trans*-$W(CO)_4PPh_3$(cyclohexane) In addition, the positioning of the triphenylphosphine *trans* to the vacant site would facilitate solvation and stabilise the *trans* species for a longer period of time relative to a non-solvated intermediate It was therefore concluded that this species was the *cis*-$W(CO)_4PPh_3$ intermediate

3.4.3.2 Second transient species

The second transient species had a lifetime of approximately 500μs under one atmosphere of CO A UV/visible difference spectrum of this transient is shown in Figure 3 4 3 2 1 As expected the intermediate exhibited a broad band with a λmax at

-430nm typical of these photocomplexes Photolysis of this species under varying concentrations of CO revealed a linear dependence of the observed rate constant with CO The second order rate constant for the reaction of this species with CO was 4 1 x 10^5 dm^3 mol^{-1} s^{-1} ± 1 5 x 10^5 and was in agreement with the second transient observed in the 355nm photolysis of $W(CO)_5PPh_3$ Therefore it may be assumed that this species was present in both 355nm and 266nm photolysis of $W(CO)_5PPh_3$ In the 355nm photolysis experiments this species was assigned to $W(CO)_5$(cyclohexane)

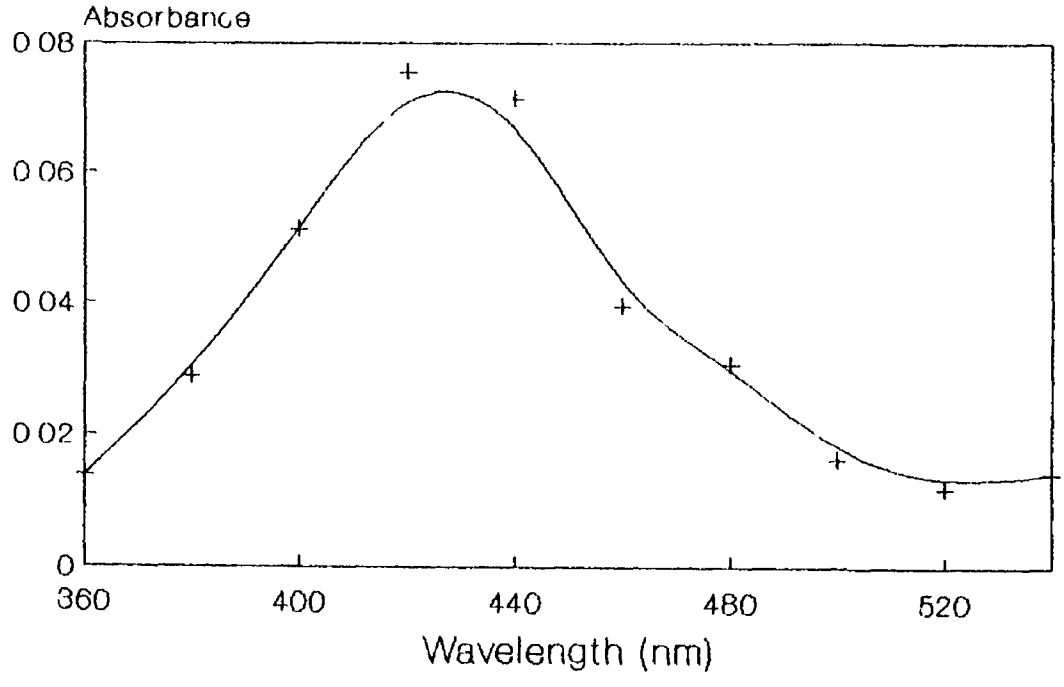

Figure 3.4.3.1.1 A UV/visible difference spectrum of *cis*-$W(CO)_4PPh_3$ obtained 5μs after the laser pulse

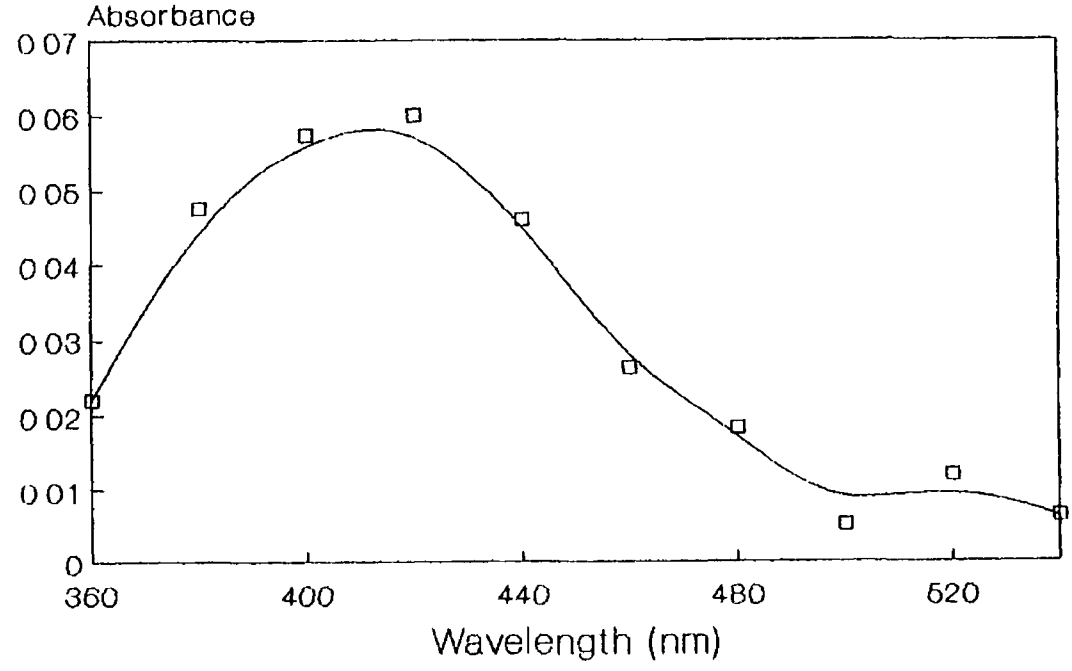

Figure 3.4.3 2.1 A UV/visible difference spectrum of the second transient species obtained 50μs after the laser pulse

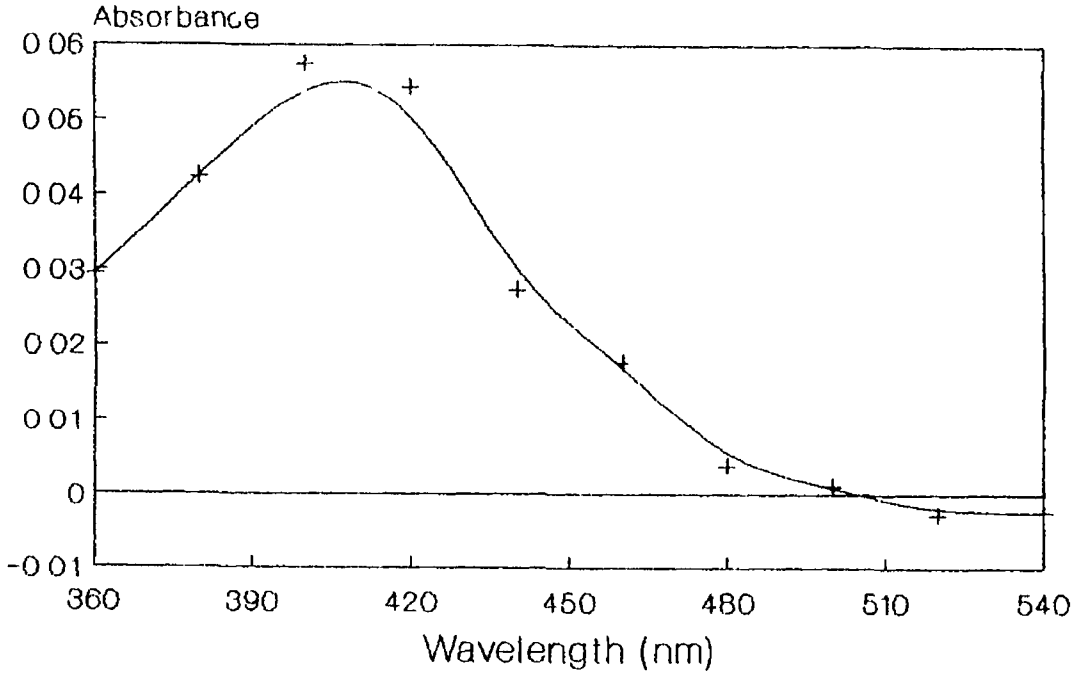

Figure 3.4 3.3.1 A UV/visible difference spectrum of the third transient species obtained 2500μs after the laser pulse

3 4 3.3 Third transient species

A third transient species was observed and had a λmax at 430nm A UV/visible difference spectrum of this species can be seen in Figure 3 4 3 3 1 The second order rate constant for the reaction of this species with CO was calculated as 1 5 x 10^4 dm^3 mol^{-1} s^{-1} ± 1 8 x 10^3 and indicates that this species was the same as that observed on 355nm photolysis In the 355nm experiments this species was tentatively assigned as *trans*-$W(CO)_5PPh_3$(cyclohexane)

Weak transients were observed for the last species presumably because of the lower concentration of $W(CO)_5PPh_3$ in solution compared to the experiments at 355nm This demonstrates that this species was a dinuclear species as the lower parent concentration would decrease the chance of a primary photoproduct reacting with parent

3.5 Conclusions

The possibility of three primary photoproducts on photolysis of compounds of the type $M(CO)_5PPh_3$ (M = Cr, Mo or W) can lead to the production of many photoproducts, both primary and secondary The reaction kinetics of the intermediates formed in the photolysis can help in identifying the nature of the transient species A summary of the second order rate constants for the transient species obtained upon 355nm photolysis of $M(CO)_5PPh_3$ complexes is presented in Table 3 5 1 It can be seen that the reactivity of the transient species was dependent on the type of metal and the metal radii i e steric and electronic requirements For the first transient species, the *cis*-$M(CO)_4PPh_3$ analogue, the reactivity of the intermediates was in the order Cr > Mo > W This order is consistent with the relative atomic radii of the metal atoms and indicates a steric requirement as generally molybdenum carbonyl complexes tend to react faster than chromium and tungsten complexes[20] The first transient species in each case was presumed to be non-solvated on the basis that the second order rate constants obtained for the reaction of the *cis* intermediate with CO were two orders of magnitude faster than the rates for the corresponding $M(CO)_5$(cyclohexane) intermediates and thereby indicating that the metal centre did not coordinate a solvent molecule on photolysis Steric effects arising from the triphenylphosphine ligand were believed to cause this difference in reactivity i e the larger solvent molecule could not coordinate to the metal because of the triphenylphosphine ligand but the smaller CO molecule could The intermediates may have been stabilised by intramolecular reaction with the triphenylphosphine ligand possibly an ortho metallation type interaction The *cis* species may be isomerising to the *trans* configuration although the evidence is not conclusive Dobson *et al* reported that the solvation of the $LW(CO)_4$ species inhibits the isomerisation process[10] Therefore if the *cis* species is not solvated then the isomerisation process may be favourable

In the case of the second transient species the results do not conclusively identify if this species was $M(CO)_5$(cyclohexane) The reactivity of the second transient species was in the order Mo > W This series reflects the relative reactivities of the metal hexacarbonyls i e molybdenum tends to be the most reactive[20] The reactivity of *trans*-$Cr(CO)_4PPh_3$ indicates that it may in fact be $Cr(CO)_5$(cyclohexane) even though spectral data indicate otherwise If one includes the *trans* - $Cr(CO)_4PPh_3$(cyclohexane) second order rate constant in the $M(CO)_5$(alkane) series, the relative rates ie Mo > Cr > W fit the reactivity series for the $M(CO)_5$(alkane) solvatocomplexes[21] The third transient species *trans*-$M(CO)_4PPh_3$(cyclohexane) also reflected this trend if the rate for the *trans*-$Cr(CO)_4PPh_3$(cyclohexane) complex was omitted from the series *trans*-$Cr(CO)_4PPh_3$(cyclohexane) appeared to react faster than the other species by an order of magnitude This species however was not observed to react with parent complex

Transient Species	Cr $k_{[CO]}$[a]	Mo $k_{[CO]}$[a]	W $k_{[CO]}$[a]
cis-$M(CO)_4PPh_3$	2 04 x 10^8	1 51 x 10^8	0 60 x 10^8
$M(CO)_5$(cyclohexane)	Absent	3 83 x 10^6	0 66 x 10^6
trans-$M(CO)_4PPh_3$-(cyclohexane)	1 92 x 10^6	4 00 x 10^5	1 27 x 10^4
dinuclear	No reaction	6 0 x 10^3	1 14 x 10^3
dinuclear	489	908	200[b]

Table 3.5 1 A table showing the second order rate constants for the reaction of the transient species produced on 355nm laser flash photolysis of $M(CO)_5PPh_3$ (M = Cr, Mo or W) with CO [a] $dm^3\ mol^{-1}\ s^{-1}$, [b] estimated from the observed rate constant under 1 atm CO

The other intermediates reacted with both CO and parent which suggested that they were primary photoproducts even though the yield of the intermediates dropped on addition of CO to the sample solutions The absence of a fourth transient species for the chromium analogue implied that the photochemical processes for $Cr(CO)_5PPh_3$ were simpler than the corresponding molybdenum and tungsten complexes It may reflect a smaller number of photoproducts on 355nm excitation producing perhaps a *cis*- and *trans*-$Cr(CO)_4PPh_3$ intermediate with a low quantum yield for loss of the unique ligand as was observed in the photochemistry of $Cr(CO)_4PMe_3$[12] The lifetimes of these transient species suggested that they were dinuclear species The lifetimes of the fifth transient species were of the order of seconds again indicating that they were dinuclear complexes The molybdenum intermediate was again the most reactive. The absence of a value for the tungsten analogue may reflect the thermal stability of tungsten complexes in general There was a decay for a fifth transient species but its lifetime was longer than the instrumentation could measure accurately In addition, diffusion of the photoproducts from the monitoring beam path can induce errors in kinetic measurements at long timescales[22] An estimate for the decay of this species under 1 atmosphere of CO gives a second order rate constant of 200 $dm^3\ mol^{-1}\ s^{-1}$ This fits in the reactivity series for the Group VIB metal carbonyl complexes

It was difficult to perceive any wavelength dependency on the 355nm and 266nm photolysis of these complexes The first transient species *cis*-$M(CO)_4PPh_3$ was present for M = Mo, W but absent for M = Cr This indicated that the higher energy excitation of $Cr(CO)_5PPh_3$ does not induce the loss of a CO ligand in the *cis* position The reduction in quantum yield could be the result of a different non-radiative pathway for the *cis* -$Cr(CO)_4PPh_3$ intermediate arising from the higher energy excitation The second transient species was present for all complexes and was identified, in all cases, as the same species present on 355nm excitation The quantum yield of this species may have increased with the move to higher energy excitation The

third species was present for chromium and tungsten but in a low yield for molybdenum This suggests that there may be wavelength dependency for ligand loss in $Mo(CO)_5PPh_3$ This third species was shown to react with parent and CO on 355nm excitation which suggests it may have been a primary photoproduct The low yield of this species on irradiation at 266nm may have reflected a change in the photochemistry of $Mo(CO)_5PPh_3$ The overall reaction schemes are shown Schemes 3 5 1, 3 5 2 and 3 5 3 for chromium, molybdenum and tungsten respectively

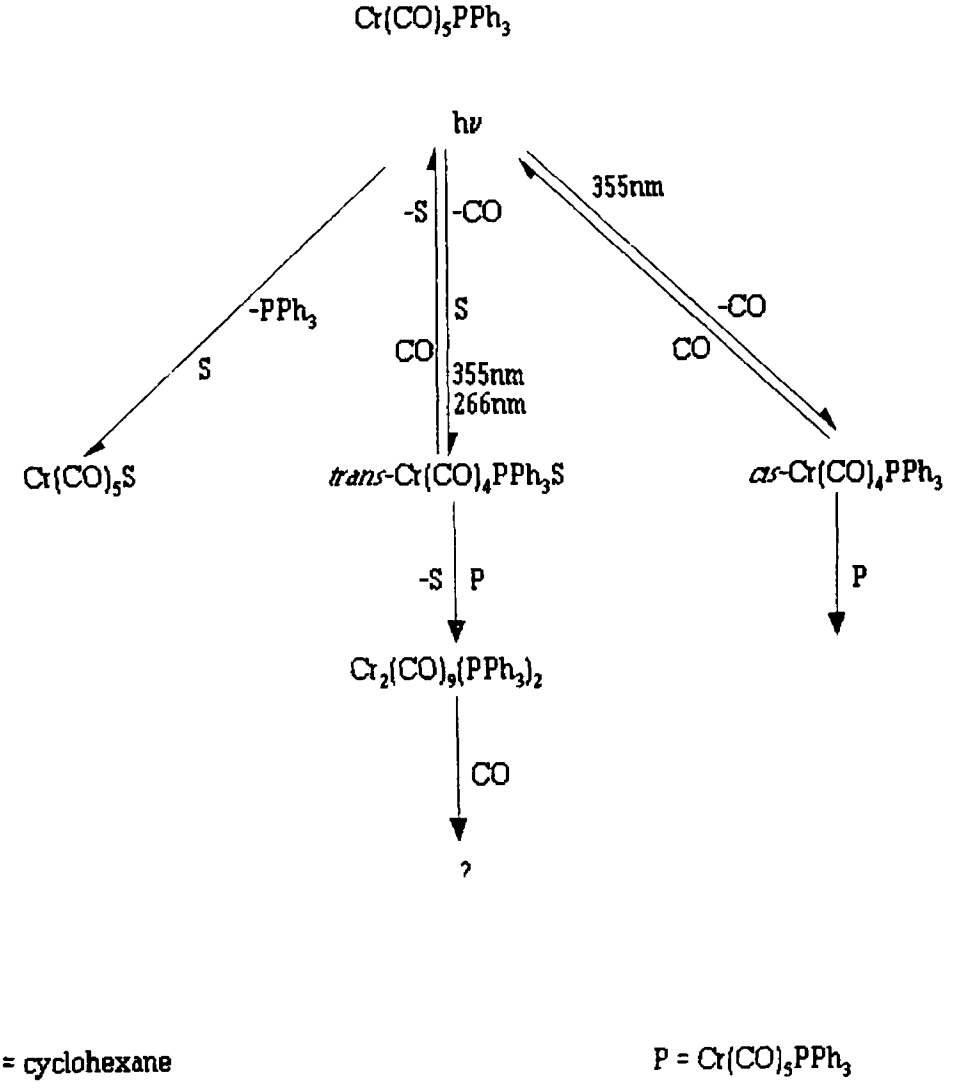

S = cyclohexane

P = $Cr(CO)_5PPh_3$

Scheme 3.5.1 The reaction scheme for the photochemical and subsequent thermal reactions on the laser flash photolysis of $Cr(CO)_5PPh_3$

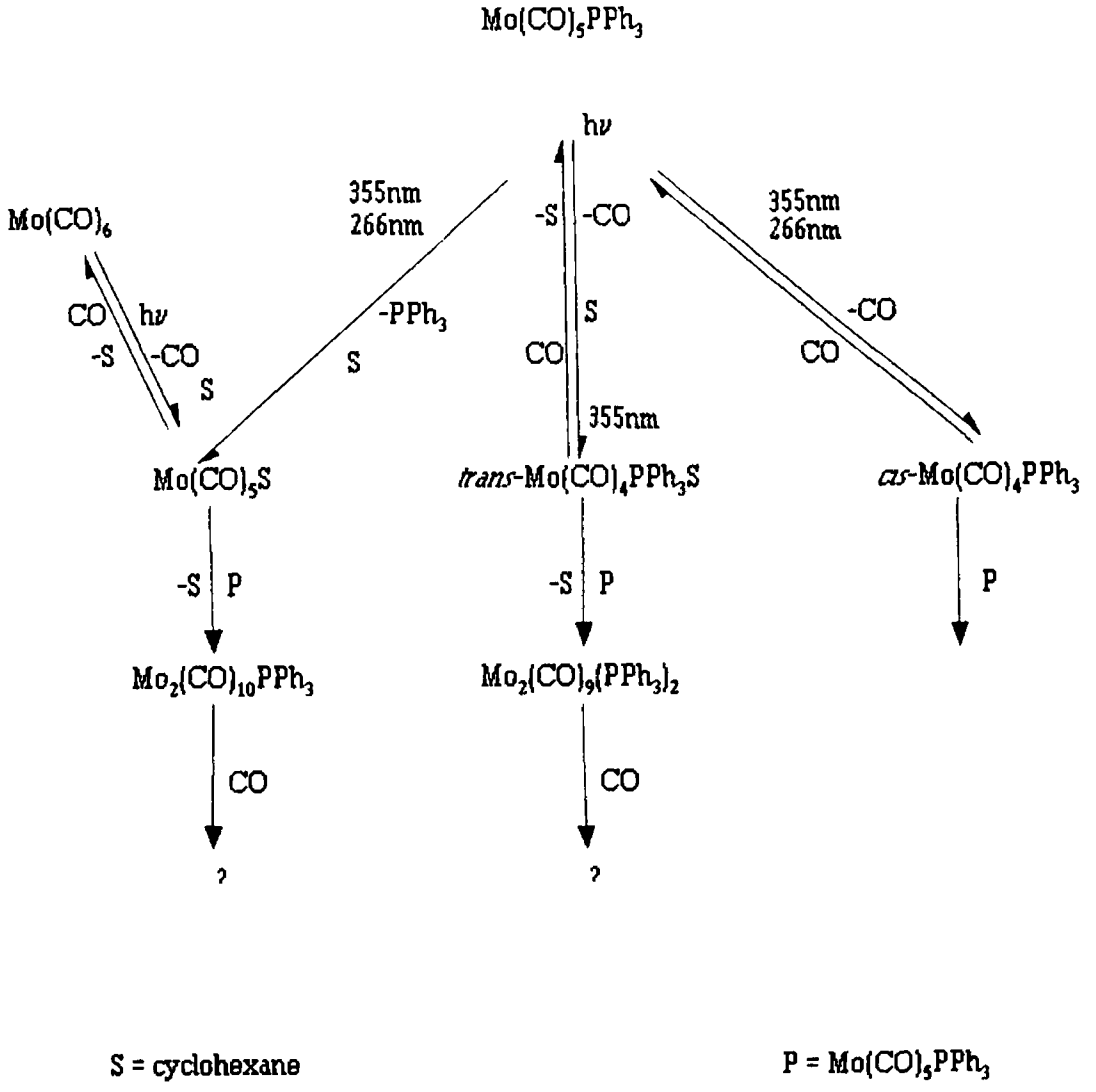

Scheme 3.5.2 The reaction scheme for the photochemical and subsequent thermal reactions on the laser flash photolysis of $Mo(CO)_5PPh_3$

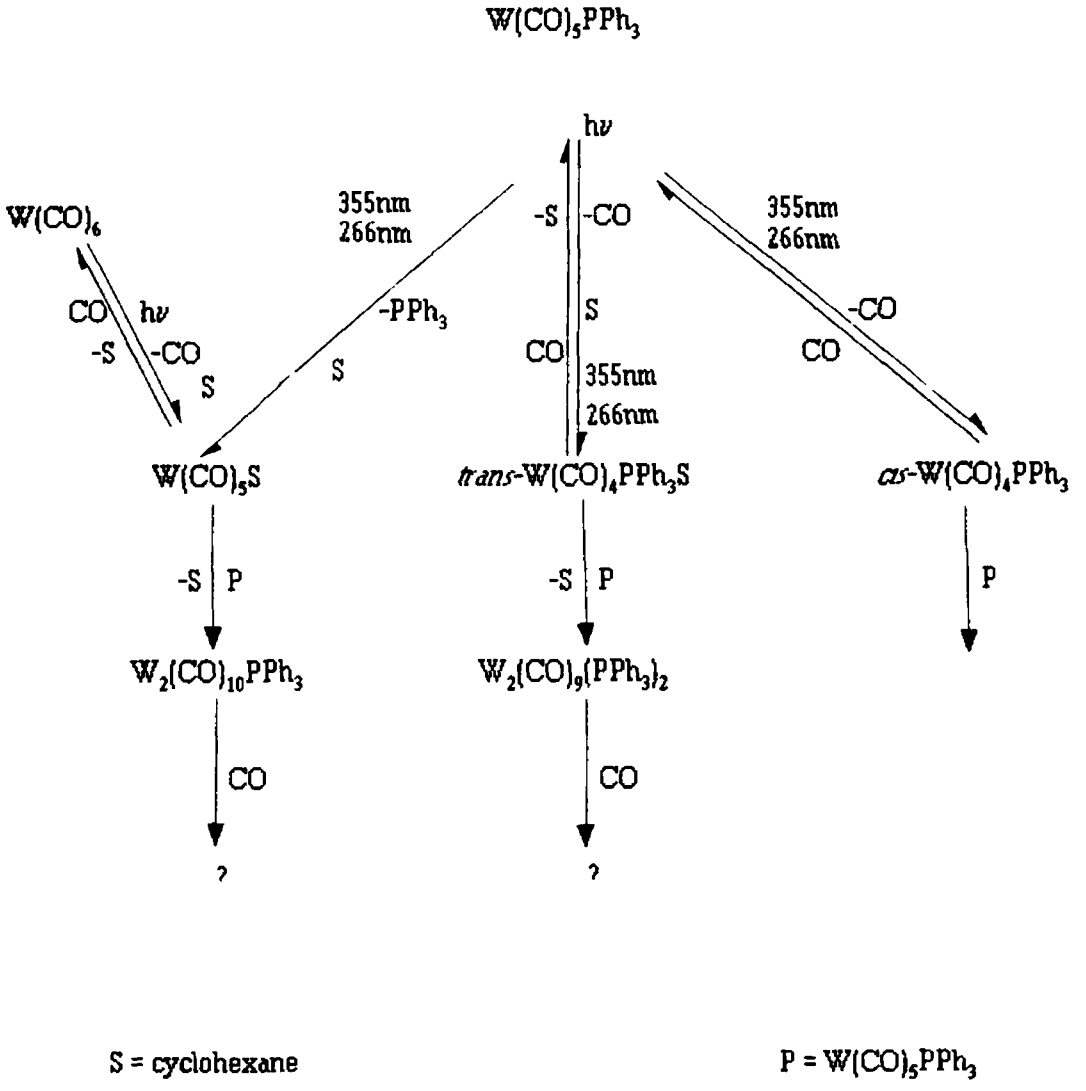

Scheme 3.5.3 The reaction scheme for the photochemical and subsequent thermal reactions on the laser flash photolysis of $W(CO)_5PPh_3$

REFERENCES

1 Geoffroy, G L, Wnghton, M S, *Organometallic Photochemistry*, Academic Press, New York, 1979

2 Strohmeier, W, *Agnew Chem Int Ed Engl*, 1964, **3(11)**, 730

3 Nayak, S K, Burkley, T J, *Organometallics*, 1991, **10**, 3745

4 Wnghton, M S, *Chem Rev*, 1974, **74**, 401

5 Darensbourg, D J, Murphy, M A, *J Am Chem Soc*, 1978, **100**, 463

6 Cotton, F A, Kraihanzel, C S; *J Am Chem Soc*, 1962, **84**, 4432

7 Kelly, J M, Hermann, H, Koerner von Gustorf, E, *J Chem. Soc, Chem Commun*, 1973, 105

8 Zhang, K, Gonzalez, A A, Mukerjee, S L, Chou, S J, Hoff, C D, Kubat-Martin, K A, Barnhart, D, Kubas, G J, *J Am Chem Soc*, 1991, **113**, 9170

9 Atwood, J D, Brown, T L, *J Am Chem Soc*, 1976, **98**, 3160

10 Dobson, G R, Hodges, P M, Healy, M A, Poliakoff, M, Turner, J J, Firth, S, Asali, K J, *J Am Chem Soc*, 1987, **109**, 4218

11 Church, S P, Grevels, F-W, Hermann, H, Schaffner, K; *Inorg. Chem*, 1985, **24**, 418

12 Boxhoorn, G, Schoemaker, G C, Stufkens, D J, Oskam, A, *Inorg Chim Acta*, 1980, **42**, 241

13 Dahlgren, R M, Zink, J I, *Inorg Chem*, 1977, **16**, 3154

14 Creaven, B S, Dixon, A J, Kelly, J M, Long, C, Poliakoff, M, *Organometallics*, 1987, **6**, 2600

15 Kelly, J M, Long, C, Bonneau, R, *J Phys Chem*, 1983, **87**, 3344

16 Creaven, B S, PhD thesis, Dublin City University, 1989

17 Dobson, G R, Bernal, I, Reisner, G M, Dobson, C B, Mansour, S E, *J Am Chem. Soc*, 1985, **107**, 525

18 Asali, K J, Basson, S S, Tucker, J S, Hester, B C, Cortés, J E, Awad, H H, Dobson, G R, *J Am Chem Soc*, **1987, 109**, 5386

19 Brown, C F, Ishikowa, Y Hackett, P A, Rayner, D M, *J Am Chem. Soc*, **1990, 112**, 2530

20 Howell, J A S; Burkinshaw, P M, *Chem, Rev*, **1983, 83**, 557

21 Zhang, S, Zang, V, Bajaj, H C, Dobson, G R, van Eldik, R, *J. Organomet Chem*, **1990, 397**, 279

22 Long, C, Cassidy, J F, *J Photochem Photobiol, A Chem*, **1990, 54**, 1

CHAPTER 4

THE CRYSTAL STRUCTURES OF $(\eta^5\text{-}C_6H_7)Mn(CO)_2(C_5H_5N)$ AND $(\eta^5\text{-}C_6H_7)Mn(CO)_2(\textit{cis}\text{-}C_8H_{14})$

4.1 Introduction

X-ray crystallography has become a very important technique in the elucidation of the structure of molecules X-rays with wavelengths of less than 2Å are used for the determination of the relative positions of atoms in crystals because their wavelengths are comparable to the spacings of atoms in a molecule X-rays interact with crystals in what can be described as a diffraction phenomenon Crystals themselves are characterised by periodicities in three dimensions i e the atomic grouping is repeated by symmetry elements so as to build up a crystal The regularity of the 3-D structure of crystals acts to reinforce the diffraction caused by any molecule in the crystal The nature of the diffraction provides a method where the molecular structure and crystal structure may be determined

The crystal structures of two manganese complexes were determined The complexes were of the type $(\eta^5\text{-}C_5H_4CH_3)Mn(CO)_2L$ where L = pyridine and *cis*-cyclooctene These compounds were examined to see if the presence of two distinctly different ligands (L) had an effect on the $(\eta^5\text{-}C_5H_4CH_3)Mn(CO)_2$ unit i e the strong σ donating capacity of the pyridine ligand and the strong π accepting capacity of the *cis*-cyclooctene ligand The structures were solved by the Patterson heavy atom method The heavy atom method can give a trial structure which can then be refined This method involves location of the heaviest atom(s) in the molecule by calculating an electron density map (Patterson map) from the collected reflection data Refinement takes place in four stages (1) A crude model of the structure is calculated from the first calculated electron density functions and the observed structure factors with the observed phases (2) A set of structure factors is calculated allowing for thermal effects A new electron density map and structure is calculated from the observed structure factors and calculated phases This procedure is repeated until a reproducible model is obtained (cyclic Fourier refinement) (3) A difference Fourier synthesis produces a

difference Fourier map which allows for further refinement to produce more precise locations of atoms, identification of missing atoms and refinement of thermal parameters Steps (2) and (3) are repeated as necessary until the discrepancy under R (see Equation 4 1 1) is reduced (4) A statistical model of the structure is obtained using least squares refinement which represents the best fit with the observed data Three positional and six thermal parameters are fitted to each atom The final result is an electron density map which correlates with the true structure At each stage an R value is calculated This value indicates the correlation of the calculated structure to the actual structure and is computed from the following equation;

$$R = \frac{\Sigma|(|Fo| - |Fc|)|}{\Sigma|Fo|} \qquad \text{Equation 4 1 1}$$

where |Fo| is the observed structure factor and |Fc| is the calculated structure factor

The reflection data were collected on a four circle diffractometer Using a four circle diffractometer allows for total freedom of rotation about three mutually perpendicular axes so that the crystal can be placed in any onentation The fourth circle is the position of the counter and the incident beam which can only be moved in the honzontal plane (Figure 4 1 1)

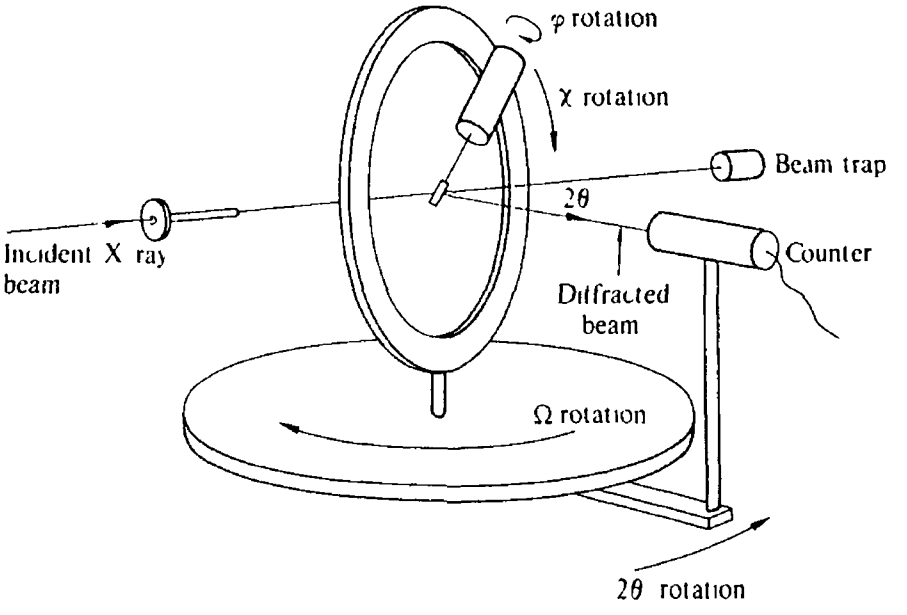

Figure 4.1.1 A schematic diagram of the geometry of a four circle diffractometer

compound	$(\eta^5\text{-}C_6H_7)Mn(CO)_2(C_5H_5N)$	$(\eta^5\text{-}C_6H_7)Mn(CO)_2(cis\text{-}C_8H_{14})$
F$_w$ a m u	269 18	300 28
space group	$P2_{1/c}$	$P2_{1/n}$
crystal	monoclinic	monoclinic
a Å	7 761(5)	6 198(5)
b Å	20 578(10)	19 476(13)
c Å	15 634(11)	12 273(10)
β deg	103 10(6)	94 21(6)
V Å^3	2432(3)	1477 6(2)
Z	8	4
density g cm^{-3}	1 45(5) (meas), 1 47 (calc)	1 35(5) (meas),1 394 (calc)
radiation	Mo K_α (λ = 0 710692Å) monochromated graphite	Mo K_α (λ = 0 710692Å) monochromated graphite
μ cm^{-1}	10 3	8 53
F(000)	1104	631.97
reflections	6196	4801
total unique reflections	5628	3774
unique reflections $I>2\sigma(I)$	3286	3191
R	0 056	0 049
R_w	0 055	0 0546
w	$w = \frac{1\ 7056}{(\sigma^2(F)+0\ 001F^2)}$	$w = \frac{0\ 4794}{(\sigma^2(F)+0\ 001F^2)}$

Table 4.1.1 A summary of the crystallographic data for the complexes $(\eta^5\text{-}C_6H_7)Mn(CO)_2L$ where L = pyridine and *cis*-cyclooctene

4.2 Data collection for $(\eta^5\text{-}C_6H_7)Mn(CO)_2(C_5H_5N)$

The synthesis of $(\eta^5\text{-}C_6H_7)Mn(CO)_2(C_5H_5N)$ is described in the experimental section The crystallographic data was collected by Dr R A Howie at the University of Aberdeen[1] A rectangular prismatic crystal of dimensions 0 3 x 0 3 x 0 5 mm^3 was selected for crystal structure determination The crystal was mounted on a Nicolet P3 four circle diffractometer Mo Kα radiation (0 71069 Å) was used in the analysis of the complex in which a total of 6196 reflections were measured in the range h -10 to 10 , k 0 to 23, l 0 to 20 out to 2θ = 55° using a $\theta/2\theta$ scan technique Of these reflections 5628 were unique of which 3286, with $I>2\sigma(I)$, were considered observed No absorption correction was applied to the data (μ = 10 3cm^{-1}) At a interval of 50 measurements standard reflections 4,0,2 and 0,12,0 were measured and their intensity decreased by 25% during the data collection The data was corrected by linear interpolation between the standard intensity values The density measurement was carried out by using the density gradient tube method[2]

The structure was solved using SHELXS86[3] by the Patterson heavy atom method followed by partial structure expansion to calculate the positions of the non-hydrogen atoms The atomic coordinates were refined by least squares refinement using SHELX76[4] Hydrogen atom positions were calculated from the positions of the non-hydrogen atoms to which they were attached Standard isothermal parameters (U_{iso}) of 0 05 $Å^2$ for the aromatic hydrogens and 0 13$Å^2$ for the methyl hydrogens were used In the final refinement stages the methyl unit was treated as a rigid body The final calculated R values were R = 0 056 and wR = 0 055 ($w = 1\ 7056/(\sigma^2(F) + 0\ 001F^2)$ The maximum and minimum values for $\Delta\rho$ in the final electron density map were 0 529 and -0 370$Å^3$ respectively The maximum least shift to squares error (Δ/σ_{max}) in the final cycle was 0 163 for non-hydrogen atoms Atomic scattering factors for manganese were taken from the International Tables for X-ray Crystallography Vol IV[5] The final atomic

coordinates are given in Appendix A for all non-hydrogen atoms A full listing of the bond distances and angles can be found in Appendix A A view of the molecular structure of two atoms of the asymmetric unit is given in Figure 4 2 1 Figure 4 2 2 shows a diagram of the unit cell A summary of the crystallographic data can be found in Table 4 1 1

4.3 Crystal structure of $(\eta^5\text{-}C_6H_7)Mn(CO)_2(C_5H_5N)$

The structure contained two independent and structurally distinct molecules per asymmetric unit The two molecules of this unit can be seen in Figure 4 2 1 This crystallographic independence has been seen in other molecules of the type $CpMn(CO)_2L$ where Cp = cyclopentadienyl and L = CMe_2[6], η^2-CH_2=CPh(OCOMe)[7] and η^2-1-diethylphosphonato-2-phenyl ethylene[8] The principal differences between the structures of the two independent molecules in the title complex were firstly that the dihedral angle C(10)-cCp-Mn(1)-N(1) (cCp = the centroid of the cyclopentadienyl ring) was 1 6(2)° in molecule 1 and 6 2(2)° in molecule 2 and secondly that the angle between the mean planes of the cyclopentadienyl and pyridine rings was 24 7(2)° in molecule 1 and 44 9(2)° in molecule 2 The Mn-N distances were also different at 2 023(4)Å for molecule one and 2 038(4)Å for molecule 2 No significant interactions were observed between the two molecules The pyridine rings were planar in both molecules The maximum deviation from the plane was 0 0183 Å for N(1) in molecule 1 and 0 0068Å for N(1A) in molecule 2 The carbon-carbon and the carbon-nitrogen distances were normal within the pyridine ring

The orientation of the methyl group was *cis* to the pyridine ligand This orientation causes the mean plane of the cyclopentadienyl ring to tilt slightly from orthogonality to the Mn ring-centroid vector (92 6(3)° for molecule 1 and 93 2(2)° for molecule 2) As a result the mean Mn-Cp(π) distances were not equivalent ranging in molecule 1 from Mn(1)-C(10) at 2 201(5)Å to Mn(1)-C(8) at 2.117(6)Å. The equivalent

values for molecule 2 were 2 209(5)Å to 2 119(6)Å This was in contrast to other compounds of the type $MeCpMn(CO)_2L$ (L = PPh_3[9] 2 132(9)-2 162(8)Å, L = menthylmethoxycarbene[10] 2 14(2)-2 16(2)Å, L = norbornadiene[11] 2 17(2)-2.19(2)Å; L = SO_2[12] 2 07(2)-2 11(1)Å) The differences in the Mn-Cp(π) may not be exclusively the result of steric factors and may be because of the increased electron density on the central metal atom This increased electron density results from the good σ-donating but poor π-accepting capacity of the pyridine ligand Carbonyl stretching frequencies are a good indicator of electron density on a metal atom[13] The greater the electron density on a metal in a carbonyl complex lowers the carbonyl stretching frequencies The values for pyridine were 1943 and 1886cm^{-1} compared to 2032 and 1945cm^{-1} for $MeCpMn(CO)_3$ (*vide infra*) This tilting of the cyclopentadienyl ring may give an indication of the early stages of a η^5 to η^3 ring slippage The η^3 complex [η^3-$MeCpMn(CO)_3$]$^{2-}$ with a negatively charged manganese centre has been observed in the infra red region[14] Therefore ring slippage may be a function of charge on the the manganese centre The five ring carbons are coplanar The maximum deviation from the mean plane was 0 002(5)Å for C(8) in molecule 1 and 0 011(5)Å for C(10) in molecule 2 The distance between the ring carbons was normal for a coordinated cyclopentadienyl ring at 1 415(9)Å for molecule 1 and 1 410(7)Å for molecule 2 The methyl carbon was displaced from the mean plane of the cyclopentadienyl ring by 0 075(5)Å in molecule 1 and 0 057(6)Å in molecule 2 This deviation from the mean plane is normal in η^5 coordinated methylcyclopentadienyl complexes[15]

The metal to carbon monoxide bond distances and angles were as expected for this type of complex No significant increase in CO bond length was noted for the increased electron density arising from coordination of the pyridine ligand The angles within the $Mn(CO)_2L$ tripod were 91 7(2)° for C(13)-Mn(1)-C(12), 93 4(2)° for C(13)-Mn(1)-N(1) and 97 3(2)° for C(12)-Mn(1)-N(1) The equilvalent values in molecule 2

were 91 6(2), 95 0(2) and 93 2(2) The angles in the tetrahedron cCp, C(13), C(12) and N(1) show distortion from ideal tetrahedral geometry

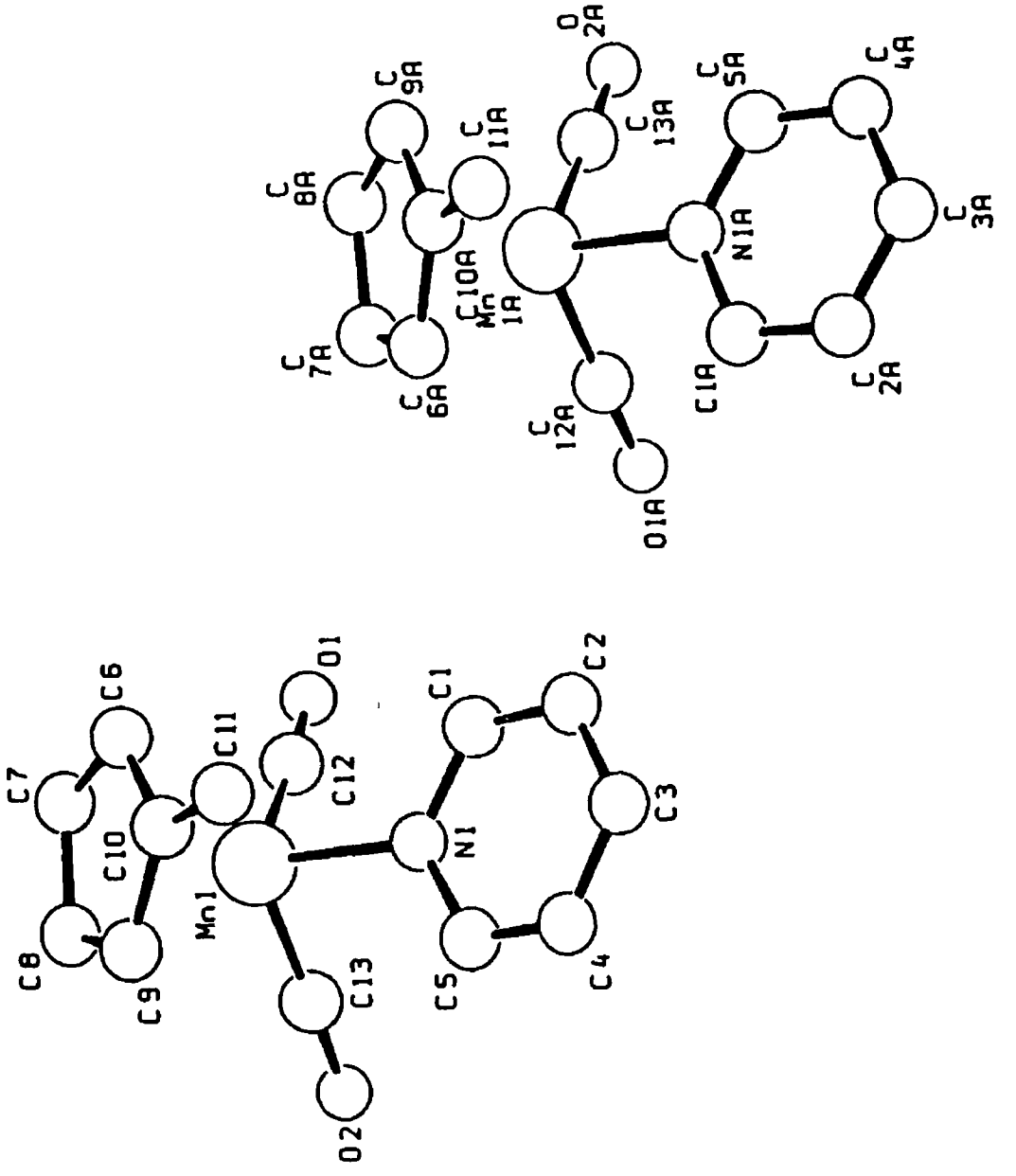

Figure 4.2.1 A SCHAKAL[16] drawing of the two molecules of the asymmetric unit in the crystal structure of $(\eta^5\text{-}C_6H_7)Mn(CO)_2(C_5H_5N)$.

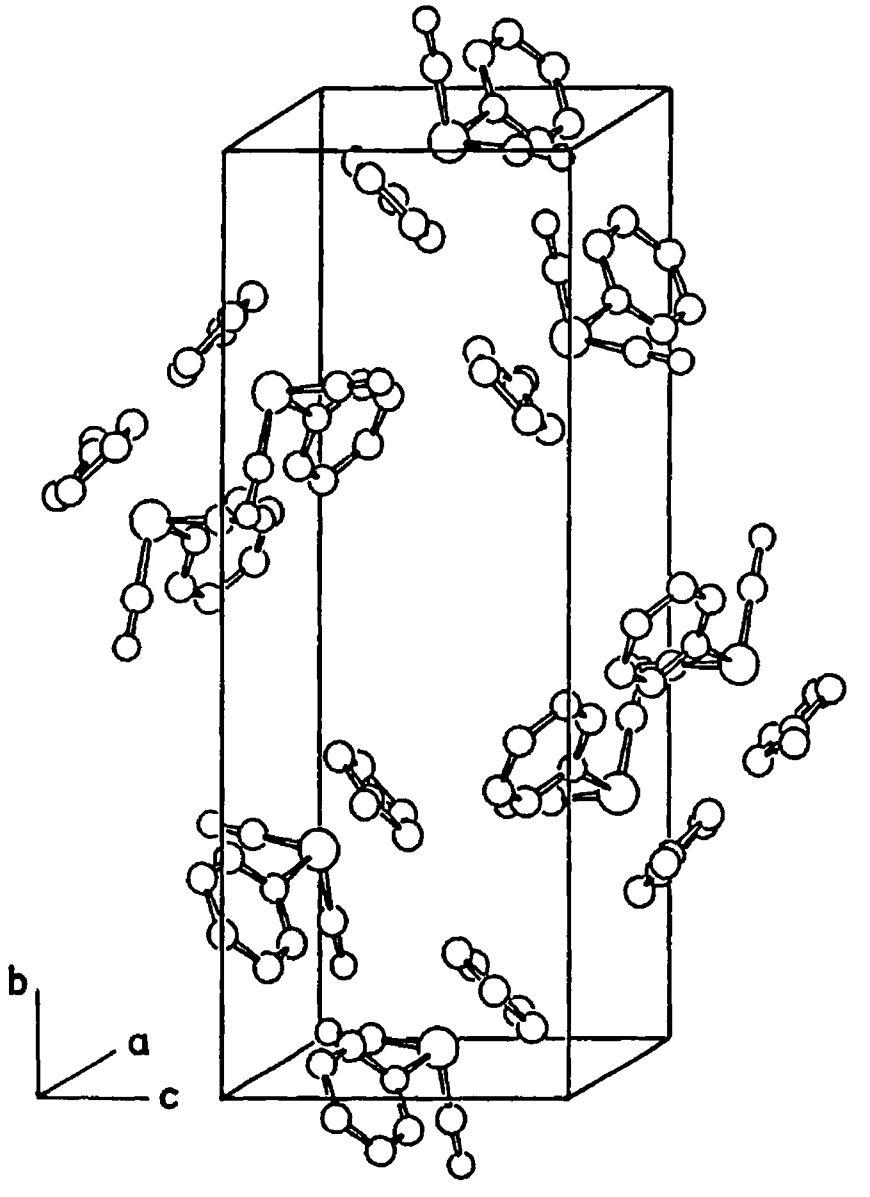

Figure 4.2 2 The unit cell of $(\eta^5\text{-}C_6H_7)Mn(CO)_2(C_5H_5N)$ (Z = 8) as represented by a SCHAKAL[16] drawing

4 4 Data collection for $(\eta^5\text{-}C_6H_7)Mn(CO)_2(\textit{cis}\text{-}C_8H_{14})$

The synthesis of $(\eta^5\text{-}C_6H_7)Mn(CO)_2(\textit{cis}\text{-}C_8H_{14})$ is described in the experimental section The X-ray data were collected by Dr R A Howie at the University of Aberdeen[1] A yellow crystal of dimensions 0 34 x0 6 x 0 56 mm^3 was selected for crystal structure analysis A Nicolet P3 four circle diffractometer was used for the determination Mo Kα radiation (0 71069Å) was used to determine 4801 reflections of which 583 were rejected by having $I < 2\sigma(I)$ and 3191 were considered observed The data was obtained by omega scan for 2θ in the range 0-60° Scan rates were in the range 1 0 to 29 3 degω min^{-1} The scan width was 0 6 degω at all times Background counts were taken at ±1 0 degω The indices were in the range h 0 to 9, k 0 to 28, l -18 to 15 Internal standards at 2,9,0 and 2,4,5 were stable to ±1 99 and ±2 11% (1 x σ) respectively No correction was applied for absorption (μ = 8 53cm^{-1}) Density measurements were carried out using the gradient tube method[2]

The structure was solved by the Patterson heavy atom method with partial structure expansion to find all non-hydrogen atoms using SHELXS86[3] The atomic coordinates were refined with full matrix least squares refinement using SHELX76[4] Hydrogen atoms were located in their calculated positions and refined using the non-hydrogen atoms to which they were attached Standard isothermal parameters (U_{iso}) of 0 5Å^2 for non-aromatic hydrogens and 0 13Å^2 for aromatic hydrogens were used In the final stages of refinement the methyl group was treated as a rigid body R values were calculated to be R = 0 049 and wR = 0 0546 where ($w = 0\ 4794/(\sigma^2(F) + 0\ 001F^2)$ The maximum and minimum values in the electron density difference map were 0 427 Å^3 and -0 452 Å^3 respectively The maximum least shift to error ratio (Δ/σ_{max}) was calculated as 0 330 for all non-hydrogen atoms. Atomic scattering factors for manganese were taken from the International Tables for X-ray Crystallography Vol IV[5] A full set of bond distances, angles and atomic coordinates can be found in Appendix B Figure

4 4 1 shows the structure of $(\eta^5\text{-}C_6H_7)Mn(CO)_2(cis\text{-}C_8H_{14})$ Figure 4 4 2 shows a representation of the unit cell A summary of the crystallographic data can be found in Table 4 1 1

4.5 Crystal structure of $(\eta^5\text{-}C_6H_7)Mn(CO)_2(cis\text{-}C_8H_{14})$

The $(\eta^5\text{-}C_6H_7)Mn(CO)_2(cis\text{-}C_8H_{14})$ complex contains one molecule per assymetric unit as represented in Figure 4 4 1 The *cis* -cyclooctene ring is η^2 coordinated to the $MeCpMn(CO)_2$ moiety *via* the ring double bond The distance between the carbon atoms of the double bond and the central manganese atom were 2 193(2)Å and 2 201(3)Å Similar distances were found for $CpMn(CO)_2(\eta^2$-cyclooctatetraene) of 2 193(2)Å and 2 202(2)Å[17] Other complexes with asymmetric η^2 coordinated ligands show unequivalent bond distances arising from either a bulky group on one of the ring carbons as in the case of η^2-anthronylketene[18] (1 976(6)Å and 2 242(6)Å) or from inductive effects from groups on one of the carbons as with η^2-methylvinylacetone[19] (2 149(8)Å and 2 175(7)Å) The length of the double bond serves as an indicator of the strength of interaction between the metal and the η^2 coordinated ligand The length of a normal carbon-carbon double bond is 1.34Å[20] On coordination, backdonation from the metal d orbitals into the ligand π^* orbitals increases the length of the double bond The η^2 *cis* -cyclooctene bond length was 1 376(4)Å This was shorter than other similar manganese complexes with η^2 ligands e.g anthronylketene[18] 1 448(8)Å, norbornadiene[21] 1 404(4)Å, cyclooctatetraene[17] 1 398(2)Å and methylvinylacetone[19] 1 390(12)Å The shorter bond length indicates that the *cis*-cyclooctene ligand may not be as tightly bound as in other complexes with η^2 ligands It may be because of inductive effects from the groups bound to the carbons in the double bond as these are known to affect bond distances in alkene compounds[20] This difference was also noted in the bond angle between the metal and the double bond carbon atoms e g C(1)-Mn(1)-C(8) in the title compound was

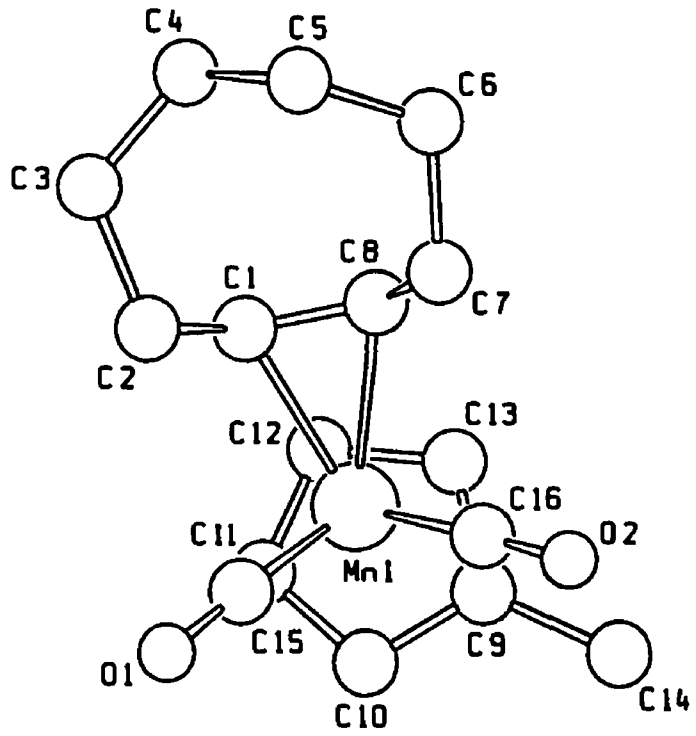

Figure 4.4.1 A SCHAKAL[16] drawing of the crystal structure of $(\eta^5\text{-}C_6H_7)Mn(CO)_2(\textit{cis}\text{-}C_8H_{14})$

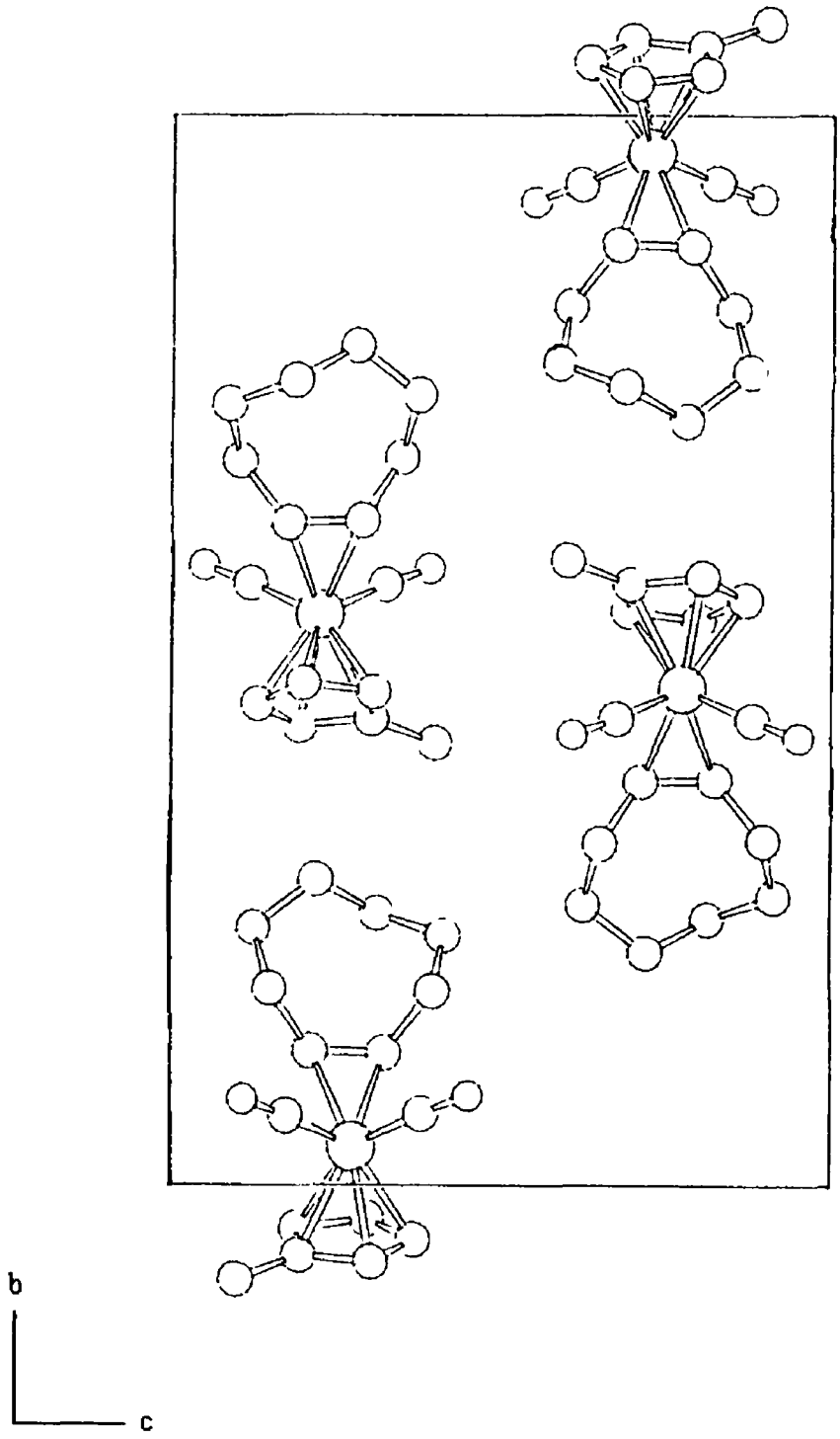

Figure 4.4.2 A SCHAKAL[16] representation of the unit cell of $(\eta^5\text{-}C_6H_7)Mn(CO)_2(\textit{cis}\text{-}C_8H_{14})$ (Z = 4)

36 5(1)°, methylvinylacetone[19] 37 5(0 3)°, norbornadiene[21] 38 0(1)° and anthronylketene[18] 39 5(2)° Disorder was noted in the cyclooctene ring system where C(4) and C(5) could be represented by two positions within the structure i e C(4A) and C(5A) This disruption was presumably because of chair and boat like conformations as observed in cyclohexane The cyclooctene carbon-carbon single bond distances were on average 1 528(9)Å for one orientation and 1 556(13) for the second orientation (C(4A),C(5A)) These were normal for C-C single bond distances (1.54Å)[20]

The cyclopentadienyl ring carbons were an average of 2 149(6)Å from the central manganese atom This value was typical of the average Mn-C(π) bond lengths as can be seen in Table 4 5 1 Some disorder may be noted in the ring where the maximum and the minimum deviations from the mean plane were 0 139 and -0 139Å respectively for C(11) and C(12) The average bond length between ring carbons was 1 394(6)Å. This distance was usual for carbon carbon bonds in cyclopentadienyl rings

COMPOUND	Mn-C (Cyclopentadienyl) (Å)	Reference
(η^5-C_5H_5)Mn(CO)$_2$(η^2-methylvinylketone)	2 137(8)	19
(η^5-C_5H_5)Mn(CO)$_2$(η^2-cyclooctatetraene)	2 156(2)	17
[(η^5-C_6H_7)Mn(CO)$_2$]$_2$N$_2$	2 144(7)	22
[(η^5-C_6H_7)Mn(CO)$_2$S(CH$_3$)$_2$C$_2$H$_5$]PF$_6$	2 141(4)	23
(η^5-C_5H_5)Mn(CO)$_2$(η^2-norbornadiene)	2 166(9)	11
(η^5-C_5H_5)Mn(CO)$_2$(η^2-anthronylketene)	2 155(7)	18
(η^5-C_6H_7)Mn(CO)$_2$(η^2-*cis*-cyclooctene)	2 149(6)	a

Table 4.5.1 The Mn-C(π) cyclopentadienyl average bond distances (Å) for manganese complexes with cyclopentadienyl ligands [a]this work

The Mn(1)-(CO) distances 1 775(3)Å and 1 762(3)Å were within the expected ranges for this type of complex, PPh_3 1 76(1)Å, 1 77(1)Å[9] The Mn-(CO) angles were 177.2(3) for Mn(1)-C(15)-O(1) and 176 1(3) for Mn(1)-C(16)-O(1) The angles in the tripod $Mn(CO)_2$(*cis*-cyclooctene) using the centre of the double bond (CDB) as the reference point for the *cis*-cyclooctene ligand were 94 5(1)° for C(16)-Mn(1)-CDB, 95 8(1)° for C(15)-Mn(1)-CDB and 90.0(2)° for C(16)-Mn(1)-C(15) The angles involving the *cis*-cyclooctene ligand show distortion in the tetrahedral geometry of the manganese complex (fourth reference point = centroid of the cyclopentadienyl ring) caused by coordination of the ligand to manganese These types of distortions have been noted in other η^2 coordinated complexes involving the $CpMn(CO)_2$ component e.g cyclooctetraene[17], norbornadiene[21] and methylvinylacetone[19]

4.6 A comparison of the crystal structures of $(\eta^5\text{-}C_6H_7)Mn(CO)_2$(pyridine) and $(\eta^5\text{-}C_6H_7)Mn(CO)_2(\eta^2\text{-}$*cis*-cyclooctene)

In the comparison of the title complexes, which are of the type $(\eta^5\text{-}C_6H_7)Mn(CO)_2L$, the only difference between the two compounds is the unique ligand L (where L = pyridine and *cis*-cyclooctene). These ligands are different in that the pyridine is a good σ donating ligand by virtue of the lone pair on the ring nitrogen but a poor π accepting ligand because of the lack of antibonding π^* orbitals to accept electron density from the low valent manganese atom In contrast, the *cis*-cyclooctene ligand is a poor σ donor because the electrons required in the σ bond to the metal are mainly involved in the ligand π system but a good π acceptor because the metal can donate electron density into the empty ligand π^* orbitals In terms of stability this means that the pyridine complex was extremely air sensitive and decomposed rapidly in aerated solvents In the solid form a layer of manganese oxide was present on the surface of the crystal and so prevented air oxidation of the complex In contrast, the *cis*-

cyclooctene complex was more stable surviving for approximately 1hr in non-degassed solvent and for a period of weeks before air oxidation decomposed the crystals The effect of the pyridine ligand was to leave more electron density on the manganese atom relative to the *cis*-cyclooctene ligand This effect can be clearly seen in the orientation of the methyl group of the cyclopentadienyl ring in the complexes In the *cis*-cyclooctene complex the methyl group was *cis* to a carbonyl ligand This orientation was the preferred position in all the complexes of the type $(\eta^5\text{-}C_6H_7)Mn(CO)_2L$ when L was a relatively good π accepting ligand Although the methyl group was not necessarily *cis* to a carbonyl in these complexes the orientation of the methyl group was always *trans* to the unique ligand L In contrast, the location of the methyl group in the pyridine complex was *cis* to the pyridine ligand This feature appears to be common to all compounds containing a nitrogen donor ligand bound to a $(\eta^5\text{-}C_5H_4R)Mn(CO)_2$ fragment Examples of this type of interaction were $[(\eta^5\text{-}C_5H_4R)Mn(CO)_2]_2N_2$ (R = H)[22] and the chelate complex $(\eta^5\text{-}C_5H_4R)Mn(CO)_2$ (R = $CH_2CH(CH_3)N(CH_3)(C_3H_5)$)[24] where the coordinating nitrogen atom was *cis* to the methyl group of the cyclopentadienyl ring The reason for the differing orientation may lie in the amount of electron density on the central manganese atoms in the complexes Pyridine is a relatively strong base and on coordination to the manganese atom the electron density from the non-bonding electrons from the nitrogen atom would reside mainly on the metal In *cis*-cyclooctene the σ bonding electrons come from the π orbitals of the double bond and therefore would not impart as much electron density on the atom relative to the pyridine In addition, the metal could remove some of the electron density into the π^* antibonding orbitals of the *cis*-cyclooctene ligand This would not be the case in the pyridine complex where the poor π accepting ability of the pyridine ligand would leave a significant amount of the electron density on the metal atom An added effect of this increased electron density on the complex was to tilt the cyclopentadienyl ring This tilting may be the result of steric interaction of the methyl group with the

pyridine ligand or as a result of the increased electron density on the manganese inducing the initial stages of a η^3 ring slippage All other aspects of these complexes were typical The metal-cyclopentadienyl ring carbon bond distances on the *cis*-cyclooctene complex were normal for these types of compounds (see Table 4 5 1) and the Mn-(CO) bond distances were also in the normal ranges

REFERENCES

1 R A Howie, University of Aberdeen, Meston Walk, Aberdeen, Scotland.

2 *International Tables for X-ray Crystallography, Vol III*, D Reidel Publishing Company, Dordrecht, Holland, 1985

3 Sheldrick, G M, *Acta Cryst*, 1990, **A46**, 467

4 Sheldrick, G M, SHELX76, Program for crystal structure determination, University of Cambridge, England, 1976

5 *International Tables for X-ray Crystallography, Vol IV*, Kynoch Press, Birmingham, England, 1974

6 Friedrich, P, Besl, G, Fischer, E O, Huttner, G, *J Organomet Chem*, 1977, **139**, C68

7 Aleksandrov, G G, Antonova, A B; Kolobova, N E, Obezyuk, N S, Struchkov, Yu T, *Koord Khim*, 1979, **5**, 279

8 Antonova, A B, Kovalinko, S V, Komiyets, E D; Johansson, A A, Struchkov Yu T, Ahmedov, A I, Yanovsky, A I, *J Organomet Chem*, 1983, **244**, 35

9 Zaworotko, M J; Shakir, R, Atwood, J L, Siryunyongwat, V, Reynolds, S D, Albright, T A, *Acta. Cryst*, 1982, **B38**, 1572

10 Fontana, S, Shubert, U, Fischer, E O; *J Organomet Chem*, 1978, **146**, 39

11 Granoff, B, Jacobson, R A, *Inorg Chem*, 1968, **7**, 2328

12 Barbeau, C, Dubey, R J, *Can J Chem*, 1973, **51**, 3684

13 Cotton, F A, Wilkinson, G, *Advanced Inorganic Chemistry, 5th Ed*, Wiley Interscience, New York, 1988

14 Lee, S; Cooper, N J; *J Am Chem Soc*, 1991, **113**, 716

15 Chinn, J W, Hall, M B, *J Am Chem Soc*, 1983, **105**, 4930.

16 Keller, E; SCHAKAL88, Program for the Graphical Representation of Molecular and Crystallographic Models, University of Freiburg, Germany, 1988

17 Benson, I B, Knox, S A R, Stansfield, R F D, Woodward, P, *J Chem Soc, Dalton Trans*, 1981, 51

18 Herrmann, W A, Plank, J, Ziegler, M A, Wiedenhammer,K; *J Am Chem Soc*, 1979, **101**, 3133

19 Le Borgne, P G, Gentric, E, Grandjean, D, *Acta Cryst*, 1975, **B31**, 2824

20 March, J, *Advanced Organic Chemistry, 3rd Ed*, Wiley Interscience, New York, 1985.

21 Vella, P A, Beno, M, Schultz, A J, Willia, J M, *J Organomet. Chem*, 1981, **205**, 71

22 Wiedenhammer, K, Herrmann, W A, Ziegler, M L, *Z. Anorg, Allg Chem*, 1979, **457**, 183

23 Adams, D A, Chodosh, D F, *J Am Chem Soc*, 1978, **100**, 812

24 Wang, T F, Lee, T Y, Wen, Y S, Liu, L K, *J Organomet Chem*, 1991, **403**, 353

CHAPTER 5

PROGRAM FOR TRANSIENT ANALYSIS

5 0 Computer program for transient analysis

5.1 Introduction

The advent of computers has greatly enhanced the speed and accuracy of data acquisition in fast kinetic experiments The original method for the analysis of transient data involved taking a picture of the recorded transient on the oscilloscope This picture was then traced onto paper, enlarged and subsequently analysed by tedious mathematical calculations to determine the order and the observed rate for the reaction Computer interfacing with modern oscilloscopes has greatly reduced the work load with the analysis times for recorded transients having been reduced from hours to seconds Commercial programs have been developed for transient analysis[1] but they usually contain more sub programs than are actually required by the user and therefore they are more complicated to use What follows is an explaination of a GW-BASIC program developed specifically for the analysis of transient data The menu-driven program allowed for the collection, accumulation, viewing, analysis and storage of transient waveforms The acquired data could be manipulated to create files compatible with other commercial analysing and graphics packages and with other developed programs The system consisted of an Olivetti PCS 286 interfaced *via* a GPIB-IEEE-488 card to a Philips PM 3311 oscilloscope The laser system has been described (*vide infra*) A modified version of this program was written to enable it to be used with a Hewlett-Packard HP54510A oscilloscope The program could be run directly from a batch file which initiated the interface card drivers and the graphics drivers A full listing of the PM 3311 program can be found in Appendix C

5.2 Computer program

The main menu for the program was as follows,

1 New Measurement
2 Decay Analysis
3 Create STATIS File
4 View Files
5 Absorbance Calculations
6 DOS Functions
7 Exit

The first section of the program was used for transient acquisition A sub-menu was used for this part of the program as the options were usually needed many times during a typical experiment Before the sub-menu appeared on the screen the program asked for title of the experiment to be performed This prevented tedious re-entering of an experiment title during data file creation The sub-menu listing was as follows,

1 Io Measurement
2 Transient Measurement
3 Exit

The Io measurement is a very important parameter which must be calculated prior to the capture of a kinetic trace It corresponds to the amount of light passing through the solution prior to photolysis by the laser pulse It is measured by getting the difference in mV of the amount of light transmitted by the solution when the shutter on the monitoring beam is closed and then opened From the Beer-Lambert law (Equation 5 2 1) the absorbance of a reactant or product is linearly proportional to its concentration in solution provided the absorbance value is within the limits of optical linearity

$$A = \varepsilon c l \qquad (5\ 2\ 1)$$

where A is the absorbance, ε is the molar extinction coefficient ($dm^3\ mol^{-1}\ cm^{-1}$), c is the concentration of the reactant or product ($mol\ dm^{-3}$) and l is the pathlength (cm)

The change in millivolts on the oscilloscope produced by a transient species is also a function of the light transmitted by a solution per unit time (It) Therefore one can calculate the absorbance value from It/Io The photomultiplier was normally adjusted to the maximum linear working range of 200mV To speed up the process of acquiring the data for the Io measurement only the first 25 channels, of the 256 channels available to store data in the oscilloscope, were averaged to obtain the values (in mV) when the shutter was closed and opened For the HP54560A scope, the data in the first 50 of the 500 available channels were transmitted The value of the voltage scale on the scopes was also sent to enable calculation of the mV values

The transient measurement function recorded transient data and wrote the data to a file The program prompted for a filename, for the wavelength of the monochromator and for Io if it had not previously been measured If Io had been measured, its value was retained to enable measurement of transients of different timebases at the same analysis wavelength It also displayed the previous filename (if any) to prevent confusion if sequential filenames were entered Pressing return (<CR>) ,recorded the data from the oscilloscope The display consisted of two halves, one which contained the averaged transient and the other containing the current transient on the oscilloscope (Figure 5 2 1) This aided enormously in the judging of the number of laser shots required to obtain good quality transient waveforms In the first acquisition, the program asked for the front panel settings from the scope i e. the voltage scale, the timebase After each acquisition, the averaged data was automatically stored on disk along with the title, timebase, number of shots, voltage scale, wavelength and the Io measurement This prevented data loss as a result of oscilloscope 'crashing'. The data were averaged by summing the channel numbers sent from the oscilloscope (0-255) after each shot and dividing the total by the number of shots This had the added effect of reducing the noise level in the traces

Part two of the program was concerned with data analysis The program prompted for a filename and searched by default the for the file from floppy disk This could be changed to search in other drives The called file was displayed on one half of the screen and the user was asked if curve smoothing was required

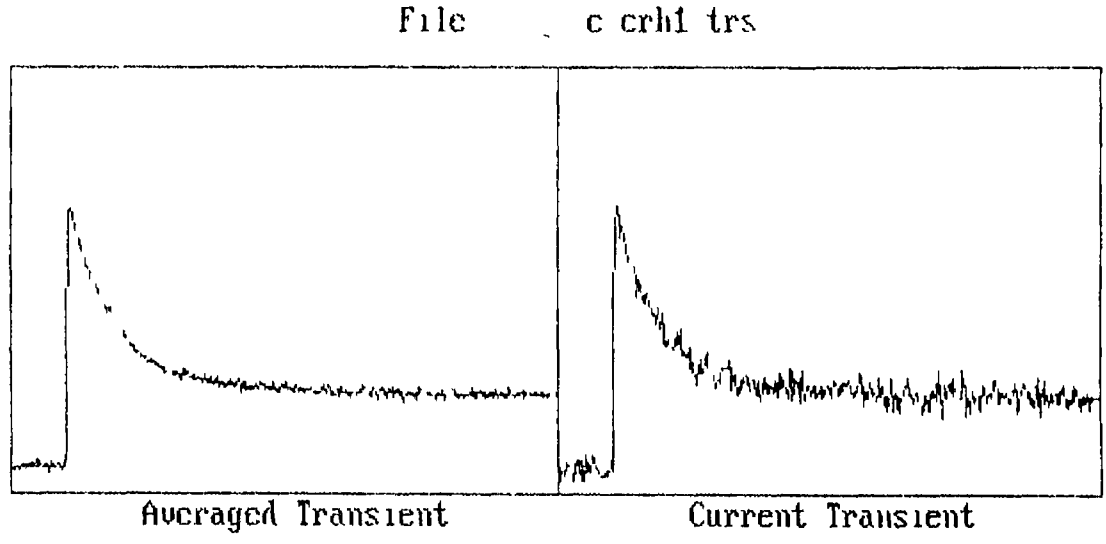

Figure 5.2.1 The split screen showing the current transient and the averaged transient in the 355nm flash photolysis of $Cr(CO)_6$ under 1 0 atmosphere of CO in hexane.

The procedure used was a Savitzky-Golay 5 point moving least squares method[2] and the equation is shown in Equation 5 2 2

$$z(i) = \frac{(-3z(i-2) + 12z(i-1) + 17z(i) + 12z(i+1) - 3z(i+2))}{35} \qquad (5\ 2\ 2)$$

where z was greater than 2 and less than n-2 (n= number of data points) This technique was ideally suited for the transient data as one of the requirements for the smoothing is that each data point must be obtained at the same time interval from each preceding point This is a feature of fast transient digitizers The effect of this smoothing procedure was to reduce noise in the transients without degrading the quality of the data The next step in the analysis process was to set a baseline where the change in slope of the transient decay was at a minimum This was extremely important as this line set the value of absorbance at infinity (A_{inf}) which was used in the first and second order rate constant calculations Next the channel numbers had to be selected, corresponding to the channel numbers on the oscilloscope, to identify the portion of the curve for analysis The typical starting channel was 32 (50 using the HP54510A oscilloscope) as in the recording of the transient data, the first portion of the trace was usually given to the millivolt reading before the photolysis of the sample by the laser pulse A typical trace is shown in Figure 5 2 2 An option then prompted the user to choose a first or second order analysis The first order analysis used Equation 5 2 3 which is derived from basic first order kinetics and the Beer-Lambert law[3]

$$k_r t = \ln (A_o - A_{inf}) - (A_t - A_{inf}) \qquad (5\ 2\ 3)$$

Where k_r is the rate constant, t is the time, A_o is the absorbance at time zero, A_{inf} is the absorbance at time infinity (calculated from the baseline) and A_t is the absorbance at time t A plot of $\ln(A_t - A_{inf})$ versus t is linear for a first order process with a slope equal

to $-k_r$ The second order rate constants were calculated from second order kinetics rate equation incorporating the Beer-Lambert law[3] (Equation 5 2 4)

$$k_r t = \frac{1}{(A_t - A_{inf})} - \frac{1}{(A_o - A_{inf})} \qquad (5\ 2\ 4)$$

The symbols are the same as for the first order equation A plot of $1/(A_t - A_{inf})$ versus t yields a straight line with a slope of k_r

On the unused half of the screen the data points were displayed on a graph of the calculated absorbance values from the rate equations versus time (Figure 5 2 3) The best line of fit was drawn through the points This was calculated using simple linear regression The observed rate constant, and its linear regression coefficient were displayed on the screen The rate constant could be recalculated by choosing a different portion of the curve

Part three of the program created files in a format which could be used with STATIS3 a data analysis program The program prompted for a filename of the file to be converted The data was then read in to the computer and the equation of the line for the first 20 points of the data was calculated The standard deviation calculated for this line was used to compute the channel number where the laser fired as the data in the file from channel numbers 1 to 20 consisted of the mV reading from the photomultiplier before the laser photolysis pulse hit the sample solution and was therefore not part of the transient decay The data after the calculated fire channel was written to the file in the form of absorbance and time so that accurate rate constants could be determined An option was given to export the file to the STATIS3 directory or to write it to disk. A second option was given whether the user wished to run STATIS3 or to return to main menu

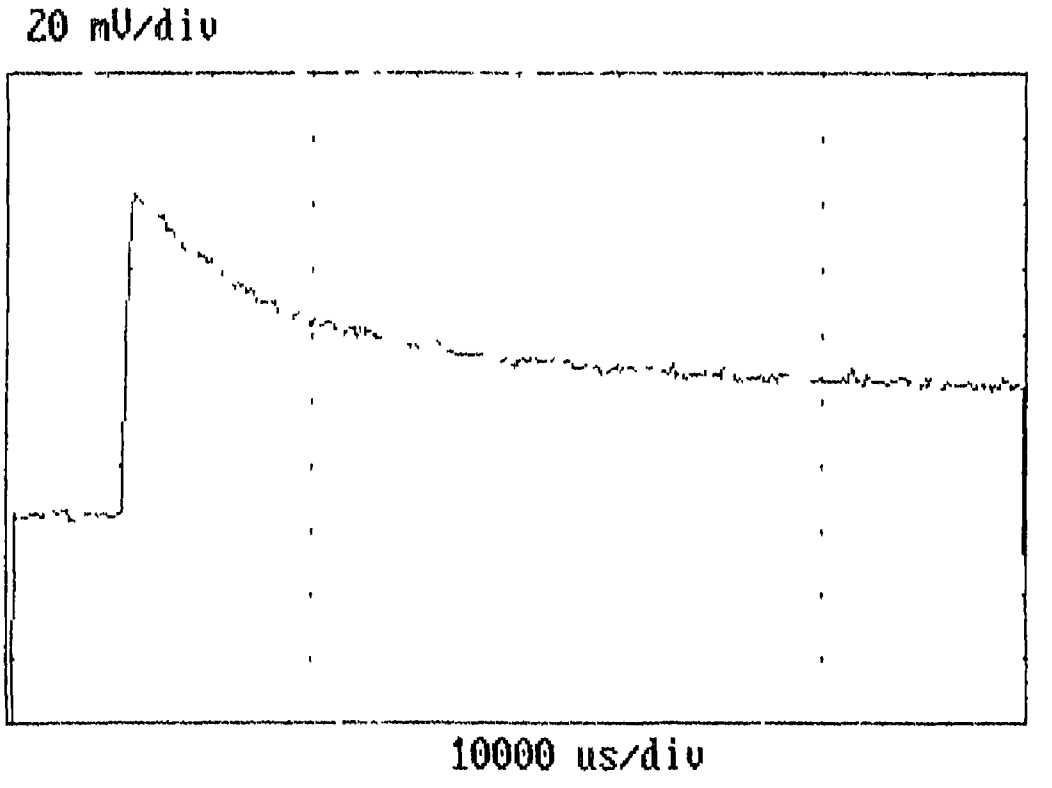

Figure 5.2.2 A typical trace of a transient species where the initial portion of the curve corresponds to the absorbance of the sample prior to the photolysis pulse

The STATIS3 package could be used to perform statistical calculations on any data set in the form required by the program The main use of this program in the analysis of transient data was in one and two exponential curve fitting These functions acted as a complement to the previously described transient analysis methods The advantages of this form of analysis over the linear regression method were that the data was not transformed, as in the linear method, and that it enabled the calculation of the intercepts on the decay curves which could be used to estimate the relative amounts of each component produced in the photolysis experiments

The fourth part of the program was used to view files An option appeared at the beginning of this function which enabled the user to examine the files contained on disk for their content This helps to find specific files but was not thought as a replacement for recording the file details on paper. A requirement to use this feature

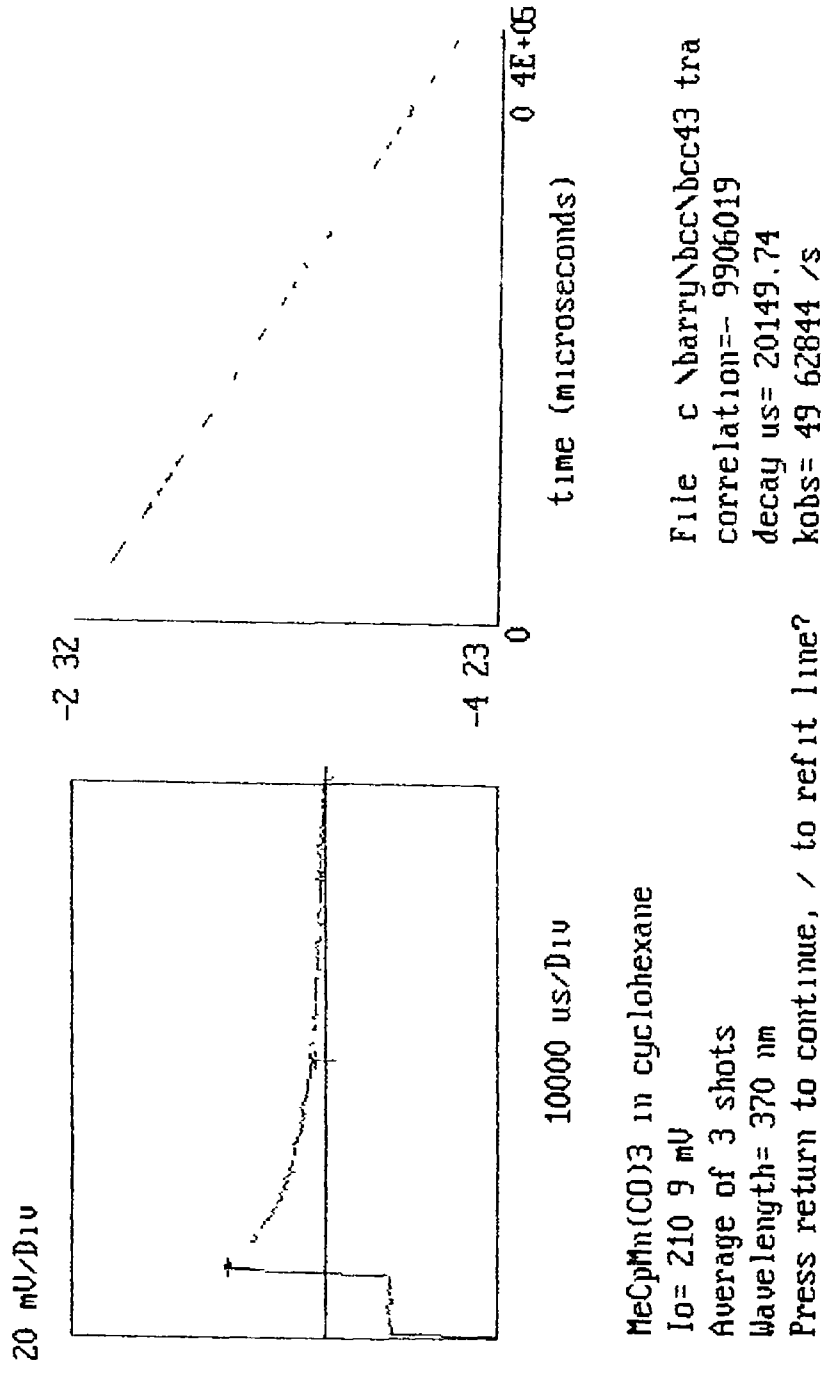

Figure 5.2.3 The analysis profile of a transient with the transient displayed on the lefthand side The arrows correspond to the analysis portion of the curve The right hand side of the screen shows a plot of the first order fit to a set of datapoints from the analysis portion of the curve against time with the line of best fit drawn though the points The file details, calculated rate constant and correlation coefficient are displayed under the graphs

was that the recalled files had to be in numerical sequence The next prompt asked for a specific filename The view files choice permitted the user to display, overlay and clear the specified files from the screen An example of this screen is shown in Figure 5 2 4 A screen dump could be carried out by pressing the print screen option on the keyboard which ran DOS graphics which was originally initiated in the laser batch file This applied to any screen in the program

The fifth section of the program was concerned with outputing data to a file which was compatible with HARVARD GRAPHICS, a program which could produce excellent spectral plots of transient species The user was prompted by a request for a common file string and the starting and ending file number and a increment to identify a certian series of filenames A maximum of four time delays could be entered An option was also displayed so the calculated absorbances could be output to a printer or to a working file for the graphics package The program systematically calculated the fire channel of the laser for each of the files and then used this channel number as time zero for the subsequent absorbance value calculations

There were many constraints on this part of the program The files had to be sequential in order for the file search loop to execute and the entered times for the absorbance calculations could not exceed the limit of the transient timescale The created file could be directly imported into HARVARD GRAPHICS A crude approximation of the spectrum could be viewed at the end of the absorbance calculation and this aided in determining if there were inconsistencies in the calculations because of incorrect fire channel selection With channel numbers greater than 35 and less than 26 the program automatically entered a fire channel number of 30 The existence of this inserted number was denoted by an asterisk A complementary program was written which plots the data in a 3-D spectrum of

absorbance against time (μs) against wavelength (nm)[4] This program more clearly demonstrated the existence or non-existence of any produced transient species

The final part of the program was a simple SHELL command This enabled the use of the DOS functions available on the computer The most important of these was the file editor EDLIN which was used to correct incorrectly entered data, e g wavelength, during the data aquisition Other uses involved the execution of other programs or packages compatible with DOS

The exit command was used to exit the program An option was given whether to exit to DOS or to GWBASIC On exiting to DOS the program returns to the default C \ directory Exiting to GWBASIC enabled the loading and executing of other basic programs

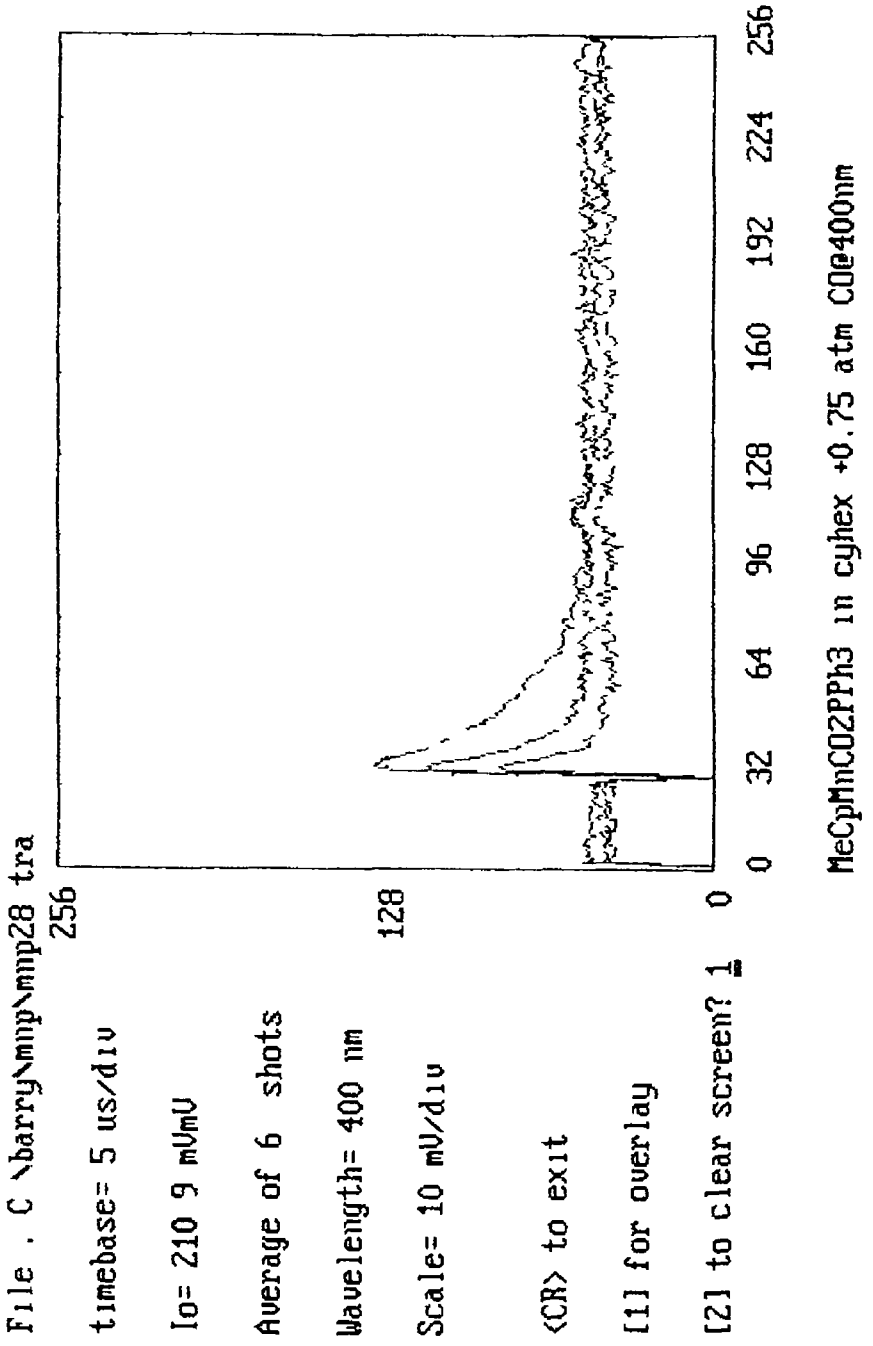

Figure 5 2.4 An example of the View Files screen with overlayed transients from the photolysis of $MeCpMn(CO)_2PPh_3$ under various pressures of CO The display shows that the transient produced was not a primary photoproduct.

REFERENCES

1 Gerber, S , Wirz, J., *EPA Newsletter*, 1989, **26**, 19

2 Savitzky, A , Golay, M J E , *Anal Chem*, 1964, **36**, 1627

3 Avery, T E ; Basic Reaction Kinetics and Mechanisms , Macmillan Education Ltd , London 1986

4 Shendan, N , M Sc thesis, Dublin City University, 1991

CHAPTER 6

EXPERIMENTAL SECTION

6.0 Experimental Section

6.1 Introduction

The photosubstitution reactions of metal carbonyl compounds are well known (Reaction 6 1 1)[1] Reactions usually involve the photolysis of the metal carbonyl complex in a donor solvent e g an alcohol, ether, cyanoalkane or in 'inert' alkane solvents The function of the donor solvent is to coordinate loosely to the site left by photolytic loss of a carbon monoxide ligand (Reaction 6 1 2) and in some cases prevent further CO loss The addition of a stronger ligand i e a good σ donor to the solution can displace the donor solvent thermally to produce the appropriate compound The solvent can alternatively be removed under reduced pressure and so drive the reaction (Reaction 6 1 3) to completion

$$M(CO)_x \xrightarrow{h\nu} M(CO)_{x-1} + CO \qquad (6\,1\,1)$$

$$M(CO)_{x-1} + S \longrightarrow M(CO)_{x-1}S \qquad (6\,1\,2)$$

$$M(CO)S + L \longrightarrow M(CO)_{x-1}L + S \qquad (6\,1\,3)$$

S = donor solvent L = ligand

If the coordinating ligand is sufficiently strong so as not to afford higher substitution products then an alkane solvent e g cyclohexane can be used Usually in these reactions it is necessary to remove oxygen as the reactive intermediates formed could coordinate to the oxygen molecules and subsequently decompose into the corresponding metal oxides This is usually performed by bubbling an inert gas through the photolysis solution and also has the added effect of removing any CO liberated in the reaction, preventing backreactions and so shortening the photolysis time

6.2 Photolysis apparatus

All the prepared photolyses were carried out in a photoreactor as in Figure 6 2 1 The double walled pyrex glass vessel contained a medium pressure mercury lamp (400W) cooled by running water The external vessel contained the solution to be irradiated Air and carbon monoxide (liberated during the reactions) were removed by bubbling nitrogen or argon through the solution The products were isolated by removing the solvent under reduced pressure and purifing by ambient or low temperature recrystallisation and/or classical chromatography depending on the air sensitivity of the compounds

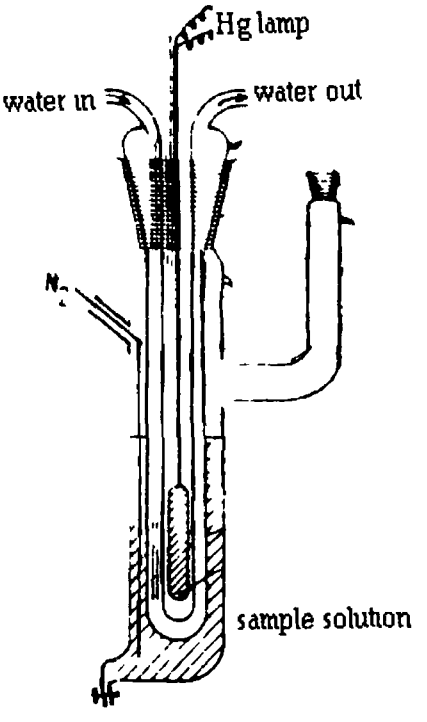

Figure 6.2.1 Photolysis apparatus used in the synthesis of substituted metal carbonyl complexes

Air sensitive solutions for IR or UV/visible spectroscopy were filled in a nitrogen atmosphere glove box

6.3 Materials

$MeCpMn(CO)_3$ (Strem chemicals), $Cr(CO)_6$ (Strem chemicals), $Mo(CO)_6$ (Strem chemicals), $W(CO)_6$ (Strem chemicals), pyridine (Aldrich Chemical Co), *cis*-cyclooctene (Aldrich Chemical Co), triphenylphosphine (BDH), and n-pentane (Reidel de Haen) were used without further purification Cyclohexane was stored under size 4A molecular sieve Argon (IIG), carbon monooxide (IIG) and oxygen free nitrogen (IIG) were used without further purification $MeCpMn(CO)_3$ for laser flash photolysis studies was vacuum distilled and stored under argon at -30°C

6.4 Equipment.

Infra red spectra were recorded on a Perkin Elmer 983-G IR spectrophototometer using sodium chloride solution cells (pathlength 0 1mm) or in KBr pellets UV/visible spectra were obtained on Hewlett Packard 8425a spectrophotometer using quartz cells (pathlength 1 0cm)

6.5 Synthesis of manganese complexes

6.5.1 Preparation of η^5-methylcyclopentadienylmanganese(I)dicarbonyl triphenylphosphine

The yellow $MeCpMn(CO)_2PPh_3$ complex was prepared by UV irradiation with a 400W medium pressure mercury lamp of a continuously N_2 purged n-pentane solution (150mls) that contained 2 3mmoles of $MeCpMn(CO)_3$ and an equimolar equivalent of PPh_3 Nitrogen purging was maintained throughout the reaction to avoid oxidation of the complex The photolysis time was 3hrs Following irradiation the solvent was removed under reduced pressure avoiding exposure to the air in the

transferring process The resultant orange residue was dissolved in a minimum of hot ethanol and on cooling the $MeCpMn(CO)_2PPh_3$ complex recrystallised as yellow crystals IR υCO n-hexane 1938, 1879cm^{-1}

6 5 2 Preparation of η^5-methylcyclopentadienylmanganese(I)dicarbonylpyridine

2 3mmoles of $MeCpMn(CO)_3$ were dissolved in 150ml of tetrahydrofuran and photolysed by UV irradiation using a 400W medium pressure mercury lamp for 3hrs The solution was continuously purged throughout the reaction by a stream of nitrogen The resultant burgundy coloured solution was transferred under argon to a 250ml flask which contained an equimolar amount of pyridine The solvent was removed under reduced pressure and the residue was redissolved in 2mls of argon degassed ethanol and filtered through cotton wool The solution was stored for 2 weeks at -30°C Brown crystals of $MeCpMn(CO)_2$(pyridine) were isolated by alternate washings with 40-60 pet-ether at -70°C and water The crystals were covered in an opaque layer of presumably MnO_2 which prevented decomposition of the complex IR υCO n-hexane 1930, 1863cm^{-1} X-ray structure see Chapter 5

6.5.3 Preparation of η^5-methylcyclopentadienylmanganese(I)dicarbonyl η^2-*cis*-cyclooctene

The $MeCpMn(CO)_2$(*cis* -cyclooctene) complex was prepared by prior photochemical generation of the tetrahydrofuran adduct $MeCpMn(CO)_2$(THF) as in the previous complex preparation When the irradiation was complete a 20 molar excess of *cis*-cyclooctene was added to the solution The THF was removed under reduced pressure and the resultant yellow oily product was placed in a low temperature circulator for 3 days at -80°C On returning to room temperature a yellow precipitate formed This was subsequently recrystallised from methanol at -30°C The

product was identified as $MeCpMn(CO)_2$(*cis*-cyclooctene) IR υCO n-hexane 1959, 1900cm^{-1} X-ray structure see Chapter 5

6.6 Synthesis of Group VIB monosubstituted triphenylphosphine pentacarbonyl complexes

6.6 1 Preparation of $Cr(CO)_5PPh_3$

A 200 mL solution of tetrahydrofuran (THF) and parent hexacarbonyl $Cr(CO)_6$ (0 5g) was degassed for 15 minutes and then irradiated with a 400W medium pressure mercury lamp for 3hrs The solution was continously purged with nitrogen throughout the irradiation to avoid oxidation of the metal After irradiation a stoichiometric amount of ligand was added to the solution and the solvent was removed using a rotary evaporator The pale yellow $Cr(CO)_5PPh_3$ complex was purified by repeated recrystalhsation from hexane and washing with methanol to remove unreacted PPh_3 Purity was confirmed by TLC and infra red spectroscopy IR υCO cyclohexane, 2066(m), 1989(w), 1945(vs) cm^{-1}

6.6.2 Preparation of $Mo(CO)_5PPh_3$

A THF solution of parent hexacarbonyl $W(CO)_6$ (0 5g) was irradiated as in the previous synthesis An equimolar amount of PPh_3 was added to the resultant solution and the solvent removed by rotary evaporation The remaining green residue was dissolved in a minimum amount of chloroform and chromatographed on a 15cm alumina column with a 5 95 ethyl acetate 40-60 pet-ether eluent The complex was purified by recrystallisation from n-hexane at -30°C to give white crystals of $Mo(CO)_5PPh_3$ IR υCO cyclohexane, 2072(m), 1989(w), 1945(vs) cm^{-1}

6.6.3 Preparation of $W(CO)_5PPh_3$

The complex was prepared as for the synthesis of the corresponding chromium compound The complex was recrystallised from ethanol to give yellow crystals of $WCO)_5PPh_3$ IR υCO cyclohexane, 2074(m), 1988(w), 1945(vs) cm^{-1}

6.7 Laser flash photolysis

6 7.1 Introduction

Laser flash photolysis has become a very important technique in the study of photoreaction intermediates In principle flash photolysis involves the generation of a high concentration of short-lived intermediate using a very high intensity pulse of radiation of very short duration A short time interval after the generating pulse the system is analysed by observing its emission or absorption charactenstics The process can be followed by photographing the emission spectrum using a spectrograph or the absorption spectrum by triggering an analytical beam passing through the reaction cell to flash at a predetermined time interval after the initial flash Alternatively the process may be followed kinetically by monitoring the emission or absorption at a particular wavelength using a detector coupled to an oscilloscope with a time-based sweep The latter process is used here Typical traces for transient absorption and decay are given in Figure 6 7 1 The polychromatic nature of the radiation from conventional discharge tubes increases the possibility of generating more than one emitting or absorbing species Lasers overcome this problem because their radiation is monochromatic Other advantages are that the pulse from a laser is of very short duration (Q-switching) and highly reproducible Frequency doubling can be employed to increase the range of the laser source from its fundamental harmonic Oscilloscope traces of the decay of the intermediate can be obtained if a high intensity monitoring beam is used to overcome problems caused by background noise with lower intensity sources Background noise can further be reduced by repeating the measurement many times and averaging the results Spectra of the decay of an intermediate can be obtained point by point on the

monitoring monochromator and recording a series of readings at a fixed time interval after the flash

6.7 2 Preparation of samples for flash photolysis

All the photolysis solutions were prepared in cyclohexane Solutions of the metal carbonyl complexes were adjusted until the absorbance readings were between 0 5 and 2 0 absorbance units Absorbance measurements were taken on a Hewlett-Packard 8452a UV/visible spectrophotometer Concentrations of the metal carbonyl compounds in solution were calculated from previously determined extinction coefficients The solutions were degassed by three cycles of a freeze pump thaw method Argon or carbon monoxide was added to prevent boiling of the solutions and to check the reversibility of the photochemical reactions observed The concentration of carbon monoxide in cyclohexane solution was calculated from reference 2 and was equal to $1\ 2 \times 10^{-2}$ mol dm^{-3} under 1 0 atmosphere of CO at 298K

6.7.3 Laser flash photolysis system with UV/visible monitoring

Flash photolysis studies were carried out using a Spectron Laser Systems Q-switched Nd YAG laser with a fundamental frequency at 1064nm This frequency can be doubled, tripled or quadrupled to generate a second (532nm), third (355nm) or fourth (266nm) harmonic The energy of the pulse can be varied by altering the voltage across the amplifier flash tube At the frequencies employed, 355nm and 266nm, the energies were typically 30mJ per pulse and 40mJ per pulse respectively The UV/visible monitoring source was an Applied Photophysics 40804 250W Xenon arc lamp The laser beam and UV light source were placed in a cross beam arrangment with the sample holder at the intersection The laser beam was directed onto the sample holder by two Pellin-Broca prisms The monitoring beam was focused onto an Applied Photophysics f3 4 monochromator using a lens Optical filters were used to cut

(a)

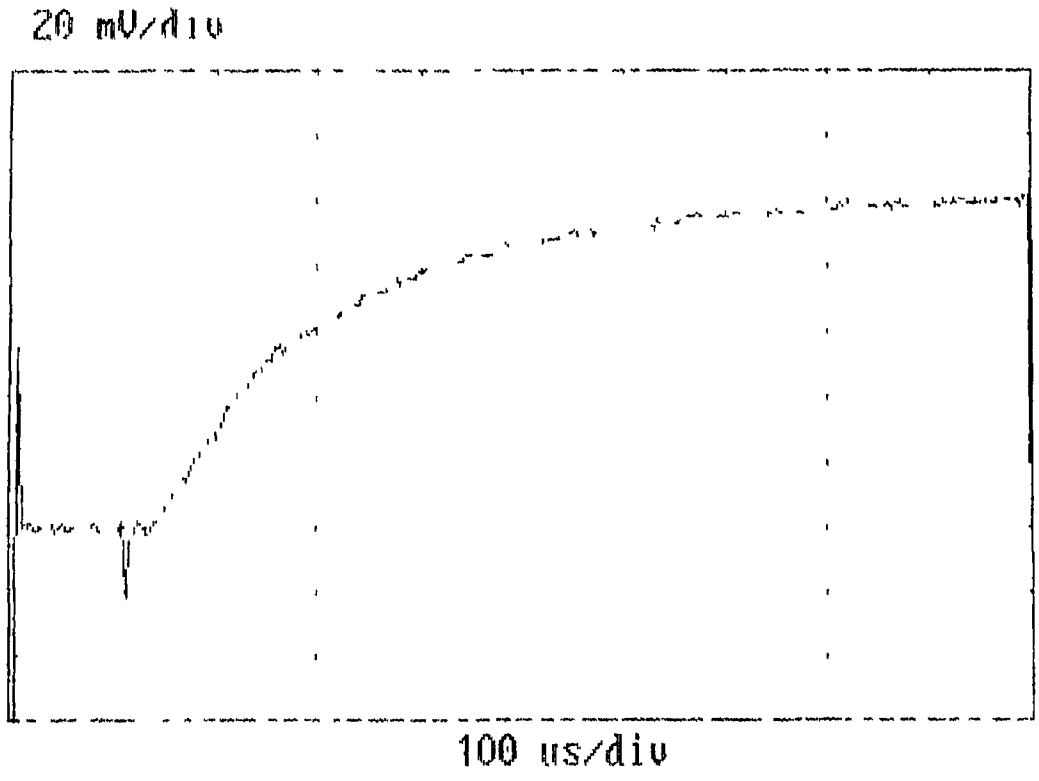

(b)

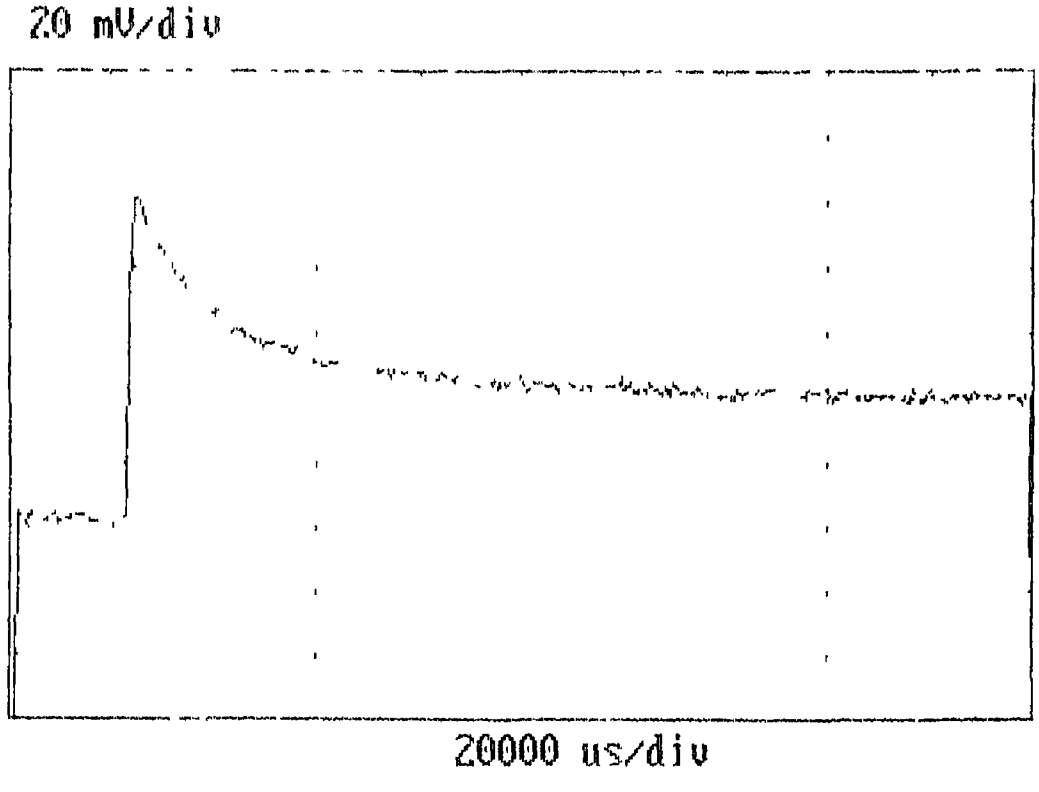

Figure 6.7.1 Typical traces obtained from an oscilloscope for transient absorption (a) and decay (b)

off the monitoring beam in order to minimise unnecessary photolysis from the Xenon arc lamp at wavelengths >345nm and >400nm At the exit slit of the monochromator a Hamamatsu five stage photomultiplier, operating at 850V, detected absorbance changes and relayed the output to a transient digitizer *via* a variable load resistor The digitizer, a Philips PM3311 storage oscilloscope, was interfaced through an IEEE card to an Olivetti 286PCS microcomputer The resultant data were stored on floppy disk A schematic diagram of the laser system is shown in Figure 6 7 3 1 In house programs were used to analyse the data The resultant transients were analysed by first order kinetics All errors on the second order rate constants are one standard deviation on the scatter of the graphical points

6 8 Transient deconvolution

Transient decays exhibiting characteristics of two first order decays can be difficult to separate in terms of their kinetic data The transient is however a linear combination of two exponential decays Therefore by fitting a double exponential curve (Equation 6 8 1) to the transient it should be possible to separate the transients into their individual components

$$Y = A_1e^{-k_1t} + A_2e^{-k_2t} \qquad (6\ 8\ 1)$$

The A_1 and A_2 terms in Equation 6 8 1 are constants, k_1 and k_2 refer to the decay constants for each of the components in the decay profile, t refers to the time and Y to the value on the resultant decay curve For a single exponential decay as in Equation 6 8 2 the inverse log of the equation (Equation 6 8 3) can be used to obtain a linear plot of lnY against time (t) to yield a slope of -k and an intercept lnA

$$Y = Ae^{-kt} \qquad (6\ 8\ 2)$$

$$\ln Y = \ln A - kt \qquad (6\ 8\ 3)$$

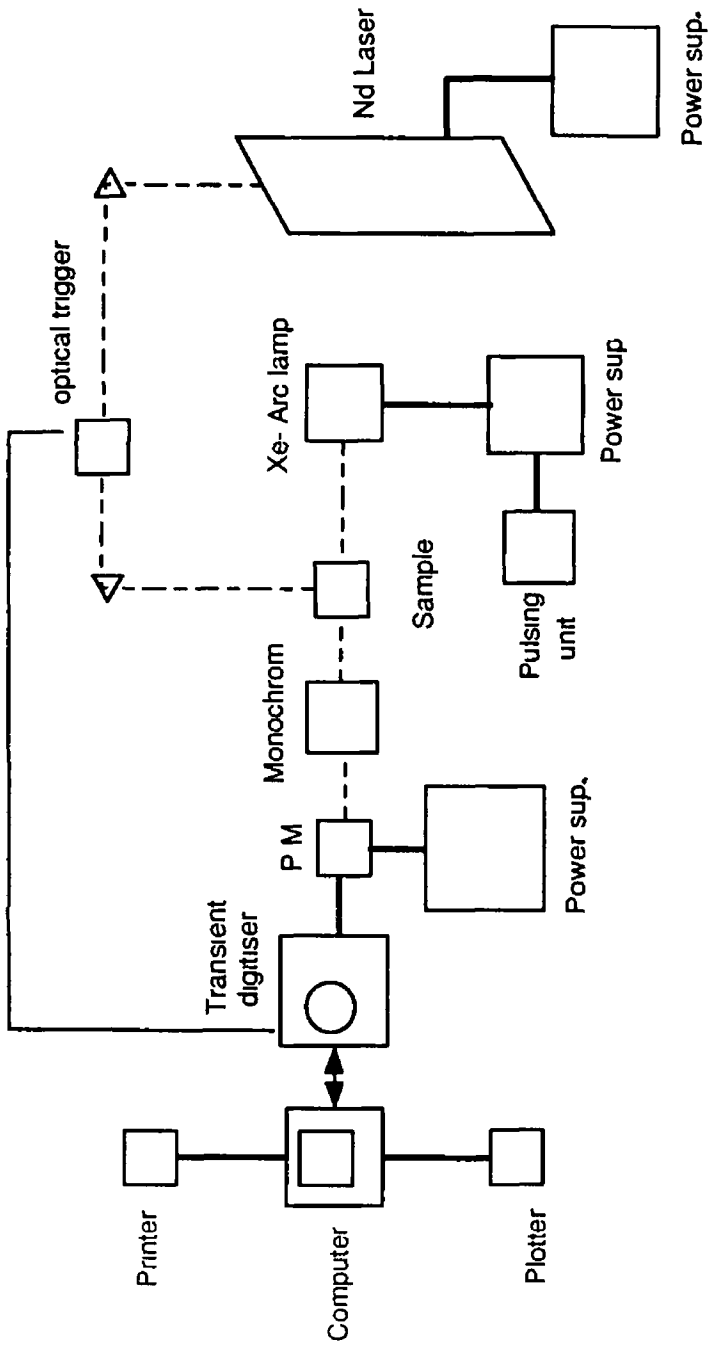

Figure 6.7.3 1 A schematic diagram of the laser system used in the laser flash photolysis experiments

Rearranging Equation 6 8 3 to give Equation 6 8 4 produces an equation which is similar in form to the spectroscopic equation for first order decay analysis[3] (Equation 6 8 5),

$$kt = \ln A - \ln Y \qquad (6\,8.4)$$

$$kt = \ln(A_o - A_{inf}) - \ln(A_t - A_{inf}) \qquad (6\,8\,5)$$

where A_o is the absorbance at time zero, A_t is the absorbance at time t, A_{inf} is the absorbance at time infinity, t is the time and k is the observed rate constant Therefore using a linear combination of the exponential decay curves it is possible to calculate the initial absorbances of the transient species and therefore the relative yields at different concentrations of CO from the A_1 and the A_2 terms for each decaying species

6.9 Activation parameter measurements

Activation parameters for the metal carbonyl complexes were calculated from the Arrhenius (Equation 6 9 1) and Eyring (Equation 6 9 2) equations

$$\ln k = \ln A - \frac{E_{act}}{RT} \qquad (6\,9\,1)$$

$$\ln \frac{k_{obs}}{T} = \ln \frac{k}{h} + \frac{\Delta S^*}{R} - \frac{\Delta H^*}{RT} \qquad (6\,9\,2)$$

In the Arrhenius equation A is the frequency factor related to the number of collisions between the reactant molecules, Eact is the activation energy , R is the universal gas constant, T is the absolute temperature and k_{obs} is the observed rate constant A plot of $\ln k_{obs}$ against $\frac{1}{T}$ should yield a straight line of slope $\frac{-E_{act}}{RT}$ from which the activation energy can be determined In the Eyring equation k is the Boltzmann constant, h is Plancks constant, R is the universal gas constant, ΔH^* is the enthalpy change of activation, ΔS^* is the entropy change of activation, T is the absolute temperature and k_{obs} is the observed rate constant A plot of $\ln \frac{k_{obs}}{R}$ against $\frac{1}{T}$ yields a slope of $\frac{-\Delta H^*}{R}$ and an

intercept equal to $\ln \frac{k}{h} + \frac{\Delta S^*}{R}$ ΔH^* and ΔS^* can be determined from the slope and the intercept respectively Temperature changes for the sample were achieved by immersing the sample cell in a temperature controlled water bath for a fixed period of time to attain equilibrium between the sample solution and the water Transient signals at this temperature were obtained and the sample was again immersed in the water bath at a different temperature Experiments were performed usually at increments of 5°C

REFERENCES

1 Strohmeier, W , *Agnew Chem Int Ed Engl*, 1964, **3(11)**, 730

2 Gjaldbæk, J C , *Acta Chem Scand*, 1952, **6**, 623

3 Avery, T E , Basic Reaction Kinetics and Mechanisms , Macmillan Education Ltd , London 1986

Further Work

The effect of a triphenylphosphine ligand on the ability of the various metal centres to coordinate to a solvent has been observed in this thesis Therefore, as a natural progression, the effects of other phosphine ligands such as trimethylphosphine, tricyclohexylphosphine etc should be investigated In addition, phosphites should be considered as the additional oxygen atom on phosphite ligands should decrease the ring strain on agostic interaction with the ligand C-H bonds The effect of different solvents should also be considered as some of these reactive intermediates appear non-solvated in cyclohexane but solvated in n-heptane solution

APPENDIX A

	x/a	y/b	z/c	U_{eq}
Mn1	342(2)	2046(1)	1303(1)	41(1)
N1	-681(11)	1710(2)	2306(3)	38(3)
C1	-16(16)	1175(3)	2769(4)	55(4)
C2	-507(18)	989(4)	3518(5)	56(5)
C3	-1729(19)	1330(5)	3816(5)	56(5)
C4	-2460(18)	1874(5)	3349(5)	64(5)
C5	-1903(16)	2038(4)	2598(4)	52(4)
C6	3083(17)	2237(4)	1870(5)	52(4)
C7	2674(17)	2397(4)	972(5)	66(5)
C8	1397(18)	2888(4)	845(6)	72(5)
C9	1054(18)	3036(3)	1684(6)	56(5)
C10	2099(15)	2641(3)	2310(4)	50(4)
C11	2246(24)	2664(5)	3272(5)	98(8)
C12	580(13)	1283(3)	829(4)	39(4)
C13	-1751(18)	2159(3)	595(4)	50(5)
O1	826(11)	801(3)	489(3)	76(3)
O2	-3143(11)	2238(3)	115(3)	74(3)
Mn2	5351(2)	339(1)	6681(1)	36(1)
N1A	4405(11)	63(3)	7737(3)	38(3)
C1A	3213(16)	437(4)	8006(5)	56(5)
C2A	2526(20)	293(5)	8725(5)	76(6)
C3A	3127(21)	-250(6)	9202(5)	81(6)
C4A	4315(19)	-632(5)	8946(5)	79(6)
C5A	4911(16)	-463(3)	8214(5)	55(6)
C6A	6005(16)	1345(3)	6931(4)	45(4)
C7A	6192(16)	1160(3)	6080(4)	51(4)
C8A	7494(15)	685(4)	6182(4)	43(4)
C9A	8122(15)	575(3)	7106(4)	47(4)
C10A	7211(14)	988(3)	7553(4)	44(4)
C11A	7482(24)	1043(4)	8537(5)	75(6)
C12A	3228(16)	390(3)	5980(4)	39(4)
C13A	5604(14)	-466(3)	6328(4)	42(4)
O1A	1812(11)	430(2)	5517(3)	57(3)
O2A	5858(10)	-979(2)	6068(3)	60(3)

Atomic coordinates x 10^4 for non-hydrogen atoms with e s d's in parentheses for (η^5-$C_5H_4CH_3$)-$Mn(CO)_2$(pyridine) U_{eq} x 10^3 ($U_{eq} = (1/3)\Sigma_i\Sigma_j U_{ij} a^*_i a^*_j a_i a_j$)

N1	---Mn1	2 023(4)	
C7	---Mn1	2 118(6)	
C9	---Mn1	2 173(6)	
C12	---Mn1	1 766(6)	
C1	---N1	1 352(6)	
C2	---C1	1 378(7)	
C4	---C3	1 393(8)	
C7	---C6	1 413(8)	
C8	---C7	1 404(9)	
C10	---C9	1 415(8)	
O1	---C12	1 163(6)	
N1A	---Mn1A	2 038(4)	
C7A	---Mn1A	2 111(5)	
C9A	---Mn1A	2 171(5)	
C12A	---Mn1A	1 778(5)	
C1A	---N1A	1 351(7)	
C2A	---C1A	1 380(8)	
C4A	---C3A	1 354(9)	
C7A	---C6A	1 418(7)	
C8A	---C7A	1 392(8)	
C10A	---C9A	1 410(7)	
O1A	---C12A	1 154(6)	
C6	---Mn1	2 162(5)	
C8	---Mn1	2 117(6)	
C10	---Mn1	2 201(5)	
C13	---Mn1	1 769(6)	
C5	---N1	1 343(6)	
C3	---C2	1 372(8)	
C5	---C4	1 374(7)	
C10	---C6	1 403(7)	
C9	---C8	1 441(9)	
C11	---C10	1 498(7)	
O2	---C13	1 159(6)	
C6A	---Mn1A	2 143(5)	
C8A	---Mn1A	2 119(5)	
C10A	---Mn1A	2 209(5)	
C13A	---Mn1A	1 761(5)	
C5A	---N1A	1 320(6)	
C3A	---C2A	1 37(1)	
C5A	---C4A	1 381(8)	
C10A	---C6A	1.403(7)	
C9A	---C8A	1 430(7)	
C11A	---C10A	1 508(7)	
O2A	---C13A	1 160(5)	

A complete listing of bond lengths (Å) for (η^5-$C_5H_4CH_3$)Mn(CO)$_2$(pyridine)

C6	-Mn1	-N1	105 0(2)	C7	-Mn1	-N1	143 5(2)
C7	-Mn1	-C6	38.5(2)	C8	-Mn1	-N1	142 6(2)
C8	-Mn1	-C6	64 4(2)	C8	-Mn1	-C7	38 7(2)
C9	-Mn1	-N1	103 4(2)	C9	-Mn1	-C6	63 4(2)
C9	-Mn1	-C7	64 7(2)	C9	-Mn1	-C8	39 2(2)
C10	-Mn1	-N1	85 3(2)	C10	-Mn1	-C6	37 5(2)
C10	-Mn1	-C7	64 1(2)	C10	-Mn1	-C8	64 5(2)
C10	-Mn1	-C9	37 8(2)	C12	-Mn1	-N1	97 3(2)
C12	-Mn1	-C6	98 1(2)	C12	-Mn1	-C7	90 5(2)
C12	-Mn1	-C8	119 2(3)	C12	-Mn1	-C9	155 2(3)
C12	-Mn1	-C10	132 9(2)	C13	-Mn1	-N1	93 4(2)
C13	-Mn1	-C6	157 8(2)	C13	-Mn1	-C7	122 1(2)
C13	-Mn1	-C8	93 4(3)	C13	-Mn1	-C9	100 7(2)
C13	-Mn1	-C10	135 3(2)	C13	-Mn1	-C12	91 7(2)
C1	-N1	-Mn1	121 8(3)	C5	-N1	-Mn1	121 6(3)
C5	-N1	-C1	116 5(4)	C2	-C1	-N1	123 8(5)
C3	-C2	-C1	118 6(6)	C4	-C3	-C2	118 9(5)
C5	-C4	-C3	118 9(6)	C4	-C5	-N1	123 3(5)
C7	-C6	-Mn1	69 1(3)	C10	-C6	-Mn1	72 7(3)
C10	-C6	-C7	108 9(5)	C6	-C7	-Mn1	72 4(3)
C8	-C7	-Mn1	70 6(4)	C8	-C7	-C6	108 1(6)
C7	-C8	-Mn1	70 7(3)	C9	-C8	-Mn1	72 5(3)
C9	-C8	-C7	107 6(5)	C8	-C9	-Mn1	68 3(3)
C10	-C9	-Mn1	72 2(3)	C10	-C9	-C8	107 5(5)
C6	-C10	-Mn1	69 7(3)	C9	-C10	-Mn1	70 1(3)
C9	-C10	-C6	107 9(5)	C11	-C10	-Mn1	128 7(4)
C11	-C10	-C6	124 9(6)	C11	-C10	-C9	127 1(6)
O1	-C12	-Mn1	175 9(5)	O2	-C13	-Mn1	178 0(5)
C6A	-Mn1A	-N1A	103 5(2)	C7A	-Mn1A	-N1A	142 0(2)

A complete listing of bond angles (°) for (η^5-$C_5H_4CH_3$)Mn(CO)$_2$(pyridine) (P T O)

C7A -Mn1A-C6A	38 9(2)	C8A -Mn1A-N1A	148 4(2)
C8A -Mn1A-C6A	64 5(2)	C8A -Mn1A-C7A	38 4(2)
C9A -Mn1A-N1A	109 5(2)	C9A -Mn1A-C6A	63 7(2)
C9A -Mn1A-C7A	64 5(2)	C9A -Mn1A-C8A	38 9(2)
C10A-Mn1A-N1A	88 5(2)	C10A-Mn1A-C6A	37 6(2)
C10A-Mn1A-C7A	63 9(2)	C10A-Mn1A-C8A	63 9(2)
C10A-Mn1A-C9A	37 6(2)	C12A-Mn1A-N1A	93 2(2)
C12A-Mn1A-C6A	101 2(2)	C12A-Mn1A-C7A	90 9(2)
C12A-Mn1A-C8A	117 3(2)	C12A-Mn1A-C9A	154 8(2)
C12A-Mn1A-C10A	137 1(2)	C13A-Mn1A-N1A	95 0(2)
C13A-Mn1A-C6A	156 8(2)	C13A-Mn1A-C7A	122 6(2)
C13A-Mn1A-C8A	92 4(2)	C13A-Mn1A-C9A	97 0(2)
C13A-Mn1A-C10A	130 9(2)	C13A-Mn1A-C12A	91 6(2)
C1A -N1A -Mn1A	119 5(4)	C5A -N1A -Mn1A	123 3(4)
C5A -N1A -C1A	117 2(5)	C2A -C1A -N1A	122 0(6)
C3A -C2A -C1A	119 7(6)	C4A -C3A -C2A	118 2(6)
C5A -C4A -C3A	119 7(6)	C4A -C5A -N1A	123 2(6)
C7A -C6A -Mn1A	69 3(3)	C10A-C6A -Mn1A	73 8(3)
C10A-C6A -C7A	108 3(5)	C6A -C7A -Mn1A	71 7(3)
C8A -C7A -Mn1A	71 1(3)	C8A -C7A -C6A	108 1(5)
C7A -C8A -Mn1A	70 5(3)	C9A -C8A -Mn1A	72 5(3)
C9A -C8A -C7A	108 1(5)	C8A -C9A -Mn1A	68 6(3)
C10A-C9A -Mn1A	72 7(3)	C10A-C9A -C8A	107 5(5)
C6A -C10A-Mn1A	68 7(3)	C9A -C10A-Mn1A	69 8(3)
C9A -C10A-C6A	108 0(4)	C11A-C10A-Mn1A	127 3(4)
C11A-C10A-C6A	126 2(5)	C11A-C10A-C9A	125 8(5)
O1A -C12A-Mn1A	178 9(4)	O2A -C13A-Mn1A	176 8(5)

A complete listing of bond angles (^{0}) for (η^5-$C_5H_4CH_3$)Mn(CO)$_2$(pyridine) (continued)

	x/a	y/b	z/c
H1	939	888	2524
H2	77	547	3865
H3	-2142	1196	4407
H4	-3426	2175	3566
H5	-2493	2462	2221
H6	4027	1862	2176
H7	3248	2167	471
H8	820	3110	215
H9	106	3401	1790
H11a	1019	2818	3402
H11b	3302	2979	3563
H11c	2549	2171	3580
H1A	2734	875	7629
H2A	1600	609	8933
H3A	2602	-390	9767
H4A	4813	-1069	9305
H5A	5919	-763	8011
H6A	5034	1694	7063
H7A	5463	1356	5463
H8A	7958	448	5667
H9A	9153	234	7405
H11Aa	7823	580	8816
H11Ab	6282	1222	8707
H11Ac	8545	1391	8800

Coordinates x 10^4 for hydrogen atoms in (η^5-$C_5H_4CH_3$)Mn(CO)$_2$(pyridine)

	U11	U22	U33	U23	U13	U12
Mn1	38(1)	37(1)	41(1)	3(1)	9(1)	0(1)
N1	33(2)	33(2)	40(2)	0(2)	3(2)	1(2)
C1	47(3)	50(3)	52(3)	6(3)	11(3)	2(3)
C2	60(4)	66(4)	51(3)	17(3)	5(3)	-7(3)
C3	54(4)	108(6)	42(3)	4(3)	12(3)	-22(4)
C4	51(4)	84(5)	49(3)	-11(3)	16(3)	-1(3)
C5	49(3)	47(3)	50(3)	-2(2)	12(3)	8(3)
C6	43(3)	38(3)	76(4)	-1(3)	5(3)	-5(3)
C7	57(4)	66(4)	69(4)	-2(3)	23(3)	-17(3)
C8	83(5)	62(4)	64(4)	24(3)	9(4)	-22(4)
C9	59(4)	35(3)	90(5)	7(3)	7(3)	0(3)
C10	45(3)	42(3)	59(3)	-4(3)	6(3)	-13(3)
C11	81(5)	85(5)	57(4)	-21(4)	8(4)	-29(4)
C12	43(3)	57(4)	44(3)	-5(3)	10(2)	-2(3)
C13	50(3)	54(3)	41(3)	1(2)	10(3)	2(3)
O1	75(3)	77(3)	83(3)	-39(2)	23(3)	3(3)
O2	58(3)	96(3)	55(2)	8(2)	-6(2)	6(2)
Mn1A	37(1)	32(1)	33(1)	-1(1)	8(1)	-3(1)
N1A	36(2)	44(2)	40(2)	1(2)	11(2)	-4(2)
C1A	51(3)	79(4)	51(3)	8(3)	16(3)	11(3)
C2A	47(4)	142(7)	48(4)	-12(4)	21(3)	-4(4)
C3A	70(5)	116(6)	40(3)	1(4)	19(3)	-43(5)
C4A	108(6)	68(4)	50(4)	11(3)	21(4)	-21(4)
C5A	70(4)	43(3)	50(3)	12(2)	18(3)	2(3)
C6A	48(3)	30(3)	62(3)	1(2)	12(3)	-4(2)
C7A	61(4)	44(3)	44(3)	11(2)	11(3)	-12(3)
C8A	56(4)	55(3)	47(3)	-5(3)	23(3)	-16(3)
C9A	36(3)	43(3)	57(3)	-4(2)	11(3)	1(2)
C10A	46(3)	40(3)	39(3)	-7(2)	9(2)	-11(2)
C11A	74(4)	73(4)	51(3)	-16(3)	8(3)	-18(4)
C12A	46(3)	40(3)	44(3)	-2(2)	12(3)	-1(3)
C13A	41(3)	40(3)	43(3)	-1(2)	9(2)	-2(2)
O1A	46(2)	69(3)	59(2)	6(2)	-7(2)	-1(2)
O2A	62(3)	45(2)	67(3)	-14(2)	10(2)	3(2)

Anisotropic temperature factors x 10^3 with e s d's in parentheses for (η^5-$C_5H_4CH_3$) Mn(CO)$_2$ (pyridine)

APPENDIX B

	x/a	y/b	z/c	Ueq
MN1	1309(1)	354(1)	2751(1)	41(1)
C1	-683(4)	1217(1)	3237(2)	48(1)
C2	192(6)	1789(2)	3978(3)	64(1)
C3	-1643(8)	2315(2)	4144(4)	92(1)
C4	-2990(18)	2526(5)	3131(11)	78(3)
C4A	-1558(43)	2889(7)	3085(21)	199(10)
C5	-1679(22)	2848(5)	2202(12)	78(3)
C5A	-2905(36)	2612(10)	2292(19)	156(9)
C6	-1373(10)	2392(2)	1248(4)	103(1)
C7	311(7)	1817(2)	1502(3)	75(1)
C8	-639(5)	1232(1)	2118(2)	51(1)
C9	1262(6)	-640(1)	1959(2)	57(1)
C10	2016(6)	-706(1)	3051(3)	62(1)
C11	356(10)	-497(2)	3701(3)	91(1)
C12	-1403(8)	-303(2)	2994(6)	105(2)
C13	-825(7)	-388(2)	1927(4)	82(1)
C14	2503(12)	-865(2)	999(4)	122(2)
C15	3175(5)	653(2)	3811(2)	53(1)
C16	3004(5)	639(2)	1752(3)	57(1)
O1	4411(4)	820(1)	4512(2)	77(1)
O2	4150(4)	788(2)	1080(2)	87(1)

Atomic coordinates x 10^4 for non-hydrogen atoms with e s d's in parentheses for (η^5-$C_5H_4CH_3$) $Mn(CO)_2$(*cis*-cyclooctene) U_{eq} x 10^3 ($U_{eq} = (1/3)\Sigma_i\Sigma_j U_{ij} a^*_i a^*_j a_i a_j$)

C1	---MN1	2.193(2)	C8	---MN1	2.201(3)
C9	---MN1	2.165(3)	C10	---MN1	2.136(3)
C11	---MN1	2.134(3)	C12	---MN1	2.150(3)
C13	---MN1	2.160(3)	C15	---MN1	1.775(3)
C16	---MN1	1.762(3)	C2	---C1	1.513(4)
C8	---C1	1.376(4)	C3	---C2	1.556(5)
C4	---C3	1.502(15)	C4A	---C3	1.717(27)
C4A	---C4	1.140(24)	C5	---C4	1.578(18)
C5A	---C4	1.049(21)	C5	---C4A	1.084(22)
C5A	---C4A	1.348(23)	C5A	---C5	0.902(23)
C6	---C5	1.493(14)	C6	---C5A	1.704(26)
C7	---C6	1.546(5)	C8	---C7	1.511(4)
C10	---C9	1.393(4)	C13	---C9	1.381(5)
C14	---C9	1.518(5)	C11	---C10	1.408(5)
C12	---C11	1.394(8)	C13	---C12	1.393(8)
O1	---C15	1.155(4)	O2	---C16	1.163(3)

A complete listing of bond lengths (Å) for (η^5-$C_5H_4CH_3$)Mn(CO)$_2$(*cis*-cyclooctene)

C8	-MN1	-C1	36.5(1)	C9	-MN1	-C1	144.9(1)
C9	-MN1	-C8	123.2(1)	C10	-MN1	-C1	143.7(1)
C10	-MN1	-C8	155.7(1)	C10	-MN1	-C9	37.8(1)
C11	-MN1	-C1	105.2(1)	C11	-MN1	-C8	129.0(2)
C11	-MN1	-C9	63.6(1)	C11	-MN1	-C10	38.5(1)
C12	-MN1	-C1	87.5(1)	C12	-MN1	-C8	95.6(2)
C12	-MN1	-C9	63.0(2)	C12	-MN1	-C10	63.5(2)
C12	-MN1	-C11	38.0(2)	C13	-MN1	-C1	107.6(1)
C13	-MN1	-C8	93.1(1)	C13	-MN1	-C9	37.2(1)
C13	-MN1	-C10	62.9(1)	C13	-MN1	-C11	63.4(2)
C13	-MN1	-C12	37.7(2)	C15	-MN1	-C1	84.2(1)
C15	-MN1	-C8	108.3(1)	C15	-MN1	-C9	127.5(1)
C15	-MN1	-C10	94.4(1)	C15	-MN1	-C11	92.6(2)
C15	-MN1	-C12	124.6(2)	C15	-MN1	-C13	155.0(1)
C16	-MN1	-C1	109.0(1)	C16	-MN1	-C8	81.4(1)
C16	-MN1	-C9	87.6(1)	C16	-MN1	-C10	107.4(1)
C16	-MN1	-C11	145.8(2)	C16	-MN1	-C12	142.7(2)
C16	-MN1	-C13	105.1(2)	C16	-MN1	-C15	91.0(1)
C2	-C1	-MN1	122.9(2)	C8	-C1	-MN1	72.1(2)
C8	-C1	-C2	123.4(2)	C3	-C2	-C1	109.3(3)
C4	-C3	-C2	116.1(4)	C4A	-C3	-C2	105.5(9)
C4A	-C3	-C4	40.8(7)	C4A	-C4	-C3	79.8(16)
C5	-C4	-C3	114.9(11)	C5	-C4	-C4A	43.4(11)
C5A	-C4	-C3	142.3(15)	C5A	-C4	-C4A	75.9(15)
C5A	-C4	-C5	33.0(13)	C4	-C4A	-C3	59.4(17)
C5	-C4A	-C3	134.8(12)	C5	-C4A	-C4	90.4(14)
C5A	-C4A	-C3	103.5(24)	C5A	-C4A	-C4	49.0(14)
C5A	-C4A	-C5	41.8(13)	C4A	-C5	-C4	46.2(14)
C5A	-C5	-C4	39.3(16)	C5A	-C5	-C4A	85.0(22)
C6	-C5	-C4	115.6(10)	C6	-C5	-C4A	145.6(9)
C6	-C5	-C5A	87.1(20)	C4A	-C5A	-C4	55.1(15)
C5	-C5A	-C4	107.8(22)	C5	-C5A	-C4A	53.2(19)
C6	-C5A	-C4	140.2(12)	C6	-C5A	-C4A	107.1(27)
C6	-C5A	-C5	61.0(21)	C5A	-C6	-C5	31.9(6)
C7	-C6	-C5	113.3(6)	C7	-C6	-C5A	115.8(6)
C8	-C7	-C6	111.4(3)	C1	-C8	-MN1	71.4(1)
C7	-C8	-MN1	122.6(2)	C7	-C8	-C1	123.6(3)
C10	-C9	-MN1	70.0(2)	C13	-C9	-MN1	71.2(2)
C13	-C9	-C10	107.9(3)	C14	-C9	-MN1	128.1(3)
C14	-C9	-C10	124.5(4)	C14	-C9	-C13	127.4(4)
C9	-C10	-MN1	72.2(2)	C11	-C10	-MN1	70.7(2)
C11	-C10	-C9	108.1(4)	C10	-C11	-MN1	70.8(2)
C12	-C11	-MN1	71.6(2)	C12	-C11	-C10	107.2(4)
C11	-C12	-MN1	70.4(2)	C13	-C12	-MN1	71.5(2)
C13	-C12	-C11	108.0(4)	C9	-C13	-MN1	71.6(2)
C12	-C13	-MN1	70.8(2)	C12	-C13	-C9	108.7(4)
O1	-C15	-MN1	177.2(3)	O2	-C16	-MN1	176.1(3)

A complete listing of bond angles (^{0}) for (η^5-$C_5H_4CH_3$)Mn(CO)$_2$(cis-cyclooctene)

	x/a	y/b	z/c
H1	-2054	1220	3732
H2a	773	1576	4758
H2b	1509	2041	3609
H3a	-892	2777	4479
H3b	-2689	2101	4722
H4a	-2600	2011	3407
H4b	-4487	2686	3452
H4Aa	-2016	3384	3392
H4Ab	-130	2707	3554
H5a	-327	2565	1923
H5b	-1803	3338	1791
H5Aa	-4255	2916	1960
H5Ab	-2839	2137	1841
H6a	-2914	2159	1000
H6b	-846	2702	588
H7a	1673	2027	1992
H7b	849	1625	743
H8	-1963	1252	1496
H10	3596	-888	3349
H11	446	-486	4583
H12	-2938	-122	3244
H13	-1852	-274	1200
H14a	1729	-567	339
H14b	2096	-1401	883
H14c	4235	-803	1008

Coordinates x 10^4 for hydrogen atoms in (η^5-$C_5H_4CH_3$)Mn(CO)$_2$(cis-cyclooctene)

	U11	U22	U33	U23	U13	U12
MN1	39(1)	35(1)	49(1)	1(1)	10(1)	-1(1)
C1	48(1)	35(1)	63(2)	0(1)	16(1)	2(1)
C2	87(2)	45(1)	60(2)	-8(1)	9(2)	8(2)
C3	122(4)	61(2)	96(3)	-14(2)	28(3)	27(2)
C4	67(5)	51(4)	121(8)	-14(5)	30(6)	23(4)
C4A	295(25)	59(7)	222(19)	-37(9)	-132(16)	84(12)
C5	90(7)	44(4)	100(7)	17(4)	0(6)	18(4)
C5A	140(14)	129(15)	186(20)	-44(14)	-67(16)	97(12)
C6	143(5)	70(2)	96(3)	33(2)	7(3)	36(3)
C7	97(3)	59(2)	69(2)	23(2)	17(2)	10(2)
C8	48(1)	43(1)	62(2)	3(1)	-1(1)	6(1)
C9	80(2)	40(1)	53(2)	-8(1)	7(1)	-7(1)
C10	85(2)	39(1)	62(2)	-2(1)	-1(2)	8(1)
C11	167(5)	40(2)	73(2)	-3(1)	56(3)	-24(2)
C12	75(3)	40(2)	209(6)	-14(3)	69(3)	-17(2)
C13	65(2)	44(2)	131(4)	3(2)	-30(2)	-11(2)
C14	198(6)	85(3)	91(3)	-35(2)	65(4)	-18(3)
C15	46(1)	53(2)	61(2)	5(1)	9(1)	0(1)
C16	47(1)	61(2)	63(2)	-1(1)	13(1)	-2(1)
O1	60(1)	99(2)	70(1)	0(1)	-12(1)	-7(1)
O2	72(2)	112(2)	82(2)	4(1)	42(1)	-12(1)

Anisotropic temperature factors x 10^3 with e s d's in parentheses for (η^5-$C_5H_4CH_3$)Mn(CO)$_2$(cis-cyclooctene)

APPENDIX C

```
10 REM Program for transient capture and analysis
20 KEY OFF
30 REM commands to set up GPIB-IEEE card
40 DEF SEG=0
50 DRIVER1=PEEK(&H4F0)+256*PEEK(&H4F1)
60 DRIVER2=PEEK(&H4F4)+256*PEEK(&H4F5)
70 DEF SEG=DRIVER1   REM SELECT CARD #1
80 INIT=3   ABORTIO=6   DEVCLEAR=9   LOCAL=12
90 LOCALLOCKOUT=15   REMOTE=18   IRESUME=21   TRIGGER=24
100 OUTPUT=27   ENTER=30   STATUS=33   SETTERMINATOR=36
110 SETTIMEOUT=39   SERIALPOLL=42   SRQCHECK=45   ERRCHECK=48
120 SETEOI=51   SETTERM=54   PARALLELPOLL=57   SRVREQ=60
130 NCINIT=63   BLOCKOUT=66   BLOCKIN=69   BYTESWAP=72
140 TRANSFER=75   TALK=78   UNTALK=81   LISTEN=84
150 UNLISTEN=87   ATTN=90   MTA=93   MLA=96
160 DIM AB(56) DIM Y%(257) DIM W%(257) DIM S(257) DIM AB1(56) DIM V$(257)
170 DIM AB2(56) DIM AB3(56) DIM DE(4) DIM DE$(4)
180 DIM S1(256) DIM OD(256) DIM X(256) DIM WL(56) DIM A(50) DIM B(50)
190 REM command to initilise the GPIB-IEEE card
200 CALL INIT
210 OSC=8 PI=3 14159
220 CLS D=0
230 SCREEN 0
240 WIDTH 80
250 REM Main Menu
260 LOCATE 8,34 COLOR 4 PRINT "      MENU"
270 LOCATE 9,30 COLOR 7 PRINT "New Measurement         [1]"
280 LOCATE 10,30 PRINT "Decay Analysis          [2]"
290 LOCATE 11,30 PRINT "Create Stats File       [3]"
300 LOCATE 12,30 PRINT "Review Files            [4]"
310 LOCATE 13,30 PRINT "Absorbance calculation [5]"
320 LOCATE 14,30 PRINT "DOS functions           [6]"
330 LOCATE 15,30 PRINT "EXIT                    [7]"
340 PRINT  LOCATE 16,34 COLOR 2 INPUT "  Enter Option ",D
350 IF D>7 OR D<1 THEN 340
360 IF D=1 THEN CLS KEY OFF
370 IF D=1 THEN LOCATE 10,5 INPUT"Enter experimental details",DT$
380 ON D GOTO  390,550,2060,2570,5190,6600,2940
390 REM ----------------------New Measurement-------------------------
400 REM  Menu for new measurement
410 SCREEN 0 CLS D=0
420 COLOR 4
430 REM LINE (210,70)-(450,125),12,B
440 LOCATE 11,30 PRINT "   New Measurement" COLOR 2
450 LOCATE 12,30 PRINT "Io measurement         [1]"
460 LOCATE 13,30 PRINT "Transient measurement [2]"
470 LOCATE 14,30 PRINT "FXIT                   [3]"
480 LOCATE 15,30 COLOR 14 INPUT "    Enter option",D
490 IF D>3 OR D<1 THEN 480
500 IF D=3 THEN 220
510 IF D=2 THEN GOSUB 5140 CLEAR ARRAYS AND CONSTANTS
520 IF D=1 THEN GOSUB 3220 IO MEASUREMENT
530 IF D=2 THEN GOSUB 3470 DRAW MEASURED TRANSIENTS
540 GOTO 410
550 REM -------------------------Decay Analysis-------------------------
560 CLS VP=0
570 KEY OFF
580 LOCATE 11,30  COLOR 4 PRINT "Decay Analysis"
590 LOCATE 14,29  COLOR 2 INPUT "Enter Filename ",FILE$
600 LOCATE 15,29 INPUT "Enter drive specification/default A",DR$
610 IF DR$="" THEN DR$="A"
620 FILE$=DR$+" "+ FILE$ +" tra"
630 ON ERROR GOTO 6720
640 OPEN FILE$ FOR INPUT AS #1
650 INPUT#1,DT$
660 INPUT#1,TMB
```

```
670 INPUT#1,W%(257)
680 INPUT#1,SCL
690 INPUT#1,WL
700 INPUT#1,INUL
710 FOR I%=1 TO 256
720 INPUT#1,S(I%)
730 NEXT I%
740 CLOSE#1
750 SCREEN 3
760 IF L=1 THEN VIEW(21,26)-(275,190) CLS
770 VIEW
780 LINE(20,25)-(276,191), B
790 X1=20+1 Y1=191-S(1)* 648
800 FOR I=1 TO 256
810 X=20+I Y=191-S(I)* 648
820 PSET (X,Y),1
830 LINE (X1,Y1)-(X,Y),1
840 X1=X Y1=Y
850 NEXT I
860 FOR I=1 TO 10
870 REM LINE (20+25 6*I,25)-(20+25 6*I,191),,,&HAAAA
880 REM LINE (20,25+16 6*I)-(276,25+16 6*I),,,&HAAAA
890 NEXT I
900 LOCATE 1,1 PRINT SCL "mV" "/Div"
910 LOCATE 14,15 PRINT TMB,"us/Div"
920 REM lOCATE 15,20 PRINT DT$,INUL,TMB,W%(257)
930 IF B$="y" THEN LOCATE 17,43 PRINT"  "
940 LOCATE 17,20 INPUT "Curve Smoothing (y/n)",B$
950 IF B$<>"y" AND B$<>"n" THEN 940
960 IF B$="n" THEN 1050
970 FOR I=3 TO 254
980 S(I)=(-3*S(I-2)+12*S(I-1)+17*S(I)+12*S(I+1)-3*S(I+2))/35
990 NEXT I L=1
1000 GOTO 760
1010 GOTO 1050
1020 LINE (21,BL)-(275,BL),0
1030 VIEW PRINT 16 TO 22
1040 CLS
1050 LOCATE 17,5 PRINT "Use arrow up and arrow down keys to set baseline and pre
ss return "
1060 VIEW PRINT
1070 WHILE EXIT$=""
1080 UPDN$=INKEY$
1090 IF UPDN$="" THEN 1080
1100 UPDN=ASC(RIGHT$(UPDN$,1))
1110 IF UPDN=72 THEN Z=Z-1
1120 IF UPDN=80 THEN Z=Z+1
1130 IF UPDN$=CHR$(13) THEN 1180
1140 IF Z<0 THEN Z=256
1150 IF Z>166 THEN Z=0
1160 GOSUB 4900  BASELINE ARROW
1170 WEND
1180 BL=25+Z
1190 LINE (20,BL)-(276,BL)
1200 VIEW PRINT 16 TO 22
1210 CLS
1220 LOCATE 17,20 INPUT"       Is the baseline correct y/n ",B$
1230 IF B$<>"y" AND B$<>"n" THEN 1220
1240 IF B$="n" THEN 1020
1250 VIEW PRINT
1260 GOTO 1290
1270 LOCATE 17,56 PRINT "         "
1280 LOCATE 19,53 PRINT "          "
1290 IF VP>0 THEN VIEW PRINT 16 TO 24 CLS
1300 IF VP>0 THEN VIEW PRINT
1310 LOCATE 17 20 INPUT 'Enter starting channel for analysis ",ST
```

```
1320 C=0 GOSUB 5010 REM Positioning arrow
1330 LOCATE 19,20 INPUT "Enter stop channel for analysis ",SP
1340 IF ST<0 OR SP>256 THEN 1270
1350 C=1 GOSUB 5010  REM Positioning arrow
1360 FOR I=ST TO 256
1370 S1(I)=(255-1 543*(BL-25)-S(I))*(SCL*10)/256
1380 NEXT I
1390 FOR I=ST TO SP
1400 OD(I)=ABS(LOG(INUL/(INUL+S1(I)))/2 303)
1410 NEXT I
1420 LOCATE 21,20 INPUT "First or Second order analysis ",RO
1430 IF RO<1 OR RO>2 THEN 1420
1440 IF RO=1 THEN 1450 ELSE 1530
1450 LOCATE 22,20 PRINT "First order "
1460 XMAX=-10 XMIN=0
1470 FOR I=ST TO SP
1480 X(I)=LOG(OD(I))
1490 IF XMAX<X(I) THEN XMAX=X(I)
1500 IF XMIN>X(I) THEN XMIN=X(I)
1510 NEXT I
1520 GOTO 1600
1530 LOCATE 22,20 PRINT "Second order"
1540 XMAX=0 XMIN=10
1550 FOR I=ST TO SP
1560 X(I)=1/OD(I)
1570 IF XMAX<X(I) THEN XMAX=X(I)
1580 IF XMIN>X(I) THEN XMIN=X(I)
1590 NEXT I
1600 XX=(XMAX-XMIN)
1610 IF VP>0 THEN VIEW (300,10)-(639,220) CLS
1620 VIEW
1630 FOR I=ST TO SP
1640 R=R+1
1650 YY=256/(SP-ST)
1660 XX1=(XMAX-X(I))/XX
1670 IF I=ST THEN R=0
1680 G=369+(R)*YY H=26+XX1*164
1690 PSET(G,H),1
1700 NEXT I
1710 SUM=0 SUMX=0 SUMY=0 SUMX2=0 SUMY2=0 SUMXY=0 SIGMA=0 CORR=1
1720 GOSUB 4690 REM statistical analysis
1730 XX1=TAU*ST+ICP XX2=TAU*SP+ICP
1740 G1=369 H1=26+((XMAX-XX1)/(XMAX-XMIN))*164
1750 G2=369+R*YY H2=26+((XMAX-XX2)/(XMAX-XMIN))*164
1760 H3=191-H2
1770 LINE (G1,H1)-(G2,H2)
1780 IF RO=2 THEN LINE (G1-(G1* 05),26)-(G1-(G1* 05),H2+H3)
1790 LINE (G1-(G1* 05),26)-(G1-(G1* 05),H2+H3)
1800 LINE(G1-(G1* 05),H2+H3)-(G2,H2+H3)
1810 IF RO=1 THEN 1820 ELSE 1850
1820 LOCATE 2,37 PRINT USING "#### ##",XX1
1830 LOCATE 12,37 PRINT USING"#### ##",XX2
1840 GOTO 1870
1850 LOCATE 2,37 PRINT USING "#### ##",XX2
1860 LOCATE 12 37 PRINT USING"#### ##",XX1
1870 A=TMB/25*(SP-ST)
1880 LOCATE 13,44 PRINT USING "#                                    # #^^^^",0,A
1890 LOCATE 14,52 PRINT "time (microseconds)"
1900 VIEW PRINT 16 TO 24 CLS
1910 LOCATE 18,50 PRINT"correlation=",CORR
1920 LOCATE 19,50 PRINT "decay us=",ABS((1/TAU)*TMB/25)
1930 RKOBS=((1/TAU)*TMB/25)* 000001
1940 KOBS=(1/RKOBS)
1950 IF RO=1 THEN LOCATE 20,50 PRINT "kobs=",ABS(KOBS),"/s"
1960 IF RO=2 THEN LOCATE 20 50 PRINT  kobs=";ABS(KOBS),"dm3/mol/s"
1970 LOCATE 17 50 PRINT "File   ",FILE$
```

```
1980 LOCATE 16,4 PRINT DT$
1990 LOCATE 17,4 PRINT"Io=",INUL,"mV'
2000 LOCATE 18,4 PRINT 'Average of",W%(257),'shots"
2010 LOCATE 19,4 PRINT "Wavelength=",WL,"nm"
2020 LOCATE 20,4 INPUT "Press return to continue, / to refit line",W$
2030 IF W$ ="/" THEN 2040 ELSE 220
2040 VP=1
2050 GOTO 1250
2060 REM ------------------Create STATIS Files------------------
2070 KEY OFF
2080 CLS
2090 LOCATE 9,32 COLOR 4 PRINT 'Create Statis File"
2100 LOCATE 11,29 COLOR 2 INPUT "Enter Filename",FILE$
2110 LOCATE 12,29 INPUT "Enter drive specification/default A",DR$
2120 IF DR$="" THEN DR$="A"
2130 FL$=DR$+" "+FILE$ +" tra"
2140 ON ERROR GOTO 6720
2150 OPEN FL$ FOR INPUT AS #1
2160 INPUT#1,DT$ INPUT#1,TMB INPUT#1,W%(257) INPUT#1 SCL INPUT#1,WL
2170 INPUT#1,INUL
2180 FOR I%=1 TO 256
2190 INPUT #1,S(I%)
2200 X(I%)=S(I%)
2210 NEXT I%
2220 CLOSE#1
2230 ST=10 SP=20
2240 SUM=0 SUMX=0 SUMY=0 SUMX2=0 SUMY2=0 SUMXY=0 SIGMA=0 CORR=1
2250 GOSUB 4690  REM statistical analysis
2260 FOR I=ST TO 256
2270 YL=TAU*I+ICP
2280 IF X(I)>YL+4*SIGMA OR X(I)<YL-4*SIGMA THEN 2300
2290 NEXT I
2300 LF=I LOCATE 14,29 COLOR 3 PRINT "laser fires at channel ",LF
2310 LOCATE 16,29 INPUT "Output file to statis (y/n)",OS$
2320 IF OS$<>"y" THEN  2370
2330 SHELL"cd\statis3"
2340 SHELL"exit"
2350 FILE$=FILE$+" sta"
2360 GOTO 2390
2370 LOCATE 17,29 INPUT "Enter drive specification",DR$
2380 FILE$=DR$+" "+FILE$+" sta"
2390 OPEN FILE$ FOR OUTPUT AS #1
2400 PRINT#1,DT$
2410 PRINT#1,2,256-LF
2420 PRINT#1,"Time(s)"
2430 PRINT#1,"Absorbance (AU)"
2440 GOSUB 5070 REM subroutine to calculate baseline voltage
2450 FOR I=LF TO 256
2460 OD(I)=LOG(INUL/(INUL-(S(I)-AQS)*SCL*10/255))/2.303
2470 PRINT#1,USING '# ####^^^^    (TMB/25*(I-LF))*10^-6,OD(I)
2480 NEXT I
2490 CLOSE#1
2500 LOCATE 21,29 INPUT "Do you wish to enter statis (y/n)",ES$
2510 IF ES$<>"y" THEN 2550
2520 CLS SHELL"cd\"
2530 SHELL"statis"
2540 SHELL"cd\basic2"
2550 LOCATE 25,30 COLOR 7 INPUT "Press return to continue",B$
2560 IF B$="" THEN 220 ELSE 2520
2570 REM -------------------------View Files---------------------
2580 O=0 CL=0
2590 SCREEN 0 CLS KEY OFF
2600 LOCATE 11,34  COLOR 4 PRINT "Review Files"
2610 LOCATE 13,30 COLOR 12 INPUT "Review file contents (y/n)",RE$
2620 IF RE$="y" THEN 6910 REM read file contents
2630 LOCATE 15,30  COLOR 3 INPUT "Enter Filename ",FILE$
```

```
2640 LOCATE 16,30 INPUT "Enter drive specification/default A",DR$
2650 IF DR$="" THEN DR$="A"
2660 IF CL=1 THEN O=1
2670 IF O=1 THEN LOCATE 20,1 PRINT "                "
2680 IF O=1 THEN LOCATE 20,1 INPUT "Enter filename",FILE$
2690 IF O=1 THEN LOCATE 20,1 PRINT "                                "
2700 FILE$=DR$+" " + FILE$ +" tra"
2710 ON ERROR GOTO 6720
2720 OPEN FILE$ FOR INPUT AS #1
2730 INPUT#1,DT$
2740 INPUT#1,TMB
2750 INPUT#1,W%(257)
2760 INPUT#1,SCL
2770 INPUT#1,WL
2780 INPUT#1,INUL
2790 FOR I%=1 TO 255
2800 INPUT#1,S(I%)
2810 NEXT I%
2820 CLOSE#1
2830 GOSUB 4370 REM draw transient data
2840 LOCATE 14,1  PRINT "<CR> to exit"
2850 LOCATE 16,1 PRINT"[1] for overlay"
2860 LOCATE 18,1 INPUT "[2] to clear screen",O
2870 IF O=0 THEN 220
2880 IF O=2 THEN 2890 ELSE 2930
2890 VIEW (217,22)-(599,276)
2900 CLS CL=1
2910 VIEW
2920 GOTO 2660
2930 IF O=1 THEN 2670
2940 REM ----------------------------EXIT---------------------
2950 LOCATE 17,35 COLOR 3 INPUT "Exit to DOS (y/n)",EX$
2960 IF EX$="y" THEN SYSTEM ELSE END
2970 REM  Subroutine for data transfer from oscilloscope
2980 CMD$="SPR 13"
2990 CALL OUTPUT(CMD$,OSC)
3000 CMD$="USP 47"
3010 CALL OUTPUT(CMD$,OSC)
3020 CMD$="WTD 30"
3030 CALL OUTPUT(CMD$,OSC)
3040 CALL OUTPUT(CM$,OSC)
3050 CALL UNLISTEN
3060 FOR I=1 TO 256
3070 V$(I)=SPACE$(20)
3080 NEXT I
3090 DELIM$=CHR$(13)
3100 CALL TALK(OSC)
3110 CALL MLA
3120 CALL IRESUME
3130 CALL TRANSFER(V$(0),COUNT,DELIM$)
3140 FOR I=1 TO COUNT
3150 Y%(I)=VAL(V$(I))
3160 NEXT I
3170 REM CMD$="FRO 0/HOR MTB/MOD REC/TRD ?"
3180 REM CALL OUTPUT(CMD$,OSC)
3190 CALL LOCAL(OSC)
3200 CALL LOCAL(OSC)
3210 RETURN
3220 REM Subroutine for Io measurement
3230 CLS
3240 REM LINE (200,70)-(460,125),12,B
3250 LOCATE 11,30 COLOR 4 PRINT "    Io Measurement" COLOR 2
3260 LOCATE 13,25 INPUT " Close Shutter and press return ",D$
3270 CM$="REG 0/VER A/FCN ON/BGN 0/END 25/CNT 1/DAT ?"
3280 COUNT =27
3290 IF D$=""  THEN GOSUB 2970
```

```
3300 FOR I%=1 TO 26
3310 AA=AA+Y%(I%)
3320 NEXT I%
3330 AA=AA/26
3340 LOCATE 13,25 COLOR 2 INPUT " Open Shutter and press return ",D$
3350 IF D$="" THEN GOSUB 2970
3360 FOR I%=1 TO 26
3370 BB=BB+Y%(I%)
3380 NEXT I%
3390 BB=BB/26
3400 LOCATE 15,30 PRINT "                    "
3410 GOSUB 4170 REM front panel oscilloscope settings
3420 INUL=(AA-BB)*(ATT*10)/256
3430 LOCATE 13,25 COLOR 7 PRINT"          Io=",INUL,"              "
3440 LOCATE 15,29 COLOR 5 INPUT "Press return to continue",W$
3450 IF W$ = "" THEN 410 ELSE 3440
3460 RETURN
3470 REM  Subroutine for to draw measured transients
3480 SCREEN 3 KEY OFF  CLS
3490 LOCATE 11,30 PRINT "Previous file ",FILE$
3500 LOCATE 13,30 INPUT "Enter filename ",FILE$
3510 FILE$="A " + FILE$ +" tra"
3520 WL1=WL
3530 LOCATE 15,30 PRINT "Enter wavelength (nm) [",WL,"] ",
3540 INPUT WL IF WL=0 THEN WL=WL1
3550 IF INUL=0 THEN LOCATE 17,30 INPUT"Enter Io",INUL
3560 LOCATE 21,30 INPUT "Press return to measure ",B$
3570 IF B$="" THEN 3580 ELSE 3560
3580 CLS
3590 GOSUB 4170 REM front panel oscilloscope settings
3600 SCL=ATT TMB=TM
3610 FOR J=1 TO 10
3620 W%(257)=W%(257)+1
3630 IF J>1 THEN VIEW (51,26)-(305,190) CLS
3640 IF J>1 THEN VIEW (307,26)-(561,190) CLS
3650 LOCATE 1,30 PRINT "File       ",FILE$
3660 IF J=1 THEN LINE (50,25)-(306,191),,B
3670 IF J=1 THEN LINE (306,25)-(562,191),,B
3680 LOCATE 13,15 PRINT"Averaged Transient"
3690 LOCATE 13,47 PRINT"Current Transient"
3700 LOCATE 15,5 PRINT "Shot No ",W%(257)
3710 LOCATE 15,25 PRINT DT$
3720 IF INUL =0 THEN LOCATE 17,5 PRINT "Io not measured" GOTO 3760
3730 LOCATE 19,5 PRINT "Wavelength=",WL,"nm"
3740 LOCATE 16,5 PRINT "Io=",INUL,"mV      "
3750 LOCATE 17,5 PRINT "Scale=",SCL,"mV/div"
3760 LOCATE 18,5 PRINT "Timebase=",TMB,"us/div"
3770 CM$="REG 0/VER A/FCN ON/BGN 0/END 255/CNT 1/DAT ?"
3780 COUNT =257
3790 GOSUB 2970 REM data transfer from oscilloscope
3800 FOR I=1 TO 256
3810 W%(I)=Y%(I)+W%(I)
3820 NEXT I
3830 VIEW
3840 X1=50+1 Y1=191-(W%(1)/W%(257))* 648
3850 FOR I=1 TO 256
3860 X=50+I Y=191-(W%(I)/W%(257))* 648
3870 PSET (X,Y),1
3880 LINE (X1,Y1)-(X,Y),1
3890 X1=X Y1=Y
3900 NEXT I
3910 X1=306+1 Y1=191-Y%(1)* 648
3920 FOR I=1 TO 256
3930 X=306+I Y=191-Y%(I)* 648
3940 PSET(X,Y),1
3950 LINE (X1,Y1)-(X,Y),1
```

```
3960 X1=X Y1=Y
3970 NEXT I
3980 ON ERROR GOTO 6790
3990 OPEN FILE$ FOR OUTPUT AS #1
4000 PRINT#1,DT$
4010 PRINT#1,TMB
4020 PRINT#1,W%(257)
4030 PRINT#1,SCL
4040 PRINT#1,WL
4050 PRINT#1,INUL
4060 FOR I=1 TO 256
4070 S(I)=W%(I)/W%(257)
4080 PRINT#1,S(I)
4090 NEXT I
4100 CLOSE#1
4110 BEEP
4120 LOCATE 22,15 PRINT "Press return for another shot measurement"
4130 LOCATE 23,15 INPUT "Enter any character to return to menu ",B$
4140 IF B$="" THEN 4150 ELSE 4160
4150 NEXT J
4160 RETURN
4170 REM Subroutine to obtain oscilloscope settings
4180 CMD$="REG 0/VER A/FCN ON/ATT ?"
4190 VOLT$=SPACE$(11)
4200 CALL OUTPUT(CMD$,OSC)
4210 CALL ENTER(VOLT$,OSC)
4220 FOR I=1 TO 1000 NEXT I
4230 CALL LOCAL(OSC)
4240 CALL LOCAL(OSC)
4250 ATT$=RIGHT$(VOLT$,7)
4260 ATT=VAL (ATT$)*200
4270 CMD$="HOR ?"
4280 CALL OUTPUT (CMD$,OSC)
4290 T$=SPACE$(100)
4300 FOR I=1 TO 5000 NEXT I
4310 CALL ENTER(T$,OSC)
4320 CALL LOCAL (OSC)
4330 CALL LOCAL (OSC)
4340 TB$=MID$(T$,21,6)
4350 TM=VAL(TB$)*10^6
4360 RETURN
4370 REM Subroutine to draw transient data
4380 KEY OFF
4390 SCREEN 3  WIDTH 80
4400 PRINT
4410 LOCATE 2,24 PRINT "256"
4420 LOCATE 10,24 PRINT"128"
4430 LOCATE 18,26 PRINT "0"
4440 PRINT
4450 LOCATE 19,28 PRINT"0    32    64    96    128    160    192    224    256"
4460 LOCATE 21,28 PRINT '                                                    "
4470 LOCATE 21,28 PRINT DT$
4480 LINE (216,21)-(600,277),,B
4490 LOCATE 3,11 PRINT "                    "
4500 LOCATE 3,1 PRINT"timebase=",TMB,"us/div"
4510 LOCATE 1,1 PRINT "                      "
4520 LOCATE 1,1 PRINT "File    " FILE$
4530 LOCATE 5,1 PRINT "Io",INUL,"mV"
4540 LOCATE 7,1 PRINT "Average of',W%(257),"shots"
4550 LOCATE 9,1 PRINT "Wavelength=",WL,"nm"
4560 LOCATE 11,1 PRINT "Scale=",SCL,"mV/div"
4570 FOR I=1 TO 10
4580 LINE(216+(25 6*I*1 5),21)-(216+(25 6*I*1 5),277),,,&H4444
4590 LINE(216,21+25 6*I)-(600,21+25 6*I),,,&H4444
4600 NEXT I
4610 X1=216+1 5 Y1=277-S(1)
```

```
4620 FOR I=1 TO 256
4630 X=216+1 5*I Y=277-S(I)
4640 PSET (X,Y),1
4650 LINE (X1,Y1)-(X,Y),1
4660 X1=X.Y1=Y
4670 NEXT I
4680 RETURN
4690 REM Subroutine for statistical calculations
4700 SUM=SP-ST+1
4710 FOR I=ST TO SP
4720 SUMX=SUMX+I
4730 SUMY=SUMY+X(I)
4740 SUMX2=SUMX2+I*I
4750 SUMY2=SUMY2+X(I)*X(I)
4760 SUMXY=SUMXY+X(I)*I
4770 NEXT I
4780 RA=SUM*SUMXY-SUMX*SUMY
4790 RB=SQR(SUM*SUMX2-SUMX^2)
4800 RC=SQR(SUM*SUMY2-SUMY^2)
4810 CORR=RA/(RB*RC)
4820 DELTA=SUM*SUMX2-SUMX^2
4830 ICP=(SUMX2*SUMY-SUMX*SUMXY)/DELTA
4840 TAU=(SUM*SUMXY-SUMX*SUMY)/DELTA
4850 FOR I=ST TO SP
4860 SIGMA=SIGMA+(X(I)-ICP-TAU*I)^2
4870 NEXT I
4880 SIGMA =SIGMA/(SP-ST-1)
4890 RETURN
4900 REM Subroutine for baseline arrow
4910 IF Z<>Z-1  THEN LINE (277,25+Z-1)-(284,25+Z-1),0
4920 IF Z<>Z-1  THEN LINE (277,25+Z-1)-(279,28+Z-1),0
4930 IF Z<>Z-1  THEN LINE (277,25+Z-1)-(279,22+Z-1),0
4940 IF Z<>Z+1 THEN LINE (277,25+Z+1)-(284,25+Z+1),0
4950 IF Z<>Z+1  THEN LINE (277,25+Z+1)-(279,28+Z+1),0
4960 IF Z<>Z+1  THEN LINE (277,25+Z+1)-(279,22+Z+1),0
4970 LINE (277,25+Z)-(284,25+Z)
4980 LINE (277,25+Z)-(279,28+Z)
4990 LINE (277,25+Z)-(279,23+Z)
5000 RETURN
5010 REM Subroutine for positioning arrow
5020 IF C=0 THEN U=ST ELSE U=SP
5030 LINE (20+U,191-S(U)* 648)-(20+U,200-S(U)* 648)
5040 LINE (20+U,191-S(U)* 648)-(16+U,192-S(U)* 648)
5050 LINE (20+U,191-S(U)* 648)-(24+U,192-S(U)* 648)
5060 RETURN
5070 REM Subroutine to calculate baseline voltage
5080 QS=0
5090 FOR I=4 TO 15
5100 QS=QS+S(I)
5110 NEXT I
5120 AQS=QS/11
5130 RETURN
5140 REM Subroutine to clear arrays and constants
5150 FOR I=1 TO 257
5160 W%(I)=0
5170 NEXT I
5180 RETURN
5190 REM--------------------Absorbance Calculation-------------------
5200 CLS KEY OFF N=4
5210 FOR I=1 TO N
5220 LOCATE 15,25 PRINT " Enter time delay No ",I,"max=4 (/ to exit)",
5230 INPUT DE$(I)
5240 LOCATE 15,68 PRINT "          "
5250 N=I-1
5260 IF I=4 THEN N=4
5270 IF DE$(I)="/" THEN 5300
```

```
5280 DE(I)=VAL(DE$(I))
5290 NEXT I
5300 GOSUB 5640 REM to read data from disk
5310 OPEN FILE$ FOR INPUT AS #1
5320 INPUT#1,DT$
5330 INPUT#1,TMB
5340 INPUT#1,W%(257)
5350 INPUT#1,SCL
5360 INPUT#1,WL
5370 INPUT#1,INUL
5380 FOR I%=1 TO 255
5390 INPUT#1,S(I%)
5400 X(I%)=S(I%)
5410 NEXT I%
5420 CLOSE#1
5430 ST=10 SP=20
5440 SUM=0 SUMX=0 SUMY=0 SUMX2=0 SUMY2=0 SUMXY=0 SIGMA=0 CORR=1
5450 GOSUB 4690  REM statistical calculations
5460 FOR I=ST TO 256
5470 YL=TAU*I+ICP
5480 IF X(I)>YL+3*SIGMA OR X(I)<YL-3*SIGMA THEN 5510
5490 YL=0
5500 NEXT I
5510 LF=I IF LF>35 OR LF<26 THEN LF=30
5520 GOSUB 5070 REM calculate baseline voltage
5530 CH=0 CH1=0
5540 CH=INT((DE(1)*256)/(TMB*10))+LF
5550 CH1=INT((DE(2)*256)/(TMB*10))+LF
5560 CH2=INT((DE(3)*256)/(TMB*10))+LF
5570 CH3=INT((DE(4)*256)/(TMB*10))+LF
5580 OD(CH)=LOG(INUL/(INUL-(S(CH)-AQS)*SCL*10/255))/2 303
5590 OD(CH1)=LOG(INUL/(INUL-(S(CH1)-AQS)*SCL*10/255))/2 303
5600 OD(CH2)=LOG(INUL/(INUL-(S(CH2)-AQS)*SCL*10/255))/2 303
5610 OD(CH3)=LOG(INUL/(INUL-(S(CH3)-AQS)*SCL*10/255))/2 303
5620 RETURN
5630 END
5640 REM Subroutine to get files from disk
5650 CLS WD=0 R=0
5660 INPUT"Enter letter code",C$
5670 INPUT"Enter start file no ",SF
5680 INPUT "Enter file stop no ",FS
5690 INPUT"Enter step",TEP
5700 INPUT"Send data to printer (y/n)",P$
5710 IF P$<>"y" AND P$<>"n" THEN 5700
5720 INPUT "Write data to file (y/n)",WD$
5730 IF WD$<>"y" AND WD$<>"n" THEN 5720
5740 IF WD$="n" THEN 5780
5750 WD=1
5760 INPUT  Enter drive specification',DR$
5770 FI$=DR$+" "+C$+" abs"
5780 FOR J=SF TO FS STEP TEP
5790 GOSUB 6120 REM convert filenumbers to strings
5800 FILE$="a "+CE$+" tra'
5810 GOSUB 5310 REM read data from disk
5820 R=R+1  IF R=1 THEN CLS
5830 IF R=1 THEN PRINT TAB(20)"Timedelay=",DE(1),"microseconds"
5840 IF R=1 AND P$="y" THEN LPRINT TAB(20)"Timedelay=",DE,"microseconds"
5850 IF R=1 THEN PRINT "  Wavelength     Absorbance      Filename       Fire cha
nnel     Timebase"
5860 IF R=1 AND P$="y" THEN LPRINT "  Wavelength     Absorbance      Filename
    Fire channel     Timebase"
5870 PRINT USING "     ###        ## ###^^^^       \            \     ##
  ###### #",WL,OD(CH) FILE$,LF,TMB
5880 IF P$="y" THEN LPRINT USING "     ###        ## ###^^^^       \
\     ##             ######",WL,OD(CH),FILE$,LF,TMB
5890 WL(R)=WL AB(R)=OD(CH) AB1(R)=OD(CH1) AB2(R)=OD(CH2) AB3(R)=OD(CH3)
```

```
5900 NEXT J
5910 CLOSE#1
5920 CO=(FS-SF)/TEP+1
5930 IF WD=1 THEN 5940 ELSE 6090
5940 OPEN FI$ FOR OUTPUT AS #1
5950 PRINT#1,DT$
5960 PRINT#1,
5970 IF N=1 THEN PRINT#1  DE(1)"us"
5980 IF N=2 THEN PRINT#1,,DE(1)"us",DE(2)"us"
5990 IF N=3 THEN PRINT#1,,DE(1)"us",DE(2)"us",DE(3)"us"
6000 IF N=4 THEN PRINT#1,,DE(1)"us",DE(2)"us",DE(3)"us",DE(4)"us"
6010 CO=(FS-SF)/TEP+1
6020 FOR I=1 TO CO
6030 IF N=1 THEN PRINT#1,USING " ###      ## ###^^^^ ",WL(I),AB(I)
6040 IF N=2 THEN PRINT#1,USING " ###      ## ###^^^^       ## ###^^^^ ",WL(I),AB(I
),AB1(I)
6050 IF N=3 THEN PRINT#1,USING " ###      ## ###^^^^       ## ###^^^^       ## ###^
^^^ ",WL(I),AB(I),AB1(I),AB2(I)
6060 IF N=4 THEN PRINT#1 USING " ###      ## ###^^^^       ## ###^^^^       ## ###^
^^^      ## ###^^^^ ",WL(I),AB(I),AB1(I),AB2(I),AB3(I)
6070 NEXT I
6080 CLOSE#1
6090 LOCATE 25,9 INPUT "Press return to plot spectrum (any character for menu)",
W$
6100 IF W$="" THEN 6190 ELSE 220
6110 REM Subroutine to convert filenumbers to strings
6120 CE$=""
6130 E$="" CE$=C$
6140 IF INT(J/10)>0 OR INT(J/10)<10 THEN E$=RIGHT$(STR$(J),2)
6150 IF INT(J/10)=0 THEN E$=RIGHT$(STR$(J),1)
6160 IF ABS(J/10)>9 899999 THEN E$=RIGHT$(STR$(J),3)
6170 CE$=CE$+E$
6180 RETURN
6190 REM Subroutine to draw line spectrum
6200 CLS
6210 SCREEN 3
6220 WIDTH 80
6230 YMAX=-10 YMIN=10
6240 XMAX=-10 XMIN=1000
6250 LINE (100,20)-(500,280),,B
6260 FOR I=1 TO CO
6270 IF WL(I)>XMAX THEN XMAX=WL(I)
6280 IF WL(I)<XMIN THEN XMIN=WL(I)
6290 IF AB(I)>YMAX THEN YMAX=AB(I)
6300 IF AB(I)<YMIN THEN YMIN=AB(I)
6310 IF DE1=0 THEN 6340
6320 IF AB1(I)>YMAX THEN YMAX=AB1(I)
6330 IF AB1(I)<YMIN THEN YMIN=AB1(I)
6340 NEXT I
6350 LOCATE 1 15 PRINT DT$
6360 LOCATE 2,7 PRINT USING"## ###",YMAX LOCATE 18,7 PRINT USING "## ###",YMIN
6370 LOCATE 19,11 PRINT XMIN LOCATE 19,61 PRINT XMAX LOCATE 19,36 PRINT (XMAX+XM
IN)/2
6380 Y1=(YMAX-YMIN)
6390 X1=(XMAX-XMIN)
6400 IF YMIN>0 THEN 6420
6410 LINE (100,20+((YMAX-0)/Y1)*260)-(500,20+((YMAX-0)/Y1)*260)
6420 PS3=500-(XMAX-WL(1))/X1*400 PS4=20+(YMAX-AB(1))/Y1*260
6430 FOR I=1 TO CO
6440 X2=(XMAX-WL(I))/X1
6450 Y2=(YMAX-AB(I))/Y1
6460 PS1=500-X2*400 PS2=20+Y2*260
6470 PSET(PS1,PS2)
6480 LINE (PS3,PS4)-(PS1,PS2)
6490 PS3=PS1 PS4=PS2
6500 NEXT I
```

```
6510 IF DE1=0 THEN 6570
6520 FOR I=1 TO CO
6530 SWAP AB(I),AB1(I)
6540 NEXT I
6550 DE1=0
6560 GOTO 6420
6570 GOTO 6090
6580 END
6590 REM ------------------------DOS Functions------------------------------
6600 CLS
6610 PRINT "  TYPE                              FUNCTION"
6620 PRINT
6630 PRINT "'A '<CR>                    Change from hard-disk to floppy disc"
6640 PRINT "'cd\trans'<CR>              Call transient directory"
6650 PRINT "'type (filename)<CR>        To list the contents of the file"
6660 PRINT "'edlin (filename)'<CR>      To edit a file"
6670 PRINT "'C <CR>                     To return to hard-disk"
6680 PRINT "'exit'<CR>                  To return to program"
6690 SHELL
6700 SHELL"cd\basic2"
6710 GOTO 220
6720 REM Subroutine for error trapping
6730 IF ERR=53 AND ERL=640 THEN ER=1
6740 IF ERR=53 AND ERL=2150 THEN ER=2
6750 IF ERR=53 AND ERL=2720 THEN ER=3
6760 IF ER=1 THEN LOCATE 17,29 PRINT "FILE NOT FOUND   SWITCH DIRECTORY?" FOR I=
1 TO 5000 NEXT I GOSUB 6820 RESUME 220
6770 IF ER=2 THEN LOCATE 17,37 PRINT "FILE NOT FOUND" FOR I=1 TO 5000 NEXT I GOS
UB 6820 RESUME 220
6780 IF ER=3 THEN LOCATE 17,34 PRINT "FILE NOT FOUND" FOR I=1 TO 5000 NEXT I IF
CL=1 THEN RESUME 2660 ELSE RESUME 220
6790 IF ERR=71 AND ERL=3990 THEN 6800 ELSE 6810
6800 LOCATE 19,40 PRINT "INSERT DISK INTO DRIVE" FOR I=1 TO 5000 NEXT I GOSUB 51
40 RESUME 3480
6810 ON ERROR GOTO 0
6820 REM Subroutine to list filenames
6830 CLS
6840 SHELL"A "
6850 SHELL"dir/w"
6860 SHELL"C "
6870 SHELL"cd\basic2"
6880 LOCATE 25,30 COLOR 7 INPUT "Press return to continue",B$
6890 IF B$="" THEN 6900  ELSE 6880
6900 RETURN
6910 KEY OFF
6920 CLS
6930 REM Subroutine to read and display file contents
6940 K=0
6950 INPUT 'Enter file string" F$
6960 INPUT "Enter file start number",FS
6970 INPUT "Enter file stop number",FE
6980 FOR I=FS TO FE
6990 K=K+1
7000 IF K=1 THEN PRINT" FILENAME "," WAVELENGTH ","TIMEBASE  ","SCALE ","
     DETAILS"
7010 REM Subroutine to convert filenumbers to strings
7020 GOSUB 7200
7030 FILE$='A '+FI$+' tra"
7040 ON ERROR GOTO 7270
7050 OPEN FILE$ FOR INPUT AS #1
7060 INPUT#1,DT$
7070 INPUT#1,TMB
7080 INPUT#1,SHOT
7090 INPUT#1,SCL
7100 INPUT#1,WL
7110 INPUT#1,INUL
```

```
7120 CLOSE#1
7130 PRINT USING"\           \ ###     ###### #  ###    \
                \",FILE$,WL,TMB,SCL,DT$
7140 IF K=22 THEN GOSUB 7380
7150 NEXT I
7160 INPUT "Another go' (y/n)",AG$
7170 IF AG$="y" THEN 6910
7180 CLS GOTO 2630 END
7190 REM Subroutine to convert filenumbers to strings
7200 FI$=""
7210 E$=""
7220 IF INT(I/10)>0 OR INT(I/10)<10 THEN E$=RIGHT$(STR$(I),2)
7230 IF INT(I/10)=0 THEN E$=RIGHT$(STR$(I),1)
7240 IF INT(I/10)>9 899999 THEN E$=RIGHT$(STR$(I),3)
7250 FI$=F$+E$
7260 RETURN
7270 CLS
7280 SHELL"a "
7290 SHELL"dir/w"
7300 LOCATE 1,1 INPUT "Switch directory A \ = [1], A \TRANS = [2], no switch = [
0]",SD
7310 IF SD=0 THEN 7340
7320 IF SD=2 THEN SHELL"cd\trans"  GOTO 7270
7330 IF SD=1 THEN SHELL"cd\"  GOTO 7270
7340 SHELL"C "
7350 SHELL"exit"
7360 GOSUB 7380
7370 RESUME 6930
7380 LOCATE 24,30 INPUT "Press return to continue",PR$
7390 IF PR$="" THEN CLS ELSE 7370
7400 K=0
7410 RETURN
```